Alma Mater Studiorum – Università di Bologna

DOTTORATO DI RICERCA IN

Scienze e Tecnologie Agrarie, Ambientali e Alimentari

Ciclo XXXI

Settore Concorsuale: 07/F1

Settore Scientifico Disciplinare: AGR/15

Optimizing quality losses and shelf-life in bakery products by edible coatings

Presentata da: Swathi Sirisha Nallan Chakravartula

Coordinatore Dottorato

Massimiliano Petracci

Supervisore

Marco Dalla Rosa

Correlatrice

Federica Balestra

Esame finale anno 2019

Abstract

Edible packaging is of increasing interest as a technological strategy for preserving quality, improving shelf-life as well as reducing the residual waste associated with food packaging. Alternative packaging systems with coatings and films that are viable have already been proven useful in fresh produce, fresh cuts; meat and milk products. However, in the past decade interest has been renewed in edible packaging application for bakery products to restrict moisture migration, texture changes, mould growth, incorporate functional compounds and reduce overall packaging impact.

The objective of this thesis was to develop edible coatings to mitigate quality losses in bakery products. The coating and product as dynamic systems with different physico-mechanical characteristics were assessed individually by, (i) development and characterization of edible coating matrices for bakery application; (ii) evaluation of the drying of edible coating on bread to optimize temperature and time of drying; (iii) effect of coating during storage as influenced by type of coating and stage of application.

Based on the obtained results, characterization of rheological, mechanical and thermal characteristics of edible coatings and films were found particularly useful to select suitable coating matrices. The use of rapid methods like near infrared spectroscopy enabled the monitoring and modelling of optimal temperature/time combinations to dry coatings. Also, a numerical model to understand the heat and mass transfer dynamics for the coated bread was designed. Furthermore, the study on storage indicated that the use of edible coatings can have a retaining effect on the moisture and textural quality of bread.

The results evidenced in this doctoral project can contribute to the understanding of the role of edible coatings for bread. They could be further designed as potential alternatives to reduce the level of barriers used for packaging, for a more sustainable and eco-friendly production chain.

List of Papers

The thesis is based on the work contained in the following papers and manuscripts as referred to in the text by their Roman numerals. The papers are attached at the end of the thesis;

I **Nallan Chakravartula SS.**, Balestra F., Lotti N., Soccio M., Siracusa V., Dalla Rosa M. (2019). Characterization of composite edible films based on Pectin/Alginate/Whey Protein concentrate (Manuscript).

II **Nallan Chakravartula SS.**, Balestra F., Romani S., Dalla Rosa M. (2019). Dehydration behaviour of pan bread with edible coating: A preliminary study (Manuscript).

III **Nallan Chakravartula SS.**, Balestra F., Cevoli C., Fabbri A., Dalla Rosa M. (2019). Evaluation of drying of edible coating on bread using NIR spectroscopy. Journal of Food engineering, 240, 29-37.

IV Cevoli C., **Nallan Chakravartula SS.**, Dalla Rosa M., Fabbri A. (2019). Drying of coating on bun bread: heat and mass transfer numerical model. Bio systems Engineering, (submitted).

V(a) **Nallan Chakravartula SS.**, Cevoli C., Balestra F., Fabbri A., Dalla Rosa M. (2019). Effect of edible coating on mini-buns during storage: Textural and near infrared spectroscopic analysis. Journal of Food Engineering, (submitted).

V(b) **Nallan Chakravartula SS.**, Balestra F., Romani S., Dalla Rosa M. (2019). Edible coatings application on bread: Effect of application stage and type of coating in storage (Manuscript).

VI **Nallan Chakravartula SS.**, Lourenço RV., Balestra F., Bittante AMBQ., Sobral PJA., Dalla Rosa M. (2019). Preparation and characterization of Cassava Starch/Chitosan films activated with Pitanga leaf extract (Eugenia Uniflora L.) and Natamycin (Manuscript).

Table of Contents

List of Figures

1. Introduction and objectives

Packaging systems aimed to improve the keeping quality of the product should contribute also to the sustainability of food production (Licciardello *et al.,* 2014; Siracusa *et al.,* 2008). The increasing concerns with regard to the environmental sustainability of traditional packaging materials has propelled in the last two decades pursuit for alternatives. One such alternative widely being investigated for applications on a wide range of food products is '*edible packaging'*. It is an age-old technique, dating back to middle-age Mesopotamia for sausage making, cheese aging and 12th century China, where wax was used to coat citrus fruits to prevent water loss (Debeaufort *et al*., 1998; Han, 2013). A radical interest resurfaced in early 21st century to develop food grade biopolymer matrices to enhance shelf-life, safety of food products with nominal costs as well investigate and mitigate the short-comings of these biodegradable polymers.

The edible packaging technology encompasses edible coatings and edible films which can be defined as a primary packaging for food, formed directly on the surface of food products or as thin stand-alone films used to wrap around or placed between the components of food products (Falguera *et al.,* 2011; Tongnuanchan and Benjakul, 2014). Edible films can be used as such or as pouches, bags, casings depending on the type of process and products, whereas, coatings are applied on the surfaces of products to form films directly by dipping, spraying or spreading (Han, 2013). These coatings are designed to be consumed along with the product and are typically prepared using hydrocolloids (polysaccharides, proteins) and composites with one or more hydrocolloids, with or without lipids (Debeaufort *et al.,* 1998; Galus and Kadzińska, 2015).

Bread is a part of everyday meal in many communities across the globe with a perishable status and limited shelf-life of 3-4 days without preservatives (Jideani and Vogt, 2016). Several additives and advanced packaging systems are used to improve the shelf-life and conserve the fresh characteristics of bread and bread products (Fadda *et al*., 2014; Gomes-Ruffi *et al*., 2012; Gutiérrez *et al*., 2011; Jideani and Vogt, 2016). In particular, pan-bread and hamburger buns are fast moving products characterized by thin crust and evenly distributed crumb, with short shelf-life and rapid staling depending on the baking and storage conditions contributing to economic losses (Soukoulis *et al.,* 2014). It is well known that ageing of crumb and paste products is due to the retrogradation of starch and the migration of moisture within the protein and starch molecules (Stanley P. Cauvain and Young, 2009; Davidou *et al*., 1996; Fadda *et al*., 2014; Gray and Bemiller, 2003; He and Hoseney, 1990). To prevent these changes bread is usually packaged

in polyethylene bags (PE) with ethanol spray (0.5-8.0 % by loaf weight), modified atmosphere packaging or by use of active packaging (Jideani and Vogt, 2016; Kotsianis *et al*., 2002). However, most practices utilize high barrier packaging to decrease food losses resulting in negative environmental impacts, estimated at 5-10% for a food item. Also, in the past decade consumers are demanding products with reduced preservatives and high quality (Licciardello *et al*., 2014). In this context edible coatings and films as primary packaging have potential to simplify and replace the traditional packaging partially or completely (Debeaufort *et al.,* 1998). The presence of active ingredients enhances the functionality by providing for additional benefits. Some researchers have identified the potential use of films and coatings to improve the shelf-life of bakery products by primarily preventing moisture migration and redistribution; microbial growth; enhance functionality by incorporating probiotics or other active components in the coatings (Altamirano-Fortoul *et al.,* 2012; Balaguer *et al.,* 2014; Bartolozzo *et al.,* 2016; Bravin *et al.,* 2006; Ferreira Saraiva *et al.,* 2016; Soukoulis *et al.,* 2017; Theóphilo Galvão *et al.,* 2018).

This renewed interest in edible coatings and films can be an alternative to increase the shelf stability of bread after opening of package and act as a carrier for functional components without compromising the primary texture characteristics of the product. The potential use of films and coatings depends on their physico-chemical characteristics similar to that of conventional petroleum based packaging materials. As well as the suitability of the biopolymer matrix as coating should be evaluated by monitoring the quality parameters of the bread. Also, it is important to consider the disintegration time of the edible films and coatings as they are expected to be longer than the product shelf-life. However, some aspects of these technologies relating to the application and subsequent effect on the product characteristics are not completely understood. To succeed the edible coatings should enhance the value of the product during storage and hence storage testing is of importance to justify the role of coatings on the product. To evaluate the effectiveness of edible coatings on the quality and shelf-life of bakery products, a simultaneous approach was considered, by characterizing the coatings and films; application methods and their effect on baked product quality by multi-analytical techniques. Accordingly the main objectives of this doctoral project were:

(i) Development and characterization of edible coatings and films for bakery applications.

(ii) Evaluation and optimization of edible coating drying conditions on bakery product (bread).

(iii) Application of edible coatings and its effect on bread quality characteristics.

Thesis Outline

To realise the stated objectives a series of research activities have been carried out during the doctoral period (November 2015 to October 2018) with specific aims and presented in three chapters as explained briefly in the schematic representation (Figure 1).

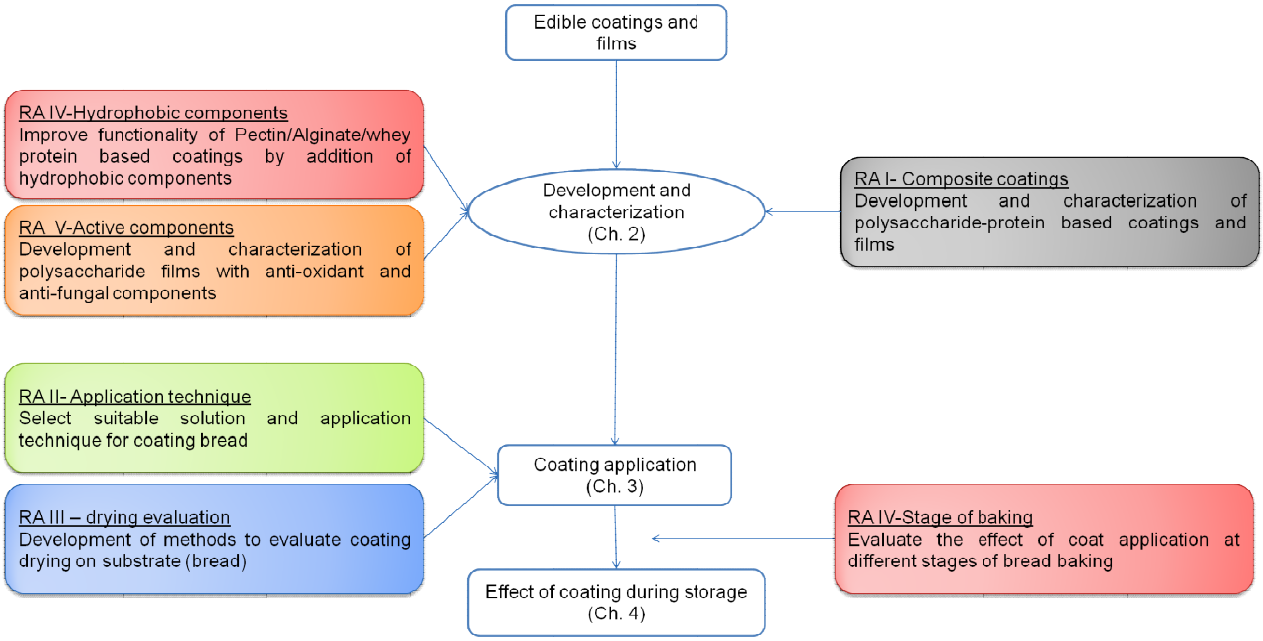

Figure 1. Schematic representation of research activities (RA) and thesis presentation.

The information presented in the chapters constituting the dissertation work is either published, submitted or is a manuscript under revision and mentioned for convenience as **Paper(s)** followed by Roman numeral **(I to VI)** unless mentioned otherwise.

2. Development and characterization of edible coatings and films

The terms edible coatings and films are sometimes used synonymously, but differ greatly in the preparation methods and characteristics. Coatings are thin layers of material applied directly on the surface of foods by dipping, spreading, spraying or other means (Falguera *et al*., 2011). The fundamental similarity is that these matrices should contain only food grade materials or in general components with GRAS (Generally Recommended as Safe) status. The use of coating to preserve citrus fruits dates back to 12th century, when fat was used as coating, also known as 'Larding' (Debeaufort *et al*., 1998; Han, 2013). The role of coatings has evolved from basic protection against moisture loss to acting as carriers for functional ingredients. Particularly, the use of edible coating as carriers of active substances has gained wide interest as it is a promising application of active packaging. According to Cuq *et al*., (1995) edible films and coatings by themselves can be considered as active packaging due to their biodegradability and edibility. In regard to their potential use, the development, application and characteristics of edible coatings and films for food products, in particular for fruits and vegetables- fresh, fresh-cut and minimally processed; meat and meat products; poultry and seafood; cheese; and cereal products has gained a wide interest and has been extensively reviewed (Cazón *et al*., 2017; Debeaufort *et al*., 1998; Dehghani *et al*., 2018; Han, 2013; Kurek *et al*., 2017; Otoni *et al*., 2017; Wu *et al*., 2002).

This chapter discusses about the development and characterization of edible coatings and films for potential application in bakery products. The research work presented within **paper I** was developed in co-operation with Prof. Valentina Siracusa (University of Catania) and that in **paper VI** with Prof. Paulo Josè Amaral do Sobral (Univerisity of Sao Paulo, Pirassununga, Brazil).

2.1. Film forming components

Edible films and coatings are processed using hydrophilic or hydrophobic components like polysaccharides, proteins and lipids from renewable sources (Galus and Kadzińska, 2015; Peressini *et al.,* 2003). All these components are usually derived from plant or animal sources like starch, cellulose, carrageen, pectin, alginate, chitosan, gums; gelatin, soy protein, wheat gluten, corn zein, whey protein being the most common industrial by-products, with some studies also focusing on non-commercial by-products like pea starch and protein, sesame seed cake, olive press cake, fish skin gelatin and similar hydrocolloids (Mellinas *et al*., 2016). The main film forming components considered in this doctoral study are components widely produced, extracts and by-products, namely, pectin, alginate, cassava starch, chitosan, whey protein concentrate and are described in this section.

2.1.1. Polysaccharides

Polysaccharides are abundantly available and act as sacrificial agents to prevent dehydration of foods. They are characterized as efficient gas, aroma and oil barriers with structural integrity and mechanical strength. The presence of hydroxyl groups and extensive Hydrogen bonding plays a significant role in the film structure and properties (Huber and Embuscado, 2009). Their wide availability, ease of preparation and known synergistic reactions with other polysaccharides and proteins makes them an ideal macro-molecule for biopolymer matrices.

Pectin can be defined as a complex polysaccharide mixture consisting of at least 65% of galaturonic acid. It is present in most plant tissues, with citrus and apple pomace being the largest sources of extraction industrially (Huber and Embuscado, 2009; Naqash *et al*., 2017). It is classified as a safe food ingredient with no assigned maximum daily intake (Baldino *et al*., 2018). It is composed of β-1,4-linked d-galacturonic acid residues interspersed with (1→2)-α-L-rhamnose residues and with fully or partially methyl esterified carboxyl groups (Sato *et al.,* 2008). The degree of methoxylation varies from <50% in low methoxyl pectin to >50% in high methoxyl pectins. Pectins are known to form strong films with good mechanical and gas barrier properties. However, pectin's alone are characterized by higher water vapor permeability and act as sacrificial agents to prevent dehydration. Although inherently they are not antimicrobial, they have the ability to act as carriers for anti-microbial components (Espitia *et al*., 2014; Naqash *et al*., 2017).

Alginate is a polysaccharide isolated from marine brown algae, widely used in the food industry as thickening agent, which also has film-forming properties (Galus and Lenart, 2013; Lee and Mooney, 2012; Silva *et al*., 2009). These structural polysaccharides are made up of alternating blocks of (1, 4)- linked mannuronic acid (M) and glucuronic acid (G) residues, extracted from brown algae (Lee and Mooney, 2012). These ionic linear co-polymers are usually used as their sodium salts of alginic acid and are also available as calcium and magnesium salts. Also, alginate is classified as GRAS material and is found to have good filmogenic capacities. Films from alginate or alginate-Calcium divalent are found to have water solubility, excellent mechanical strength, low permeability to oils and oxygen with ability to restrict moisture transfer (Tavassoli-Kafrani *et al*., 2016). One important characteristic of Pectin and alginate polyuronates is that these natural anionic polysaccharides are known to possess biopolymer compatibility and form synergistic gels and films with improved mechanical and barrier properties (Galus and Lenart, 2013; Silva *et al.,* 2009).

Starch is another extensively used polymer in coating production, mainly due to low cost, high availability and the relative ease of use. Among the various starches like rice starch, corn starch, potato, wheat, yam and tapioca/ cassava starch studied, **cassava starch** is considered as a promising polymer due to its wide availability, pricing and thermoplastic behavior with an estimated global production of 54% (Bangyekan *et al.,* 2006; Valencia-Sullca *et al.,* 2018a). It is a natural polymer, abundantly available with ease of casting as films due to its viscous and gelling properties. Also, they are known to have low water vapor permeability (Bergo *et al.,* 2008; Pelissari *et al.,* 2009). Despite the advantages, it is considered to have poor mechanical strength which is usually compensated by blending with plasticizers and other biopolymers that are either synthetic to produce bio-degradable films (Bonilla *et al.,* 2014; Valencia-Sullca *et al.,* 2018b) or other biopolymers to produce edible films (Bonilla and Sobral, 2017) with successful improvement in the overall properties of the films.

Chitosan $(C_6H_{11}O_4N)_n$, a linear polysaccharide, deacetylated derivative of chitin is the second most abundant polymer after cellulose with increasing applications as edible coatings and films due to its non-toxicity, biocompatibility, antimicrobial and antifungal properties (Bonilla and Sobral, 2016; Elsabee and Abdou, 2013; Hosseini *et al.,* 2009; Valencia-Sullca *et al.,* 2018a). Moreover it is a polysaccharide which is found to form synergistic gels with cassava starch resulting in improved film mechanical and barrier properties (Bangyekan *et al.,* 2006; Chillo *et al.,* 2008; Valencia-Sullca *et al.,* 2018b; Vásconez *et al.,* 2009). Studies show that these blends

are also suitable for industrial scale up by use of extrusion and thermal compression molding (Pelissari *et al*., 2009; Valencia-Sullca *et al*., 2018a; Valencia *et al*., 2018).

2.1.2. Proteins

Proteins, even though are not completely hydrophobic, can constitute an effective barrier for gas and water (Miller and Krochta, 1997). Their hydrophilic and barrier properties are determined by the quantity of plasticizer and moisture content Fang *et al*., (2002). These are among the commonly used film forming materials, with collagen and gelatin studied extensively followed by soy and whey protein isolates. The ease of modification of the secondary, tertiary and quaternary structures of protein makes them ideal film forming components.

Whey protein, apart from nutritive value, possesses excellent mechanical and barrier properties (Cecchini *et al.,* 2017; Ramos *et al.,* 2012). The tightly packed, ordered hydrogen bonds in proteins give them excellent oxygen barrier ability along with amino acid residues that inhibit enzymatic activity, and the low amounts of triglycerides contributing to water barrier activity (Banerjee and Chen, 1995; Galus and Kadzińska, 2016a; Osés *et al*., 2009; Ramos *et al*., 2012). Whey proteins are exploited in forms of isolates and concentrates with isolates being extensively used. However, **whey protein concentrates (WPC)** available as different standards such as 35, 50, 65 and 80% (w/w) protein, are low cost alternatives with potential for good film performance (Bahram *et al*., 2014; Pérez *et al*., 2016; Ramos *et al*., 2013). Moreover they can be used as functional components in context of the emerging evidence that the bioactive peptides produced upon digestion of proteins have antihypertensive and radical scavenging health benefits (Smithers, 2008).

2.1.3. Lipids

Lipids are hydrophobic compounds that reduce the water vapor permeability of coatings and films which are used mostly as adjunct components owing to their poor film forming properties. However, the incorporation of lipids into polysaccharide matrices emulsified with use of proteins or emulsifiers were observed to be suitable for forming hydrophobic coatings with good adhesion and film forming characteristics (Debeaufort and Voilley, 2009; Galus and Kadzińska, 2015; Huber and Embuscado, 2009). These components as emulsion particles or components of multi layer coatings increase the resistance to water penetration and thereby improve barrier effects (Perez-Gago and Krochta, 2002). Different lipids in form of oils, fats, waxes have been investigated for forming emulsion based matrices (Bravin *et al*., 2006; Cerqueira *et al*., 2012;

Gontard *et al*., 2007; Javanmard and Golestan, 2008). These components were observed to improve the water barrier properties of the films albeit with plasticized and weakened mechanical characteristics. Moreover, the vegetable oils like corn oil, olive oil and fats like butter, cocoa-butter are non-toxic and non volatile with saturated fats exhibiting lower moisture transfer than unsaturated ones (Cerqueira *et al*., 2012; Galus and Kadzińska, 2015; Ma *et al*., 2012).

2.1.4. Additives

2.1.4.1. Plasticizers and Surfactants

Plasticizers are low molecular weight, non- volatile agents that improve flexibility and extensibility by reducing the intermolecular forces. These agents increase the molecular mobility and are observed to increase diffusion coefficients and film flexibility (Bergo and Sobral, 2007; Chillo *et al.,* 2008; Liu *et al.,* 2013; Pérez *et al.,* 2016; Vieira *et al.,* 2011). The level of plasticizer depends on the desired properties of the film, as they cause significant reductions in the barrier properties and cohesion. Several food grade substances like polyols (glycerol, sorbitol), sugars (glucose, fructose) and some lipids (mono glycerides, phospholipids) were investigated for their compatibility and efficiency. Among them polyols, mono- and oligo-saccharides have been systematically investigated and used for biopolymer plasticization (Bergo and Sobral, 2007; Pérez *et al*., 2016; Vieira *et al*., 2011).

Surfactants are surface active components incorporated into the formulations to reduce the surface tension, improve the wettability and adhesion of the coating onto substrates. Usually, these compounds are amphiphilic in nature with both polar lipophilic end and non polar hydrophilic end. The balance between these two ends; known as hydrophilic-lipophilic balance (HLB) governs the final coating and film properties, and usually improve the barrier properties. However, it is important to note that above the threshold limit the addition of surfactant does not change the surface tension even though it is a linear function of concentration (Rodríguez *et al*., 2006). Various anionic and non-ionic surfactants like tween (20, 80), Lecithin, Span were used for different hydrocolloid matrices (Alexandre *et al*., 2016; Bravin *et al*., 2004; Rodríguez *et al*., 2006). However, tween®20 (polyoxyethylene -20- sorbitan monolaurate) is a non-ionic surfactant, with a HLB index of 16.0, was found to be synergistic with glycerol for plasticizing the films (Bravin *et al.,* 2004).

2.1.4.2. Functional components

Incorporation of active components renders edible coatings and films with unique functions like antioxidant, antimicrobial capacity and to act as carriers for probiotics, prebiotics, nutrients and flavours, colours. These additives can be defined as substances intended to be used directly or indirectly, as a component or otherwise which affects the food characteristics. In general, the substance and also the intended use should be classified under GRAS exemption. In particular, antioxidant and anti-microbial agents received high attention as promising technologies to extend product shelf-life (Balaguer *et al*., 2013; Campos *et al*., 2011; Sánchez-González *et al*., 2011; Zhao *et al*., 2018). As from literature, a wide range of additives of both natural and synthetic origin have been studied extensively for incorporation in traditional and edible packaging (Bonilla *et al*., 2012; Campos *et al*., 2011; Kechichian *et al*., 2010). In the recent past, the use of natural antioxidants and anti-microbials as coarse or fine emulsions, as nano-emulsions; as dispersions and encapsulates have been considered advantageous due to the raising consumer concerns over synthetic additives (Bonilla *et al.,* 2017, 2013; Campos *et al.,* 2011; Ramos *et al.,* 2012; Soares *et al.,* 2009). Also, most active compounds are compatible with the sensory characteristics of different products, and are particularly used for application in fruits and vegetables.

As in **paper I** pectin from citrus peel with methoxylation degree > 75%, sodium alginate and whey protein concentrate of 80% w/w at a maximum concentration of 3% (w/w) and in **paper VI** a blend of cassava starch and chitosan with deacetylation degree > 75% at 2:1 ratio were used with an aim to produce and characterize coating solutions and edible films. Glycerol (99% pure) was used at 33% and 25% w/w on dry basis of the polymers for different studies, following the preliminary trials. In particular, it was observed that films with glycerol at lower levels cracked and at higher levels were sticky to handle. As to the advantages stated and the synergistic effects of surfactants to reduce surface tension, improve wettability and thereby adhesion; tween®20 was used as surfactant as reported in **paper I.** All the solutions were prepared as dispersions or emulsions as they have higher commercial appeal in terms of ease of preparation and post application stability. The solutions were added with corn oil and butter in the study presented in **paper V(b)**. The presence of lipid component was expected to improve the water barrier properties and simultaneously increase heterogeneity within the matrix. However, the presence of both protein and polysaccharide is an advantage, as the lipid droplets are embedded in the heterogeneous matrix of the different hydrocolloids. Furthermore, to obtain films with active

functions, ethanolic extracts of Pitanga leaves and commercial Natamycin as described in **paper VI** were used as anti-oxidant and anti-fungal agents with Cassava starch/chitosan matrix.

2.2. Film forming conditions

The film forming components with or without the additives are required to be homogenously dispersed to produce coating solutions and subsequently stand alone films. These biopolymers interact by intermolecular, electrostatic, hydrophobic or ionic interactions that are strongly dependent on the film forming mechanisms used like heating, pH modification, salt addition, enzyme treatment and the solvents (Kester and Fennema, 1986). The conditions are in general standardized and controlled as they alter the mass transfer kinetics and reactions between components. Films are formed either by dry casting or wet casting methods (Gontard *et al.,* 2007; Peressini *et al.,* 2003). The dry process uses extrusion techniques based on the thermoplastic properties of the polymers. The wet process uses solvents for dispersion of film forming materials followed by solvent removal step. These solvents are restricted to water, ethanol or diluted acetic or lactic acid owing to the edibility (Campos *et al*., 2011). This technique is preferred methodology and is used in this doctoral study to form edible pre-formed films and to apply coatings directly onto the food surfaces.

Formation of whey protein films generally involves heat denaturation in aqueous solutions at 75-100°C during 20 min (Khwaldia *et al*., 2004; Perez-Gago and Krochta, 2002). Whey protein is comprised of several individual proteins, majorly with beta-lactoglobulins, alpha-lactalbumins, serum albumins and immune-globulins with the net negative charge evenly distributed over the protein chain. Thermal degradation denatures whey protein and results in more cohesive and stronger films than native proteins due to the exposure of free thiol groups of ß-lactoglobulin (Pérez-Gago *et al*., 1999). Heating modifies the three dimensional structure of proteins (i.e. above 65 ºC, the β-Lg globular structure opens) thus exposing internal sulfhydryl (–SH) and hydrophobic groups that promote intermolecular S-S bonding and hydrophobic interactions during drying; which are partially responsible for film structure (Perez-Gago and Krochta, 2002). Also, non-covalent aggregation due to the hydrophobic and ionic interactions between the exposed thiol groups increases as the pH decreases towards the iso-electric point. Furthermore, when heated at temperatures greater than 65°C as in **paper I**, intermolecular disulfide bond exchange takes place resulting in polymerization. Whereas, for pectin and alginate different authors suggested methodologies with pre-dissolution and heating (Coughlan *et al*., 2004; Galus and Lenart, 2013; Silva *et al*., 2009). However, with respect to the dry blending procedure used

an optimum of 75°C was used so as to dissolve the components as reported in **table 1 (paper I)** with heating and continuous stirring to 75°C (±0.1°C) within first 15 min and holding for 30 min to facilitate complete dissolution of the components.

In case of polysaccharides like starch they are to be gelatinized either by cold gelatinization by addition of alkaline substances or by thermal gelatinization. In general, authors observed the use of cold gelatinization results in weaker films in terms of mechanical and barrier properties compared to that of heat treated films (Jiménez *et al*., 2012; Romero-Bastida *et al*., 2005). Starch is heated in excess of water so as to disrupt the crystalline structure and cause interaction of amylose and amylo-pectins resulting in solubilized starch (Jiménez *et al*., 2012). However, heating in temperatures between 65-100°C depending on the source of starch causes irreversible gelatinization and thereby a homogenous solution. Different authors reported various conditions of heating for cassava starch (Chillo *et al.,* 2008; Parra *et al.,* 2004; Pelissari *et al.,* 2009). As for chitosan, the addition of excess water and heating is not adequate to render film forming characteristics as chitosan loses its cationic nature above pH ~6.5 and requires acidic conditions for dissolution and forming a gelatinous mass. In general acetic acid, a mono-carboxylic acid is used as a proton donor in a number of studies. Researchers have also explored other mono-, di- and tri-carboxylic acids like formic acid, citric acid, lactic acid (Park *et al*., 2002). The prime purpose of acidic conditions is to form polycationic polymer by the protonation of the amino groups of the polymer. As described in **paper VI**, cassava starch was gelatinized at 90°C for 30 min and chitosan was dissolved overnight in 1% v/v acetic acid solution at 40°C with continuous stirring.

Furthermore, the film forming solutions can be formed by dry-blending as described in **paper I** or by blending of solutions at different ratios as in **paper VI** (Bonilla *et al.,* 2018; Coughlan *et al.,* 2004). To prevent the interruption in gelatinization process for cassava starch in **paper VI** additives were added towards the end of the process. Once the compounds are gelatinized and added with the plasticizers, surfactants or other additives, homogenization is carried out to obtain a stable dispersion or emulsion by use of a rotor stator homogenizer (Cecchini *et al*., 2017; Galus and Kadzińska, 2016b, 2016a; Vásconez *et al*., 2009). Subsequently, the conditions of homogenization like the speed, time and number of cycles have been varied according to the polymer matrix under investigation in this dissertation. However, a recurring problem post homogenization in most film forming solutions (FFS) is the foam, particularly in presence of gums and proteins. This foam or air bubbles are removed either by use of vacuum or by ultra-

sound. It is of interest to note that the use of vacuum is sometimes linked to the formation of micro-pores in the dried films.

As mentioned previously, a common practice in film formation is to cast the film forming solutions (FFS) over polystyrene or Teflon petri-plates or plates to obtain the films. The casted FFS are then left to dry at a wide range of time-temperature conditions as reported in literature to remove the solvent (Alcantara *et al.,* 1998; Bergo *et al.,* 2008; Galus and Lenart, 2013; Guillard *et al.,* 2004; Xiao *et al.,* 2014). Controlling the drying process is crucial, since faster drying produces stiffer, less flexible films, with a less extensive effect upon film tensile strength and elongation. This is attributed to changes in film morphology, with subsequent thinner film drying achieved at a higher rate (Guilbert *et al.,* 1996; Alcantara *et al.,* 1998; Guillard *et al.,* 2004). In this context a relative humidity of 50-55% and a temperature of 25°C for 18-24h was used to dry P/A/WP films **(paper I)** and a temperature of 30°C for 16-20h was used to dry CS/CH films **(paper VI).**

Consequently, for the food coating process the liquid is deposited onto the substrate directly by dipping, spreading or spraying as singular or multiple layers. Spreading is frequently used technique in coating of bakery products due to the low mechanical stresses involved in comparison to spraying. This consideration is vital as most edible coatings are shear thinning in nature and the viscosity perceived depends on the shear rates when being applied to the substrate. The coating was applied directly onto the substrate and subjected to the film forming conditions as discussed in detail in **chapter 3**.

2.3. Coating characteristics

The design of the process operations, like dipping, spreading, spraying or casting necessitates information on the characteristics of the dispersions or solutions, particularly the rheological characteristics (Chen *et al*., 2009). These properties influence the film formation characteristics and the homogeneity post application, i.e., the presence or absence of defects. The defects are important for coating integrity and functionality as well as the appearance of the product (Peressini *et al*., 2003; Zhong *et al*., 2014). Moreover, fluid viscosity directly influences the ability of the solution to adhere onto the substrates along with their wetting properties, impact behavior, mechanisms of application and associated phase changes (Andrade *et al*., 2015; Peressini *et al*., 2003). Therefore, it is necessary to evaluate the relationship between the dispersion composition and the basic rheology, like flow behavior of the solutions.

In general most coating systems exhibit pseudoplastic, viscoelastic and thixotropic behaviors and as a consequence are highly influenced by the type and magnitude of operating shears. The flow properties are important for the coating quality, as the coating levels on the surface during drying. For this, it is necessary for the coating to have an apparent viscosity (η_0) adequate to prevent the gravity effects and allow the capillary-driven leveling. Accordingly, very high viscosities result in problems with dispersing onto surfaces and elimination of air bubbles causing discontinuities in the films or coatings post drying. It is suggested that a viscosity lower than 700 mPa.s is desirable to appropriately cast films (Cuq *et al*., 1995; Peressini *et al*., 2003). Usually when two or more biopolymers are mixed, the behavior of the individual components is affected by the interactions. Furthermore, it influences the solutions ability to form a continuous network.

Several mathematical models are available for modeling of fluid rheological behaviour and for non-Newtonian fluids. In particular, Herschel-Bulkley model, Ostwald de Waale model and Bingham model (Cevoli *et al*., 2013; Kennedy *et al*., 2015; Kontogiorgos *et al*., 2012; Meza *et al*., 2015; Mezger, 2006; Silva-Weiss *et al*., 2013) are frequently utilized. In this **Ph. D study**, the rheological data were fitted to Carreau and Ostwald de Waale models to elaborate selected rheological parameters pertaining to the flow behavior and fluid consistency. The decrease in values of flow behavior index indicates increase in pseudo-plasticity of the fluids, and consequently increase in consistency coefficient indicates higher apparent viscosity at a given shear-rate. Higher η_0 values indicate strong interactions between the bio-polymers, and subsequently register higher flow rates and lower relaxation times, indicating higher shear-stress requirement for structural breakdown and lower time for structural recovery respectively.

As in **paper I** and **VI**, the rheology of the solutions was carried out using controlled stress rheometer with increasing shear rates. Time and temperature effects were not considered in these works. As in **table 3** (**paper I)** and **table 2** (**paper VI)**, the viscosity decreased with increasing shear rate, indicating shear thinning behavior with characteristic flow index less than 1. The blends containing pectin and alginate exhibited higher apparent viscosity in accordance with their gelling and thickening behavior. However, the incorporation of whey protein concentrate in the pectin-alginate blend decreased the viscosity of the solution due to associative interactions between the polysaccharides and proteins (Zhu *et al*., 2019). As for CS/CH solutions, the incorporation of active ingredients like Pitanga extract and Natamycin did not significantly affect the flow behavior of cassava-chitosan blend solutions. A good agreement between the

experimental data and the models was obtained as can be observed with $R^2 > 0.75$ for the solutions studied. This characterization holds importance in adjusting the coating formulation according to the surface characteristics of the targeted food product for adhesion and leveling of the coating (Falguera *et al.,* 2011; Ma *et al.,* 2014).

2.4. Edible film characterization

The potential use of films depend on their intrinsic physico-chemical and functional properties that are influenced by the formulation (film forming bio-polymer, solvent and additives); film forming techniques (solution formation, drying and conditioning) (Gontard *et al.,* 2007; Guillard *et al.,* 2004; Peressini *et al.,* 2003; Wu *et al.,* 2002).

2.4.1. Optical and surface characteristics

The optical properties like colour and transparency are essential sensory aspects for edible films and coatings for consumer acceptance, as they are generally expected to be colourless similar to that of polymeric packaging materials or as close to the food colour onto which the coating will be applied (Galus and Kadzińska, 2016a; Galus and Lenart, 2013). The commonly used methodologies to measure colour are Hunter Lab, CIE L*a*b*, CIE LCH, CIE xyz that measure colours in three basic colours (red, green and blue) and their mixtures. For food products apart from the basic scale the differences in the colour perception can be expressed as total colour difference, yellowness index, whiteness index and browning index based on the final product characteristics as a numeric value indicating the magnitude of difference (Galus and Kadzińska, 2016b; O'Connor *et al*., 2018; Saberi *et al*., 2016). For both the edible films based on P/A/WP and CS/CH the optical properties were observed to be dependent on the ratio of components and the presence or absence of additives**.** Figure 2 depicts a representative comparison of parameters evaluated for colour in **paper I.** The edible films were characterized on both support and air sides for luminosity (fig. 2a), whiteness index (fig. 2b), total colour difference (fig. 2c) and yellowness index (fig. 2d) to evaluate the component interactions. The interaction of whey protein with pectin was found to significantly increase the yellowness of the films. This interpretation is useful to understand the application of film and its subsequent influence on product visual characteristics.

Moreover, other characteristics like gloss and transparency are evaluated as an estimate to structural heterogeneity. This is usually carried out using UV-VIS spectroscopy or gloss meters and expressed as transparency, opacity or gloss. These values are of importance to the product

appearance and were found in studies to be affected by drying conditions, relative humidity and storage time apart from composition (Monedero *et al*., 2009; Ozdemir and Floros, 2008; Villalobos-Carvajal *et al*., 2009).

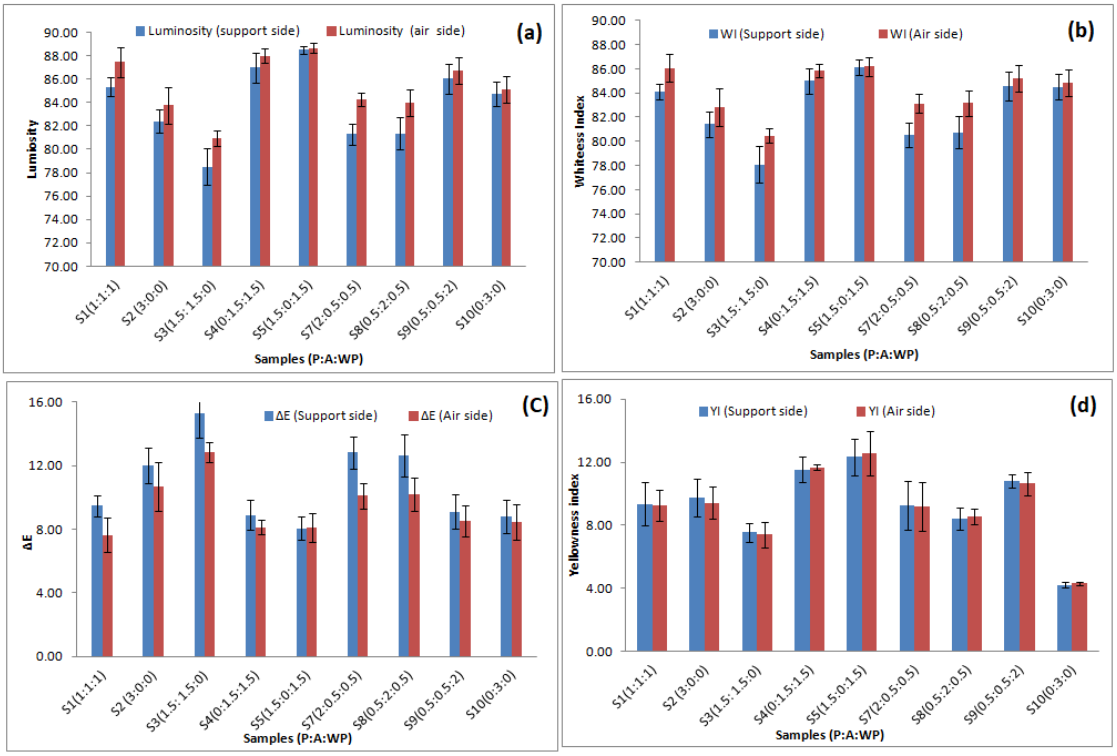

Figure 2 (a-d). Representative graphs for Luminosity (a); Whiteness index (b); Total colour difference (c) and yellowness index (d) of P/A/WP films.

Also, the film microstructure and roughness of the surface influences these properties. The effect of surface roughness on the film opacity has been observed in **paper VI** and UV-VIS spectra were useful to estimate the barrier capacity of the films, which is important to prevent light induced oxidation in foods (Bonilla and Sobral, 2016)**.**

2.4.2. Mechanical characteristics

Biopolymer films are expected to maintain integrity and withstand the handling stresses, particularly when used as wraps and films rather than coating. Also, they should have a longer durability than the food they are protecting. These properties depend on the type of biopolymers, solvent type, additives (plasticizers, surfactants, lipids), functional components (antioxidants, antimicrobials), process (temperature, time, shear) and film or coat formation (spreading, spraying, rate of drying) parameters and techniques (Bergo and Sobral, 2007; Maftoonazad *et al.,* 2007; Mathew *et al.,* 2006; Perez-gago and Krochta, 2001; Pérez *et al.,* 2016). Furthermore, it is important to control the film thickness and speed of testing uniformly for the sample set being

tested. These abilities are in general evaluated using different mechanical tests, with the common tests being ASTM D882-02 method (ASTM, 2002b) tensile testing for thin films. Other tests include puncture tests (Bergo and Sobral, 2007), dynamic mechanical testing with the most common parameters assessed being tensile strength (MPa), elongation at break (%), elastic modulus, percent deformation (%) and puncture strength (N). Tensile strength is the maximum load exerted on and sustained by the specimen; elongation at break is the maximum change in length before breaking and elastic modulus is the ratio of stress and strain in the linear part of stress-strain curve, under given test conditions. Puncture strength is the maximum force exerted per unit area of the film and the percent deformation is the maximum elongation of the film under given puncture settings.

In this **Ph. D study** it was observed in both P/A/WP and CS/CH films, the differences observed in the mechanical strength was due to the composition and also to the slight differences in moisture content arising thereby. The amount of plasticizer is kept constant as the increase in plasticizer content leads to increased flexibility in films. However, the addition of additives decreased greatly the mechanical strength of the film, rendering them more brittle and rigid as depicted in figure 3, with differences in the deformation at strain greater than 10%.

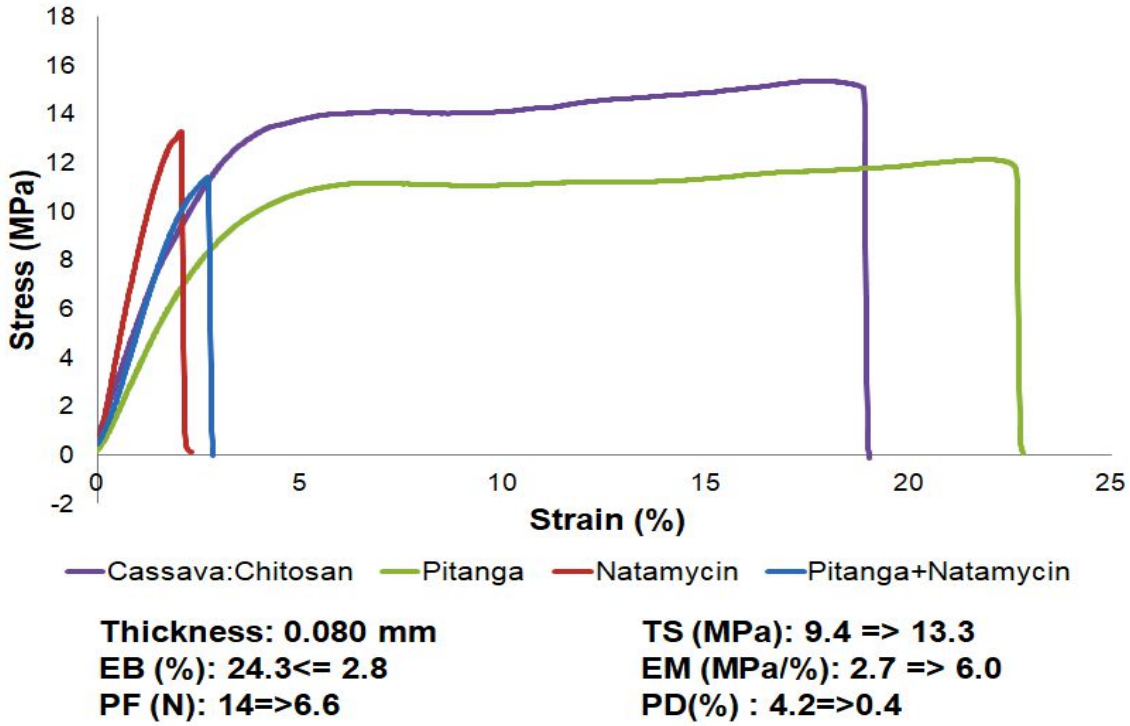

Figure 3. Representative mechanical behavior of CS/CH films with and without pitanga extract and natamycin (paper VI).

2.4.3. Barrier properties

Barrier properties are important functional parameters and are determined to evaluate the ability of films to protect the food product from detrimental effects of primarily gases like O_2, CO_2 and moisture transfer. Permeability is defined as the rate of transmission of water vapor or gas through unit area of flat material, due to a unit pressure gradient across the film of unit thickness under specified temperature and relative humidity. The basic mechanism of this transfer is active diffusion and is mathematically described by Fick's first law. The barrier properties that are usually measured are water vapor according to ASTM E96-95 (ASTM, 1995) expressed as WVP (g mm cm^{-2} h^{-1} kPa^{-1}) and gas barrier properties according to ASTM 1434 (standard test method for determining gas permeability characteristics of plastic film and sheeting, 2009) expressed as (cm^3/m^2 d bar).

The assessment of moisture barrier capacity is widely done based on the water vapour permeability and related physical properties like moisture content, solubility (Bourlieu *et al.,* 2009). This property can be used as a comprehensive indicator as it is dependent on both the compatibility between water molecule and barrier material as well as the diffusion rate influenced by the morphology of the films. Hence it necessary to explicitly mention the testing conditions as the specific rate is inherent property of the barrier material at a given test condition (Gennadios *et al.,* 1994; Sobral *et al.,* 2001). Another important factor is the thickness, as the barrier effect decreases above or below a critical thickness owing to the swelling, sorption phenomena and the inherent film defects, particularly for hydrophilic films (Guillard *et al.,* 2004, Debeaufort 2000). Also, the degree of crystallinity as can be calculated from thermal and diffraction experiments of the material is an important parameter affecting the spatial distribution of water during transport. Since, most bio-polymer films are amorphous to semi-crystalline in nature, the major transport phenomenon is considered to take place through the amorphous zones. However, this property measured on self supporting films is not directly transferrable to that of coatings on food as additional parameters of food surface heterogeneity, adhesion quality and drying rate on composite food systems are to be considered (Guillard *et al.,* 2003, 2006). In this **Ph. D study** this affinity to water was measured in terms of water vapour permeability with gravimetric procedure detailed by ASTM E96 (cup assembly used in figure 4) and also data of moisture content and water solubility to understand the probable barrier effect exhibited by the films.

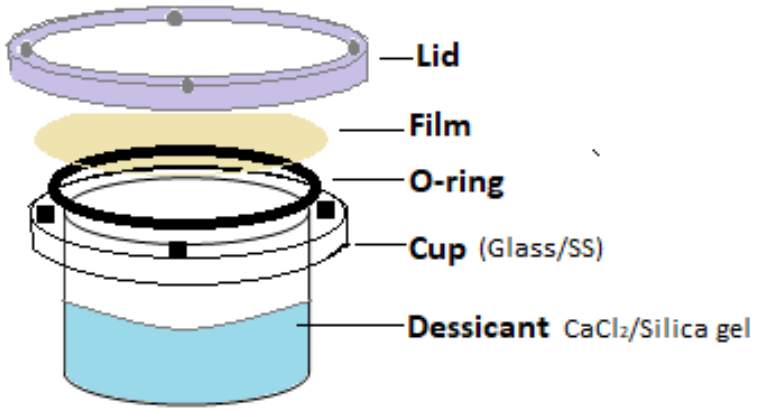

Figure 4. Schematic of cup assembly for water vapor permeability measurement.

Gas barrier properties are of great interest, particularly for applications intended to protect products from oxidation and for modified atmosphere effect on fresh produce (Baldwin *et al*., 2011; Huber and Embuscado, 2009). Thus, oxygen and carbon dioxide gas permeabilities are frequently estimated by semi to fully automatic permeability gauges. Similar to the water vapor permeability the transfer of gas or aromas, in general take place due to the combined effects of diffusion, solubility and permeability. These factors are affected by the chemical nature, structure, cohesive energies, cross linking and arrangement of the polymer chains, crystallinity and the amorphous fraction of the films (Miller and Krochta, 1997b; Siracusa *et al*., 2018). The gas barrier properties of P/A/WP films were evaluated as presented in **paper I** by ASTM 1434 (standard test method for determining gas permeability characteristics of plastic film and sheeting, 2009), DIN 53536 (gas permeability determination), ISO 15105-1 (Plastics film and sheeting determination of gas transmission rate - Part I: Differential pressure methods, 2007) procedures. The oxygen permeability of whey protein-based films are lower than most synthetic films and consequently it was observed that blending of films lowered the gas transmission rates.

2.4.4. Structural characteristics

The interactions between components can be evaluated by techniques like diffraction, spectroscopic and thermal analyses. These techniques are used to decipher the nature of the polymer, helpful in understanding the mechanical and barrier strength of the films. Fourier transform infrared (FTIR) spectroscopy and X-ray diffraction (XRD) techniques are used in this **Ph.D study** to elaborate the structure and state of the bio-polymer components in the films. FTIR spectroscopy is a non-invasive and rapid technique used to understand the molecular and conformational transitions in macromolecules. Attenuated total reflection FTIR facilitates for superior spectral resolution, detection sensitivity and lower noise. Also, it is potentially applied

in material identification and quantification of chemical composition, particularly in composite biopolymer systems. As reported in **paper I** and **VI,** FTIR spectra were analyzed to identify the functional groups and potential interactions among components. Figure 5(a) presents the characteristic bands observed in the pectin, alginate and whey protein films as singular, binary and tertiary composite films. As for **paper VI,** the pure components of pitanga and natamycin were also characterized as depicted in figure 5(b). The characteristic wave numbers and the corresponding functional groups of interest are presented in detail in respective papers.

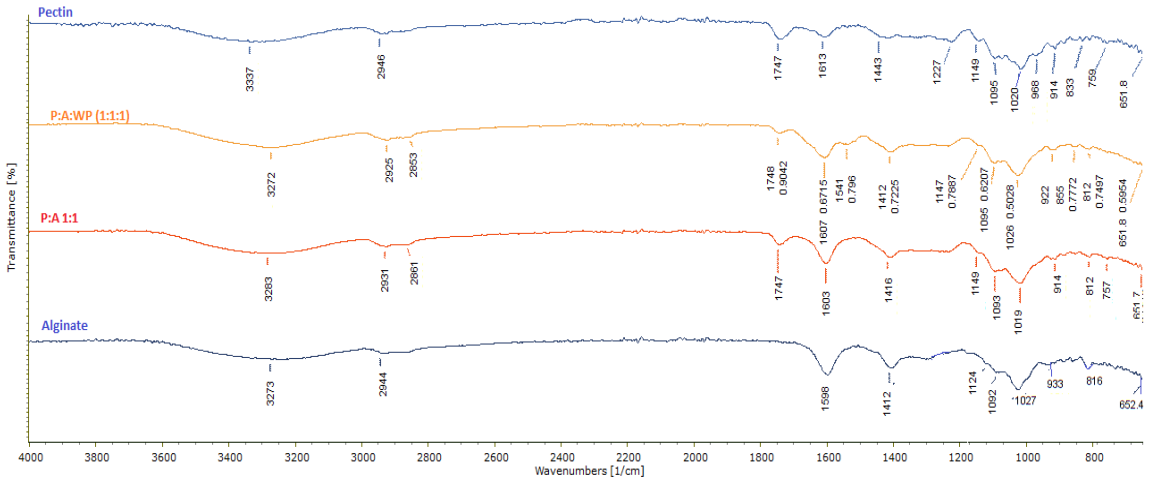

Figure 5(a). Representative FTIR spectral patterns of pectin (P), alginate (A), pectin/alginate (P/A) and pectin/alginate/whey protein (P/A/WP) films.

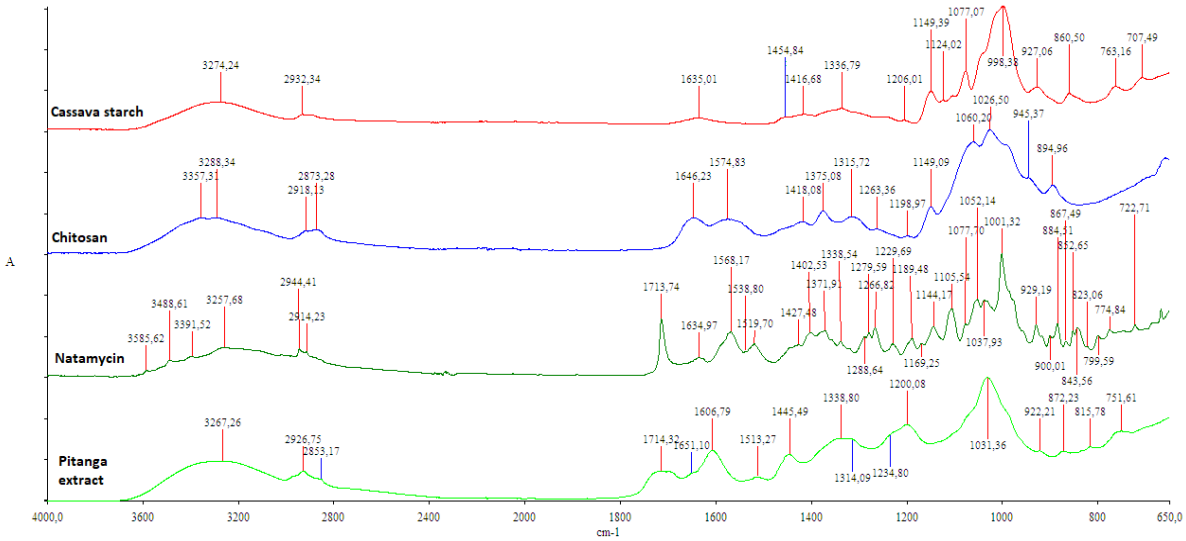

Figure 5(b). Representative FTIR spectral patterns of pure components of cassava starch, chitosan, natamycin and pitanga extract.

Similarly, X-ray diffraction (XRD) patterns are fingerprints of the specific chemical and atomic arrangement within the biopolymer mixtures. The diffraction pattern enables the separation of crystal and amorphous forms. However these patterns cannot be used to estimate the relative amounts of components based on the intensity of the diffraction peaks. The intensities vary based on the efficiency of the molecule to diffract x-rays. Some characteristic peaks are shifted to different positions or completely disappear due to rearrangement of the polymer network as a result of polymer-polymer, polymer-plasticizer, and polymer-additive interactions (Bergo and Sobral, 2007; Bergo *et al*., 2008; Dang and Yoksan, 2015; Thakur *et al*., 2016). As expected the crystalline fractions immiscible were reflected in the XRD patterns of Cassava/Chitosan films as explained in **paper VI**.

2.4.5. Thermal characteristics

Thermal behavior of polymers is another indicator of the miscibility and compatibility of the polymers. The common techniques include DSC (differential scanning calorimetry), TG (thermogravimetric analysis), DTG (differential thermal analysis) and DMA (dynamic mechanical analysis) (Bonilla *et al.,* 2017). The compatibility of polymers in reflected in the thermal events that shift in comparison to pure polymers. Glass transition temperature (Tg) is known to be associated to the structural transition from amorphous to rubbery state, indicative of the film strength. The glass transition Tg temperature reflects the polymer branching/ cross-linking and the intermolecular interactions. Similarly, enthalpy and melting transitions reflect the strength of the polymer interactions. Also, thermogravimetric analysis data relating to degradation onset and peak temperatures reflect thermal stability and strength of the films. Moreover, the phases of weight change allow the researcher to understand the steps in dissociation and degradation of the polymers (**paper I** and **VI**) which can be used to moderate the film forming and coat drying conditions. The typical DSC and TGA curve obtained for pectin, alginate and whey protein concentrate films along with some parameters considered are presented in figure 6(a-b).

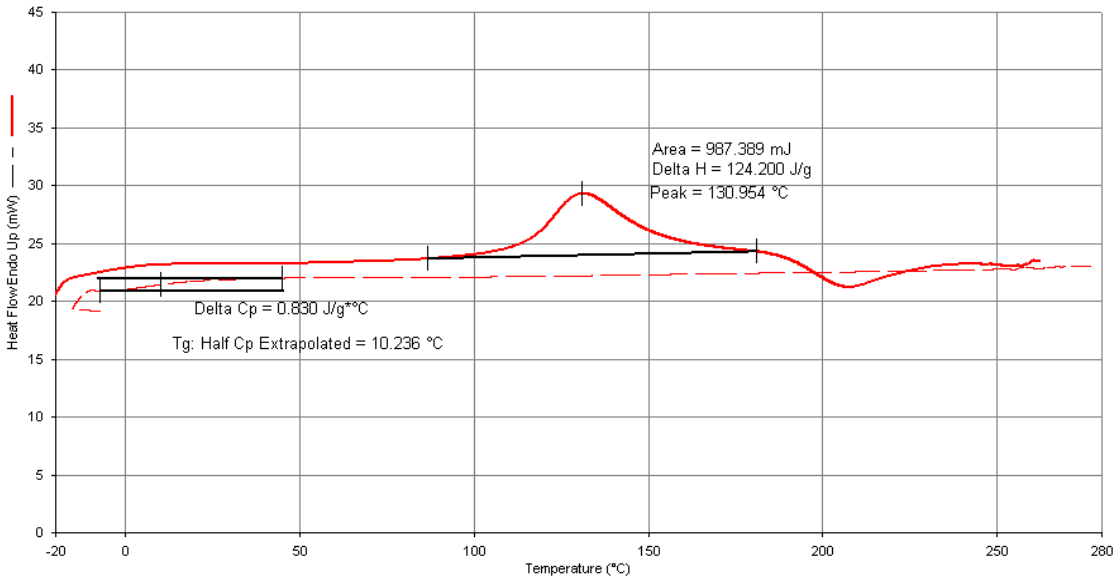

Figure 6(a). DSC thermograms representative of the first scan and second scan of P/A/WP films of P/A/WP (1:1:1).

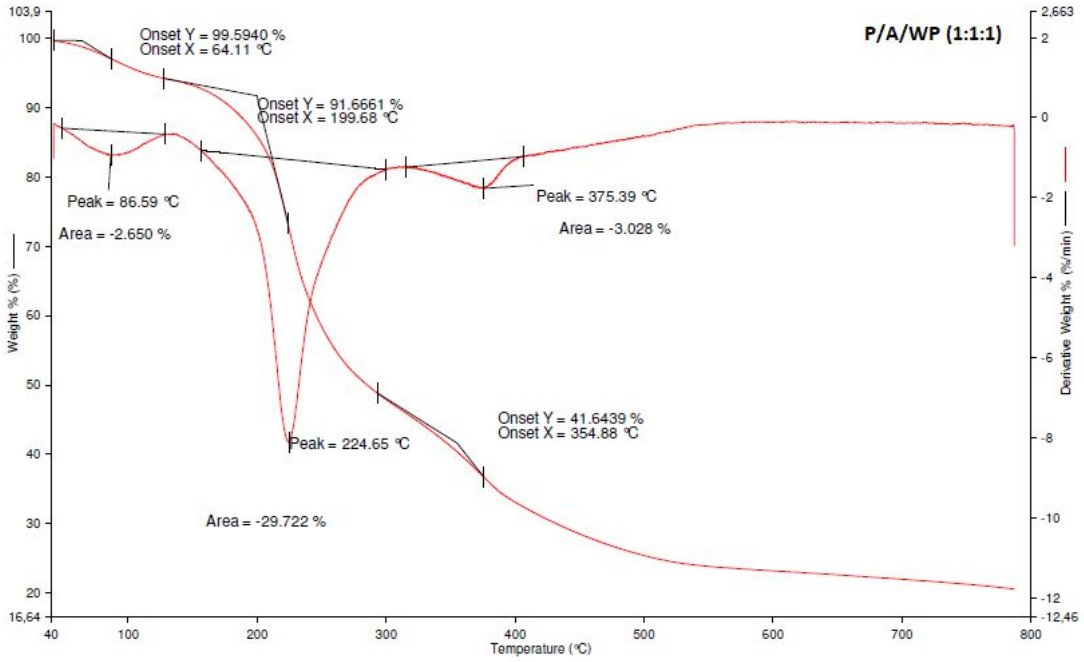

Figure 6(b). Representative TGA spectra and the subsequent first derivative of P/A/WP film.

3. Coating application and evaluation of its drying on bakery product - Bread

The functionality of coating depends not only on the composition, presence of additives but also on the method of application, homogeneity and coat formation conditions. Different techniques like dipping, spreading, spraying and electro-spraying have been described in literature (Bartolozzo *et al.*, 2016; Khan *et al.*, 2013; Zhong *et al*., 2014). Each technique encompasses advantages and disadvantages owing to technical or economical feasibility and functionality. Bravin *et al.,* (2006) used spraying to coat crackers with methyl cellulose based edible coating in their study. Theóphilo Galvão *et al.,* (2018) in their study on application of tomato powder enriched coating on frozen dough used dipping technique. Other studies by Bartolozzo *et al.,* (2016); Ferreira Saraiva *et al.,* (2016); Soukoulis *et al.,* (2014) chose spreading to apply singular or multiple layers of coating, owing to its feasibility and availability.

These biopolymer matrices are usually applied in their liquid form and entail a drying step for the formation of an individual layer on the product surfaces. Hence, drying forms the preliminary step and is important to be controlled as it affects the eventual water activity. Different researchers utilized a range of temperatures and drying conditions like 60°C for 10 min and 180°C for 2 min on probiotic breads (Soukoulis *et al.,* 2014); 180°C for 5 min on mini-panettone (Ferreira Saraiva *et al.,* 2016) and 40°C on muffin (Bartolozzo *et al.,* 2016). Drying temperatures are found to have significant effect on the crust and crumb moisture contents. Thus, it is necessary to understand the drying process and estimate drying time for each product. The kinetics of drying when edible coating is applied onto bread can be evaluated by weight loss and moisture loss during drying for a given temperature and humidity, similar to that of fruit and vegetable matrices (Di Scala and Crapiste, 2008; Planinić *et al.,* 2005).

This chapter focuses on different applicable techniques and methodologies that can be utilized to monitor and evaluate the drying of coating on the surface of the chosen product, bread. The work as presented within **paper III** and **IV** was developed in cooperation with Prof. Angelo Fabbri and Dr. Chiara Cevoli (DiSTAL, University of Bologna).

3.1. NIR Spectroscopy

Near infrared spectroscopy is a non-destructive and rapid technique being used increasingly for food quality evaluation and online process monitoring. The basic advantage is that, it is a non destructive technique with higher precision for larger samples (Huang *et al*., 2008). Several studies utilized NIR spectroscopy in the determination of moisture, protein and other constituents in cereal grains and their products for which the weak absorption of water molecules facilitates also for the analysis of high moisture foods (Büning-Pfaue, 2003; Huang *et al*., 2008). In particular, it is efficient and rapid compared to traditional techniques like oven drying or vacuum drying for estimating moisture content of foods (He *et al*., 2013). Also NIR is successfully applied for moisture analysis of intact products as well as their evolution during drying and storage, particularly, for factors related to staling in products like cereals, bread, flat breads, biscuits and cakes (Cevoli *et al*., 2015; Osborne, 1996; Sørensen, 2009; Xie *et al*., 2003).

These advantages of minimal sample preparation and rapid assessment make NIR a suitable choice to monitor the surface moisture of coated breads during drying. In particular, the wavelength region between 1100nm and 2300nm are utilized to reflect the fundamental vibrations of overtones and combinational bands (Büning-Pfaue, 2003; Nallan Chakravartula *et al*., 2019). As mentioned, film formation process is complex involving the solvent-polymer and polymer–polymer interactions affected continuously by the removal of water. However, when the coating is on a substrate, it also involves in the interaction of food surface, polymer and solvent. The water component instantaneously increases upon spreading on the substrate, making the substrate high in moisture. During drying this moisture evaporates leaving the protein fraction on the surface which can be observed in the spectral band at 1500nm concerning the first overtone.

Further, the spectral treatment with exploratory analysis as explained in **section 2.5** of **paper III** provides information on the sample discrimination during the drying time as well as the surface of the bread. The statistical analysis and the criteria selected are critical as they determine the acceptability of the predictions. Principal Component Analysis (PCA) is largely used to reduce the spectral data to independent variables which express the variations among the samples. The spectral data extracted and the corresponding moisture content values measured are used to establish quantitative relationship between the predictive and experimental values by PLSR modelling (He *et al.,* 2013). To establish this quantitative relation selected wavelengths between

1100nm and 2400nm corresponding to the moisture and protein content in the coated bread surfaces was utilized as depicted in **figure 7** adapted from **paper III**.

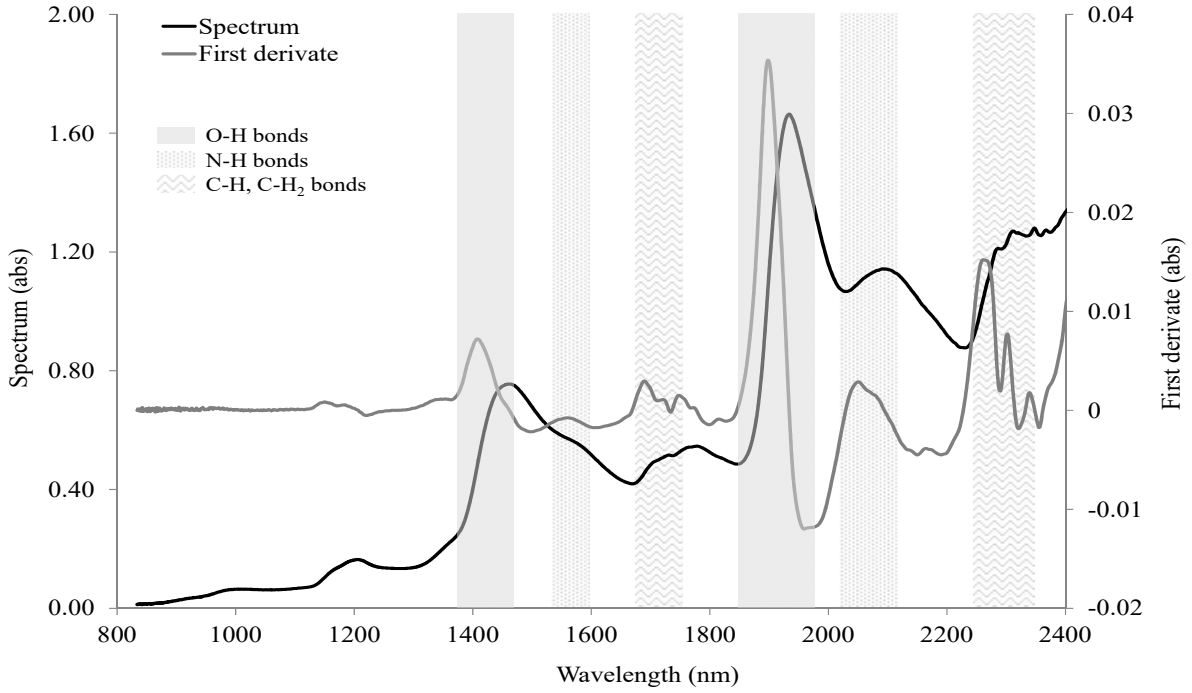

Figure 7. Representative NIR spectrum of coated bread and the relative first derivate (Paper III).

The NIR spectral band was characterized in this doctoral study by use of published infrared regions as reported by Cevoli *et al.,* (2015) on piadina (a thin Italian flatbread, typically prepared in Romagna region); Giangiacomo, (2006) on sucrose-water interactions; Osborne *et al.,* (1984) and Suzuki *et al.,* (1986) on wheat and rye-bread. As in the initial stages, corresponding to high water activity i.e., > 80% water in the coating, the spectral absorption up to 1400nm can be considered due to the first and second overtones of water. Also bands in region of 1900-1950nm are linked to the water content that can be quantified. These bands are affected by the process of drying as the hydrogen bonding and degree of hydration are altered, and are reflected in the spectra owing to its detection sensitivity (Özdemir *et al.,* 2018; Sinelli *et al.,* 2011).

As presented in **Paper III,** the extracted spectral data with the spectral regions associated to the water and protein bands were found to be aligned with their respective drying times. Similar trend was observed for both the temperatures of 25°C and 60°C and also the number of layers of coating. Also, a clear discrimination of the surfaces of the bread buns was observed, along the

drying time. However, a drawback observed was that the time ranges were estimated rather than precise timing.

To overcome this regression modelling with partial least squares (PLS) was utilized to define the optimal drying moment based on the percent moisture. The results in reference to the regression models were observed to be satisfactory, with reliable prediction of coat drying at a given time. However, it is important to note that these models hold good for the tested time/temperature conditions.

3.2. Numerical modelling

Drying is a multifaceted process involving different inter-phases between the dryer and the product with simultaneous transfer of heat and mass (Defraeye, 2014). A suitable drying procedure considers the product shape, dimension, coating formulation, processing factors (temperature, time) and coating properties (solvent, density, viscosity). Numerical simulation and modeling can be a potential alternative to experimental procedures as described in previous **section (3.1)** as the product drying dynamics can be provided in time and space continuum. A numerical model essentially consists of a set of differential equations that are solved numerically on the geometrical design for a given physical problem (Fabbri *et al.,* 2012). The main advantages of this technique are limited experimentation thereby reducing inherent biological variability, computational power for various geometrical designs and high spatial and temporal resolution for moisture transport predictions (Cevoli *et al.,* 2018; Defraeye, 2014; Fabbri *et al.,* 2012).

Finite elements method (FEM) is an established engineering tool known for simulating heat and mass transfer in foods. The advantage of FEM is its ability to represent different structures and orientations that influence the thermo-physical properties of the food in consideration (Martins, 2006). The main physical phenomenon during drying is diffusion of the solvent in the coating matrix and its evaporation. As coating formulation and processing factors determine the functionality of film, it is necessary to establish relation between the drying conditions. Moreover, the coating forms a thin film on the substrate for which parameters like thickness, solvent concentration, positioning can be controlled effectively.

As defined in **paper III**, the optimal drying time can be considered as time required for removing the solvent present in coating without provoking internal dehydration. This involves in main processes of transfer of heat from the drying air to the liquid layer, diffusion of the liquid

through the solution and subsequent mass flux due to evaporation of water. The air-coating interface is considered as the main region of evaporation. For this, the product was categorized into different zones based on the product and coating position. In this context, one dimensional and 2D axisymmetric finite element models were developed to describe the heat and moisture transfer from the surface as well as the internal regions of the product.

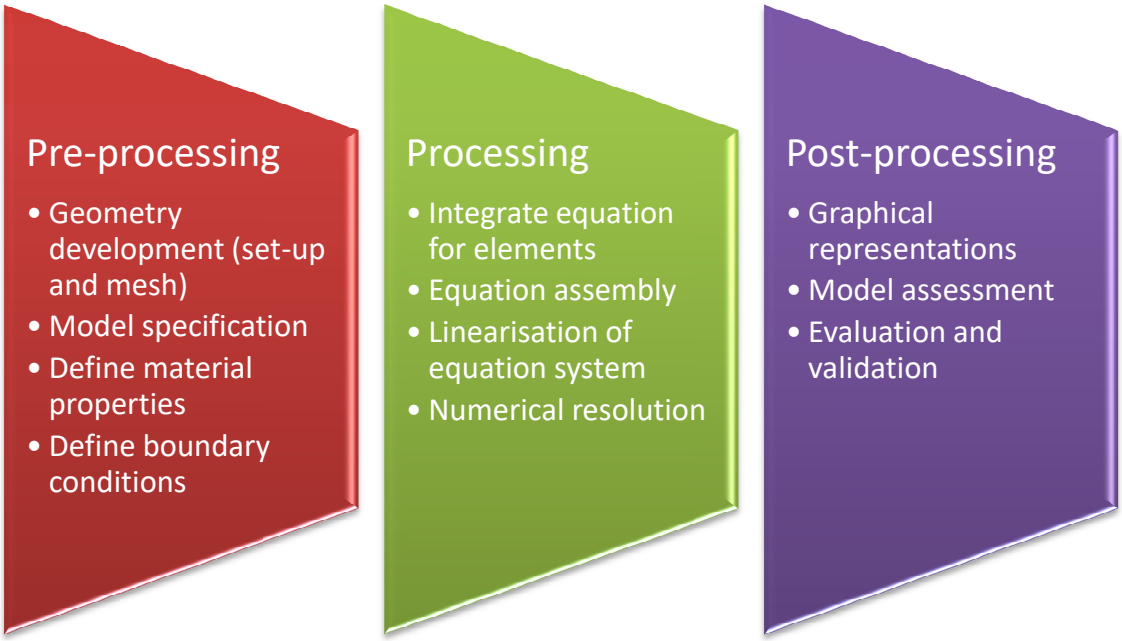

Figure 8. Steps in numerical model construction (adapted from *Fabbri et al., 2012*).

The 1D model was characterized by edge elements distributed symmetrically from the geometrical centre. Subsequently, the 2D model with triangular mesh and quadrilateral boundaries was generated to evaluate the effect of temperature distribution on mass flux. The main steps in the development of the geometry and numerical model are depicted in figure 8. The FEM was developed and validated as in **paper IV** to describe the drying of a Pectin-Alginate-Whey Protein concentrate edible coating on a bun bread, varying several process conditions (temperature, time and heating properties), coating properties (moisture content, thickness, position) and product characteristics. The observed optimal drying time values and moisture contents appeared to be in good agreement with the calculated values.

4. Coating application and evaluation of its effect on bakery product storage quality - Bread

Bread is a staple product and is benefitted from extended shelf-life, as it continuously undergoes changes after production. The major cause of deterioration is moisture migration, staling and mold growth that affect the product singularly or collectively as a result of storage conditions. Shelf-life in general is extended by adjusting the equilibrium relative humidity (ERH) and adding preservatives. Other techniques include use of ethanol spray, packaging with Modified atmosphere, and use of ultraviolet or Infra-red irradiation prior to packaging (Licciardello *et al*., 2017; Smith *et al*., 2004; Upasen and Wattanachai, 2018). As such the use of edible coatings and films can be a potential alternative to extend the texture without '*overpackaging'* and eventually reduce the packaging environmental impact.

This chapter describes the works presented on the potential use of edible coatings to retain moisture and texture during the storage of bread. Different aspects such as effect during short storage, application at different stages of baking, type of coatings are discussed as presented in **paper II, paper V(a), V(b)**. The work as presented within **paper II, V(b)** was developed in cooperation with Prof. Santina Romani (DiSTAL, University of Bologna) and that in **V(a)** was carried out in co-operation with Prof. Angelo Fabbri and Dr. Chiara Cevoli (DiSTAL, University of Bologna).

4.1. Effect on dehydration

Shelf-life extension by reducing moisture migration in heterogeneous food is a prime objective of food industries. The migration of moisture occurs when there is a difference in water activity among components which acts as a driving force. In general, water diffuses from '*wet component'* to *'dry component'* as defined by Guillard *et al*., (2003), say for example from cream or savoury filling to the pastry or cake. This results in relative firming of the water losing component and sogginess in the moisture retaining component. Furthermore, the increase in moisture of the components may promote microbial growth. However the balance of moisture is more complex for products like bread and cakes, as the moisture is both redistributed and lost during storage (Gray and Bemiller, 2003; He and Hoseney, 1990). The presence of free water is an important aspect of bread as it directly affects the freshness. The loss or gain of water both within and out of the product matrix results in the acceptance or rejection by consumer depending on the type of bread. Some of the parameters routinely evaluated for the presence of water are product weight, moisture content and the ratio of free to bound water.

Bread is an intermediate moisture product with moisture content ranging from 38-44% depending on type of bread (Stanley P Cauvain and Young, 2009). The moisture redistribution from crumb to crust initiates during post bake cooling step and continues in the storage time, leading to the formation of a leathery crust and dry crumb. Finally, the level of water loss or retention is also related to the physico-chemical changes in product during storage referred to as staling (Fadda *et al*., 2014; He and Hoseney, 1990; Kulp *et al*., 1981; Rayas-Duarte and Mulvaney, 2012). Weight loss, caused by moisture movement from the product to the environment is affected by the product, type of packaging material and usually increases along the storage time. Water within the product acts as a lubricating agent during the mastication and greatly affects the perception of freshness or staleness.

Traditional polymers are efficient to minimise this transfer of water, however, the use of edible barriers can also help prevent this migration, without need for changes in formulation or addition of preservatives with potential to reduce overall packaging impact. As stated in previous sections, the mechanical and barrier property of these coatings and films is to be evaluated (chapter 2). Ideally, they should be non-toxic, maintain quality characteristics and adhere to the surface of the food after application and during drying (chapter 3) with reliable barrier effects. Also, employing water insoluble or poorly soluble components in edible coating formulation reduces their water vapour permeability (WVP) and inhibits weight loss.

As the key parameter for packaging selection for bread is moisture migration, knowledge of moisture loss or gain was considered important criteria to evaluate the effectiveness of edible coating. Accordingly, the weight loss was measured with a semi-analytical balance and the water activity was measured by an aqua-lab. As for dehydration behaviour of bread during short storage, the weight and moisture loss were modelled with semi-empirical Peleg's model as detailed in **paper II**. However, for moisture content methods like hot air oven drying (AOAC 2002, **paper V(a)/(b)**) and near infrared spectroscopy (NIR, **paper V(a)),** were used. Baeva and Panchev (2005) and Panchev *et al.,* (2005) in their study on sucrose free dietetic sponge cake have extensively evaluated the moisture retaining effects of edible coatings and films. Also, as water plays a major role in the product texture from oven to the point of consumption, the management of water within the product matrix can help retain the textural characteristics.

In this **Ph. D study**, it was observed that the edible coating significantly ($p<0.05$) increased the crust moisture content irrespective of stage of application by 3-6%. However, the crumb moisture content ranged between 40-43% in comparison to the 40-41% for the control samples with differences between the stages of application. Application of coating before baking as in **paper V(b)** had noticeably higher values due to the restriction of moisture migration during baking from the bread surface. As for the storage period, the coated samples registered 1-2% lower weight loss than the control samples irrespective of the number of layers. Subsequently, the moisture content was 2-4% higher in the coated samples depending on the number of layers. However, the moisture content decreased along the storage time and a marginal retention effect was observed both in case of unpackaged or packaged storage.

4.2. Effect on textural quality

Texture is set of physical characteristics related to the structure of the food which can be measured by objective instrumental or subjective sensory analyses or a combination thereof. Most bakery products, particularly bread proceed to deteriorative changes after baking and packaging until the point of consumption. These deteriorative physico-chemical changes that occur during the storage time are termed as staling (Gray and Bemiller, 2003; He and Hoseney, 1990). Staling is defined as a process other than microbial spoilage by which consumer acceptance decreases due to change in the crumb characteristics. As known, bread is elastic foam, with cross-linked gluten and leached amylose forming the continuous matrix and the gelatinized starch forming the entrapped, discontinuous matrix. During ageing crumb firmness

increases and crust crispiness decreases, leading to poor quality and loss of marketability (Licciardello *et al*., 2017, 2014; Vodovotz *et al*., 2018).

Staling is a time dependent and multifaceted process resulting in physical, chemical and sensory changes with most studies relating to the effect of crumb firming. Starch is one of the main components involved in this process with amylose and amylopectin segments that recrystallize. Furthermore, gluten crosslink's with a part of starch and water that acts as a plasticizer migrates from amorphous to crystalline regions resulting in further hardness. The initial stages of staling were linked to starch retrogradation and long term staling is linked to loss of moisture from gluten, which serves as moisture reservoir to buffer changes in starch hydration. However, the complete mechanism of staling is not fully understood, with the loss of moisture evidenced to accelerate these changes (Fadda *et al.,* 2014; Gray and Bemiller, 2003; Ribotta and Le Bail, 2007).

In brief, crumb can be described as a gel penetrated and separated by aqueous mobile phase, which facilitates its displacement from crumb to crust. This results in drying of crumb alveoli, causing crumb firmness and subsequent hydration of crust regions, although the overall moisture is maintained by packaging. In case of unwrapped bread, this moisture retained in the crust evaporates into the surrounding atmosphere to attain equilibrium. The loss of oven-fresh nature of bread can be encompassed as the changes depicted in figure 9.

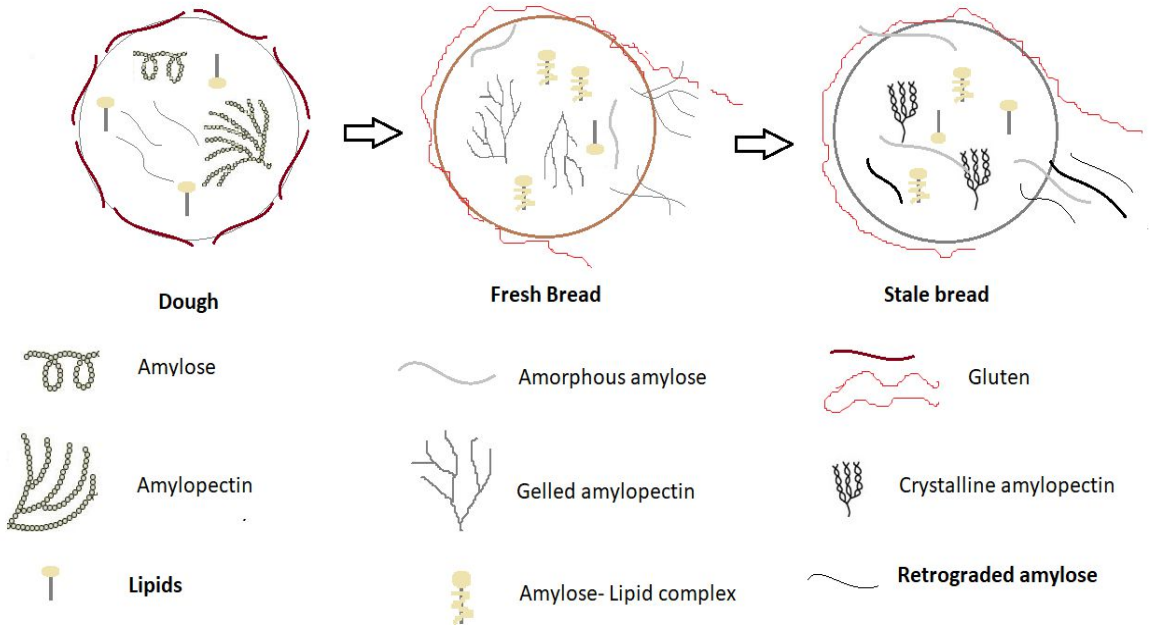

Figure 9. Mechanism of bread staling (adapted from *Kulp and Ponte, 1981*).

Techniques to measure texture changes

Bread staling comprises of changes in physico-chemical and organoleptic characteristics which can be evaluated instrumentally at macroscopic, microscopic and molecular levels (Vodovotz *et al*., 2018). As the events of staling occur concurrently, it is useful to have multi-analytical approach for better understanding. The macroscopic tests include subjective sensory tests and objective analyses, of which textural properties received wide attention. The main textural attribute routinely evaluated is firmness which directly affects the consumer's decision to procure the product. It can be defined as the force required to compress crumb to a pre-defined percent of deformation and is strongly correlated to sensory hardness. However it is important to note that there is no universally accepted methodology for complete measurement of staling in similar terms as that of consumer.

A wide range of instruments like Instron Universal Testing Machine (IUTM), Baker Compressimeter (BC), Texture Analyzer (TA) and Precision Penetrometer (PP) are available for measuring this parameter. Instrumental Texture Profile Analysis (TPA) has evolved as a preferable method, as it measures not only firmness, but also other attributes like springiness, resilience and chewiness that imitate parameters of sensory evaluation (Breene, 1975; Conte *et al*., 2018; Gámbaro *et al*., 2002; Jekle *et al*., 2018). As described in **paper V(a)** and **V(b)** texture profile analysis (TPA) has been used to evaluate the crumb parameters and penetration tests have been used to evaluate the crust parameters, particularly, the hardness (figure 10 (a-b)). Apart from direct measurement by texture analyzer, other microscopic and molecular techniques are widely employed for both physical and chemical information. Among them microscopy (light and polarized, electron, confocal laser) techniques are used to study bread components and their structural resolution with techniques like Magnetic resonance imaging (MRI) that provide three-dimensional representation of the molecules. As for the structural properties differential scanning calorimetry (DSC) is used to monitor physico-chemical changes of material as function of temperature. Dynamic mechanical analysis (DMA) is a thermo-mechanical technique useful to monitor the segmental mobility of the polymers by transition either from crystal-to-melt or glassy-to-rubbery regions as a function of temperature. Moreover, to understand the molecular changes taking place during staling, spectroscopic techniques such as Infrared spectroscopy (Fourier transformed, near infrared, mid infrared) and Nuclear magnetic resonance (NMR) are finding increased application (Baeva and Panchev, 2005; Piccinini *et al*., 2012; Ribotta and Le Bail, 2007; Ringsted *et al*., 2017; Schiraldi *et al*., 1996; Vodovotz *et al*., 2018).

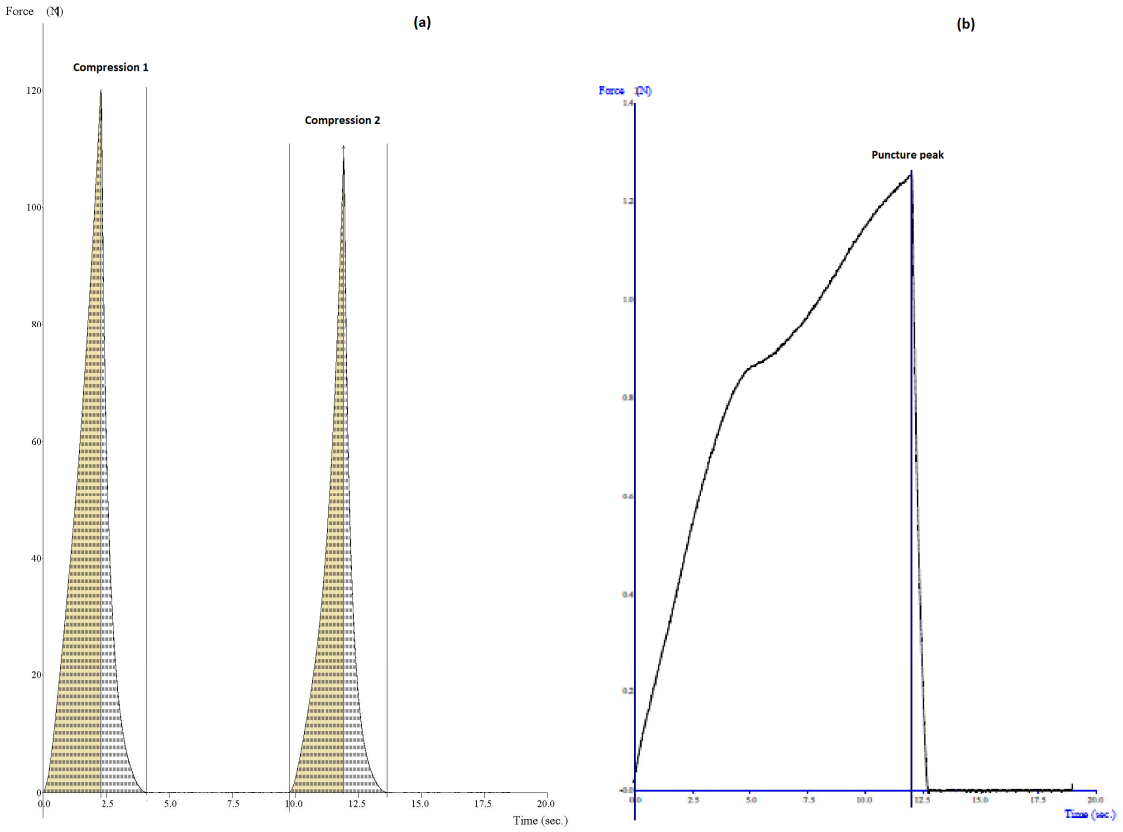

Figure 10. Representative graphs for (a) texture profile analysis depicting both compressions for crumb characteristics (b) Puncture test for crust characteristics.

Specifically, near infrared spectroscopy (NIR) either singularly or in combination with hyper-spectral imaging is a non-destructive, physical method with high precision that can be effectively used for online quality monitoring (Huang *et al*., 2008). Also, it is cost effective in comparison to traditional methods with information on both physical and chemical aspects of staling related to the hydrogen bonding. In relation to staling, the spectral wavelengths relating to the amylo-pectin retrogradation was observed to be the main factor for differentiating the staling. Cocchi *et al*., (2005) found that the first PC was influenced by the typical bond vibrations in stored breads analyzed with combination of FT-MIR and PCA. The absorption bands of water molecules in particular reflect the evolution in starch and protein along the storage time, and have found application in monitoring products like bread, flat breads, cakes and biscuits (Al-Mahsaneh *et al*., 2018; Cevoli *et al*., 2015; Cocchi *et al*., 2005; Osborne, 1996; Ringsted *et al*., 2017). In context of non-destructive analysis, NIR technique was used to simultaneously evaluate the textural changes as described in **paper V(a).**

In this **Ph. D study**, the texture of the product as affected by the loss of moisture was hypothesized to a certain extent to be mitigated by use of edible coatings. Some researchers have found that the use of edible coatings delayed crumb firming kinetics and textural changes in bread and cake type products (Baeva and Panchev, 2005; Bartolozzo *et al.,* 2016; Ferreira Saraiva *et al.,* 2016). This is due to the presence of poorly soluble or water insoluble components in the coating formulation which can reduce the textural changes (Vargas *et al.,* 2008).

As in **Paper V(a)** TPA and NIR were used to evaluate the texture parameters of the coated whole buns to simulate the eating character over a short storage period. From the use of TPA, the attributes of hardness, chewiness and cohesivity were calculated. Further, hardness and chewiness were considered to be modeled with PLS by analyzing the NIR spectra of the bread top surface. The typical spectrum along with its first derivative utilized for this purpose is reported in **figure 7 (section 3.1)**. It was observed that 2L of coating provided the best model to predict the hardness evolution during storage. Considering the overall results, coated samples exhibited retaining effect even though the initial hardness was higher due to the presence of coating. The percentage increase in hardness was higher in the control samples (Control: 271.8%) than those of the coated samples (1L: 126.5% and 2L: 231.2%). These limited results were similar to those observed by Soukoulis *et al.,* (2014) and Altamirano-Fortoul *et al.,* (2012) in their studies on probiotic coatings on pan breads and partially baked pan breads as evaluated by thermal analysis.

Following these results, the coatings were added with hydrophobic components and applied at various stages of baking as presented in **paper V(b).** Furthermore in this study to understand the effect of coating on crust, the textural parameters of crust and crumb were evaluated separately by puncture tests and texture profile analysis respectively as explained in **section 2.8 (paper V(b))**. During storage, the presence of coating was found to reduce the crust firming rate indicative of slower crust softening, although there was not a substantial reduction in crumb firming rate. The lower firming rates observed in treated samples were generally preceded by higher moisture content in the crust or crumb, as also observed in case of glazed breads by Chin *et al.,* (2011). Also, the application of coating before baking, at par-baked stage or after baking significantly affected the initial firmness of bread along with the type of coatings with or without hydrophobic component. Indeed both the hydrophilic and hydrophobic coatings used in this study, were observed to extend moisture and texture retaining effect on the bread during storage albeit with few significant reductions in firming rates.

4.3. Effect on microbial quality

Bread and most bread products are susceptible to rapid microbial deterioration due to microbial growth with fungi being the most common spoilage organisms. This is a significant economic problem for the storage that depends on the temperature, pH, water activity and the condensation in packages (Smith *et al*., 2004). The presence of spores and bread being high water activity, nutrient rich product leads to mould growth within days in preservative free breads. At a water activity greater than 0.60, the large visible blemishes due to fungi indicate the end of shelf-life. This expression of mould depends on the initial level of contamination, water activity of the product and the storage conditions. However, a contrast to be noted for bread and bread type products is that the loss of water slightly increases the mould free shelf-life (MFSL). Apart from visible contamination, fungi also results in off-flavours and mycotoxins with imminent health effects.

This contamination of bread products is linked to the post baking handling, usually by *Rhizophus*, *Aspergillus* and *Pencilium* genera of fungi. This confirms that use of preservatives in bread formulations is not suggestible as most of this is surface growth. As well, the consumers demand for preservative free foods with more bio-degradable packaging makes preservative use an unacceptable method. As well for the frequently used alternative of alcohol spraying (0.2-8.0%) prior to sealing of the packages requires label declaration. Alternatively, incorporation of antimicrobials in packaging materials, with low diffusion rate and high surface retention is found to be an effective method to extend the MFSL of baked goods (Jideani and Vogt, 2016). Also recent studies show that incorporation of the antimicrobial compounds in edible coatings and films improved the bread and cake type product keeping quality (Altan *et al*., 2018; Balaguer *et al*., 2014; Kechichian *et al*., 2010; Lopes *et al*., 2014). As observed in **paper VI**, the coatings with active components were found effective against *A. flavus* and *A. parasiticus*, as evaluated by disc diffusion assay on agar plates.

5. Conclusions

The objectives of the work described in this dissertation were to develop and characterize edible coatings and films in order to better understand the compositional effects and secondly, apply coatings to evaluate their behavior and effectiveness on chosen substrate, bread. In this regard, the various research activities as discussed resulted in interesting findings that can be underlined as:

- The physico-mechanical characterization of edible coatings and films is influenced by the formulation and processing conditions. In particular, the rheological and thermal characterization provided insights to select coatings suitable for a specific application technique and drying steps, respectively. Also, the mechanical and barrier characterization may contribute to the understanding of eventual coating efficacy although the values obtained on stand-alone films are not directly transferable to the coating-product interface.
- An important aspect required for the scale-up is efficient drying of the coating on the substrate, without compromising the quality and safety of the product. In this regard, methodologies developed with near infrared spectroscopy and numerical model were found optimal to evaluate coat drying on the product surface. These results are helpful to apply coatings without compromising coating functionality and product integrity.
- With regard to the application of edible coatings on bread, as an innovative packaging enhancement, different methodologies were adapted for commercial and in-house baked breads. The edible coatings, particularly with addition of hydrocolloid components, were found to mitigate the moisture loss and retain texture during storage. Also, the coatings were found to not alter the mechanical characteristics of fresh bread, and can be a potential option to develop functional coated breads.

The results of this doctoral study indicate that a multi-analytical evaluation of the coating, film and bread characteristics simultaneously can contribute to better design of edible packaging for complex products like bread. However, further research is needed to design an industrial and fully functional edible packaging system which is efficient, safe and sustainable.

References

Al-Mahsaneh, M., Aljarrah, M., Rababah, T., Alu'datt, M., 2018. Using MR-FTIR and Texture Profile to Track the Effect of Storage Time and Temperature on Pita Bread Staling. J. Food Qual. 2018, 1–9. https://doi.org/10.1155/2018/8252570

Alcantara, C.R., Rumsey, T.R., Krochta, J.M., 1998. Drying rate effect on the properties of whey protein films. J. Food Process Eng. 21, 387–405. https://doi.org/10.1111/j.1745-4530.1998.tb00460.x

Alexandre, E.M.C., Lourenço, R.V., Bittante, A.M.Q.B., Moraes, I.C.F., Sobral, P.J. do A., 2016. Gelatin-based films reinforced with montmorillonite and activated with nanoemulsion of ginger essential oil for food packaging applications. Food Packag. Shelf Life 10, 87–96. https://doi.org/10.1016/j.fpsl.2016.10.004

Altamirano-Fortoul, R., Moreno-Terrazas, R., Quezada-Gallo, A., Rosell, C.M., 2012. Viability of some probiotic coatings in bread and its effect on the crust mechanical properties. Food Hydrocoll. 29, 166–174. https://doi.org/https://doi.org/10.1016/j.foodhyd.2012.02.015

Altan, A., Aytac, Z., Uyar, T., 2018. Carvacrol loaded electrospun fibrous films from zein and poly(lactic acid) for active food packaging. Food Hydrocoll. 81, 48–59. https://doi.org/https://doi.org/10.1016/j.foodhyd.2018.02.028

Andrade, R., Skurtys, O., Osorio, F., 2015. Development of a new method to predict the maximum spread factor for shear thinning drops. J. Food Eng. 157, 70–76. https://doi.org/10.1016/j.jfoodeng.2015.02.017

Baeva, M., Panchev, I., 2005. Investigation of the retaining effect of a pectin-containing edible film upon the crumb ageing of dietetic sucrose-free sponge cake. Food Chem. 92, 343–348. https://doi.org/10.1016/j.foodchem.2004.03.060

Bahram, S., Rezaei, M., Soltani, M., Kamali, A., Ojagh, S.M., Abdollahi, M., 2014. Whey Protein Concentrate Edible Film Activated with Cinnamon Essential Oil. J. Food Process. Preserv. 38, 1251–1258. https://doi.org/10.1111/jfpp.12086

Balaguer, M.P., Fajardo, P., Gartner, H., Gomez-Estaca, J., Gavara, R., Almenar, E., Hernandez-Munoz, P., 2014. Functional properties and antifungal activity of films based on gliadins containing cinnamaldehyde and natamycin. Int. J. Food Microbiol. 173, 62–71. https://doi.org/https://doi.org/10.1016/j.ijfoodmicro.2013.12.013

Balaguer, M.P., Lopez-Carballo, G., Catala, R., Gavara, R., Hernandez-Munoz, P., 2013. Antifungal properties of gliadin films incorporating cinnamaldehyde and application in active food packaging of bread and cheese spread foodstuffs. Int. J. Food Microbiol. 166, 369–77. https://doi.org/10.1016/j.ijfoodmicro.2013.08.012

Baldino, N., Mileti, O., Lupi, F.R., Gabriele, D., 2018. Rheological surface properties of commercial citrus pectins at different pH and concentration. LWT 93, 124–130.

https://doi.org/10.1016/j.lwt.2018.03.037

Baldwin, E.A., Hagenmaier, R., Bai, J., 2011. Edible Coatings and Films to Improve Food Quality, Second Edition. CRC Press.

Banerjee, R., Chen, H., 1995. Functional Properties of Edible Films Using Whey Protein Concentrate. J. Dairy Sci. 78, 1673–1683. https://doi.org/10.3168/jds.S0022-0302(95)76792-3

Bangyekan, C., Aht-Ong, D., Srikulkit, K., 2006. Preparation and properties evaluation of chitosan-coated cassava starch films. Carbohydr. Polym. 63, 61–71. https://doi.org/10.1016/j.carbpol.2005.07.032

Bartolozzo, J., Borneo, R., Aguirre, A., 2016. Effect of triticale-based edible coating on muffin quality maintenance during storage. J. Food Meas. Charact. 10, 88–95. https://doi.org/10.1007/s11694-015-9280-1

Bergo, P., Sobral, P.J.A., 2007. Effects of plasticizer on physical properties of pigskin gelatin films. Food Hydrocoll. 21, 1285–1289. https://doi.org/10.1016/j.foodhyd.2006.09.014

Bergo, P.V.A., Carvalho, R.A., Sobral, P.J.A., Dos Santos, R.M.C., Da Silva, F.B.R., Prison, J.M., Solorza-Feria, J., Habitante, A.M.Q.B., 2008. Physical properties of edible films based on cassava starch as affected by the plasticizer concentration. Packag. Technol. Sci. 21, 85–89. https://doi.org/10.1002/pts.781

Bonilla, J., Atarés, L., Vargas, M., Chiralt, A., 2012. Edible films and coatings to prevent the detrimental effect of oxygen on food quality: Possibilities and limitations. J. Food Eng. 110, 208–213. https://doi.org/10.1016/J.JFOODENG.2011.05.034

Bonilla, J., Bittante, A.M.Q.B., Sobral, P.J.A., 2017. Thermal analysis of gelatin–chitosan edible film mixed with plant ethanolic extracts. J. Therm. Anal. Calorim. 130, 1221–1227. https://doi.org/10.1007/s10973-017-6472-4

Bonilla, J., Fortunati, E., Atarés, L., Chiralt, A., Kenny, J.M., 2014. Physical, structural and antimicrobial properties of poly vinyl alcohol-chitosan biodegradable films. Food Hydrocoll. 35, 463–470. https://doi.org/10.1016/j.foodhyd.2013.07.002

Bonilla, J., Poloni, T., Sobral, P.J.A., 2018. Active edible coatings with Boldo extract added and their application on nut products: reducing the oxidative rancidity rate. Int. J. Food Sci. Technol. 53, 700–708. https://doi.org/10.1111/ijfs.13645

Bonilla, J., Sobral, P.J.A., 2017. Antioxidant and physicochemical properties of blended films based on gelatin-sodium caseinate activated with natural extracts. J. Appl. Polym. Sci. 134. https://doi.org/10.1002/app.44467

Bonilla, J., Sobral, P.J.A., 2016. Investigation of the physicochemical, antimicrobial and antioxidant properties of gelatin-chitosan edible film mixed with plant ethanolic extracts.

Food Biosci. 16, 17–25. https://doi.org/10.1016/j.fbio.2016.07.003

Bonilla, J., Talón, E., Atarés, L., Vargas, M., Chiralt, A., 2013. Effect of the incorporation of antioxidants on physicochemical and antioxidant properties of wheat starch-chitosan films. J. Food Eng. 118, 271–278. https://doi.org/10.1016/j.jfoodeng.2013.04.008

Bourlieu, C., Guillard, V., Vallès-Pamiès, B., Guilbert, S., Gontard, N., 2009. Edible moisture barriers: how to assess of their potential and limits in food products shelf-life extension? Crit. Rev. Food Sci. Nutr. 49, 474–99. https://doi.org/10.1080/10408390802145724

Bravin, B., Peressini, D., Sensidoni, A., 2006. Development and application of polysaccharide–lipid edible coating to extend shelf-life of dry bakery products. J. Food Eng. 76, 280–290. https://doi.org/10.1016/j.jfoodeng.2005.05.021

Bravin, B., Peressini, D., Sensidoni, A., 2004. Influence of Emulsifier Type and Content on Functional Properties of Polysaccharide Lipid-Based Edible Films. J. Agric. Food Chem. 52, 6448–6455. https://doi.org/10.1021/jf040065b

Breene, W.M., 1975. Application of texture profile analysis to instrumental food texture evaluation. J. Texture Stud. 6, 53–82. https://doi.org/10.1111/j.1745-4603.1975.tb01118.x

Büning-Pfaue, H., 2003. Analysis of water in food by near infrared spectroscopy. Food Chem. 82, 107–115. https://doi.org/10.1016/S0308-8146(02)00583-6

Campos, C.A., Gerschenson, L.N., Flores, S.K., 2011. Development of Edible Films and Coatings with Antimicrobial Activity. Food Bioprocess Technol. 4, 849–875. https://doi.org/10.1007/s11947-010-0434-1

Cauvain, S.P., Young, L.S., 2009. Flours and grains, in: Cauvain, S.P., Young, L.S.B.T.-M.B.P.S. (Eds.), More Baking Problems Solved. Elsevier, pp. 33–51. https://doi.org/10.1533/9781845697204.33

Cauvain, S.P., Young, L.S., 2009. Bread and fermented products, in: Cauvain, S.P., Young, L.S.B.T.-M.B.P.S. (Eds.), More Baking Problems Solved. Elsevier, pp. 83–127. https://doi.org/10.1533/9781845697204.83

Cazón, P., Velazquez, G., Ramírez, J.A., Vázquez, M., 2017. Polysaccharide-based films and coatings for food packaging: A review. Food Hydrocoll. 68, 136–148. https://doi.org/https://doi.org/10.1016/j.foodhyd.2016.09.009

Cecchini, J.P., Spotti, M.J., Piagentini, A.M., Milt, V.G., Carrara, C.R., 2017. Development of edible films obtained from submicron emulsions based on whey protein concentrate, oil/beeswax and brea gum. Food Sci. Technol. Int. 23, 371–381. https://doi.org/10.1177/1082013217695170

Cerqueira, M.A., Souza, B.W.S., Teixeira, J.A., Vicente, A.A., 2012. Effect of glycerol and corn oil on physicochemical properties of polysaccharide films – A comparative study. Food

Hydrocoll. 27, 175–184. https://doi.org/10.1016/j.foodhyd.2011.07.007

Cevoli, C., Balestra, F., Ragni, L., Fabbri, A., 2013. Rheological characterisation of selected food hydrocolloids by traditional and simplified techniques. Food Hydrocoll. 33, 142–150. https://doi.org/10.1016/j.foodhyd.2013.02.022

Cevoli, C., Fabbri, A., Tylewicz, U., Rocculi, P., 2018. Finite element model to study the thawing of packed frozen vegetables as influenced by working environment temperature. Biosyst. Eng. 170, 1–11. https://doi.org/10.1016/j.biosystemseng.2018.03.005

Cevoli, C., Gianotti, A., Troncoso, R., Fabbri, A., 2015. Quality evaluation by physical tests of a traditional Italian flat bread Piadina during storage and shelf-life improvement with sourdough and enzymes. Eur. Food Res. Technol. 240, 1081–1089. https://doi.org/10.1007/s00217-015-2429-7

Chen, C.-H., Kuo, W.-S., Lai, L.-S., 2009. Rheological and physical characterization of film-forming solutions and edible films from tapioca starch/decolorized hsian-tsao leaf gum. Food Hydrocoll. 23, 2132–2140. https://doi.org/10.1016/j.foodhyd.2009.05.015

Chillo, S., Flores, S., Mastromatteo, M., Conte, A., Gerschenson, L., Del Nobile, M.A., 2008. Influence of glycerol and chitosan on tapioca starch-based edible film properties. J. Food Eng. 88, 159–168. https://doi.org/10.1016/j.jfoodeng.2008.02.002

Chin, N.L., Abdullah, R., Yusof, Y.A., 2011. Glazing effects on bread crust and crumb staling during storage. J. Texture Stud. 42, 459–467. https://doi.org/10.1111/j.1745-4603.2011.00307.x

Cocchi, M., Foca, G., Marchetti, A., Sighinolfi, S., Tassi, L., Ulrici, A., 2005. Use of multivariate analysis of MIR spectra to study bread staling. Ann. Chim. 95, 657–666. https://doi.org/10.1002/adic.200590076

Conte, P., Del Caro, A., Balestra, F., Piga, A., Fadda, C., 2018. Bee pollen as a functional ingredient in gluten-free bread: A physical-chemical, technological and sensory approach. LWT 90, 1–7. https://doi.org/10.1016/j.lwt.2017.12.002

Coughlan, K., Shaw, N.B., Kerry, J.F., Kerry, J.P., 2004. Combined Effects of Proteins and Polysaccharides on Physical Properties of Whey Protein Concentrate-based Edible Films. J. Food Sci. 69, E271–E275. https://doi.org/10.1111/j.1365-2621.2004.tb10997.x

Cuq, B., Aymard, C., Cuq, J.-L., Guilbert, S., 1995. Edible Packaging Films Based on Fish Myofibrillar Proteins: Formulation and Functional Properties. J. Food Sci. 60, 1369–1374. https://doi.org/10.1111/j.1365-2621.1995.tb04593.x

Dang, K.M., Yoksan, R., 2015. Development of thermoplastic starch blown film by incorporating plasticized chitosan. Carbohydr. Polym. 115, 575–581. https://doi.org/10.1016/j.carbpol.2014.09.005

Davidou, S., Le Meste, M., Debever, E., Bekaert, D., 1996. A contribution to the study of staling of white bread: effect of water and hydrocolloid. Food Hydrocoll. 10, 375–383. https://doi.org/https://doi.org/10.1016/S0268-005X(96)80016-6

Debeaufort, F., Quezada-Gallo, J.A., Voilley, A., 1998. Edible films and coatings: tomorrow's packagings: a review. Crit. Rev. Food Sci. Nutr. 38, 299–313. https://doi.org/10.1080/10408699891274219

Debeaufort, F., Voilley, A., 2009. Lipid-Based Edible Films and Coatings, in: Huber, K.C., Embuscado, M.E. (Eds.), Edible Films and Coatings for Food Applications. Springer New York, New York, NY, pp. 135–168. https://doi.org/10.1007/978-0-387-92824-1_5

Defraeye, T., 2014. Advanced computational modelling for drying processes – A review. Appl. Energy 131, 323–344. https://doi.org/10.1016/j.apenergy.2014.06.027

Dehghani, S., Hosseini, S.V., Regenstein, J.M., 2018. Edible films and coatings in seafood preservation: A review. Food Chem. 240, 505–513. https://doi.org/10.1016/j.foodchem.2017.07.034

Di Scala, K., Crapiste, G., 2008. Drying kinetics and quality changes during drying of red pepper. LWT - Food Sci. Technol. 41, 789–795. https://doi.org/10.1016/j.lwt.2007.06.007

Elsabee, M.Z., Abdou, E.S., 2013. Chitosan based edible films and coatings: A review. Mater. Sci. Eng. C 33, 1819–1841. https://doi.org/10.1016/j.msec.2013.01.010

Espitia, P.J.P., Du, W.-X., Avena-Bustillos, R. de J., Soares, N. de F.F., McHugh, T.H., 2014. Edible films from pectin: Physical-mechanical and antimicrobial properties - A review. Food Hydrocoll. 35, 287–296. https://doi.org/10.1016/j.foodhyd.2013.06.005

Fabbri, A., Cevoli, C., Silaghi, F.A., Guarnieri, A., 2012. Numerical Simulation of Physical Systems in Agri-Food Engineering. J. Agric. Eng. 42, 1. https://doi.org/10.4081/jae.2011.4.1

Fadda, C., Sanguinetti, A.M., Del Caro, A., Collar, C., Piga, A., 2014. Bread staling: Updating the view. Compr. Rev. Food Sci. Food Saf. 13, 473–492. https://doi.org/10.1111/1541-4337.12064

Falguera, V., Quintero, J.P., Jiménez, A., Muñoz, J.A., Ibarz, A., 2011. Edible films and coatings: Structures, active functions and trends in their use. Trends Food Sci. Technol. 22, 292–303. https://doi.org/10.1016/j.tifs.2011.02.004

Fang, Y., Tung, M.A., Britt, I.J., Yada, S., Dalgleish, D.G., 2002. Tensile and Barrier Properties of Edible Films Made from Whey Proteins. J. Food Sci. 67, 188–193. https://doi.org/10.1111/j.1365-2621.2002.tb11381.x

Ferreira Saraiva, L.E., Naponucena, L. de O.M., da Silva Santos, V., Silva, R.P.D., de Souza, C.O., Evelyn Gomes Lima Souza, I., de Oliveira Mamede, M.E., Druzian, J.I., 2016.

Development and application of edible film of active potato starch to extend mini panettone shelf life. LWT 73, 311–319. https://doi.org/10.1016/j.lwt.2016.05.047

Galus, S., Kadzińska, J., 2016a. Moisture Sensitivity, Optical, Mechanical and Structural Properties of Whey Protein-Based Edible Films Incorporated with Rapeseed Oil. Food Technol. Biotechnol. 54, 78–89. https://doi.org/10.17113/ftb.54.01.16.3889

Galus, S., Kadzińska, J., 2016b. Whey protein edible films modified with almond and walnut oils. Food Hydrocoll. 52, 78–86. https://doi.org/10.1016/j.foodhyd.2015.06.013

Galus, S., Kadzińska, J., 2015. Food applications of emulsion-based edible films and coatings. Trends Food Sci. Technol. 45, 273–283. https://doi.org/10.1016/j.tifs.2015.07.011

Galus, S., Lenart, A., 2013. Development and characterization of composite edible films based on sodium alginate and pectin. J. Food Eng. 115, 459–465. https://doi.org/10.1016/j.jfoodeng.2012.03.006

Gámbaro, A., Varela, P., Giménez, A., Aldrovandi, A., Fiszman, S.M., Hough, G., 2002. Textural quality of white pan bread by sensory and instrumental measurements. J. Texture Stud. 33, 401–413. https://doi.org/10.1111/j.1745-4603.2002.tb01356.x

Gennadios, A., Weller, C.L., Gooding, C.H., 1994. Measurement errors in water vapor permeability of highly permeable, hydrophilic edible films. J. Food Eng. 21, 395–409. https://doi.org/10.1016/0260-8774(94)90062-0

Giangiacomo, R., 2006. Study of water–sugar interactions at increasing sugar concentration by NIR spectroscopy. Food Chem. 96, 371–379. https://doi.org/10.1016/j.foodchem.2005.02.051

Gomes-Ruffi, C.R., Cunha, R.H. da, Almeida, E.L., Chang, Y.K., Steel, C.J., 2012. Effect of the emulsifier sodium stearoyl lactylate and of the enzyme maltogenic amylase on the quality of pan bread during storage. LWT - Food Sci. Technol. 49, 96–101. https://doi.org/https://doi.org/10.1016/j.lwt.2012.04.014

Gontard, N., Duchez, C., Cuq, J.-L., Guilbert, S., 2007. Edible composite films of wheat gluten and lipids: water vapour permeability and other physical properties. Int. J. Food Sci. Technol. 29, 39–50. https://doi.org/10.1111/j.1365-2621.1994.tb02045.x

Gray, J.A., Bemiller, J.N., 2003. Bread Staling: Molecular Basis and Control. Compr. Rev. Food Sci. Food Saf. 2, 1–21. https://doi.org/10.1111/j.1541-4337.2003.tb00011.x

Guillard, V., Broyart, B., Bonazzi, C., Guilbert, S., Gontard, N., 2004. Effect of temperature on moisture barrier efficiency of monoglyceride edible films in cereal-based composite foods. Cereal Chem. 81, 767–771. https://doi.org/10.1094/CCHEM.2004.81.6.767

Guillard, V., Broyart, B., Bonazzi, C., Guilbert, S., Gontard, N., 2003. Preventing moisture transfer in a composite food using edible films: Experimental and mathematical study. J.

Food Sci. 68, 2267–2277. https://doi.org/10.1111/j.1365-2621.2003.tb05758.x

Gutiérrez, L., Batlle, R., Andújar, S., Sánchez, C., Nerín, C., 2011. Evaluation of antimicrobial active packaging to increase shelf life of gluten-free sliced bread. Packag. Technol. Sci. 24, 485–494. https://doi.org/10.1002/pts.956

Han, J.H., 2013. Edible Films and Coatings: A Review, in: Innovations in Food Packaging: Second Edition. Elsevier, San Diego, pp. 213–255. https://doi.org/10.1016/B978-0-12-394601-0.00009-6

He, H.-J., Wu, D., Sun, D.-W., 2013. Non-destructive and rapid analysis of moisture distribution in farmed Atlantic salmon (Salmo salar) fillets using visible and near-infrared hyperspectral imaging. Innov. Food Sci. Emerg. Technol. 18, 237–245. https://doi.org/https://doi.org/10.1016/j.ifset.2013.02.009

He, H., Hoseney, R.C., 1990. Changes in Bread Firmness and Moisture During Long-Term Storage. Cereal Chem. 67, 603–605.

Hosseini, M.H., Razavi, S.H., Mousavi, M.A., 2009. Antimicrobial, physical and mechanical properties of chitosan-based films incorporated with thyme, clove and cinnamon essential oils. J. Food Process. Preserv. 33, 727.

Huang, H., Yu, H., Xu, H., Ying, Y., 2008. Near infrared spectroscopy for on/in-line monitoring of quality in foods and beverages: A review. J. Food Eng. 87, 303–313. https://doi.org/10.1016/j.jfoodeng.2007.12.022

Huber, K.C., Embuscado, M.E. (Eds.), 2009. Edible Films and Coatings for Food Applications. Springer New York, New York, NY. https://doi.org/10.1007/978-0-387-92824-1

Javanmard, M., Golestan, L., 2008. Effect of olive oil and glycerol on physical properties of whey protein concentrate films. J. Food Process Eng. 31, 628–639. https://doi.org/10.1111/j.1745-4530.2007.00179.x

Jekle, M., Fuchs, A., Becker, T., 2018. A normalized texture profile analysis approach to evaluate firming kinetics of bread crumbs independent from its initial texture. J. Cereal Sci. 81, 147–152. https://doi.org/10.1016/j.jcs.2018.04.007

Jideani, V.A., Vogt, K., 2016. Antimicrobial Packaging for Extending the Shelf Life of Bread—A Review. Crit. Rev. Food Sci. Nutr. 56, 1313–1324. https://doi.org/10.1080/10408398.2013.768198

Jiménez, A., Fabra, M.J., Talens, P., Chiralt, A., 2012. Edible and Biodegradable Starch Films: A Review. Food Bioprocess Technol. 5, 2058–2076. https://doi.org/10.1007/s11947-012-0835-4

Kechichian, V., Ditchfield, C., Veiga-Santos, P., Tadini, C.C., 2010. Natural antimicrobial ingredients incorporated in biodegradable films based on cassava starch. LWT - Food Sci.

Technol. 43, 1088–1094. https://doi.org/10.1016/j.lwt.2010.02.014

Kennedy, J.R.M., Kent, K.E., Brown, J.R., 2015. Rheology of dispersions of xanthan gum, locust bean gum and mixed biopolymer gel with silicon dioxide nanoparticles. Mater. Sci. Eng. C 48, 347–353. https://doi.org/10.1016/j.msec.2014.12.040

Kester, J.J., Fennema, O.R., 1986. Edible Films and Coatings - a Review. Food Technol.

Khan, M.K.I., Maan, A.A., Schutyser, M., Schroën, K., Boom, R., 2013. Electrospraying of water in oil emulsions for thin film coating. J. Food Eng. 119, 776–780. https://doi.org/10.1016/j.jfoodeng.2013.05.027

Khwaldia, K., Perez, C., Banon, S., Desobry, S., Hardy, J., 2004. Milk Proteins for Edible Films and Coatings. Crit. Rev. Food Sci. Nutr. 44, 239–251. https://doi.org/10.1080/10408690490464906

Kontogiorgos, V., Margelou, I., Georgiadis, N., Ritzoulis, C., 2012. Rheological characterization of okra pectins. Food Hydrocoll. 29, 356–362. https://doi.org/10.1016/j.foodhyd.2012.04.003

Kotsianis, I.., Giannou, V., Tzia, C., 2002. Production and packaging of bakery products using MAP technology. Trends Food Sci. Technol. 13, 319–324. https://doi.org/10.1016/S0924-2244(02)00162-0

Kulp, K., Ponte, J.G., D'Appolonia, B.L., 1981. Staling of white pan bread: Fundamental causes∗. C R C Crit. Rev. Food Sci. Nutr. 15, 1–48. https://doi.org/10.1080/10408398109527311

Kurek, M., Ščetar, M., Galić, K., 2017. Edible coatings minimize fat uptake in deep fat fried products: A review. Food Hydrocoll. 71, 225–235. https://doi.org/https://doi.org/10.1016/j.foodhyd.2017.05.006

Lee, K.Y., Mooney, D.J., 2012. Alginate: Properties and biomedical applications. Prog. Polym. Sci. 37, 106–126. https://doi.org/10.1016/j.progpolymsci.2011.06.003

Licciardello, F., Cipri, L., Muratore, G., 2014. Influence of packaging on the quality maintenance of industrial bread by comparative shelf life testing. Food Packag. Shelf Life 1, 19–24. https://doi.org/10.1016/j.fpsl.2013.10.001

Licciardello, F., Giannone, V., Del Nobile, M.A., Muratore, G., Summo, C., Giarnetti, M., Caponio, F., Paradiso, V.M., Pasqualone, A., 2017. Shelf life assessment of industrial durum wheat bread as a function of packaging system. Food Chem. 224, 181–190. https://doi.org/10.1016/j.foodchem.2016.12.080

Liu, H., Adhikari, R., Guo, Q., Adhikari, B., 2013. Preparation and characterization of glycerol plasticized (high-amylose) starch–chitosan films. J. Food Eng. 116, 588–597. https://doi.org/10.1016/j.jfoodeng.2012.12.037

Lopes, F.A., Soares, N.F.F., Lopes, C.C.P., Silva, W.A., Júnior, J.C.B., Medeiros, E.A.A., 2014. Conservation of Bakery Products Through Cinnamaldehyde Antimicrobial Films. Packag. Technol. Sci. 27, 293–302. https://doi.org/10.1002/pts.2033

Ma, J., Lin, Y., Chen, X., Zhao, B., Zhang, J., 2014. Flow behavior, thixotropy and dynamical viscoelasticity of sodium alginate aqueous solutions. Food Hydrocoll. 38, 119–128. https://doi.org/10.1016/j.foodhyd.2013.11.016

Ma, W., Tang, C.H., Yin, S.W., Yang, X.Q., Wang, Q., Liu, F., Wei, Z.H., 2012. Characterization of gelatin-based edible films incorporated with olive oil. Food Res. Int. 49, 572–579. https://doi.org/10.1016/j.foodres.2012.07.037

Maftoonazad, N., Ramaswamy, H.S., Marcotte, M., 2007. Evaluation of factors affecting barrier, mechanical and optical properties of pectin-based films using response surface methodology. J. Food Process Eng. 30, 539–563. https://doi.org/10.1111/j.1745-4530.2007.00123.x

Martins, R.C., 2006. Simple finite volumes and finite elements procedures for food quality and safety simulations. J. Food Eng. 73, 327–338. https://doi.org/10.1016/j.jfoodeng.2005.01.033

Mathew, S., Brahmakumar, M., Abraham, T.E., 2006. Microstructural imaging and characterization of the mechanical, chemical, thermal, and swelling properties of starch–chitosan blend films. Biopolymers 82, 176–187. https://doi.org/10.1002/bip.20480

Mellinas, C., Valdés, A., Ramos, M., Burgos, N., Del Carmen Garrigós, M., Jiménez, A., 2016. Active edible films: Current state and future trends. J. Appl. Polym. Sci. 133, n/a-n/a. https://doi.org/10.1002/app.42631

Meza, B.E., Peralta, J.M., Zorrilla, S.E., 2015. Rheological Properties of a Commercial Food Glaze Material and Their Effect on the Film Thickness Obtained by Dip Coating. J. Food Process Eng. 38, 510–516. https://doi.org/10.1111/jfpe.12181

Mezger, T.G., 2006. The Rheology Handbook: For Users of Rotational and Oscillatory Rheometers, Coatings compendia. Vincentz Network.

Miller, K.S., Krochta, J.M., 1997a. Oxygen and aroma barrier properties of edible films: A review. Trends Food Sci. Technol. 8, 228–237. https://doi.org/10.1016/S0924-2244(97)01051-0

Miller, K.S., Krochta, J.M., 1997b. Oxygen and aroma barrier properties of edible films: A review. Trends Food Sci. Technol. 8, 228–237. https://doi.org/10.1016/S0924-2244(97)01051-0

Monedero, F.M., Fabra, M.J., Talens, P., Chiralt, A., 2009. Effect of oleic acid–beeswax mixtures on mechanical, optical and water barrier properties of soy protein isolate based films. J. Food Eng. 91, 509–515. https://doi.org/10.1016/j.jfoodeng.2008.09.034

Nallan Chakravartula, S.S., Cevoli, C., Balestra, F., Fabbri, A., Dalla Rosa, M., 2019. Evaluation of drying of edible coating on bread using NIR spectroscopy. J. Food Eng. 240, 29–37. https://doi.org/10.1016/j.jfoodeng.2018.07.009

Naqash, F., Masoodi, F.A., Rather, S.A., Wani, S.M., Gani, A., 2017. Emerging concepts in the nutraceutical and functional properties of pectin—A Review. Carbohydr. Polym. 168, 227–239. https://doi.org/10.1016/J.CARBPOL.2017.03.058

O'Connor, L.J., Favreau-Farhadi, N., Barrett, A.H., 2018. Use of edible barriers in intermediate moisture food systems to inhibit moisture migration. J. Food Process. Preserv. 42. https://doi.org/10.1111/jfpp.13512

Osborne, B.G., 1996. Near Infrared Spectroscopic Studies of Starch and Water in Some Processed Cereal Foods. J. Near Infrared Spectrosc. 4, 195–200. https://doi.org/10.1255/jnirs.90

Osborne, B.G., Fearn, T., Miller, A.R., Douglas, S., 1984. Application of near infrared reflectance spectroscopy to the compositional analysis of biscuits and biscuit doughs. J. Sci. Food Agric. 35, 99–105. https://doi.org/10.1002/jsfa.2740350116

Osés, J., Fabregat-Vázquez, M., Pedroza-Islas, R., Tomás, S.A., Cruz-Orea, A., Maté, J.I., 2009. Development and characterization of composite edible films based on whey protein isolate and mesquite gum. J. Food Eng. 92, 56–62. https://doi.org/10.1016/j.jfoodeng.2008.10.029

Otoni, C.G., Avena-Bustillos, R.J., Azeredo, H.M.C., Lorevice, M. V., Moura, M.R., Mattoso, L.H.C., McHugh, T.H., 2017. Recent Advances on Edible Films Based on Fruits and Vegetables-A Review. Compr. Rev. Food Sci. Food Saf. 16, 1151–1169. https://doi.org/10.1111/1541-4337.12281

Özdemir, İ.S., Öztürk, B., Çelik, B., Sarıtepe, Y., Aksoy, H., 2018. Rapid, simultaneous and non-destructive assessment of the moisture, water activity, firmness and SO 2 content of the intact sulphured-dried apricots using FT-NIRS and chemometrics. Talanta 186, 467–472. https://doi.org/10.1016/j.talanta.2018.05.007

Ozdemir, M., Floros, J.D., 2008. Optimization of edible whey protein films containing preservatives for mechanical and optical properties. J. Food Eng. 84, 116–123. https://doi.org/10.1016/j.jfoodeng.2007.04.029

Panchev, I.N., Baeva, M.R., Lambov, S.I., 2005. Influence of Edible Films upon the Moisture Loss and Microstructure of Dietetic Sucrose-Free Sponge Cakes during Storage. Dry. Technol. 23, 925–940. https://doi.org/10.1081/DRT-200054241

Park, S.Y., Marsh, K.S., Rhim, J.W., 2002. Characteristics of different molecular weight chitosan films affected by the type of organic solvents. J. Food Sci. 67, 194–197. https://doi.org/10.1111/j.1365-2621.2002.tb11382.x

Parra, D.F., Tadini, C.C., Ponce, P., Lugão, A.B., 2004. Mechanical properties and water vapor

transmission in some blends of cassava starch edible films. Carbohydr. Polym. 58, 475–481. https://doi.org/https://doi.org/10.1016/j.carbpol.2004.08.021

Pelissari, F.M., Grossmann, M.V.E., Yamashita, F., Pineda, E.A.G., 2009. Antimicrobial, Mechanical, and Barrier Properties of Cassava Starch−Chitosan Films Incorporated with Oregano Essential Oil. J. Agric. Food Chem. 57, 7499–7504.

Peressini, D., Bravin, B., Lapasin, R., Rizzotti, C., Sensidoni, A., 2003. Starch–methylcellulose based edible films: rheological properties of film-forming dispersions. J. Food Eng. 59, 25–32. https://doi.org/10.1016/S0260-8774(02)00426-0

Perez-Gago. Maria B and Krochta. John M, 2002. Formation and Properties of Whey Protein Films and Coatings, in: Protein-Based Films and Coatings. CRC Press, pp. 159–181. https://doi.org/10.1201/9781420031980.ch4

Perez-gago, M.B., Krochta, J.M., 2001. Denaturation time and temperature effects on solubility, tensile properties, and oxygen permeability of whey protein edible films. J. Food Sci. 66, 705–710. https://doi.org/10.1111/j.1365-2621.2001.tb04625.x

Pérez-Gago, M.B., Nadaud, P., Krochta, J.M., 1999. Water Vapor Permeability, Solubility, and Tensile Properties of Heat-denatured versus Native Whey Protein Films. J. Food Sci. 64, 1034–1037. https://doi.org/10.1111/j.1365-2621.1999.tb12276.x

Pérez, L.M., Piccirilli, G.N., Delorenzi, N.J., Verdini, R.A., 2016. Effect of different combinations of glycerol and/or trehalose on physical and structural properties of whey protein concentrate-based edible films. Food Hydrocoll. 56, 352–359. https://doi.org/10.1016/j.foodhyd.2015.12.037

Piccinini, M., Fois, S., Secchi, N., Sanna, M., Roggio, T., Catzeddu, P., 2012. The Application of NIR FT-Raman Spectroscopy to Monitor Starch Retrogradation and Crumb Firmness in Semolina Bread. Food Anal. Methods 5, 1145–1149. https://doi.org/10.1007/s12161-011-9360-8

Planinić, M., Velić, D., Tomas, S., Bilić, M., Bucić, A., 2005. Modelling of drying and rehydration of carrots using Peleg's model. Eur. Food Res. Technol. 221, 446–451. https://doi.org/10.1007/s00217-005-1200-x

Ramos, Ó.L., Fernandes, J.C., Silva, S.I., Pintado, M.E., Malcata, F.X., 2012. Edible Films and Coatings from Whey Proteins: A Review on Formulation, and on Mechanical and Bioactive Properties. Crit. Rev. Food Sci. Nutr. 52, 533–552. https://doi.org/10.1080/10408398.2010.500528

Ramos, Ó.L., Reinas, I., Silva, S.I., Fernandes, J.C., Cerqueira, M.A., Pereira, R.N., Vicente, A.A., Poças, M.F., Pintado, M.E., Malcata, F.X., 2013. Effect of whey protein purity and glycerol content upon physical properties of edible films manufactured therefrom. Food Hydrocoll. 30, 110–122. https://doi.org/10.1016/j.foodhyd.2012.05.001

Rayas-Duarte, P., Mulvaney, S., 2012. Bread staling, in: Breadmaking. Elsevier, pp. 580–596. https://doi.org/10.1533/9780857095695.3.580

Ribotta, P.D., Le Bail, A., 2007. Thermo-physical assessment of bread during staling. LWT - Food Sci. Technol. 40, 879–884. https://doi.org/https://doi.org/10.1016/j.lwt.2006.03.023

Ringsted, T., Siesler, H.W., Engelsen, S.B., 2017. Monitoring the staling of wheat bread using 2D MIR-NIR correlation spectroscopy. J. Cereal Sci. 75, 92–99. https://doi.org/10.1016/j.jcs.2017.03.006

Rodríguez, M., Osés, J., Ziani, K., Maté, J.I., 2006. Combined effect of plasticizers and surfactants on the physical properties of starch based edible films. Food Res. Int. 39, 840–846. https://doi.org/10.1016/J.FOODRES.2006.04.002

Romero-Bastida, C.A., Bello-Pérez, L.A., García, M.A., Martino, M.N., Solorza-Feria, J., Zaritzky, N.E., 2005. Physicochemical and microstructural characterization of films prepared by thermal and cold gelatinization from non-conventional sources of starches. Carbohydr. Polym. 60, 235–244. https://doi.org/10.1016/J.CARBPOL.2005.01.004

Saberi, B., Thakur, R., Vuong, Q. V., Chockchaisawasdee, S., Golding, J.B., Scarlett, C.J., Stathopoulos, C.E., 2016. Optimization of physical and optical properties of biodegradable edible films based on pea starch and guar gum. Ind. Crops Prod. 86, 342–352. https://doi.org/10.1016/j.indcrop.2016.04.015

Sánchez-González, L., Vargas, M., González-Martínez, C., Chiralt, A., Cháfer, M., 2011. Use of Essential Oils in Bioactive Edible Coatings: A Review. Food Eng. Rev. 3, 1–16. https://doi.org/10.1007/s12393-010-9031-3

Sato, A.C.K., Oliveira, P.R., Cunha, R.L., 2008. Rheology of mixed pectin solutions. Food Biophys. 3, 100–109. https://doi.org/10.1007/s11483-008-9058-7

Schiraldi, A., Piazza, L., Riva, M., 1996. Bread staling: A calorimetric approach. Cereal Chem. 73, 32–39.

Silva-Weiss, A., Bifani, V., Ihl, M., Sobral, P.J.A., Gómez-Guillén, M.C., 2013. Structural properties of films and rheology of film-forming solutions based on chitosan and chitosan-starch blend enriched with murta leaf extract. Food Hydrocoll. 31, 458–466. https://doi.org/https://doi.org/10.1016/j.foodhyd.2012.11.028

Silva, M.A. da, Bierhalz, A.C.K., Kieckbusch, T.G., 2009. Alginate and pectin composite films crosslinked with Ca2+ ions: Effect of the plasticizer concentration. Carbohydr. Polym. 77, 736–742. https://doi.org/10.1016/j.carbpol.2009.02.014

Sinelli, N., Casiraghi, E., Barzaghi, S., Brambilla, A., Giovanelli, G., 2011. Near infrared (NIR) spectroscopy as a tool for monitoring blueberry osmo-air dehydration process. Food Res. Int. 44, 1427–1433. https://doi.org/10.1016/j.foodres.2011.02.046

Siracusa, V., Rocculi, P., Romani, S., Rosa, M.D., 2008. Biodegradable polymers for food packaging: a review. Trends Food Sci. Technol. 19, 634–643. https://doi.org/10.1016/j.tifs.2008.07.003

Siracusa, V., Romani, S., Gigli, M., Mannozzi, C., Cecchini, J., Tylewicz, U., Lotti, N., 2018. Characterization of Active Edible Films based on Citral Essential Oil, Alginate and Pectin. Materials (Basel). 11, 1980. https://doi.org/10.3390/ma11101980

Smith, J.P., Daifas, D.P., El-Khoury, W., Koukoutsis, J., El-Khoury, A., 2004. Shelf Life and Safety Concerns of Bakery Products—A Review. Crit. Rev. Food Sci. Nutr. 44, 19–55. https://doi.org/10.1080/10408690490263774

Smithers, G.W., 2008. Whey and whey proteins—From 'gutter-to-gold.' Int. Dairy J. 18, 695–704. https://doi.org/10.1016/J.IDAIRYJ.2008.03.008

Soares, N.F.F., Pires, A.C.S., Camilloto, G.P., Santiago-Silva, P., Espitia, P.J., Silva, W.A., 2009. Recent patents on active packaging for food application. Recent Pat. Food, Nutr. Agric. 1, 171.

Sobral, P.J.A., Menegalli, F.C., Hubinger, M.D., Roques, M.A., 2001. Mechanical, water vapor barrier and thermal properties of gelatin based edible films. Food Hydrocoll. 15, 423–432. https://doi.org/10.1016/S0268-005X(01)00061-3

Sørensen, L.K., 2009. Application of reflectance near infrared spectroscopy for bread analyses. Food Chem. 113, 1318–1322. https://doi.org/10.1016/j.foodchem.2008.08.065

Soukoulis, C., Behboudi-Jobbehdar, S., Macnaughtan, W., Parmenter, C., Fisk, I.D., 2017. Stability of Lactobacillus rhamnosus GG incorporated in edible films: Impact of anionic biopolymers and whey protein concentrate. Food Hydrocoll. 70, 345–355. https://doi.org/10.1016/j.foodhyd.2017.04.014

Soukoulis, C., Yonekura, L., Gan, H.H., Behboudi-Jobbehdar, S., Parmenter, C., Fisk, I., 2014. Probiotic edible films as a new strategy for developing functional bakery products: The case of pan bread. Food Hydrocoll. 39, 231–242. https://doi.org/10.1016/j.foodhyd.2014.01.023

Suzuki, K., McDonald, C.E., D'Appolonia, B.L., 1986. Near-infrared reflectance analysis of bread. Cereal Chem.

Tavassoli-Kafrani, E., Shekarchizadeh, H., Masoudpour-Behabadi, M., 2016. Development of edible films and coatings from alginates and carrageenans. Carbohydr. Polym. 137, 360–374. https://doi.org/10.1016/j.carbpol.2015.10.074

Thakur, R., Saberi, B., Pristijono, P., Golding, J., Stathopoulos, C., Scarlett, C., Bowyer, M., Vuong, Q., 2016. Characterization of rice starch-ι-carrageenan biodegradable edible film. Effect of stearic acid on the film properties. Int. J. Biol. Macromol. 93, 952–960. https://doi.org/10.1016/j.ijbiomac.2016.09.053

Theóphilo Galvão, A.M.M., de Oliveira Araújo, A.W., Carneiro, S.V., Zambelli, R.A., do Socorro Rocha Bastos, M., 2018. Coating development with modified starch and tomato powder for application in frozen dough. Food Packag. Shelf Life 16, 194–203. https://doi.org/https://doi.org/10.1016/j.fpsl.2018.04.003

Tongnuanchan, P., Benjakul, S., 2014. Essential oils: extraction, bioactivities, and their uses for food preservation. J. Food Sci. 79, R1231-49. https://doi.org/10.1111/1750-3841.12492

Upasen, S., Wattanachai, P., 2018. Packaging to prolong shelf life of preservative-free white bread. Heliyon 4, e00802. https://doi.org/10.1016/j.heliyon.2018.e00802

Valencia-Sullca, C., Atarés, L., Vargas, M., Chiralt, A., 2018a. Physical and Antimicrobial Properties of Compression-Molded Cassava Starch-Chitosan Films for Meat Preservation. Food Bioprocess Technol. 11, 1339–1349. https://doi.org/10.1007/s11947-018-2094-5

Valencia-Sullca, C., Vargas, M., Atarés, L., Chiralt, A., 2018b. Thermoplastic cassava starch-chitosan bilayer films containing essential oils. Food Hydrocoll. 75, 107–115. https://doi.org/10.1016/j.foodhyd.2017.09.008

Valencia, G.A., Luciano, C.G., Lourenço, R.V., do Amaral Sobral, P.J., 2018. Microstructure and physical properties of nano-biocomposite films based on cassava starch and laponite. Int. J. Biol. Macromol. 107, 1576–1583. https://doi.org/10.1016/j.ijbiomac.2017.10.031

Vásconez, M.B., Flores, S.K., Campos, C.A., Alvarado, J., Gerschenson, L.N., 2009. Antimicrobial activity and physical properties of chitosan–tapioca starch based edible films and coatings. Food Res. Int. 42, 762–769. https://doi.org/10.1016/j.foodres.2009.02.026

Vieira, M.G.A., da Silva, M.A., dos Santos, L.O., Beppu, M.M., 2011. Natural-based plasticizers and biopolymer films: A review. Eur. Polym. J. 47, 254–263. https://doi.org/10.1016/j.eurpolymj.2010.12.011

Villalobos-Carvajal, R., Hernández-Muñoz, P., Albors, A., Chiralt, A., 2009. Barrier and optical properties of edible hydroxypropyl methylcellulose coatings containing surfactants applied to fresh cut carrot slices. Food Hydrocoll. 23, 526–535. https://doi.org/https://doi.org/10.1016/j.foodhyd.2008.02.008

Vodovotz, Y., Baik, M., Vittadini, E., Chinachoti, P., 2018. Instrumental techniques used in bread staling analysis, Bread Staling. CRC Press. https://doi.org/10.1201/9781351070348

Wu, Y., Weller, C.L., Hamouz, F., Cuppett, S.L., Schnepf, M.B.T.-A. in F. and N.R., 2002. Development and application of multicomponent edible coatings and films: A review. Academic Press, pp. 347–394. https://doi.org/https://doi.org/10.1016/S1043-4526(02)44007-7

Xiao, Q., Gu, X., Tan, S., 2014. Drying process of sodium alginate films studied by two-dimensional correlation ATR-FTIR spectroscopy. Food Chem. 164, 179–184. https://doi.org/https://doi.org/10.1016/j.foodchem.2014.05.044

Xie, F., Dowell, F.E., Sun, X.S., 2003. Comparison of near-infrared reflectance spectroscopy and texture analyzer for measuring wheat bread changes in storage. Cereal Chem. 80, 25–29. https://doi.org/10.1094/CCHEM.2003.80.1.25

Zhao, Y., Teixeira, J.S., Gänzle, M.M., Saldaña, M.D.A., 2018. Development of antimicrobial films based on cassava starch, chitosan and gallic acid using subcritical water technology. J. Supercrit. Fluids 137, 101–110. https://doi.org/https://doi.org/10.1016/j.supflu.2018.03.010

Zhong, Y., Cavender, G., Zhao, Y., 2014. Investigation of different coating application methods on the performance of edible coatings on Mozzarella cheese. LWT - Food Sci. Technol. 56, 1–8. https://doi.org/10.1016/j.lwt.2013.11.006

Zhu, Y., Bhandari, B., Prakash, S., 2019. Tribo-rheology characteristics and microstructure of a protein solution with varying casein to whey protein ratios and addition of hydrocolloids. Food Hydrocoll. 89, 874–884. https://doi.org/10.1016/J.FOODHYD.2018.12.005

I

Characterization of composite edible films based on Pectin/Alginate/Whey Protein concentrate

Manuscript

Nallan Chakravartula SS., Balestra F., Lotti N., Soccio M., Siracusa V., Dalla Rosa M. (2019)

Characterization of composite edible films based on Pectin/Alginate/Whey Protein concentrate

Swathi Sirisha Nallan Chakravartula[a], Federica Balestra[a], Nadia Lotti[b], Michela Soccio[b], Marco Dalla Rosa[a], Valentina Siracusa[c],*

[a] *Department of Agricultural and Food Sciences- DISTAL, University of Bologna, Campus of Food Science, P.zza Goidanich 60, 47521 Cesena, Italy; swathisirisha.nalla2@unibo.it (S.S.N.C.); federica.balestra@unibo.it (F.B.); marco.dallarosa@unibo.it (M.D.L.)*

[b] *Department of Civil, Chemical, Environmental and Materials Engineering, University of Bologna, Via Terracini 28, 40131 Bologna, Italy; nadia.lotti@unibo.it (N.L.), m.soccio@unibo.it (M.S.)*

[c] *Department of Chemical Science, University of Catania, Viale A. Doria 6, 95125 Catania (CT), Italy; vsiracus@dmfci.unict.it (V.S.)*

* Corresponding author: vsiracus@dmfci.unict.it

Abstract

Composite edible films from different proportions of Pectin (P), Alginate (A) and whey protein concentrate (WP) were formulated with a simplex centroid mixture design for which the physico-chemical characteristics were determined to understand the effects of individual components. The studied matrices exhibited good film forming capacity, except whey protein at chosen concentration with thickness, elastic and optical properties dependent on the solution viscosity. Whey protein component lowered the viscosity of the solutions followed by alginate, while, pectin resulted in higher viscosities. Also, WP component lowered the mechanical strength as well as affinity to water decreased as seen by increasing contact angle. The effect of pectin was reflected in the yellowness index whereas; alginate and whey protein affected the opacity of films. Whey protein favoured higher opacity, lower gas barrier values and dense structures resulting from the polysaccharide-protein aggregates. All films displayed good thermal stability with degradation onset temperatures higher than 170°C.

Keywords: biopolymers; edible film; composite film; physical-chemical properties; thermal characteristics; barrier properties; response surface.

[1]

[1]List of symbols and abbreviations

P- Pectin; A- Alginate; WP- Whey proteins concentrate; T.S.S- Total soluble solids; Δe- Total colour difference; YI- Yellowness Index; σ^B- Tensile strength; E- Elastic modulus; ε^B- Elongation at break; WVP- Water vapour permeability; WCA (Θ)- Water contact angle; DSC- Differential scanning calorimetry; TGA- Thermogravimetric analysis

1. Introduction

The changing concerns of consumers and industry increased research in edible films and coatings for both application on foods and packaging, due to their bio-degradability and potential use as carrier systems for active substances (Campos, Gerschenson, & Flores, 2011; Falguera, Quintero, Jiménez, Muñoz, & Ibarz, 2011; Ramos, Fernandes, Silva, Pintado, & Malcata, 2012). Edible films are defined as thin layer(s) of edible polymers formed on surfaces or wrapped around food products as primary packaging, and generally with supplementary benefits. The terms edible films and coatings are defined by their method of application, with films applied after being formed and coatings formed directly onto the product surfaces (Falguera et al., 2011). These films and coatings are widely reported to have uses in limiting moisture, lipid migration and have found varied applications in conservation of highly perishable products, especially, fresh and minimally processed fruits, vegetables; semi-perishable products like processed meats (sausages) and cheese; also as barriers to reduce oil absorption in fried foods as extensively reviewed (Frédéric Debeaufort, Quezada-Gallo, & Voilley, 1998; Kurek, Ščetar, & Galić, 2017; Otoni et al., 2017; Tongnuanchan & Benjakul, 2014).

Polysaccharides, are widely used in forming edible coatings and films, and are characterized by poor gas and water barrier properties, usually acting as sacrificing agents for moisture loss (Kester & Fennema, 1986). Proteins are known for their ability to form films, similar to that of polysaccharides and are in general characterized by excellent mechanical and barrier properties, albeit with poor water vapour barrier property. Literature suggests various methods to improve the properties of edible films, and one approach is blending polysaccharides and proteins, an area of interest in material sciences to develop new functionalities within well characterized components or new components (Coughlan, Shaw, Kerry, & Kerry, 2004; Vieira, da Silva, dos Santos, & Beppu, 2011). The water barrier efficiency is important to decrease the dehydration in fresh foods, whereas prevent loss of crispiness and moisture migration in dry foods.

Pectin is an anionic polysaccharide present in most plant tissues and is made up of 1,4-D-galacturonic acids with fully or partially methyl esterified carboxyl groups and interspersed with (1→2)-α-L-rhamnose residues (Sato, Oliveira, & Cunha, 2008). It is a major by-product of fruit and vegetable industry and is widely studied for formation of edible films (Galus & Lenart, 2013;

Galus, Turska, & Lenart, 2012; Silva, Bierhalz, & Kieckbusch, 2009). However, pectin's alone are characterized by higher water vapor permeability and act as sacrificial agents to prevent dehydration. Alginates are structural polysaccharides made up of alternating blocks of (1,4)-linked mannuronic acid (M) and glucuronic acid (G) residues, extracted from brown algae (Lee & Mooney, 2012). These ionic linear co-polymers are known to be polyuronates and under suitable pH, soluble solids form synergistic gels with pectin and are also studied in preparation of edible films (Galus & Lenart, 2013).

Whey protein is a by-product from the cheese making industry, which has received great attention from nutrition to polymer industry in form of concentrates and isolates which contain 20% to 80% and >90% protein, respectively. They have been observed to possess excellent mechanical and barrier properties as studied and reviewed by various researchers (Banerjee & Chen, 1995; Galus & Kadzińska, 2016a; Osés et al., 2009; Ramos et al., 2012). They are characterized by their uniform negative charge of the protein chain, unlike casein and are comprised majorly of beta-lactoglobulins, alpha-lactalbumins, serum albumins and immunoglobulins. Many studies investigated the potential use of whey protein isolates and concentrates to form edible films and coatings (Khwaldia et al. 2004). Whey protein films are transparent, bland, flexible, and have good water, oxygen, aroma and oil barrier characteristics. Thermal degradation denatures whey protein and results in more cohesive and stronger films than native proteins (Pérez-Gago, Nadaud, & Krochta, 1999).

Composite films can be designed to achieve synergistic effects of the pure components, but are largely dependent on the characteristics and compatibility of the individual components. The blending of two or more hydrocolloids can result in improved film properties reflecting the properties of both individual components. studies were carried out extensively on forming films with two polysaccharides, polysaccharide-protein, and polysaccharide-protein-polysaccharide films (Basiak, Galus, & Lenart, 2015; Galus & Lenart, 2013; Kurek, Galus, & Debeaufort, 2014). However, it is interesting to understand the three way interaction of these components for forming edible coatings and films.

Therefore, the objective of this study was to investigate the Pectin-Alginate-whey protein concentrate blend solutions for physico-chemical characteristics and films for selected physico-chemical, mechanical and thermal properties by use of simplex centroid design.

2. Materials and Methods

2.1. Materials

The raw materials used for the preparation of films were Pectin (from citrus peel, Galacturonic acid ≥ 74%, Sigma, Denmark), Sodium alginate (Sigma Aldrich, China) and Whey protein concentrate (Protein ˷80%, Prodotti-Gianni, Italy). Glycerol (≥99.5% Purity, Sigma Aldrich, Germany) and Tween®20 (Sigma Aldrich, Germany) were used as plasticizer and emulsifier respectively.

2.2. Film formation and conditioning

The components for each composition as reported in table 1, were weighed and heated on a heating plate with magnetic stirrer (ARE Heating Magnetic stirrer, Velp Scientific) to 75°C (±0.1°C) for 45 min with continuous stirring until complete dissolution. The solutions were cooled to room temperature and then homogenized at 6000 rpm for one minute (IKA Ultra Turrax® T 25 Digital, Germany) and degassed under vacuum (100mb) with a pump (SC 920, KNF ITALIA, Milano) for ten minutes (F. Debeaufort, Martin-Polo, & Voilley, 1993). Subsequently 10 (±1) g of solutions were plated in 9 cm diameter petri-dishes and dried for 18-24h at 25(±1) °C and 50(±2) % relative humidity in controlled atmospheric chamber (Constant Climate Chamber with Peltier technology, model HPP 108/749- Memmert, Germany). The dried films are detached from the Petri-plates carefully by peeling, stored in desiccator (silica gel) prior to testing.

2.3. Film forming solutions characterization

The film forming solutions (FFS) were monitored at room temperature for pH by digital pH meter (EUTECH Instruments, Cyberscan mod.510, D, Italy) and T.S.S (°Brix) by digital refractometer (Atago Co. Ltd, mod. PR-1, Tokyo, Japan). Density was calculated as ratio of weight to volume (g/ml) with analytical weighing balance (Kern & Sohn, model: ABJ 220-4M, Germany) to the nearest 0.0001g according to Zhong et al., (2014).

Rheological measurements were performed at 25°C, with a stress-strain rheometer (model: MCR 102, Anton Paar GmbH, Inc., Graz, Austria), using a coaxial cylinder (CC27) apparatus. Samples of 20ml in duplicates were deposited carefully into the sample holder and pre-sheared at $10s^{-1}$ and rested for 60s for equilibration. Steady-state flow measurements were carried out in the range of $3s^{-1}$to $500s^{-1}$ with a rate of $10s^{-1}$/min in 30 min. The resulting flow curves (viscosity vs. Shear rate) were fitted to using Carreau and power law models to obtain selected rheological parameters namely, flow index (n, dimensionless) and consistency index (K, $Pa.s^{-n}$).

2.4. Edible Film characterization

2.4.1. Optical parameters

The colour of the films was measured with a Spectrophotocolorimeter (HunterLab ColorFlexTM, mod. A60-1010-615, U.S.A) using CIE L*a*b* parameters. The instrument was calibrated with a black tile and white standard tile. The white standard with L*: 93.47, a*: -0.83 and b*: 1.33 was used as background for colour measurements under illumination D65 (6500K). The total colour difference (ΔE), whiteness index (WI) and yellowness index (YI) were calculated as described by Saberi et al., (2016).

The opacity of the films was calculated as ratio of absorbance to the film thickness using an UV-VIS spectrophotometer (Shimadzu Italia srl, mod. UV-1601, Italia) according to Galus and Kadzinska, (2016). Rectangular film strips (1cm x 4cm) of films were placed directly in glass cuvette and absorbance was measured at 600nm.

2.4.2. Microstructure

The film structural morphology was determined by using a Nikon upright microscope (Eclipse Ti-U, Nikon Co.) with a standard light. Samples were observed in black and white and the images were recorded at a 4x magnification.

2.4.3. Thickness and mechanical properties

Film thickness was measured at ten random points as using a thickness tester DM-G with a digital dial indicator (model: MarCartor 1086, Mahr GmbH, Germany) with associated DM-G software. The minimum, maximum and average of each reading was recorded in triplicates at room temperature and reported as mean thickness value.

Mechanical properties were evaluated using Texture Analyser (ModZ2.5, Zwick Roell) equipped with 500N load cell in accordance with ASTM D882-09 (standard test method for Tensile properties of Thin plastic sheeting-2009). Rectangular strips (5mm width x 50mm length) were loaded with an initial grip separation of 20mm and crosshead speed of 5mm/min. Tensile strength (σ^B, MPa), Elongation at break (ε^B, %) and Elastic modulus (E, MPa/%) were evaluated by associated software for an average of 6 different samples.

2.4.4. Moisture

The moisture content was measured according to Galus & Lenart, (2013) with 1.5 x 1.5cm films weighed to the nearest ±0.0001 g and dried in hot air oven (UF110, Memmert, Germany) at 105 °C for 4h in triplicates and calculated as percent loss in the weight compared to that of initial sample weight.

2.4.5. Water Contact Angle

Static contact angle (θ) of the films was measured by sessile drop method using KSV CAM101 (KSV Instrument, Elsinki, Finland) as described by Siracusa et al., (2018). The measurements were carried out on both sides of the films and reported as an average of at least 5 individual determinations on each side.

2.4.6. Water vapour barrier properties

The gravimetric method of ASTM E-96-95 (2005) and Cecchini et al., (2017) with modifications was used to determine the WVP of films. In brief, glass cups with cylindrical base were deposited with 4 g of $CaCl_2$. The support side of the film was fixed onto the opening so as to face the low RH environment with paraffin in triplicates and placed in pre-equilibrated atmospheric chamber (Constant Climate Chamber with Peltier technology, model HPP 108/749- Memmert, Germany) controlled at 25±1 °C and 50 (±2) % R.H. The weight of the assembled cups was periodically recorded for 72h until $CaCl_2$ was visibly wet. The water vapour transfer rates were determined from slope of weight gain versus time plots for each sample as in equation (2);

$$WVTR\ (g.cm^{-2}h^{-1}) = \frac{\Delta m}{\Delta t} * \frac{1}{A} \quad (1)$$

Where, Δm is weight gain of the test setup (g), Δt is time (h) and A is the area of film exposed which was 23.76cm^2. Water vapour permeability was calculated by the following equation (3);

$$WVP\left(g.mm.cm^{-2}Pa^{-1}h^{-1}\right) = WVTR * \frac{x}{\Delta P} \quad (2)$$

Where, x is the average thickness of the films in mm and ΔP is partial difference of water vapour between the 50% RH of the chamber and 0% RH of $CaCl_2$, which was 1579.09Pa.

2.4.7. Gas barrier properties

Oxygen and carbon dioxide gas barrier properties were measured using a manometric method on a Permeance Testing Device, type GDP-C (Brugger Feinmechanik GmbH), in accordance with the ASTM 1434(standard test method for determining gas permeability characteristics of plastic film and sheeting, 2009), DIN 53536 (gas permeability determination), ISO 15105-1(Plastics film and sheeting determination of gas transmission rate-Part I : Differential pressure methods, 2007) and with the Gas Permeability Testing Manual-2008 (Registergericht München HRB 77020, Brugger Feinmechanik GmbH). The film sample of approximately 3x3cm in size was mounted between the two chambers of the equipment with the help of a film mask. The top chamber was filled with the dry test gases at ambient pressure and subsequent gas permeation was determined by evaluating the pressure increase in the evacuated bottom chamber. Test conditions used were: 23°C, gas stream of 100 cm^3/ min; 0% of Gas RH; sample area of 0.785 cm^2 with the temperature regulated by external thermostat (HAAKE-circulator DC10-K15 type, Thermoscientific, Selangor Darul Ehnsan, Malaysia). The gas transmission rate (GTR) value was determined considering the pressure increase in relation to the duration of the test and the volume of the gas. Method B with evacuation of bottom chamber was employed in the analysis, as reported in the Gas Permeability Testing Manual (2008). 100% dry pure food grade gases of O_2 and CO_2 were used.

2.4.8. Thermal analysis

Differential Scanning Calorimetry (DSC) test to evaluate the phase change enthalpies and temperatures were carried out using a Perkin-Elmer type Pyris DSC-6 differential scanning calorimeter (Waltham, MA, USA), equipped with a liquid sub-ambient accessory and calibrated with high purity standards. Polymer films were cut into small pieces of about 2 mm^2 and 10-12 mg in weight and placed in a 50 µL sealed aluminum pan. After an isotherm of 5 minutes at -20°C, weighed samples were heated with a scanning rate of 10°C/min, from -20 to 280°C (first scan) and then, after a further isotherm of 2 minutes at 280°C, were cooled to -20°C at a rate of

80°C/min. Finally, after an isotherm of 3 minutes, samples were reheated from -20°C to 280°C at 10°C/min (second scan). All the experiments were performed under nitrogen flow (20 cm^3/ min). The melting temperature (T_m) was determined as the peak value of the endothermic phenomena in the DSC curve. The melting enthalpy (ΔH_m) of the crystal phase was calculated from the area of the DSC endothermic peak and T_m values were collected from the first scan.

Thermo-gravimetric Analysis (TGA) was carried out under nitrogen atmosphere by means of a Perkin Elmer TGA7 apparatus (Waltham, MA, USA). Gas flow of 30 mL/min and heating scan of 10°C/min, over a temperature range 40–800 °C, were used for the analyses. Initially, the samples were held at 40 °C for 1 min.

2.4.9. Fourier Transform Infrared Analysis

Absorbance spectra were collected on a Perkin Elmer FTIR (Waltham, MA, USA) by attenuated spectroscopy over the range 650 - 4000 cm^{-1}, with a resolution of 4.0 cm^{-1}. The results are presented as an average of 64 scans recorded on each sample. The experiments were performed at room temperature, directly on the samples, without any preliminary treatment.

2.5. Experimental Design and Analysis

An augmented simplex centroid mixture design was used to find the optimum combination of constituents using Statistica (*Version 8.0)*. The 10 runs obtained, as in table 1 were coded as $S_{1\text{-}10}$ (P: A: WP) where 'S' represents sample, the numbers '1-10', the different formulations and P: A: WP represents different combinations of pectin (P), alginate (A), and whey protein concentrate (WP). The proportions of components are dependent on each other and hence the selection of design points is based on the basic constraint for the mixture design as in equation (1);

$$\sum_{i=1}^{n} x_i = x_1 + x_2 + \ldots + x_n = 1 \qquad (3)$$

Where x_i is the proportion of 'i^{th}' component in the mixture and 'n' is the number of components in the mixture. From the preliminary experiments pectin, alginate and whey protein concentrate were chosen as input factors with their proportions restricted to a total sum of '3' for actual values by weight, i.e.,

- $0 \leq$ P (Pectin) ≤ 3
- $0 \leq$ A (Alginate) ≤ 3

- $0 \leq$ WP (Whey Protein Concentrate) ≤ 3

The concentrations of glycerol and Tween®20 were determined from preliminary experiments to a constant of 1% and 0.1% concentrations respectively. Water was considered as a bulk agent and was not included in the design.

Table 1. Composition of the film forming solutions formulated with Pectin, Alginate and Whey protein concentrate by Simplex centroid mixture design.

Sample	% W/W		
	P	A	WP
S_1	1.00	1.00	1.00
S_2	3.00	0.00	0.00
S_3	1.50	1.50	0.00
S_4	0.00	1.50	1.50
S_5	1.50	0.00	1.50
S_6	0.00	0.00	3.00
S_7	2.00	0.50	0.50
S_8	0.50	2.00	0.50
S_9	0.50	0.50	2.00
S_{10}	0.00	3.00	0.00

*P- Pectin, A- Alginate, WP- Whey protein concentrate

The coefficients of the models adjusted for each response were estimated by the polynomial models. The models were subjected to analysis of variance (ANOVA) to assess the level of significance, the coefficient of determination (R^2) and the lack of fit of the model. The program Statistica 7.0 (StatSoft, 2004) was used to generate the experimental design and regression coefficients, as well as for construction of the graphs**.** The analysis of variance (ANOVA) with Tukey HSD for homogenous variances and Kruskall-wallis tests for non-homogenous variances were performed to detect significant differences in properties of films. The significance level used was 0.05.

3. Results and Discussions

3.1. Model fitting

Table 1 presents the mixture design for film forming solutions and films made from Pectin, Alginate and Whey protein concentrate. The dependent and independent variables were fitted to linear, quadratic and cubic models. The residual plots and normality plots were generated to verify the goodness of model. The analysis of variance was evaluated for the coefficients of the models

which were significant ($p \leq 0.05$) and with R^2 values ≥ 0.75. The models with high r-square, significant p-value and insignificant lack of fit were chosen. Following the stated parameters selected experimental responses and their regression coefficients are presented in table 2.

3.2. Properties of Film forming Solutions

The pH of the film forming solutions (FFS) was measured to understand the ionic nature as they affect the stability, functionality and characteristics of the solution and films (Zhong et al., 2014). It varied significantly between different solutions and ranged from 3.43 to 6.29 as reported in table 3. The pH was observed to be influenced by the components, with Alginate, whey protein interaction increasing and pectin decreasing the pH to acidic values. This is expected as commercial pectin is known to form solutions of pH 3.0 - 4.0.

Total soluble solids and density were observed to be 3.5 (±0.2) °Brix and 0.94 g/L (±0.03), respectively. There were no significant differences between compositions and the slight variation between values might be a function of components and their interactions. This might also be due to degree of bonding between the hydrophilic groups of the polysaccharides with the solvent, water as observed in sodium alginate/chitosan solutions by Zhong et al., (2014).

Viscosity of the film forming solution is a detrimental parameter for the levelling of coating, spreadabilty, absorption by substrate, adhesion to substrate and also the final film thickness, uniformity and microstructure (Cuq, Aymard, Cuq, & Guilbert, 1995; Peressini, Bravin, Lapasin, Rizzotti, & Sensidoni, 2003; Zhong et al., 2014). All the solutions exhibited characteristic shear thinning behaviour with decrease in viscosity as shear rates increased. In particular, for edible coatings some authors suggest a viscosity less than 700mPa.s for casting and film forming (Peressini et al., 2003). All the film forming solutions tested were found to have viscosity in range of 120 to 250 mPa.s at a shear rate of 100s-1 except for samples S4, S6, and S9 with WP content higher than 1% w/w had values less than 50 mPa.s. Furthermore,T the rheological data were fitted to Carreau model and the parameters (a, p and Ƞ0) with R2 > 0.75 are presented in Table 3, except for S5 and S6 which fitted power law model. The decrease in values of flow behaviour index indicated increase in pseudo-plasticity of the fluids, and consequently increase in consistency coefficient indicates indicated higher apparent viscosity at a given shear rate. All the solutions exhibited higher Ƞ0 values and lower ‘a’ (relaxation time) values with exception of S4 and S1.

These higher Ƞ0 values indicate strong interactions between the bio-polymers, and subsequently the lower 'a' (relaxation time) values, indicate the requirement of higher shear stress for structural breakdown and lower time for structural recovery respectively. Moreover, the presence of WP tended to decrease the viscous nature of pectin and alginate which might be attributed to the associative interactions between the polysaccharide and protein components. Similar inferences were found by Zhu, Bhandari, & Prakash, (2019) in case of casein and whey protein isolates in combination with gelatin, pectin, and carrageen.

Table 2. Regression coefficients of the response variables for pseudo-components and analysis of variance for the fitted models

Term	Response variables									
	Y_1 (pH)	Y_2 (thickness)	Y_3 (Opacity)	Y_4 (ΔE)	Y_5 (YI)	Y_6 (Θ)	Y_7 (σ^B)	Y_8 (E)	Y_9 (WVP)	Y_{10} (MC)
P (β_1)	3.43	34.32	3.57	11.26	9.63	40.21	58.25	1473.6	1.59	8.97
A(β_2)	5.83	40.70	3.35	8.75	4.31	55.40	39.14	606.9	1.92	6.33
WP (β_3)	6.21	2.81	0.27	0.73	0.05	0.38	2.60	0.3	0.12	0.44
P X A (β_{12})	-2.07	11.99	-3.07	12.94	2.40	15.76	20.54	-327.9	-0.88	-
P X WP (β_{13})	-1.40	185.94	6.25	7.49	30.87	163.75	-87.07	-1504.5	7.09	20.23
A X WP (β_{23})	1.03	107.07	12.22	15.08	38.10	206.07	-5.23	413.4	4.02	36.04
P X A X WP (β_{123})	-3.31	-398.45	54.96	-	-76.88	291.07	-	-2410.9	-14.69	-
$\beta_{12(1-2)}$	5.08	-	-	-	4.01	-8.90	-	-3062.9	-	-
$ß_{23(2-3)}$	0	-	-	-	0	0	-	-	-	-
$\beta_{13(1-3)}$	0.06	-	-	-	-31.54	-316.54	-	-2043.4	-	-
Model-p	0.00	0.00	0.00	0.00	0.00	0.00	0.00	0.00	0.00	0.00
R^2	0.99	0.88	0.79	0.84	0.97	0.99	0.86	0.98	0.87	0.81
Lack of fit	0.41	0.12	0.09	0.09	0.29	0.00	0.12	0.92	0.14	0.01

3.3. Edible Film Characterization

All the films were visibly transparent to translucent, flexible and easily detached from the petri plates, without cracks or pores except WP when used at a concentration of 3% did not form any film, as expected due to the low protein concentration chosen. This might be due to the fact that

formation of whey protein films usually requires 8-12% (w/w) of protein solutions (Khwaldia et al., 2004; Perez-gago & Krochta, 2001).

3.3.1. Colour and opacity

The optical properties of edible films are an essential sensory aspect for edible films and coatings to be accepted by consumers. They are generally expected to be colourless similar to that of polymeric packaging materials or as close to the food colour onto which the coating will be applied (Galus & Kadzińska, 2016a; Galus & Lenart, 2013). The alginate films were more transparent visually followed by pectin and whey protein concentrate containing films were. Also, the films were glossier on the support side compared to the air side, which were more dull and rough. Similar observations have been reported by Kokoszka et al., (2010) in their study on whey protein isolate films. In context of colour, the total colour difference (ΔE), and yellowness index (YI) were evaluated as presented in table 4.

Table 3. Physico-chemical, rheological properties of the edible coating solution

Sample	Carreau Parameters			
	pH	p	a	η◦
S_1 (1:1:1)	4.8 ± 0.01^{d}	0.10 ± 0.00^{de}	0.24 ± 0.00^{cd}	247.0 ± 1.27^{cd}
S_2 (3:0:0)	3.4 ± 0.01^{a}	0.08 ± 0.01^{cb}	0.02 ± 0.00^{ab}	272.0 ± 7.00^{d}
S_3(1.5:1.5:0)	4.1 ± 0.01^{b}	0.07 ± 0.00^{abc}	0.05 ± 0.008^{c}	249.0 ± 1.53^{cd}
S_4(0:1.5:1.5)	6.3 ± 0.03^{h}	0.07 ± 0.01^{ab}	0.01 ± 0.00^{a}	46.2 ± 2.26^{a}
S_5(1.5:0:1.5)	4.5 ± 0.04^{c}	*	*	*
S_6(0:0:3)	6.2 ± 0.06^{h}	*	*	*
S_7(2:0.5:0.5)	4.1 ± 0.03^{b}	0.05 ± 0.00^{a}	0.05 ± 0.01^{c}	154.0 ± 7.83^{b}
S_8(0.5:2:0.5)	5.0 ± 0.1^{e}	0.08 ± 0.00^{bd}	0.02 ± 0.00^{a}	143.0 ± 2.47^{b}
S_9(0.5:0.5:2)	5.5 ± 0.01^{f}	0.05 ± 0.00^{a}	0.20 ± 0.06^{cd}	45.1 ± 0.88^{a}
S_{10}(0:3:0)	5.8 ± 0.03^{g}	0.09 ± 0.01^{de}	0.02 ± 0.00^{ab}	224.0 ± 6.95^{c}

Means ± SD in a column without a common superscript letter differ significantly (P<0.05)
η0 = viscosity at low shear rate, a = characteristic time constant, p = dimensionless Carreau exponent
**Sample 5 (P: A: WP = 1.5: 0: 1.5) and Sample 6 (P: A: WP = 0:0:3) were modeled using Power-law equation as they did not fit Carreau model. The theoretical values of 'k (consistency index, Pa.s-n) and 'n' (flow behavior index, dimensionless) were k=0.912 and n=-0.352 for S5and k=0.002 and n=1.00 for S6 respectively.*

The total colour difference values ranged from 8.0 to 14.50, with P-based sample showing higher values and WP and A generally decreasing the values. Similar behaviour was observed for Pectin by Galus & Lenart, (2013) and Siracusa et al., (2018) in P/A based films. Furthermore, the yellowness Index (YI) was calculated to estimate the perceived yellowness, as a low yellow value is generally favoured (Saberi et al., 2016). The interaction of P and WP was observed in particular

to increase the yellowness index, probably due to the pectin which usually favours yellow coloration. A similar inference was found by Yasmin, Saeed, Pasha, & Zia, (2018) in their study of Pectin-whey protein beads with b* value increasing with higher pectin content. Furthermore, the opacity was observed to be ranging from 2.9 to 5.9 mm^{-1} with significant difference among samples ($p>0.05$). The presence of WP was observed to increase the opaqueness which might be due to the formation of soluble or insoluble 'Protein-polysaccharide' aggregates and presence of immiscible dispersed phases in the composite films (Ghosh & Bandyopadhyay 2012; Galus & Kadzińska 2016). Also, only a moderate correlation ($r^2< 0.75$) was observed between ΔE and opacity which might be due to the interactions of components, network rearrangement and formation of aggregates during drying (Ozdemir & Floros 2008).

3.3.2. Microstructure

The micrographs of the film surfaces were studied to detect the surface homogeneity and structure as presented in figure 1. It can be seen that A-based film (S_{10}) presented a more homogenous and uniform structure than P-based film (S_2), as also observed by Siracusa et al., (2018) for P/A films. However, blend films were observed to have non-uniform surfaces with formation of aggregates which can be attributed to the composition, miscibility and arrangement of the Polysaccharide-Protein matrices (Galus & Lenart, 2013). In particular, the films were noticed to be grainier and dense for secondary interactions (Polysaccharide-polysaccharide, polysaccharide-protein) and with agglomerates for tertiary interactions (polysaccharide-polysaccharide-protein). These observations are in accordance with the increased opacity in the films due to protein-polysaccharide interactions as also observed by Al-Hassan and Norziah, (2012); Liu et al.,(2007) for starch-gelatin films and pectin-gelatin films.

3.3.3. Mechanical Properties

The thickness of composite films varied from 41µm to 50µm, with exception of P (S_2) and P: WP (S_5) films recording extreme values of 36 µm and 64 µm, respectively, as reported in table 4. The interactions of components, as also reported by Galus & Lenart (2013) were observed to affect the thickness values ($p<0.05$) in the following order of interactions, A>P/WP>P>A/WP> P/A/WP. This variance in thickness despite constant weight of solution casted can also be attributed to the viscosity and thickness of the dispersion. These factors were found to effect the film drying

kinetics, final thickness and structure of the film (Debeaufort & Voilley 2007; Kokoszka et al. 2010).

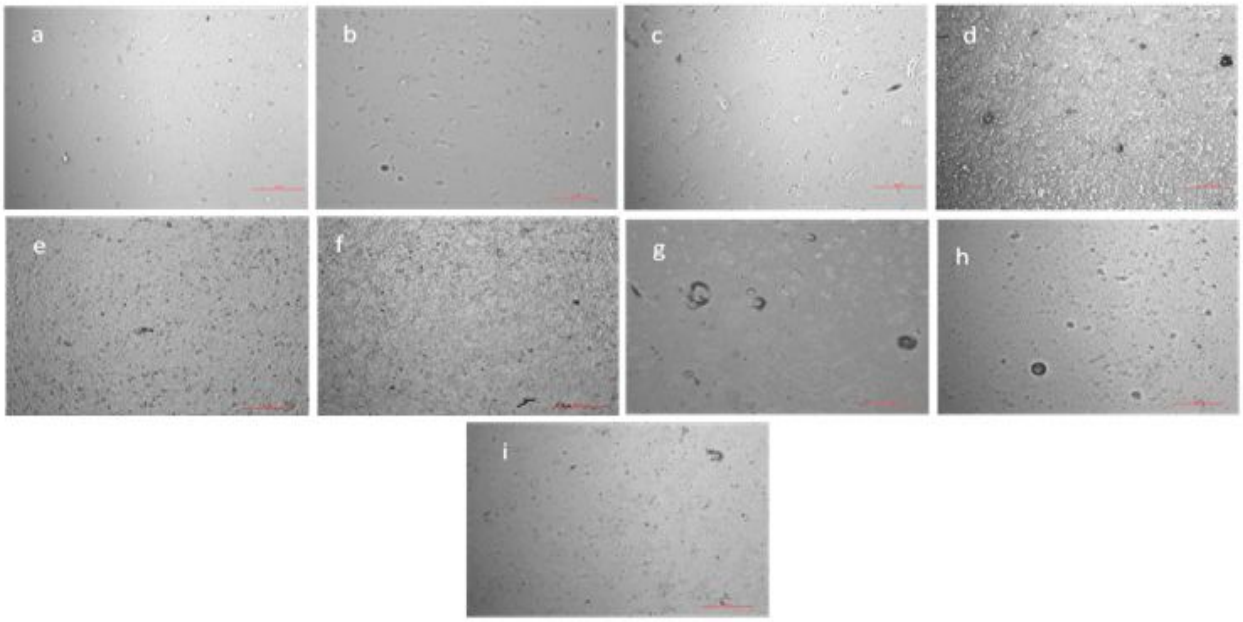

Figure 1. Surface Micrographs of the edible films with P: A: WP (a) S_2 (b) S_{10} (c) S_1 (d) S_3 (e) S_4 (f) S_5 (g) S_7 (h) S_8 (i) S_9

The mechanical properties of the edible films in terms of tensile strength at break (σ^B), elongation at break (ε^B) and elastic modulus (E) representing the film's mechanical resistance, plasticity and stiffness or elasticity respectively are reported in table 4. These material characteristics are related to the chemical structure of the films. Generally, films with high tensile strength have lower values for elongation at break and hence must be estimated simultaneously (Galus & Lenart, 2013; Silva et al., 2009). In fact, only P (S_2), A (S_{10}) and P/A (S_3) films exhibited this trend as can be observed from the data whereas, for composite films with this trend was not observed.

The tensile strength values ranged from 11 Mpa to 62 Mpa with highest values recorded for samples S_2 (3:0:0) and S_3 (1.5:1.5:0) and lowest values for S_9 (0.5:0.5:2) and S_5 (1.5:0:1.5). P, A and interaction of P/WP were observed to be the the primary factors affecting the tensile strength of the films, with P, A increasing and P/WP interaction decreasing the values. However, the interactions between A/WP though non-significant, generally decreased the tensile strength. Similar trend was observed in case of elastic modulus (E) with P, A increasing the value, whereas, the linear interaction between A/WP and P/WP decreased the value. Also, these results were

positively correlated (r^2>0.75) to the film forming solution viscosity. This might be due to the fact that more water was available for plasticization rendering flexible films at lower viscosities. However, lower values of elastic modulus can be considered desirable, as higher values indicate stiffer and brittle films. Subsequently, the elongation at break was effected positively by the interaction between A/WP with increase in the value, indicative of higher elasticity. This decrease in tensile strength and elastic modulus upon addition of whey protein was similar to that of whey protein isolate and whey protein concentrate films observed by Ramos et al., (2013) with glycerol concentrations ≥ 50% of the formulation.

Table 4. Physico-chemical and mechanical properties of the edible films

Sample	Thickness (μm)	ΔE	YI	Opacity	E (Mpa)	σ^B (MPa)	ε^B (%)
S_1 (1:1:1)	45± 4^{b}	8.6±0.4^{a}	9.3±0.9^{cd}	6.0±0.2^{f}	444±107^{abc}	23±6^{abc}	22±9
S_2 (3:0:0)	36± 1^{a}	11.3±1.1^{b}	9.6±1.1^{cd}	3.4±0.1^{bc}	1467±303^{d}	62±20^{d}	20±8
S_3 (1.5:1.5:0)	43± 2^{b}	14.1±1.0^{c}	7.5±0.4^{b}	2.9±0.1^{a}	958±240^{d}	61±11^{d}	23±10
S_4 (0:1.5:1.5)	47± 1^{bc}	8.5±0.5^{a}	11.6±0.5^{ef}	5.0±0.2^{e}	406±145^{ab}	22± 9^{abc}	40±23
S_5 (1.5:0:1.5)	64 ± 2^{d}	8.1±0.6^{a}	12.5±0.9^{f}	3.0±0.1^{ab}	352±140^{ab}	13 ± 4^{ab}	16±7
S_7 (2:0.5:0.5)	43 ± 2^{b}	11.5±0.9^{b}	9.2±1.3^{cd}	5.3±0.2^{e}	555±129^{abc}	27 ± 5^{abc}	26±4
S_8 (0.5:2:0.5)	41± 1^{b}	11.42±1.0^{b}	8.5±0.5^{bc}	4.1±0.3^{d}	746±127^{cd}	31±10^{bc}	24±12
S_9 (0.5:0.5:2)	49± 1^{c}	8.8±1.0^{a}	10.7±0.4^{de}	5.2±0.2^{e}	288±59^{a}	11 ± 3^{a}	19±2
S_{10} (0:3:0)	42± 1^{b}	8.6±0.8^{a}	4.3±0.1^{a}	3.7±0.4^{cd}	607±243^{bc}	39±16^{c}	27±14

Means ± SD in a column without a common superscript letter differ significantly (P<0.05)

3.3.4. Moisture content (MC), water vapour permeability (WVP) and Water contact angle (WCA)

The moisture content of the films was evaluated for the residual water content and the water bonding capacity of the films. The moisture content of the tested films ranged from 6.62 to 13.72% (table 5) with significant influence of WP and linear interactions. The hygroscopic nature of glycerol, favours the absorption of water molecules and formation of hydrogen bonds in film matrix, which leads to higher moisture content of the films as in film samples S_4 (Galus et al., 2012). However, the moisture content values for all the films were observed to be lower than those presented for pectin, alginate or whey protein films (Ramos et al., 2013).

Water vapour permeability for the tested films ranged from 7.1 to 9.6 (10^{10}g.mm/h.cm.Pa) for different formulations (table 5). P and A-based films recorded lower values whereas, WP slightly

increased the permeability values which could be attributed to the higher number of free hydroxyl groups thereby, enhancing interaction with water and favouring water vapour transmission. Also, this is dependent on the number of polar groups the polymer contains, and on the diffusivity and solubility of water molecules in the film matrix (Gontard, Guilbert, & Cuq, 1992). However, it was interesting to note that the water barrier property of high WP containing films might be attributed to the presence of lactose that exerts plasticizing effect on the polymer which facilitates water transfer. In accordance to the moisture results, the linear interaction of P and A with WP was found to have significant effect on the barrier property.

Table 5. Moisture content (MC), water vapour permeability (WVP) and Water contact angle (WCA) of composite films

Sample	Moisture content (%)	Water Vapour Permeability (10^{10}g.mm/h.cm.pa)	Water Contact Angle (Θ)
S_1 (1:1:1)	12.2±1.7^{cd}	7.9±0.4^{ab}	83±4.1^{de}
S_2 (3:0:0)	8.6±1.1^{ab}	7.3±0.4^{a}	40±2.1^{a}
S_3 (1.5:1.5:0)	6.6±1.3^{a}	7.4±0.3^{a}	51±1.4^{b}
S_4 (0:1.5:1.5)	13.7±1.4^{d}	8.7±1.1^{ab}	79±0.9^{d}
S_5 (1.5:0:1.5)	11.9±0.6^{cd}	9.6±0.5^{b}	60±2.5^{c}
S_7 (2:0.5:0.5)	6.8±1.1^{a}	7.9±0.2^{ab}	51±1.5^{b}
S_8 (0.5:2:0.5)	7.4±0.5^{a}	7.5±0.4^{a}	81±1.2^{de}
S_9 (0.5:0.5:2)	10.8±1.3^{bc}	9.0±0.1^{b}	83±2.1^{e}
S_{10} (0:3:0)	8.5±1.6^{a}	7.2±0.1^{a}	55±1.1^{b}

Means ± SD in a column without a common superscript letter differ significantly (P<0.05)

However, an opposite effect was observed concerning the surface hydrophobicity of the films, with P and A decreasing and WP increasing the surface hydrophobicity as reported in table 5. A water contact angle (θ) of generally θ <65 represents a hydrophilic character and a value θ >65 represents hydrophobic character (Karbowiak, Debeaufort, Champion, & Voilley, 2006; Vogler, 1998)**.** This was observed to be slightly higher on the air side than the support side of the films (data not shown) as also observed in a study on chitosan and whey protein films (Kurek et al., 2014). The lowest value was observed in P-based films, whereas, addition of A and WP significantly increased the WCA from 40° to around 50° and >60° respectively (table 5). The significant lack of fit with full cubic model was due to low pure error; however it did not affect the predicting ability of the model. A, A/WP, P, P/WP, P/A/WP had significant positive influences whereas, the interaction of components was found to negatively affect this response.

Furthermore, a significant positive correlation (r^2> 0.75) was observed between these three parameters confirming the increase in moisture content leads to increased water vapour permeability and hydrophilicity of the films.

3.3.5. Gas Barrier Properties

Gas barrier properties of films for gases, particularly, O_2 and CO_2 are important as they affect the respiration or oxidation reactions in foods and are useful to identify niche applications. The gas transmission rate (GTR) was found to be significantly affected by the composition of the films as can be observed in table 6. The addition of WP in general decreased the transmission rates, although the film exhibited heterogeneous behaviour when observed under optical microscope. Also, CO_2 permeation was in general higher compared to that of O_2. However, the relative permeability of CO_2 to O_2 was observed to be lower in films with WP and is in accordance to the thermal data, confirming the positive role of WP. The gas selectivity ratio (CO_2/O_2) was relatively low for all films with a value below 5.0 equivalent to synthetic polymers except for pectin with a value of 12.4, higher than those observed by Siracusa et al., (2018).

Table 6. Oxygen and Carbon dioxide permeability data for edible films

Sample	O_2 (cm^3/m^2dbar)	CO_2 (cm^3/m^2dbar)	CO_2/O_2
S_1 (1:1:1)	1023±21f	115±2ab	0.1
S_2 (3:0:0)	10±2a	119±2ab	12.4
S_3 (1.5:1.5:0)	16±3a	68±2a	4.3
S_4 (0:1.5:1.5)	83±1c	87±2a	1.0
S_5 (1.5:0:1.5)	49±3b	123±4ab	2.5
S_7 (2:0.5:0.5)	166±1d	303±6c	1.8
S_8 (0.5:2:0.5)	0.00	75±4a	0.0
S_9 (0.5:0.5:2)	149±4d	152±4b	1.0
S_{10} (0:3:0)	438±16e	1043±59d	2.4

Means ± SD in a column without a common superscript letter differ significantly (P<0.05)

3.3.6. Thermal Properties

The effect of protein interaction with polysaccharides on the thermal properties such as temperature at maximum degradation (T_m, °C) and enthalpy of fusion (ΔH_m, J/g) were measured by the first scan of DSC as reported in table 7. The T_g was observed to be ranging from 9.5°C to 14.0°C for different films. However, the observed change in heat capacity was too low to

elaborate the T_g values (Kokoszka et al., 2010). The T_m of P-based film (98°C) was observed to be significantly lower than the A-based film (124°C) and composite films, indicative of higher hydrophilic nature of P-based films, as also observed for water contact angle (Ramos et al., 2013). The films were observed to have a T_m in range of 116°C to 133°C with WP significantly increasing the T_m upon interaction with P. Pure alginate films showed the highest enthalpy, and pure pectin had the lowest values. The presence WP increased the enthalpy values, indicative of increased thermal stability as a consequence of inter chain interactions. P/A/WP films in equal quantities were observed to have both high melting temperature and enthalpy values, indicative of miscibility and polymer interaction.

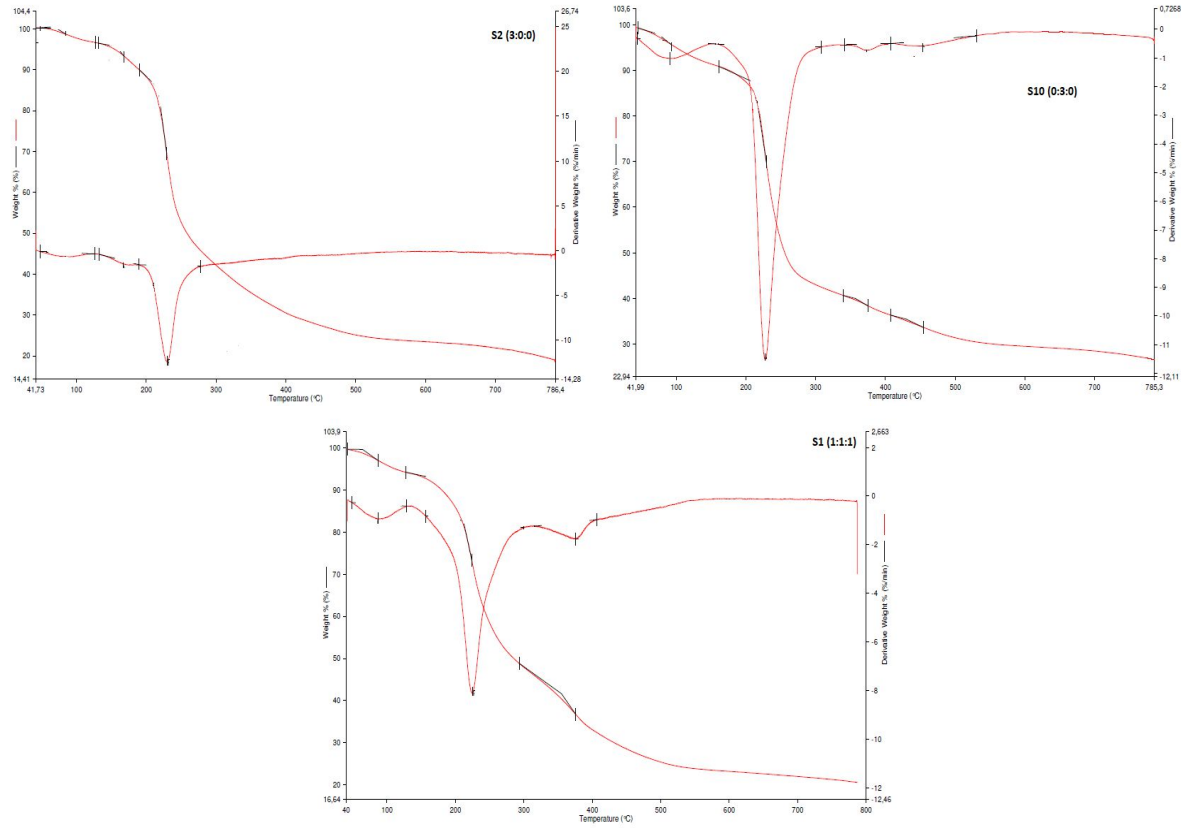

Figure 2. Representative TGA spectra Pectin (S_2), Alginate (S_{10}) and P/A/ WP (S_1) films

The thermal degradation of the films was analyzed by TGA to understand the stability of the films and potential interactions among the macromolecules (Bonilla, Fortunati, Atarés, Chiralt, & Kenny, 2014). Figure 2 depicts representative curves of mass loss and the first derivatives of thermal degradation. All films had similar trend of weight loss with an initial weight loss below 130°C indicative of loss of adsorbed and bound water (Valencia-Sullca, Vargas, Atarés, & Chiralt, 2018). All the films studied exhibited good thermal stability upto 200°C. The degradation

onset was between 175°C to 221°C and the peak was between 217°C to 235°C. The degradation was observed to be sharper in pure pectin and alginate films. In the tertiary blend films the loss of weight was more gradual, typically initiating at slightly lower temperatures than pure films as reported in table 7. The final residue at 600°C was observed to be between 22- 25% except for pure alginate films which was at 29%. The observed results are in accordance to those observed by Ramos et al., 2013 on WPC films and Siracusa et al., (2018) on Alginate-Pectin films.

Table 7. Differential scanning calorimetry and thermogravimetric data for edible films

Sample	Degradation onset (°C)	Degradation Peak (°C)	T_m (°C)	ΔHm (J/g)
S_1 (1:1:1)	207±10 ^{a}	224±1 ^{a}	130±1^{b}	124±5^{cd}
S_2 (3:0:0)	220±4 ^{a}	231±2 ^{a}	98±7^{a}	89±8^{ab}
S_3 (1.5:1.5:0)	205±3 ^{a}	217±1 ^{a}	133±2^{b}	112±11^{abcd}
S_4 (0:1.5:1.5)	222±1 ^{a}	235±1 ^{a}	121±7^{b}	122±10^{cd}
S_5 (1.5:0:1.5)	212±12 ^{a}	229±1 ^{a}	125±6^{b}	93±6^{abc}
S_7 (2:0.5:0.5)	202±0 ^{a}	222±0 ^{a}	127±8^{b}	81±17^{a}
S_8 (0.5:2:0.5)	208±3 ^{a}	222±1 ^{a}	127±2^{b}	139±11^{d}
S_9 (0.5:0.5:2)	175±6 ^{a}	225±3 ^{a}	116±8^{b}	114±10^{abcd}
S_{10} (0:3:0)	211±2 ^{a}	225±4 ^{a}	124±7^{b}	117±19^{bcd}

Means ± SD in a column without a common superscript letter differ significantly (P<0.05)

3.3.7. Infrared spectroscopy

Infrared spectroscopy was used to characterize the interaction between components at molecular level as observed from the shift in typical bands of transmission. The FTIR spectra of the films with various mixtures of P/A/WP are displayed in figure 3. The pure pectin film was characterized by a broad band at 3343cm^{-1}(O-H stretch); a small peak and a shoulder at 2934 cm^{-1} and 2884 cm^{-1} (C-H vibrations of methyl esters); 1744 cm^{-1} (C=O bonds of esters); 1607 cm^{-1} and 1416 cm^{-1} the carboxyl symmetric and asymmetric vibrations respectively and the typical saccharide finger print region from 800 cm^{-1} to 1300 cm^{-1}. The pure alginate film was characterized by a broad band at 3252cm^{-1}(O-H stretch); a small peak and a shoulder at 2920 cm^{-1} and 2853 cm^{-1} (asymmetric C-H vibrations); 1599cm^{-1} and 1407 cm^{-1} the carboxyl asymmetric vibrations and C-OH deformation vibrations respectively and the typical saccharide from 800 cm^{-1} to 1300 cm^{-1}. However, given the case pure WP films were not characterized and literature was used to identify the probable interactions. For the blend films the total number and the intensities of the peaks varied based on their compositions. All the blend films exhibited the typical peaks with respect to the pectin and alginate. A marked difference is the presence of an additional peak at 1530-1550 cm^{-1} in films

with higher whey protein, indicative of the N-H bend of amide II. Also, in these films small peaks at 1200-1230 cm^{-1} were observed indicative of the C-N stretch vibrations of amide III. However, the C-N stretch typical at 1600-1700 cm^{-1} was camouflaged by the -COO symmetric vibrations and only shift in wave numbers can be observed. These observations confirm the interaction between pectin, alginate and whey protein concentrate.

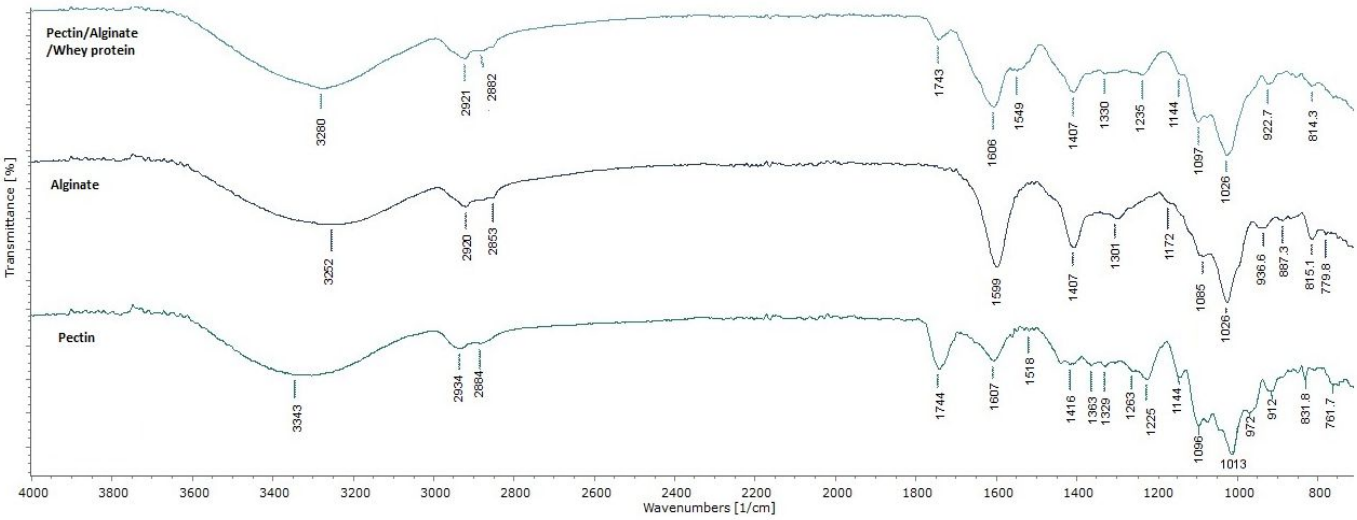

Figure 3. Representative FTIR Spectral patterns of Pectin (S_2), Alginate (S_{10}) and Pectin/Alginate /Whey protein (S_1) films

4. Conclusion

The design of mixtures is found to be a useful tool to study the effect of component concentrations on the physico-chemical properties of the film forming solutions and edible films. Whey protein was observed to have significant effect on physico-chemical, rheological properties of the solutions as well as the optical and mechanical properties of the films formed. The increase in whey protein contributed to lowering of the viscosity but significantly favoured hydrophobicity of the films. The models generated can be subjected to constrained study so as to allow for formation of films with desired characteristics.

References

Al-Hassan, A. A., & Norziah, M. H. (2012). Starch-gelatin edible films: Water vapor permeability and mechanical properties as affected by plasticizers. *Food Hydrocolloids*, *26*(1), 108–117. https://doi.org/10.1016/j.foodhyd.2011.04.015

Banerjee, R., & Chen, H. (1995). Functional Properties of Edible Films Using Whey Protein Concentrate. *Journal of Dairy Science*, *78*(8), 1673–1683. https://doi.org/10.3168/jds.S0022-0302(95)76792-3

Basiak, E., Galus, S., & Lenart, A. (2015). Characterisation of composite edible films based on wheat starch and whey-protein isolate. *International Journal of Food Science & Technology*, *50*(2), 372–380. https://doi.org/10.1111/ijfs.12628

Bonilla, J., Fortunati, E., Atarés, L., Chiralt, A., & Kenny, J. M. (2014). Physical, structural and antimicrobial properties of poly vinyl alcohol-chitosan biodegradable films. *Food Hydrocolloids*, *35*(Supplement C), 463–470. https://doi.org/10.1016/j.foodhyd.2013.07.002

Campos, C. A., Gerschenson, L. N., & Flores, S. K. (2011). Development of Edible Films and Coatings with Antimicrobial Activity. *Food and Bioprocess Technology*, *4*(6), 849–875. https://doi.org/10.1007/s11947-010-0434-1

Cecchini, J. P., Spotti, M. J., Piagentini, A. M., Milt, V. G., & Carrara, C. R. (2017). Development of edible films obtained from submicron emulsions based on whey protein concentrate, oil/beeswax and brea gum. *Food Science and Technology International*, *23*(4), 371–381. https://doi.org/10.1177/1082013217695170

Coughlan, K., Shaw, N. B., Kerry, J. F., & Kerry, J. P. (2004). Combined Effects of Proteins and Polysaccharides on Physical Properties of Whey Protein Concentrate-based Edible Films. *Journal of Food Science*, *69*(6), E271–E275. https://doi.org/10.1111/j.1365-2621.2004.tb10997.x

Cuq, B., Aymard, C., Cuq, J.-L., & Guilbert, S. (1995). Edible Packaging Films Based on Fish Myofibrillar Proteins: Formulation and Functional Properties. *Journal of Food Science*, *60*(6), 1369–1374. https://doi.org/10.1111/j.1365-2621.1995.tb04593.x

Debeaufort, F., Martin-Polo, M., & Voilley, A. (1993). Polarity Homogeneity and Structure Affect Water Vapor Permeability of Model Edible Films. *Journal of Food Science*, *58*(2), 426–429. https://doi.org/10.1111/j.1365-2621.1993.tb04290.x

Debeaufort, F., Quezada-Gallo, J. A., & Voilley, A. (1998). Edible films and coatings: tomorrow's packagings: a review. *Critical Reviews in Food Science and Nutrition*, *38*(4), 299–313. https://doi.org/10.1080/10408699891274219

Debeaufort, F., & Voilley, A. (1995). Effect of surfactants and drying rate on barrier properties of emulsified edible films. *International Journal of Food Science & Technology*, *30*(2), 183–190. https://doi.org/10.1111/j.1365-2621.1995.tb01370.x

Falguera, V., Quintero, J. P., Jiménez, A., Muñoz, J. A., & Ibarz, A. (2011). Edible films and coatings: Structures, active functions and trends in their use. *Trends in Food Science & Technology*, *22*(6), 292–303. https://doi.org/10.1016/j.tifs.2011.02.004

Galus, S., & Kadzińska, J. (2016a). Moisture Sensitivity, Optical, Mechanical and Structural Properties of Whey Protein-Based Edible Films Incorporated with Rapeseed Oil. *Food Technology and Biotechnology*, *54*(1), 78–89. https://doi.org/10.17113/ftb.54.01.16.3889

Galus, S., & Kadzińska, J. (2016b). Whey protein edible films modified with almond and walnut oils. *Food Hydrocolloids*, *52*, 78–86. https://doi.org/10.1016/j.foodhyd.2015.06.013

Galus, S., & Lenart, A. (2013). Development and characterization of composite edible films based on sodium alginate and pectin. *Journal of Food Engineering*, *115*(4), 459–465. https://doi.org/10.1016/j.jfoodeng.2012.03.006

Galus, S., Turska, A., & Lenart, A. (2012). Sorption and wetting properties of pectin edible films. *Czech Journal of Food Science*, *30*(5).

Ghosh, A. K., & Bandyopadhyay, P. (2012). Polysaccharide-Protein Interactions and Their Relevance in Food Colloids. In *The Complex World of Polysaccharides*. INTECH Open Access Publisher. https://doi.org/10.5772/50561

Gontard, N., Guilbert, S., & Cuq, J.-L. (1992). Edible Wheat Gluten Films: Influence of the Main Process Variables on Film Properties using Response Surface Methodology. *Journal of Food Science*, *57*(1), 190–195. https://doi.org/10.1111/j.1365-2621.1992.tb05453.x

Karbowiak, T., Debeaufort, F., Champion, D., & Voilley, A. (2006). Wetting properties at the surface of iota-carrageenan-based edible films. *Journal of Colloid and Interface Science*, *294*(2), 400–410. https://doi.org/10.1016/j.jcis.2005.07.030

Kester, J. J., & Fennema, O. R. (1986). Edible Films and Coatings - a Review. *Food Technology47-59*.

Khwaldia, K., Perez, C., Banon, S., Desobry, S., & Hardy, J. (2004). Milk Proteins for Edible Films and Coatings. *Critical Reviews in Food Science and Nutrition*, *44*(4), 239–251. https://doi.org/10.1080/10408690490464906

Kokoszka, S., Debeaufort, F., Lenart, A., & Voilley, A. (2010). Water vapour permeability, thermal and wetting properties of whey protein isolate based edible films. *International Dairy Journal*, *20*(1), 53–60. https://doi.org/10.1016/j.idairyj.2009.07.008

Kurek, M., Galus, S., & Debeaufort, F. (2014). Surface, mechanical and barrier properties of bio-based composite films based on chitosan and whey protein. *Food Packaging and Shelf Life*, *1*(1), 56–67. https://doi.org/10.1016/j.fpsl.2014.01.001

Kurek, M., Ščetar, M., & Galić, K. (2017). Edible coatings minimize fat uptake in deep fat fried products: A review. *Food Hydrocolloids*, *71*(Supplement C), 225–235. https://doi.org/https://doi.org/10.1016/j.foodhyd.2017.05.006

Lee, K. Y., & Mooney, D. J. (2012). Alginate: Properties and biomedical applications. *PROGRESS IN POLYMER SCIENCE*, *37*(1), 106–126. https://doi.org/10.1016/j.progpolymsci.2011.06.003

Liu, L. S., Liu, C. K., Fishman, M. L., & Hicks, K. B. (2007). Composite films from pectin and fish skin gelatin or soybean flour protein. *Journal of Agricultural and Food Chemistry*, *55*(6), 2349–2355. https://doi.org/10.1021/jf062612u

Osés, J., Fabregat-Vázquez, M., Pedroza-Islas, R., Tomás, S. A., Cruz-Orea, A., & Maté, J. I. (2009). Development and characterization of composite edible films based on whey protein isolate and mesquite gum. *Journal of Food Engineering*, *92*(1), 56–62. https://doi.org/10.1016/j.jfoodeng.2008.10.029

Otoni, C. G., Avena-Bustillos, R. J., Azeredo, H. M. C., Lorevice, M. V., Moura, M. R., Mattoso, L. H. C., & McHugh, T. H. (2017). Recent Advances on Edible Films Based on Fruits and Vegetables-A Review. *Comprehensive Reviews in Food Science and Food Safety*, *16*(5), 1151–1169. https://doi.org/10.1111/1541-4337.12281

Ozdemir, M., & Floros, J. D. (2008). Optimization of edible whey protein films containing preservatives for mechanical and optical properties. *Journal of Food Engineering*, *84*(1), 116–123. https://doi.org/10.1016/j.jfoodeng.2007.04.029

Peressini, D., Bravin, B., Lapasin, R., Rizzotti, C., & Sensidoni, A. (2003). Starch–methylcellulose based edible films: rheological properties of film-forming dispersions. *Journal of Food Engineering*, *59*(1), 25–32. https://doi.org/10.1016/S0260-8774(02)00426-0

Perez-gago, M. B., & Krochta, J. M. (2001). Denaturation time and temperature effects on solubility, tensile properties, and oxygen permeability of whey protein edible films. *Journal of Food Science*, *66*(5), 705–710. https://doi.org/10.1111/j.1365-2621.2001.tb04625.x

Pérez-Gago, M. B., Nadaud, P., & Krochta, J. M. (1999). Water Vapor Permeability, Solubility, and Tensile Properties of Heat-denatured versus Native Whey Protein Films. *Journal of Food Science*, *64*(6), 1034–1037. https://doi.org/10.1111/j.1365-2621.1999.tb12276.x

Ramos, Ó. L., Fernandes, J. C., Silva, S. I., Pintado, M. E., & Malcata, F. X. (2012). Edible Films and Coatings from Whey Proteins: A Review on Formulation, and on Mechanical and

Bioactive Properties. *Critical Reviews in Food Science and Nutrition*, *52*(6), 533–552. https://doi.org/10.1080/10408398.2010.500528

Ramos, Ó. L., Reinas, I., Silva, S. I., Fernandes, J. C., Cerqueira, M. A., Pereira, R. N., … Malcata, F. X. (2013). Effect of whey protein purity and glycerol content upon physical properties of edible films manufactured therefrom. *Food Hydrocolloids*, *30*(1), 110–122. https://doi.org/10.1016/j.foodhyd.2012.05.001

Saberi, B., Thakur, R., Vuong, Q. V., Chockchaisawasdee, S., Golding, J. B., Scarlett, C. J., & Stathopoulos, C. E. (2016). Optimization of physical and optical properties of biodegradable edible films based on pea starch and guar gum. *Industrial Crops and Products*, *86*, 342–352. https://doi.org/10.1016/j.indcrop.2016.04.015

Sato, A. C. K., Oliveira, P. R., & Cunha, R. L. (2008). Rheology of Mixed Pectin Solutions. *Food Biophysics*, *3*(1), 100–109. https://doi.org/10.1007/s11483-008-9058-7

Silva, M. A. da, Bierhalz, A. C. K., & Kieckbusch, T. G. (2009). Alginate and pectin composite films crosslinked with Ca2+ ions: Effect of the plasticizer concentration. *Carbohydrate Polymers*, *77*(4), 736–742. https://doi.org/10.1016/j.carbpol.2009.02.014

Siracusa, V., Romani, S., Gigli, M., Mannozzi, C., Cecchini, J., Tylewicz, U., & Lotti, N. (2018). Characterization of Active Edible Films based on Citral Essential Oil, Alginate and Pectin. *Materials*, *11*(10), 1980. https://doi.org/10.3390/ma11101980

Tongnuanchan, P., & Benjakul, S. (2014). Essential oils: extraction, bioactivities, and their uses for food preservation. *Journal of Food Science*, *79*(7), R1231-49. https://doi.org/10.1111/1750-3841.12492

Valencia-Sullca, C., Vargas, M., Atarés, L., & Chiralt, A. (2018). Thermoplastic cassava starch-chitosan bilayer films containing essential oils. *Food Hydrocolloids*, *75*, 107–115. https://doi.org/10.1016/j.foodhyd.2017.09.008

Vieira, M. G. A., da Silva, M. A., dos Santos, L. O., & Beppu, M. M. (2011). Natural-based plasticizers and biopolymer films: A review. *European Polymer Journal*, *47*(3), 254–263. https://doi.org/10.1016/j.eurpolymj.2010.12.011

Vogler, E. A. (1998). Structure and reactivity of water at biomaterial surfaces. *Advances in Colloid and Interface Science*, *74*(1), 69–117.

Yasmin, I., Saeed, M., Pasha, I., & Zia, M. A. (2018). Development of Whey Protein Concentrate-Pectin-Alginate Based Delivery System to Improve Survival of B. longum BL-05 in Simulated Gastrointestinal Conditions. *Probiotics and Antimicrobial Proteins*, 1–14. https://doi.org/10.1007/s12602-018-9407-x

Zhong, Y., Cavender, G., & Zhao, Y. (2014). Investigation of different coating application methods on the performance of edible coatings on Mozzarella cheese. *LWT - Food Science and Technology*, *56*(1), 1–8. https://doi.org/10.1016/j.lwt.2013.11.006

Zhu, Y., Bhandari, B., & Prakash, S. (2019). Tribo-rheology characteristics and microstructure of a protein solution with varying casein to whey protein ratios and addition of hydrocolloids. *Food Hydrocolloids*, *89*, 874–884. https://doi.org/10.1016/J.FOODHYD.2018.12.005

II

Dehydration behaviour of pan bread with edible coating: A preliminary study

Manuscript

Nallan Chakravartula SS., Balestra F., Romani S., Dalla Rosa M. (2019)

Dehydration behaviour of pan bread with edible coating: A preliminary study

Swathi Sirisha Nallan Chakravartula[a, b], Federica Balestra[b], Santina Romani [a, b],Marco Dalla Rosa[a, b]

[a] *Department of Agricultural and Food Sciences, Alma Mater Studiorum, University of Bologna, Campus of Food Science, Cesena, Italy.*

[b] *Interdepartmental Centre for Agri-Food Industrial Research, Alma Mater Studiorum, University of Bologna, Campus of Food Science, Cesena, Italy.*

Abstract

Edible coatings, are gaining importance as promising technological strategy for preserving quality and thereby, shelf-life of foods. This study aims to assess the effect of edible coating on the dehydration characteristics of soft bread under storage conditions. An edible coating based on Pectin, Alginate and Whey protein concentrates at 1.5% w/w each was prepared as an aqueous solution with 1% Glycerol as plasticizer and 0.1% tween®20 as emulsifier. The coating solution was applied onto samples of soft bread (pane cassetta), in the form of slices and mini-loaves, as a single layer by brushing. The coating was dried at 25°C, 50 % RH with predetermined times for Fette (slices) and Mini-pagnotte (muffins). For assessment of dehydration, the samples were stored without packaging at 25°C and 50 % RH for a maximum of 48 hours and monitored for weight loss, water activity and moisture content at predetermined times. The weight loss and moisture loss are modelled by using Peleg's equation to elaborate the kinetics of dehydration for which the r^2 was >0.90 confirming that the kinetics of sample moisture loss in the range of the experimental conditions used has been well described by the equation. The results, in terms of 'k' values indicate that the initial loss of humidity was higher in control samples for coated fette. In the case of mini-pagnotte, the values were higher in the coated crust in comparison to the control crust, indicating a higher rate of loss of moisture initially from the coated sample. However, the tendency of the curve exhibits more linearity for the control samples in contrast to the coated samples. The data obtained exhibits that the coating has a significant but not substantial effect for a period of 24 hours during bread storage.

Keywords: bread; dehydration kinetics; edible coating; Peleg's model

1. Introduction

Edible films and coatings are known to improve the quality and shelf life of foods as shown in various studies and reviewed by many authors (Ferreira Saraiva et al. 2016; Tongnuanchan & Benjakul 2014; Debeaufort et al. 1998). Edible films can be of heterogeneous nature, consisting of a blend of Polysaccharides, proteins and / or lipids as it allows the improvement of functional characteristics of each class of compound that forms the film (Kester & Fennema 1986). Also, the main objective of multi-component films is to improve the mechanical and permeability properties of the film formed and applied either as emulsions or multi-layer single components. However, studies show that the method of application can influence the film barrier properties. Linnemann (2007) described different methodologies for the application of edible coatings like dipping, spreading, spraying, including electro-spraying.

Edible films and coatings are advantageous due to their biodegradability and ability to act as a component of the food system. They can act as active food package systems by delaying the detrimental effects of moisture and oxygen resulting in quality losses and also incorporate bio-active components in packaged bakery products to practically extend their shelf life by retarding textural and microbial changes (Passarinho et al. 2014). The significant problem for bakery products, however, are the changes in moisture content leading to textural changes, apart from microbial deterioration. This is usually resolved by use of selective packaging for moisture, such as Polyethylene packages. Also, the redistribution of moisture and starch retrogradation, as observed in numerous studies is the main cause for increase in hardness and loss of aroma. Products with high moisture content like bread and cakes are observed to retrograde faster than low or intermediate moisture products (biscuits, crackers).

In a recent study by Bartolozzo et al. 2016 examined the use of triticale flour based coatings on muffins and observed that the application of film on the texture of muffins. They observed that the coating of muffins exhibited softer texture compared to uncoated ones during storage of 10 days, indicating that the staling was effectively delayed by the presence of coating. In another study on mini-panettones (Ferreira Saraiva et al. 2016), coating incorporated with potassium sorbate and citric acid exhibited three times higher shelf life than the product without coating.

Also, other studies evidence that coatings can exhibit protective effect on low as well as high moisture products during storage (Baeva & Panchev 2005). However data on the dehydration characteristics of bread when coated were not studied. Our objective was to assess the possible effect

of coating on the dehydration behaviour of pan bread (*pane in cassetta*) during storage by modelling the moisture loss characteristics by Peleg's model.

Background

In order to simplify the water loss data, the two parameter, non-exponential, empirical equation as proposed by Peleg (Peleg 1988) was utilised;

$$M_t = M_0 \pm \frac{t}{k1+k2(t)} \quad (1)$$

where; M_t is moisture content to a known time (t);M_0 is initial moisture content; t is wetting time (h); k1 is constant speed Peleg (% h -1); k2 is constant of Peleg capacity (% -1) and '±' becomes '+' if the process involves adsorption and '-' if the process is the desorption. The time constant of Peleg, K_1 refers to the rate of absorption / desorption at the initial time (t_0) and the constant K_2 refers to the maximum absorption / desorption humidity at infinite time.

The moisture content calculated at predetermined time intervals is expressed as dimensionless moisture as described by Planinić et al. 2005;

$$M' = {}^{M_t}/_{M_0} \quad (2)$$

Where, M_t is the moisture content at time't' and M_0 is the moisture content at initial time '0', before drying. The equation for Peleg's model can be rewritten as;

$$M' = 1 \pm \frac{t}{k_1+k_2(t)} \quad (3)$$

where k'_1 and k'_2 constants are dimensionless. The linearization of the equation against time t, gives a straight line with K_1 and K_2 as intercepts of ordinates as slope of the line which allows to determine Peleg constants (Jideani & Mpotokwana 2009).

Whereas, to model the data for weight loss, the change in weight was calculated at predefined intervals of time for the samples and modelled using Peleg's model as described by Nussinovitch & Peleg, 1990. The following equation is obtained by linearization of equation 1 and the terms 'M_t, M_0' as replaced by 'W_t, W_0' indicative for weight loss;

$$W' = 1 \pm \frac{t}{k'_1+k'_2(t)} \quad (4)$$

Where, W' is the ratio of weight change W_t/W_0; 't' is the storage time and k'_1, k'_2 representing the Peleg's rate constant and capacity constant for weight loss. Further calculating the inverse of the Peleg's rate constant (1/k1) the initial velocity of moisture and mass transfer can be obtained as described by Sopade & Obekpa 1990.

2. Materials and methods

Edible coating was prepared with sodium alginate (Sigma-Aldrich, St. Louis Missouri USA); pectin (derived from Citrus peel, Sigma-Aldrich, St. Louis Missouri USA); Whey protein concentrate (80% protein, Products-Gianni SRL, Milan Italy); glycerol (≥99.5%) (Sigma-Aldrich, St. Louis Missouri USA) and Tween® 20 (Sigma-Aldrich, St. Louis Missouri USA).

The pan bread (*Pane in cassetta*) was prepared with Wheat flour - Type '0' (Molino Sapignoli SNC, Forlì-Cesena, Italy); Extra virgin olive oil (Monini SPA, Perugia, Italy); Salt; Sugar, dried brewer's yeast (Paneangeli, Brescia, Italy). The bread was made with modifications from preliminary trials following AACC method 10-09, 1995 in forms in forms of *Fette* (*FM*; slices) representing crumb and *mini-pagnotte* (*P*; muffins*)* representing crust (*PC*) and crumb *(PM)*.

The film forming solution for the formation of coatings were prepared with a mixture of pectin, alginate and whey protein with the addition of 1.0% of glycerol and 0.1% Tween®20,used respectively as plasticizer and emulsifier. The dispersion was continually agitated with a magnetic stirrer and heated to a temperature of 75°C for 45 minutes. The solution was then cooled to room temperature and homogenized at 6000 rpm for 1 minute with a homogenizer (Model ULTRA-TURRAX T 25 digital, IKA). Further the solution was placed under vacuum using a pump (SC 920, KNF ITALY, Milan) for 10 minutes in order to degas the solution. The solution was then spread onto the surface of bread as a single layer with the aid of a confectionery brush. The samples were bought to 25°C for 270 minutes and 180 minutes respectively in a drying chamber.

The samples along with control are further stored in an atmospheric chamber at 25°C and 50% RH for 48 hours and their dehydration behaviour was characterized by monitoring weight loss, moisture content and water activity during the storage period. Water activity was determined with Aqualab-Water activity Meter, (Decagon Devices, Inc., Nelson Court, NE). Moisture content was determined by placing approximately 3g of sample in hot air oven at 105°C for 12 hours, until a constant weight in accordance with the AOAC method (1980). Also, the change in weight was monitored during the storage time.

The results were reported as mean of at least three determinations related to content of humidity and two determinations for weight loss. The dehydration curves were plotted between dimensionless moisture content (as in eq. 2) vs drying time. The data were used to estimate the Peleg model constants by use of non-linear statistical regression in Statistics for windows (Statsoft, Tulsa, OK, v.

6.0) and the reliability of the model was tested using the coefficient of determination (r^2) and value of significance related to it (p).

3. Results and Discussion

Figure 1a shows the water activity values of the FM samples with coating and control. From the graph it can be observed that the coated bread maintained higher water activity than the control. The higher water activity values in the first 24 hours can be therefore considered as a positive effect of coating which decreased loss of moisture. Probably the rapid decrease in a_w after 24 hours in both samples is to be attributed to a tendency towards achieving the equilibrium between a_w values of the bread and those of relative humidity of the surrounding environment. Subsequently, figure 1b shows the values of a_w respectively of the crust (PC) and of the (PM) of coated and control mini-pagnotte. It can be noted that the coated PC registered higher a_w values compared to control samples for all the storage time (48 hours). However the values of a_w relative to the crumb did not differ between the coated and control throughout the storage time. Moreover, the trend of water activity reduction was found to be similar in all samples.

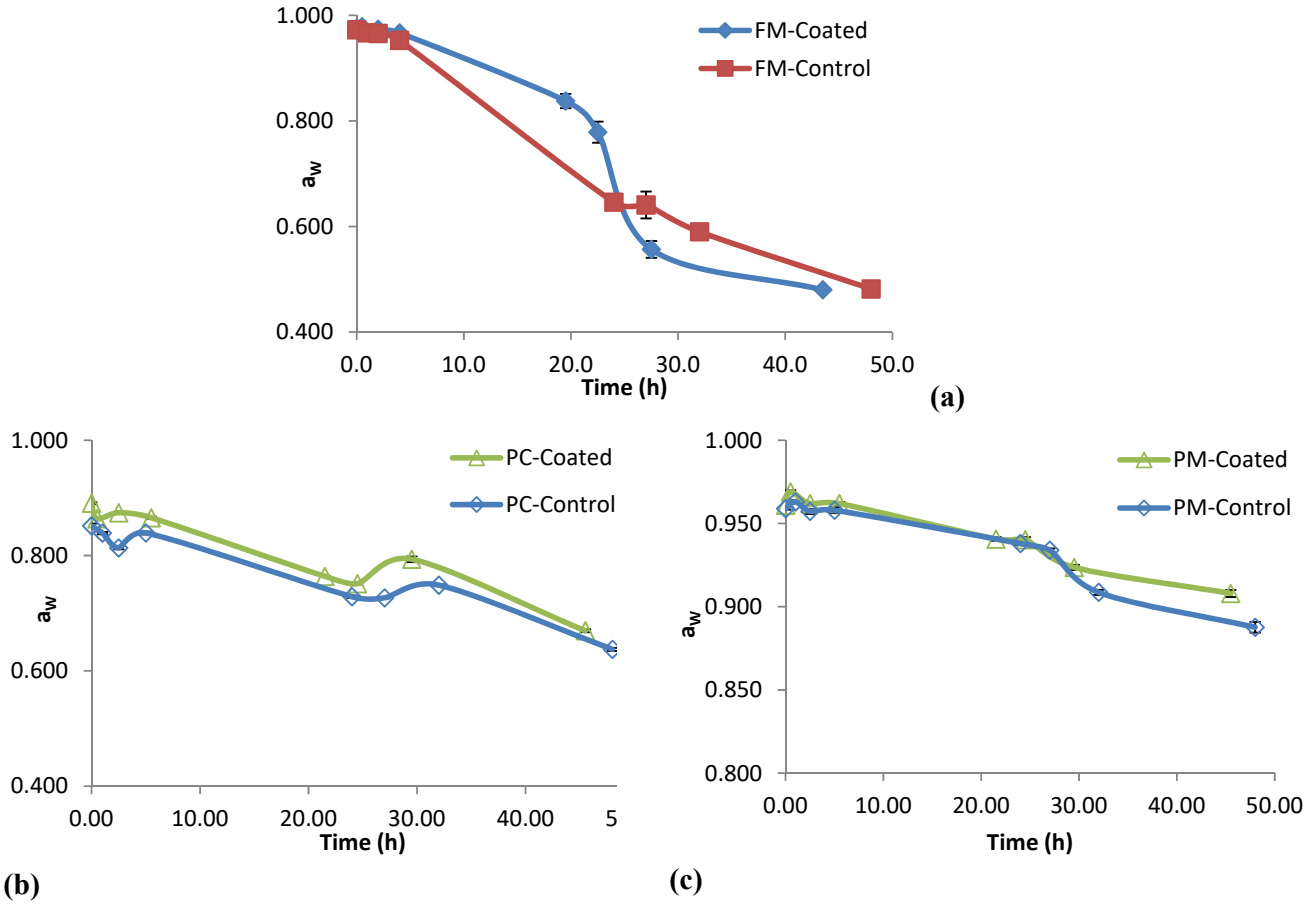

Figure 1. Water activity of the coated and control bread samples during storage (a) fette (FM) (b) mini-pagnotte crust (PC) and (c) mini-pagnotte crumb (PM)

The moisture loss of bread in form of fette (FM) and mini-pagnotte (P) as in figure 2 are fit to Peleg's equation (Eq. 3) for the experimental data obtained for both coated and control samples as shown in tables 1. The coefficients of determination, r^2 values varied from 0.900 to 0.999 indicating a good fit to the experimental data. The drying curves were characteristic indicating an initial high rate of moisture loss with similar pattern of curves for both coated and control samples. The level of significance for drying constant k_1 and k_2 for both coated and uncoated FM were high ($p<0.01$), whereas for PC they were significant $p<0.05$ and for PM varied from highly significant to non significant.

Table 1. Peleg's kinetic constants ($1/k_1$, $1/k_2$) of the moisture loss in Fette (FM), Mini-pagnotte crust (PC) and crumb (PM) during storage

Sample	Control			Coated		
	$1/k_1$	$1/k_2$	r^2	$1/k_1$	$1/k_2$	r^2
Fette (FM)	0.062***	1.114***	0.995	0.054**	1.322***	0.989
Crust (PC)	0.019*	0.757*	0.963	0.0297*	0.718**	0.968
Crumb (PM)	0.023**	0.538**	0.977	0.007*	$-3.664^{n.s}$	0.922

<0,05; **<0,01; *<0,001; n.s. = non significant*

Sopade & Obekpa (1990) observed that the k'_1 is inversely correlated to the temperature and its reciprocal better defines the initial rate of dehydration (t = 0). The kinetics of dehydration for the control and coated bread for moisture loss during storage are presented in table 1. The values of $1 / k_1$ for FM are slightly higher in control with respect to that of coated indicating that the initial rate of moisture loss is higher in control samples. However, $1/k_2$ was observed to be higher in case of coated FM indicating higher equilibrium moisture content (46.99% for coated, 42.31% for control)**.** However, according to previous studies (Nellist, 1971; Susana, 2005), k_2 values given by the more rapidly decaying term of the double exponential are stated to be related neither to drying air temperature or initial moisture content.

In the case of Mini-pagnotte crust (PC), the values of $1 / k_1$ are higher in the crust of coated samples in comparison to the control, indicating higher rate of initial moisture loss from the coated sample. On the contrary, the values for PM are significantly lower in the coated samples to those of the control. The $1/k_2$ values PC coated are slightly lower compared to the control whereas for the PM coating resulted in non significant value. Considering the moisture values of the samples, respectively FM and PM the presence of coating has resulted in slightly higher moisture for the first

24 hours of storage. In the case of the PC samples with coating retained values slightly higher than the control until the end of storage similar to the values of water activity.

The weight loss of bread in form of fette (FM) and mini-pagnotte (P) as in figure 3 are also fit to Peleg's equation (Eq. 4) for both coated and control samples. The coefficients of determination, r^2 values varied from 0.980 to 0.999 as in table 2, indicate a good fit. The level of significance for drying constant k_1 and k_2 for both coated and uncoated FM were high ($p<0.01$), whereas for P they varied from highly significant $p<0.01$ to non significant.

Table 2. Peleg's kinetic constants ($1/k'_1$, $1/k'_2$) of the weight loss in Fette (FM), Mini-pagnotte (P) during storage.

Weight Loss	Control			Coated		
	$1/k'_1$	$1/k'_2$	r^2	$1/k'_1$	$1/k'_2$	r^2
Fette (FM)	0.036^{***}	0.517^{***}	0.995	0.034^{*}	0.651^{**}	0.989
Mini pagnotte (P)	0.004^{**}	$0.408^{n.s}$	0.983	0.010^{**}	0.222^{***}	0.992

<0,05; **<0,01; *<0,001; n.s. = non significant*

The values of $1 / k'_1$ and $1/k'_2$ for FM for both coated and control samples followed similar pattern to that of moisture loss. In the case of Mini-pagnotte (P), the values of $1 / k'_1$ are higher in coated samples in comparison to control, indicating higher rate of initial weight loss from the coated sample, similar to that of PC values. From the data obtained it was observed that Peleg's model can adequately describe the dehydration behaviour of coated bread in different forms during storage. However, from the absolute data (not presented) the effect of coating in terms of protection was significant but not substantial for the fette and crumb of the mini-pagnotte.

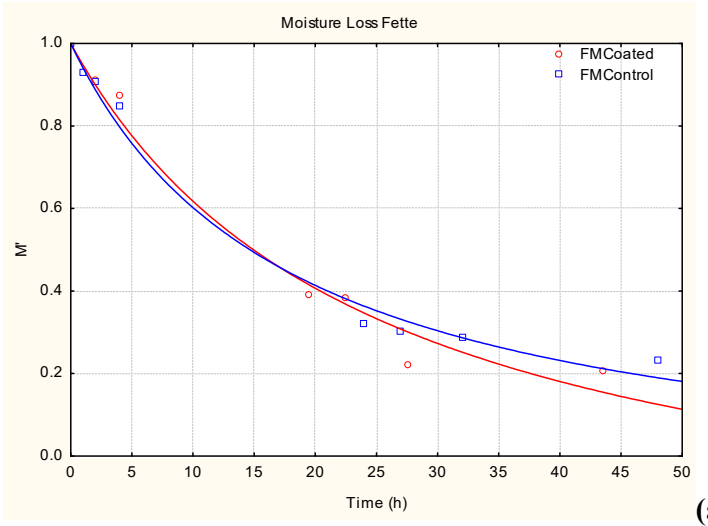

(a)

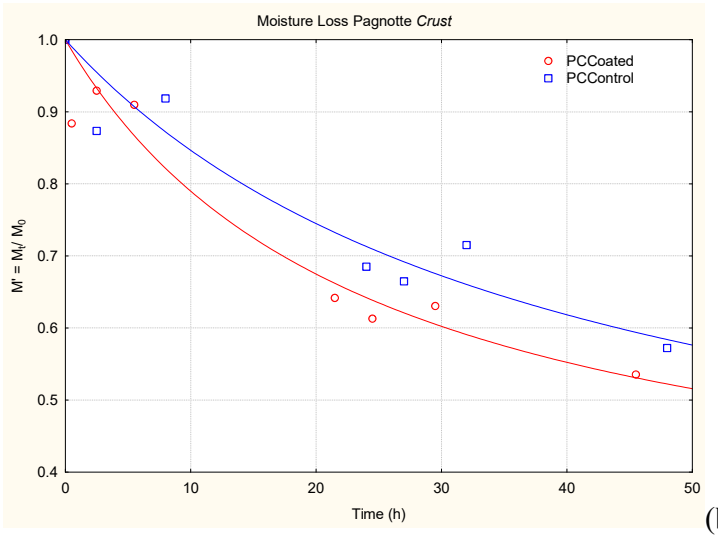

(b)

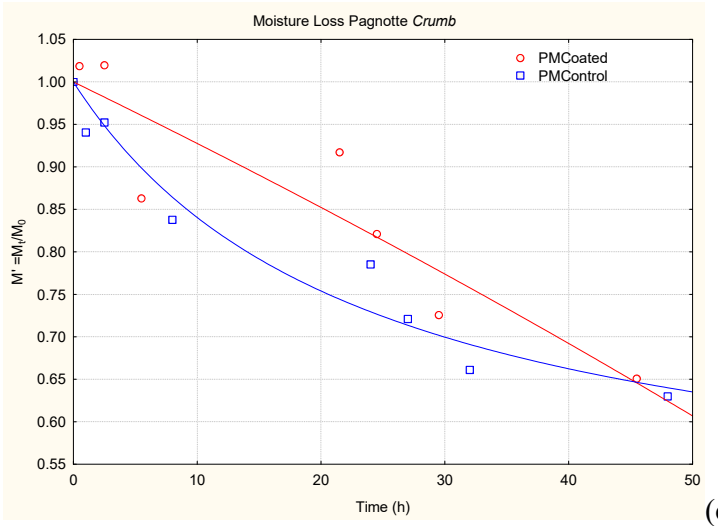

(c)

Figure 2. Moisture loss of Fette (a), Mini-pagnotte Crust (b) and Crumb (c) as a function of storage time (h) fitted by Peleg's equation.

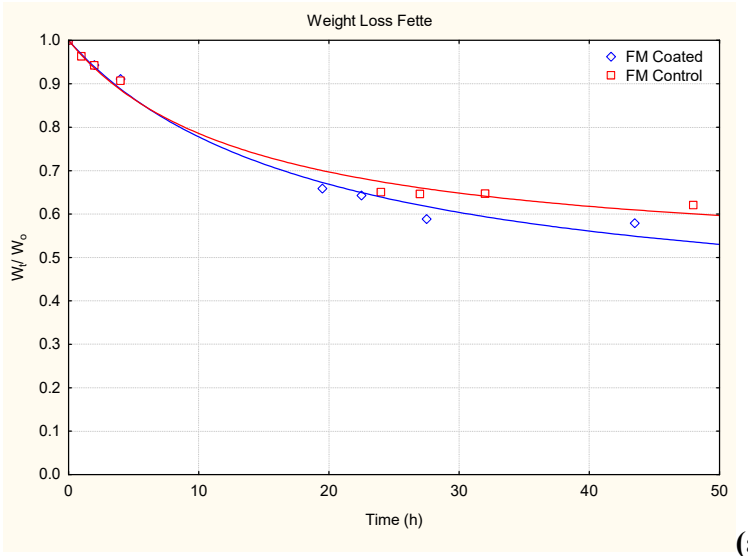

(a)

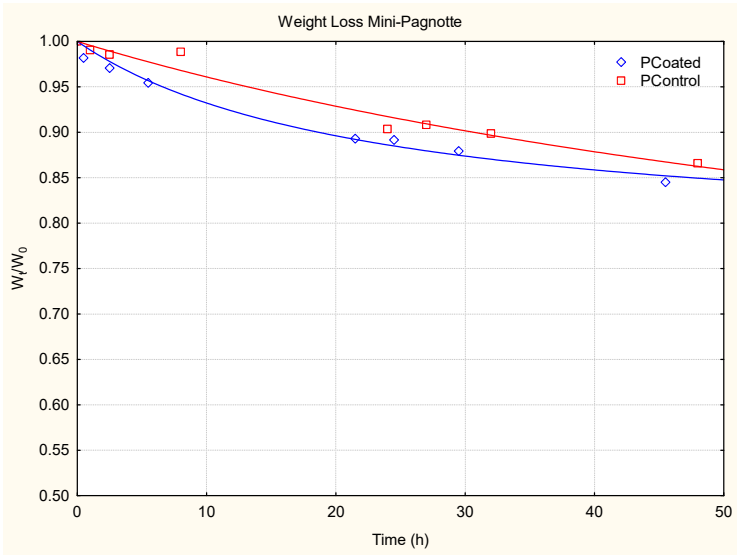

(b)

Figure 3. Weight loss of Fette (a) and Mini Pagnotte (b) as a function of storage time (h) fitted by Peleg's equation.

4. Conclusions

Peleg's equation was found to be suitable for modelling the water removal from bread at the tested time period and storage conditions. Peleg's drying rate constant (k_1), in general was affected by the presence of coating for the tested product and conditions. Peleg's capacity constant was observed to be increasing or decreasing depending on the constituent of bread under examination and not necessarily on the presence or absence of coating. Further studies are however necessary in order to understand the extent of suitability of edible film application to maintain the qualitative characteristics and shelf-life of bread, and in general bakery products.

References

Baeva, M. & Panchev, I., 2005. Investigation of the retaining effect of a pectin-containing edible film upon the crumb ageing of dietetic sucrose-free sponge cake. *Food Chemistry*, 92(2), pp.343–348. Available at: http://www.sciencedirect.com/science/article/pii/S0308814604006004 [Accessed May 6, 2016].

Bartolozzo, J., Borneo, R. & Aguirre, A., 2016. Effect of triticale-based edible coating on muffin quality maintenance during storage. *Journal of Food Measurement and Characterization*, 10(1), pp.88–95. Available at: http://dx.doi.org/10.1007/s11694-015-9280-1.

Debeaufort, F., Quezada-Gallo, J.A. & Voilley, A., 1998. Edible films and coatings: tomorrow's packagings: a review. *Critical reviews in food science and nutrition*, 38(4), pp.299–313. Available at: http://www.ncbi.nlm.nih.gov/pubmed/9626488.

Ferreira Saraiva, L.E. et al., 2016. Development and application of edible film of active potato starch to extend mini panettone shelf life. *LWT*, 73, pp.311–319. Available at: http://linkinghub.elsevier.com/retrieve/pii/S0023643816303292 [Accessed September 29, 2016].

Fiszman, S.M., Salvador, A. & Varela, P., 2005. Methodological developments in bread staling assessment: Application to enzyme-supplemented brown pan bread. *European Food Research and Technology*, 221(5), pp.616–623.

Jideani, V.A. & Mpotokwana, S.M., 2009. Modeling of water absorption of Botswana bambara varieties using Peleg's equation. *Journal of Food Engineering*, 92(2), pp.182–188. Available at: http://linkinghub.elsevier.com/retrieve/pii/S0260877408005384 [Accessed December 19, 2016].

Kester, J.J. & Fennema, O.R., 1986. Edible Films and Coatings - a Review. *Food Technology47-59*, 40(12), pp.47–59.

Nussinovitch, A. & Peleg, M., 1990. An empirical model for describing weight changes in swelling and shrinking gels. *Food Hydrocolloids*, 4(1), pp.69–76.

Passarinho, A.T.P. et al., 2014. Sliced Bread Preservation through Oregano Essential Oil-Containing Sachet. *Journal of Food Process Engineering*, 37(1), pp.53–62. Available at: http://doi.wiley.com/10.1111/jfpe.12059.

Peleg, M., 1988. An Empirical Model for the Description of Moisture Sorption Curves. *Journal of Food Science*, 53(4), pp.1216–1217. Available at: http://dx.doi.org/10.1111/j.1365-2621.1988.tb13565.x.

Planinić, M. et al., 2005. Modelling of drying and rehydration of carrots using Peleg's model. *European Food Research and Technology*, 221(3), pp.446–451. Available at: http://dx.doi.org/10.1007/s00217-005-1200-x.

Sopade, P.A. & Obekpa, J.A., 1990. Modelling Water Absorption in Soybean, Cowpea and Peanuts at Three Temperatures Using Peleg's Equation. *Journal of Food Science*, 55(4), pp.1084–1087. Available at: http://doi.wiley.com/10.1111/j.1365-2621.1990.tb01604.x [Accessed March 6, 2017].

Tongnuanchan, P. & Benjakul, S., 2014. Essential oils: extraction, bioactivities, and their uses for food preservation. *Journal of food science*, 79(7), pp.R1231-49. Available at: http://www.sciencedirect.com/science/article/pii/S0924224415001788.

III

Evaluation of drying of edible coating on bread using NIR spectroscopy

Journal of Food Engineering, 240, 29-37

Nallan Chakravartula SS., Balestra F., Cevoli C., Fabbri A., Dalla Rosa M. (2019)

Evaluation of drying of edible coating on bread using NIR spectroscopy

Swathi Sirisha Nallan Chakravartula[a, b*], Federica Balestra[b], Chiara Cevoli[b], Angelo Fabbri[a, b], Marco Dalla Rosa[a, b]

[a] *Department of Agricultural and Food Sciences, Alma Mater Studiorum, University of Bologna, Campus of Food Science, Cesena, Italy.*

[b] *Interdepartmental Centre for Agri-Food Industrial Research, Alma Mater Studiorum, University of Bologna, Campus of Food Science, Cesena, Italy*

*Corresponding author: swathisirisha.nalla2@unibo.it

Abstract

Edible coatings are recently gaining attention for potential applications in bakery products to extend the shelf-life and incorporate functional characteristics, like probiotics, antimicrobial or an antioxidant compound, for which drying of the coating is an essential step. The aim of this work was to utilize near infrared (NIR) spectroscopy as a tool to rapidly monitor and develop predictive model for the drying of edible coating on bread (mini-burger buns) surfaces. The buns coated with edible coating were dried at two different temperature regimes, at 25 °C and 60 °C for one layer of coating and one temperature regime at 60 °C for two layers of coating. NIR spectra were collected and moisture content was determined at different drying times. The spectral data were pre-treated and subjected to Principal component analysis (PCA) for discrimination of drying times and subsequently to Partial least squares (PLS) regression for moisture prediction for given temperature, time and surface. Results show that NIR spectroscopy was able to reflect the drying process and discriminate between the various surfaces of bread and times of drying, primarily by the differences in water and protein absorption bands (1940nm, 1500nm, 2050nm). Also, the subsequent PLS regression of the spectral data was found to describe satisfactorily the drying behaviour and the optimal drying moment with RMSE values ≤ 3% for the calibration and cross validation data sets. The procedure proposed could be used for faster quantification of moisture during drying process.

Keywords: NIR; drying behaviour; PLS regression; Process monitoring

[1]

[1]List of symbols and abbreviations

1L- Single layer of coating; 2L- Two layers of coating; a_w- Water activity; B- Bottom crust of the bread; T- Top crust of the bread; EC- Edible Coatings; EF- Edible Films; LV- Latent variable; MC- Moisture Content; PC- Principal Components; RH- Relative Humidity; HSI- Hyper-spectral Imaging; MSC- Multiplicative Scatter Correction; NIR- Near Infrared; PCA- Principal Component Analysis; PLS- Partial Least Square; SVN- Standard Normal Variate; TSS- Total Soluble Solids; RMSE- Root Mean Square Error; RMSEC- Root Mean Square Error Calibration set; RMSECV- Root Mean Square Error Cross Validation set; RMSET- Root Mean Square Error Test set; SAVGOL- Savitzky–Golay derivate.

1. Introduction

Bread is a staple food and an important commodity in daily nutrition of many cultures, generally viewed as a perishable product with limited shelf-life that is affected by staling and mould spoilage (Amigo et al., 2016; Licciardello et al., 2017). Staling is a complex phenomenon influencing the textural quality and consumer acceptance of bread contributing to economic losses besides mould growth (Besbes et al., 2014; Chin et al., 2011; Licciardello et al., 2014). Staling of bread is linked strongly to the retrogradation of starch, moisture loss and redistribution resulting in decreased softness, cohesiveness and loss of fresh flavour (Gray and Bemiller, 2003; He and Hoseney, 1990). The objective of bread packaging is to prevent rapid loss of moisture and ensure longer shelf- life. An efficient packaging system not only effectively maintains quality characteristics, but also has lower environmental and cost impacts (Licciardello et al., 2017).

Edible films (EF) and edible coatings (EC) have garnered increasing attention in the past decade as a novel alternative to lower synthetic packaging and improve biodegradability. They can be described as thin layers or films of material formed on the surface of the food or used as stand-alone films that provide protection to food products by acting as moisture, gas and aroma barriers as well as provide secondary functions like anti-oxidant or antimicrobial activity (Falguera et al., 2011; Galus and Kadzińska, 2015). Edible coatings can constitute one or more proteins, polysaccharides and lipids or a combination thereof resulting in composite coatings applied as bi-layer systems or emulsions (Debeaufort et al., 1998; Kester and Fennema, 1986). Edible films and coatings have been proven to improve the quality and shelf-life of foods as shown in various studies and mentioned extensively in reviews (Baeva and Panchev, 2005; Bartolozzo et al., 2016; Campos et al., 2011; Costa et al., 2018; Debeaufort et al., 1998; Dehghani et al., 2018; Ferreira Saraiva et al., 2016; Guldas et al., 2010; Ncama et al., 2018; Otoni et al., 2017; Tongnuanchan and Benjakul, 2014; Yousuf et al., 2018).

In recent studies, application of active films directly onto sliced bread and use of edible coated films for packaging of sliced bread were found to be effective in reducing the mould growth and preserving freshness of bread (Balaguer et al., 2013; Otoni et al., 2014). In few studies related to crumb firming kinetics of cake and cake type products it was observed that the textural changes related to staling were delayed by the use of edible coatings (Baeva and Panchev, 2005; Bartolozzo et al., 2016; Ferreira Saraiva et al., 2016).

These edible coatings are singular or composite materials, generally in their liquid form that are spread or sprayed and dried to render an individual layer on the product surfaces. Hence, drying is considered an important step in the formation of edible coating that influences the water activity of the food. In a study on probiotic breads by Soukoulis et al., (2014) two different temperature and time regimes, a low temperature drying at 60°C for 10 min and high temperature drying at 180°C for 2 min, were utilized to dry coating. Ferreira Saraiva et al., (2016) in their study on efficacy of active coatings dried the coating on *mini-panettone* at 180°C for 5 min. In another study on effect of coating on muffin quality a temperature of 40°C was utilized (Bartolozzo et al., 2016). A significant effect of drying temperatures was found on the crust and crumb moisture contents, which decreased by drying at higher temperatures. However, in our knowledge, no available study relates to the monitoring of drying process and kinetics of edible coat drying when applied onto bread. Thus, it is of importance to understand the drying process in order to dry the coating applied on surface but not of the internal product.

In general, the drying kinetics of foods are evaluated by weight loss and moisture loss during drying for a given temperature and humidity (Di Scala & Crapiste, 2008; Lahsasni, Kouhila, Mahrouz, & Jaouhari, 2004; Planinić, Velić, Tomas, Bilić, & Bucić, 2005). However, analyzing moisture content by oven-drying or vacuum-drying is destructive and time consuming requiring extensive sample preparation, unsuitable for large number of samples and also contributes to product wastage. Different non-destructive techniques based on the electrical, magnetic properties; spectral-scattering and imaging have been developed in the past few years as tools for measuring moisture content and recently for online quality monitoring (Büning-Pfaue, 2003; Chen et al., 2013; He et al., 2014; Mohammadi-Moghaddam et al., 2018; Özdemir et al., 2018; Todt et al., 2006; Wu et al., 2013). Near Infrared (NIR) spectroscopy is one such tool widely applied, with increasing interest in recent times, for online quality monitoring of various food products, particularly cereal and cereal products (Cevoli et al., 2015; Czaja et al., 2018; Foca et al., 2011; Huang et al., 2008; Jirsa et al., 2007; Osborne, 1996; Sørensen, 2009). It is a physical, non destructive method for measuring the physico-chemical properties of foods with high precision and minimal sample preparation.

Several studies utilized NIR spectroscopy in the determination of moisture, protein and other constituents in cereal grains and their products as stated; in which the weak absorption of water molecules facilitates also for the analysis of high moisture foods (Osborne et al., 1984). Suzuki, McDonald, & D'Appolonia (1986) applied NIR to evaluate the moisture, protein and lipid fractions of both dried and fresh bread and found that sample preparation does not

increase the accuracy of readings. Sørensen, (2009) in his extensive study described the feasible use of NIR spectroscopy to analyze the composition of wheat and rye breads and found values comparable to that of chemical analyses. Several studies show successful application of NIR for moisture analysis of intact products as well as their evolution during storage, particularly, for factors related to staling in products like cereals, bread, flat breads, biscuits and cakes (Cevoli et al., 2015; Osborne, 1996; Osborne et al., 1984; Wilson et al., 1991; Xie et al., 2003). Other studies related to osmo-air dehydration of blueberries, sulphured drying of Apricots used NIR spectroscopy as a tool to evaluate the drying process and differentiate the pre-treatments (Özdemir et al., 2018; Sinelli et al., 2011). Moreover, the perceived advantages of this method like minimal sample preparation, rapid assessment and scope for assembly in production line make it a suitable choice to provide continuous monitoring of the conditions and detect changes in the product characteristics in a production line. These attributes of NIR spectroscopy can also be extended for evaluating the surface moisture of coated breads during drying.

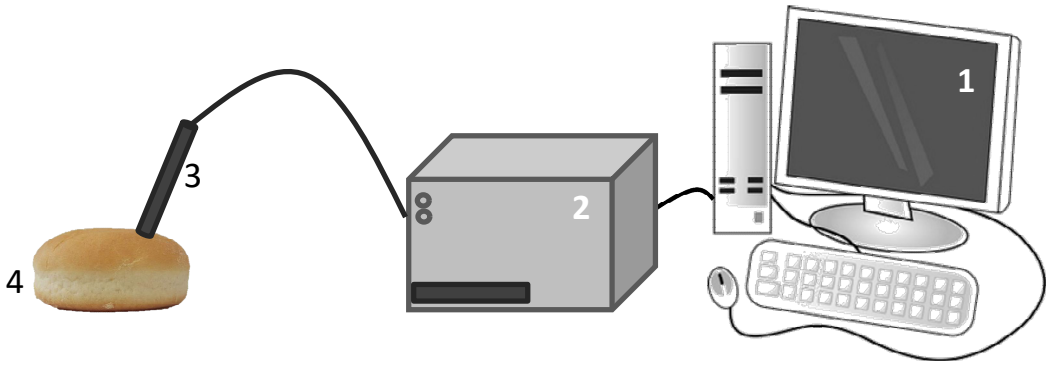

Figure 1. Schematic representation of the NIR measurement: 1) personal computer, 2) NIR device, 3) fiber probe, 4) bread sample.

In this context, the objective of the present study is to use NIR spectroscopy as a tool to evaluate the drying time of coating on the selected bakery product (mini-burger buns) and develop a predictive model for the drying of the utilized edible coating on bread surface.

2. Materials and methods

2.1 Materials

Sodium alginate (Sigma-Aldrich, St. Louis Missouri USA); pectin (derived from Citrus peel, Sigma-Aldrich, St. Louis Missouri USA); whey protein concentrate (80% protein, Products-Gianni SRL, Milan Italy) were used to prepare edible coating solution. Glycerol (≥99.5%)

(Sigma-Aldrich, St. Louis Missouri USA) and Tween® 20 (Sigma-Aldrich, St. Louis Missouri USA) were used as plasticizer and surfactant respectively. Industrially manufactured "mini-burger buns" were procured from the local market (Ipercoop, Cesena, IT). The ingredients of the mini-burger buns as per the packaging were wheat flour, water, rapeseed oil, yeast, Glucose-Fructose syrup, sugar, salt and emulsifiers.

2.2 Preparation of coated bread

The film forming solution was prepared by dispersing 1.5% w/w each of pectin, alginate and whey protein concentrate with addition of 33% of glycerol and 3.5% Tween®20 for 100g biopolymer. The dispersion was heated up to a temperature of 75°C for 45 minutes while being continually stirred on a hot plate with magnetic stirrer (ARE Heating Magnetic stirrer, Velp Scientific USA). The solution was subsequently cooled to room temperature and homogenized at 6000 rpm for 1 minute with a homogenizer (Model Ultra-Turrax T-25 digital, IKA). Further, the solution was placed under vacuum (100mb,10 minutes) using a pump (SC 920, KNF ITALY, Milan) in order to degas the solution (Javanmard and Golestan, 2008). The coating solution (pH - 4.7± 0.01, TSS – 5.4 ± 0.06, a_w – 0.97 ±0.001) was then spread onto the surface of mini-burger buns (Height- 30 mm, Diameter – 70 mm, Weight – 25.65 ± 0.7g) with the aid of a clean confectionery brush as a single layer (1L) or two layers (2L) with a 3-minute interval between applications. The average weight of the coating before drying was 2.4 (± 0.2) g for 1L and 3.6 (± 0.2) g for 2L of coating.

2.3 Drying Time Evaluation

The coated bread samples were dried by use of drying equipment (CLW 400 TOP+, POL-EKO Apparatus SP. J) and the moisture content of the Top (T) and bottom (B) surfaces of the breads were evaluated separately. In order to identify the optimal drying time, two temperature regimes were examined, 25°C (50% RH) and 60°C (10% RH) to dry the coating. The samples with single layer of coating (1L) were dried at 25°C and 60°C, while those coated with two layers (2L) only at 60°C (10% RH). The samples were subjected to NIR spectroscopy and moisture content was monitored subsequently at predetermined time intervals, in particular 1L at 25°C every 30 min; 1L at 60°C every 5 min and 2L at 60°C every 10 min.

The moisture content of at least five breads in batches was calculated by carefully separating approximately 1g of bread crust from both top and bottom surfaces, individually onto the aluminium pans of Thermo balance (i-Thermo 163M, Exacta-Optech, Italy). The samples were dried at 130°C until constant weight was achieved. A set of bread samples without

coating (Control) at time zero were analyzed in order to identify the initial moisture content of the bread surfaces (T, B) which were considered as the moisture contents to be reached approximately at the optimum drying time of the coated samples.

2.4 NIR spectroscopy

The control and coated samples were submitted to near-infrared spectroscopy (NIR) for acquisition of the spectra using a FT-NIR spectrophotometer (MATRIX ™ -F, Bruker Optics) in diffuse reflectance in the range of 12,000 and 4,000 cm^{-1} (8 cm^{-1} resolution). A schematic representation of the measurement with NIR probe is shown in figure 1. An average of 32 scans were obtained for each sample and for each drying time by placing the optical fiber probe (IN 261, Bruker Optics, Mass., USA) in direct contact with the coated bread surface. The probe is characterized by a diameter of 10 mm and uses a bifurcated fiber bundle to illuminate the sample and collect the refracted light. For each spectrum acquired, the background was acquired by placing the probe in the specific support covered with quartz under the same environmental conditions as the sample (25°C) which was subtracted. The bread was scanned at 3 central points of the top and bottom crust; and subsequently for each surface, the average spectrum of the three acquisitions was calculated.

2.5 Data analysis

Significant differences (at p-level <0.05) between means of the moisture content at different drying times were explored by means of the analysis of variance (ANOVA with post-hoc Tukey HSD); and Kruskal-Wallis test was used if significant differences emerged between variance of means of the Levene test (Statistica-StatSoft, version 7). The NIR spectra acquired on the different bread samples were analyzed by multivariate analyses (The Unscrambler ver. 9.7, CAMO, Oslo, Norway). The first part of the spectra until 1,100 nm was deleted before processing because it contains no useful chemical information, but only instrumental noise. To remove the scatter effects from spectra, the data were normalized by Standard Normal Variate (SNV) or Multiplicative Scatter Correction (MSC); following this the spectra were pre-treated by the Savitzky–Golay derivate, (SAVGOL) to enhance resolution. Spectral data were subjected to Principal Component Analysis (PCA) and Partial Least Square (PLS) regression.

PCA was applied as an exploratory analysis in order to define a possible discrimination among samples dried for different times. PLS, predictive analysis of the water content (dependent variable) was then carried out for both drying temperature and bread surfaces (top and bottom). The predictive power of the obtained models were tested by analyzing the calibration results and by performing the full cross and test set validation. For the test set validation, the

dataset was randomly divided into two sub-sets, one to calibrate the system (70% of the entire dataset) and the other (30%) to validate it. To avoid the model over-fitting, the optimal number of latent variables (LV) was chosen by plotting the root mean square error (RMSE) as a function of the number of components and by identifying where the curve reaches a minimum.

3. Results & Discussions

Concerning the drying at 25 °C, the mean moisture content values (%) over the drying time are reported in figure 2, for the top (grey diamond) and bottom (black triangle) surfaces, respectively. The dotted lines identify the moisture content of the control samples at time zero without coating for the top (grey) and for the bottom (black). It can be seen that the moisture content decreased rapidly for about 90-120 minutes and after that tended to reach an equilibrium state. This value was however observed to be influenced by the relative humidity of the drying cabinet (RH=50%). This is because of the proportionality between the humidity ratio at the product surface and the rate of moisture evaporation (Kozempel et al., 2003).

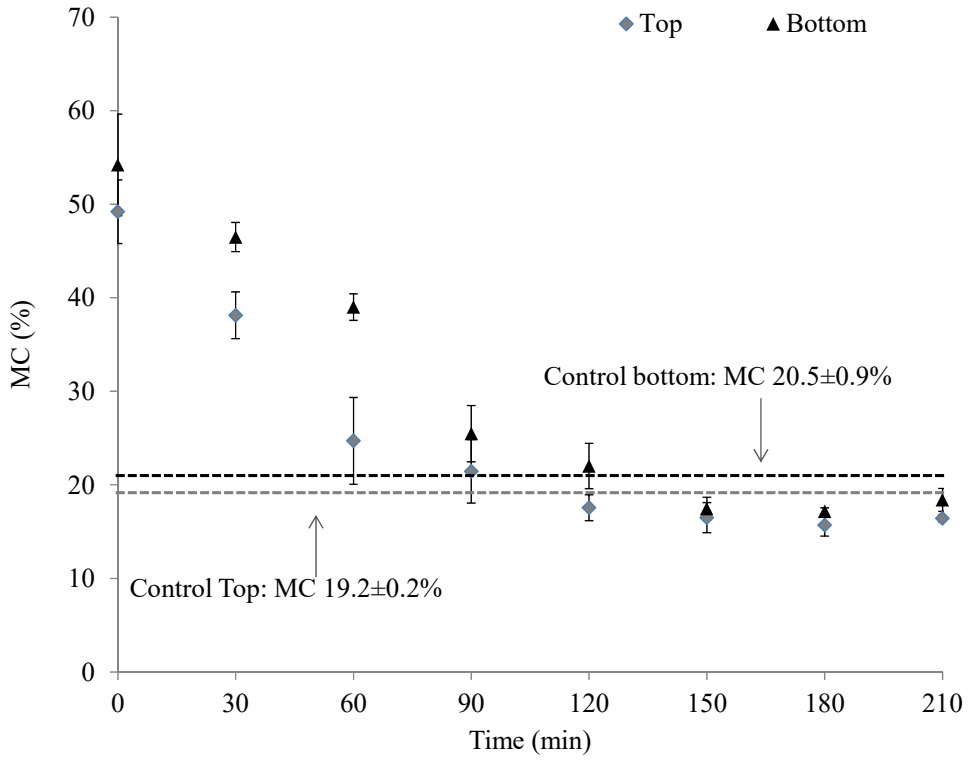

Figure 2. Moisture content (%) for 1L of coating against the drying time for temperature of 25 °C.

The dispersion around the mean value, especially for the partially dried samples, is probably due to the sample preparation and the non-uniform evaporation of the water from the surface. The crust and crumb separation from the whole bread is not perfect and when the coating is in semi-liquid form (during initial stages of drying), the operation of crust separation was rendered even more complicated. The dotted lines in figure 2 point the moisture content value of the control samples at time zero without coating (top: 19.2±0.2%; bottom: 20.5±0.9%). Comparing these values with those measured at different drying times (table 1), it is possible to observe that these initial values were achieved within 90-120 minutes and at around 120 minutes, for the top and bottom surfaces respectively. However, due to the high variance of the moisture content at same drying time, the optimal drying time for the top surface ranged from 90-120 min and for the bottom surface was at 120 min.

Table 1. Moisture content (%) during drying for coated bread with 1 Layer (1L) at 25°C, 1 Layer (1L) at 60°C and 2 Layers (2L) at 60°C

	Time (min)	Moisture content (%)	
		Top	Bottom
25°C	0	49.2±3.4 ^{a}	54.2±5.4^{a}
	30	38.1±2.5 ^{b}	46.5±1.6^{b}
	60	24.7±4.7 ^{c}	39.0±1.4^{c}
	90	21.4±3.4 ^{cd}	25.5±3.0^{d}
	120	17.6±1.4^{d}	22.0±2.4^{de}
	150	16.5±1.6^{d}	17.5±1.3^{e}
	180	15.7±1.2^{d}	17.1±0.4^{e}
	210	16.4±0.4^{d}	18.4±1.2^{e}
60°C 1L	0	47.1±1.5 ^{a}	48.4±4.4^{a}
	5	41.6±0.9 ^{a}	47.8±3.2^{a}
	10	28.5±4.9^{b}	38.1±4.0^{b}
	15	25.0±3.2^{b}	32.2±2.7^{c}
	20	19.7±2.1^{c}	27.8±2.0^{c}
	25	17.3±1.1^{c}	20.9±1.2^{d}
	30	16.0±1.1^{c}	20.0±1.1^{d}
60°C 2L	0	53.5±4.4^{a}	57.9±3.8^{a}
	10	44.8±3.2^{b}	51.9±2.8^{b}
	20	32.0±4.0^{c}	39.9±3.5^{c}
	30	19.2±2.7^{d}	28.8±2.7^{d}
	40	16.7±2.0^{de}	23.9±3.8^{de}
	50	15.1±1.2^{e}	18.7±2.3^{ef}
	60	13.6±1.1^{e}	16.6±1.9^{f}

Mean ± SD in a column without a common superscript letter differ significantly ($P<0.05$)

For drying at 60 °C, both one and two layers of coating have been considered and the moisture values are reported in table 1. The moisture content at different drying times are shown in figure 3, for the top (a) and bottom (b) surfaces, respectively. Considering the low relative humidity set up in the cabinet (RH=10%), a rapid decrease of moisture was observed for all samples. This trend is better observed for the samples with 2 layers of coating that dried for longer time. It can be observed clearly, that at any given drying time, the moisture content of the 2L samples is higher than 1L samples until 30 min of drying with the percentage difference being 25.8±10.5% and 26.0±5.1% for the top and bottom surfaces, respectively. After this time, the moisture content of the samples with one layer was not measured as the reference value of the control (top: 19.2±0.5%; bottom: 20.5±0.6%) was achieved. Also in this case, the dotted lines in figure 3 (3a, 3b) indicate the moisture content of the samples at time zero without coating. At the top surface, the optimal drying time was achieved at about 20 min for one layer and 30 min, for two layers; while at the bottom, the time was about 25-30 min and 40-50 min, for one and two layers, respectively. The drying time decreased by about 80% when the drying temperature increased from 25°C to 60 °C, both for the top and bottom surface (1L). Whereas, for the drying temperature of 60 °C, the drying time increased by 50% from one layer to two layers of coating for both the top and bottom surfaces evaluated.

The FT-NIR spectral band characterization was accomplished by comparing wavelengths with published infrared region data (Cevoli et al., 2015; Giangiacomo, 2006; Osborne et al., 1984; Suzuki et al., 1986). The NIR light molecular absorption of coated bread provided characteristic broad and overlapping peaks between 1100 and 2400 nm spectral region. All the analyzed samples show same spectral behaviour and are featured by the main absorption bands of water, protein and fat, as depicted in the representative spectra in figure 4. The Savitzky–Golay first derivative clearly allowed the extraction of useful spectral band information. As reported by Cevoli et al (2015), at about 1,450 and 1,940, the resonance bands of the O–H bonds related to water and starch were observed, while at about 1,500–1,570 and 2,050– 2,070 nm the presence of N–H bonds can be hypothesized. The absorption peaks at 1,730 1,770 and 2,310 nm correspond to lipids and can be ascribed to the first overtone of a C–H stretch and to C–H_2 group.

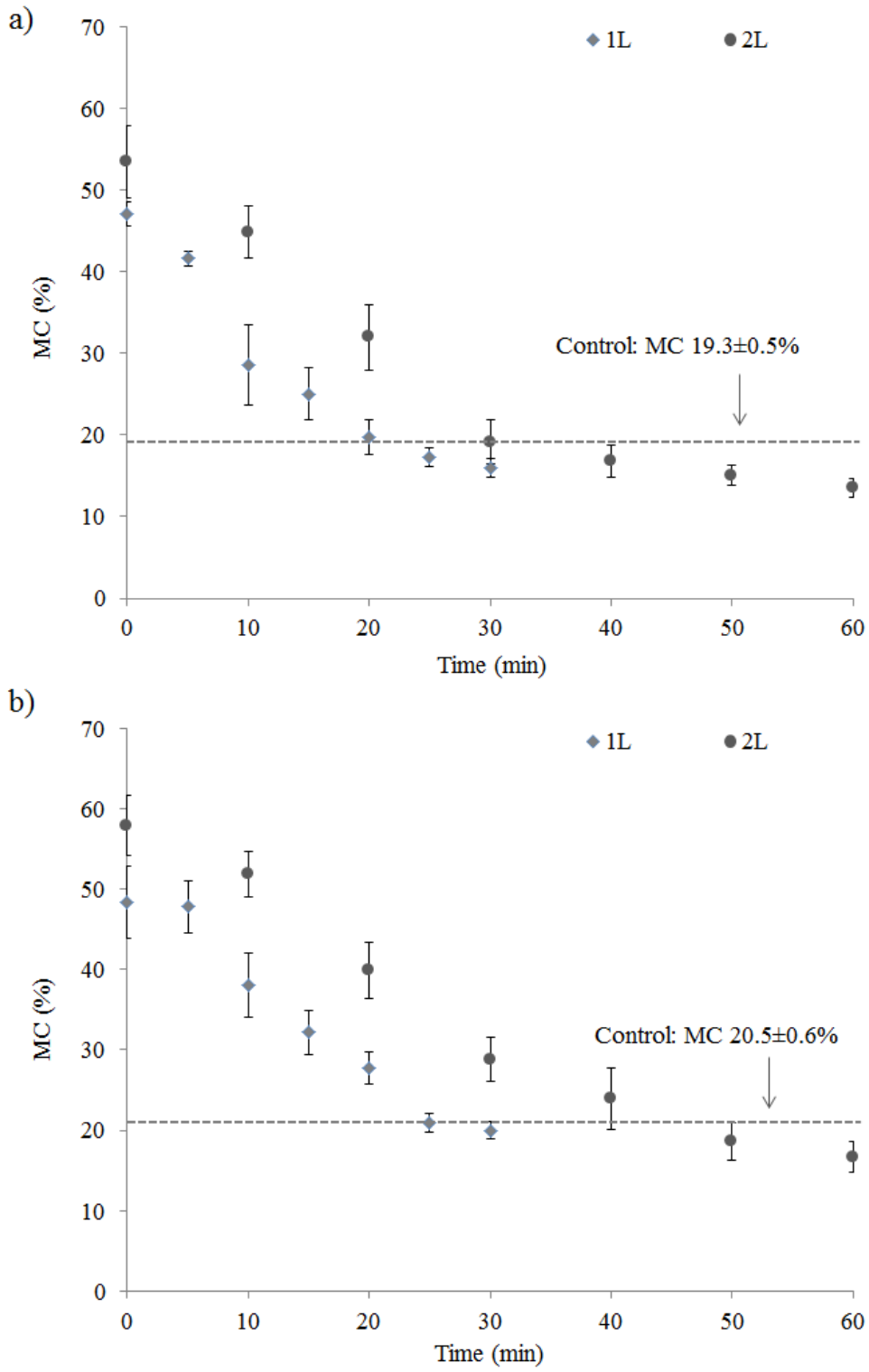

Figure 3. Moisture content (%) for 1L and 2L of coating against the drying time for temperature of 60 °C; a) top surface, b) bottom surface.

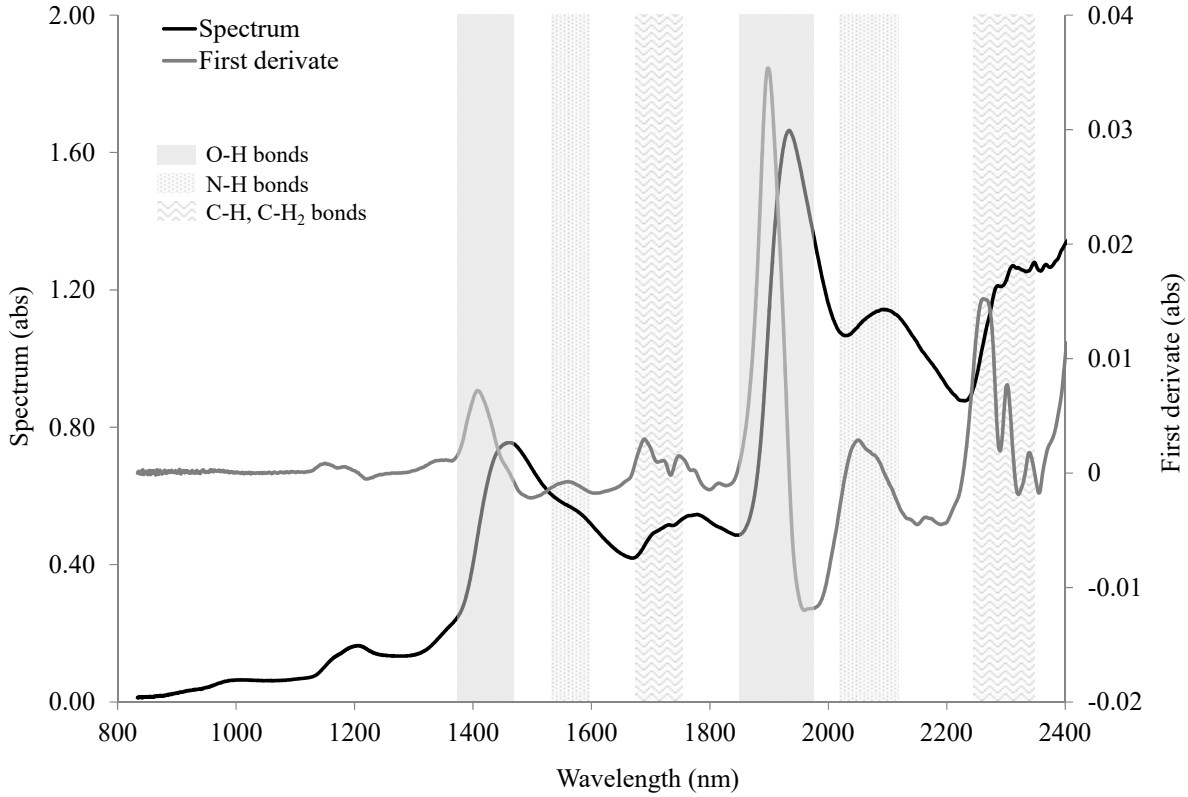

Figure 4. Representative NIR spectrum of coated bread and the relative first derivate

The PCA score plots for the NIR spectra concerning the drying at 25°C was performed to discriminate between samples at different drying times. The best results were obtained by using the SNV spectral pre-treatment. As reported in figure 5, for both the bread surfaces (top (5a) and bottom (5b)), a clear separation along the drying time was observed. The samples were arranged along the PC1 (explained variance: 93% and 79%) from right to left, on the basis of the drying time (from 0 to 210 min). The loading plots suggested that the discrimination might be attributed to spectral regions associated with moisture and protein contribution. However, the protein information is submerged in the water bands, for the first overtone concerning 1,500nm (Wu et al., 2013). During the drying, the water evaporates and the protein fraction of the coating remains on the surface of the bread, resulting in the decrease of the moisture fraction and increase of the protein fraction. Similar inference has been found by Bouman et al., (2015) on drying of protein coatings using magnetic resonance imaging. However, a clear distinction was not observed, probably due to the variable moisture content at the same drying time related to non-uniform evaporation of water from the surface. This similar interference of spectra between samples was observed by Sinelli et al., (2011) and Wu et al., (2013) in their studies on dehydration of food products using NIRS and Hyper-spectral

imaging (HSI). Moreover, it can be seen that the control samples (C) are placed along the PC1 in the same zone (grey area) of the samples dried for 90-120 minutes and 120-150 minutes, for the top and the bottom surfaces, respectively. These times are very similar to those previously reported in figure 2 and are comparable to the moisture content values.

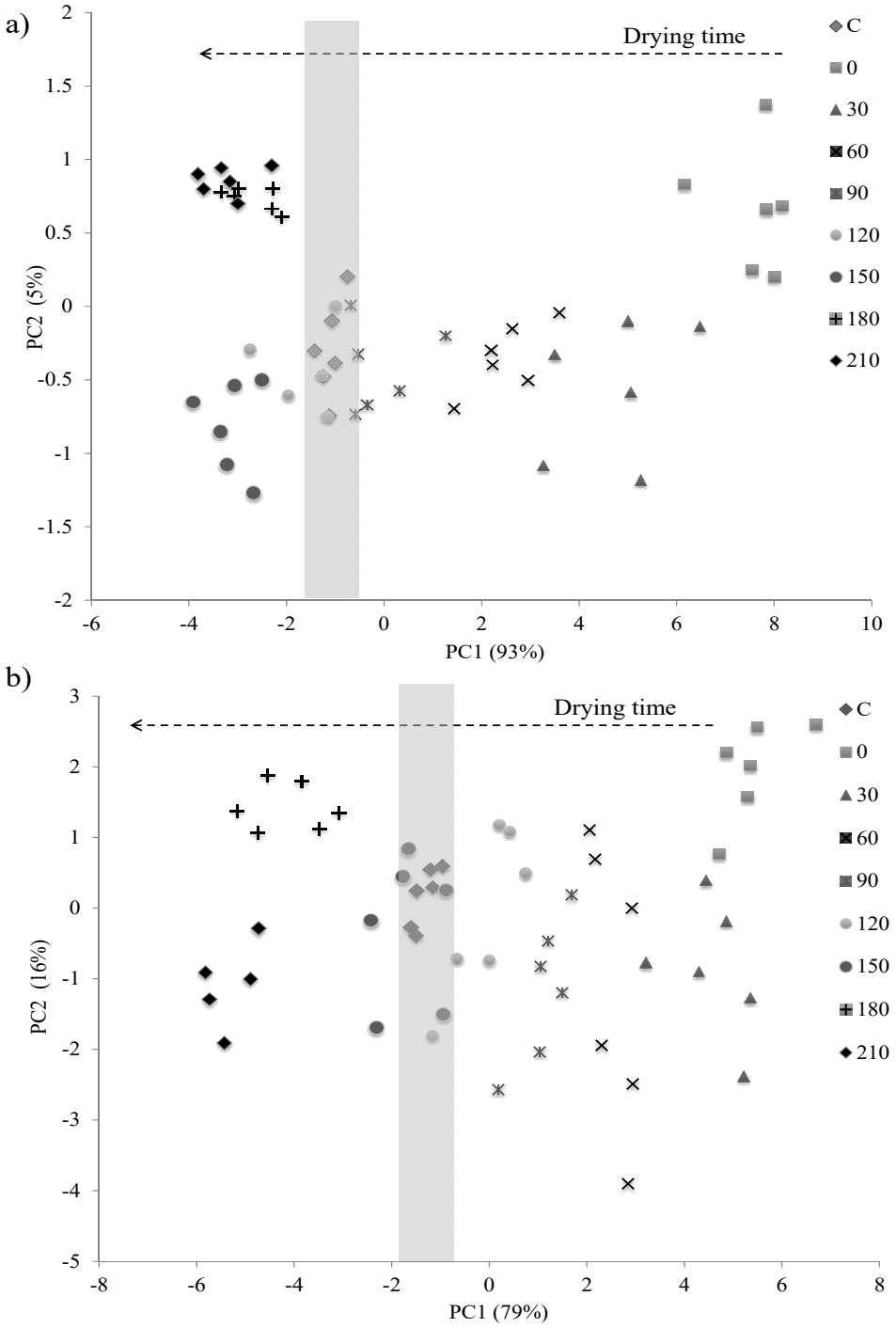

Figure 5. PCA Score plots of the NIR spectra of the top (a) and bottom (b) surfaces of the samples dried at 25 °C (C: control samples; 0, 30, 60, 90, 120, 150, 180 and 210 min: samples at respective drying times).

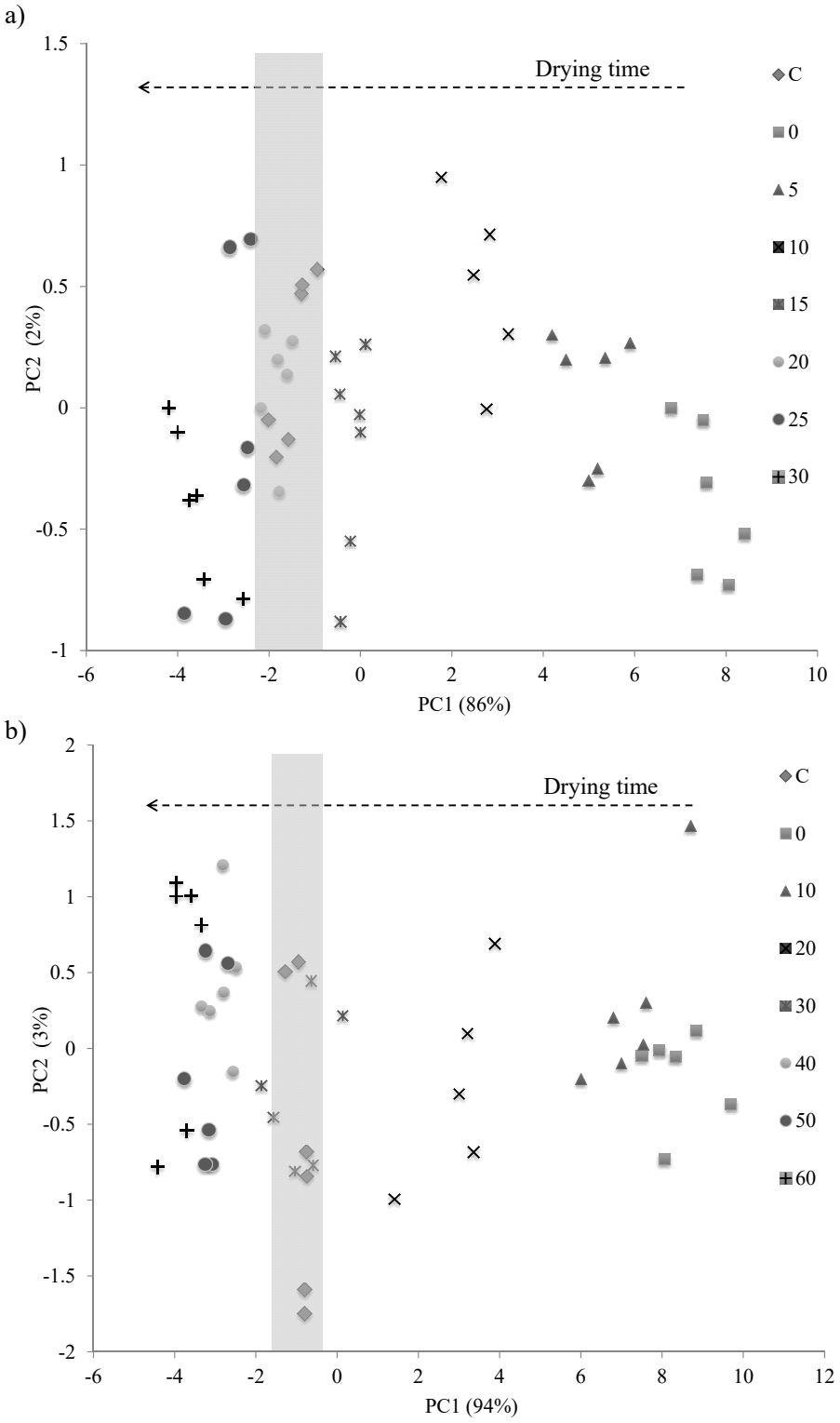

Figure 6. PCA Score plots of the NIR spectra of the top surface of the samples with one layer of coating (a) and two layers of coating (b) dried at 60 °C (C: control samples; 0, 5,10, 15, 20, 25, 30, 40, 50 and 60 min: samples at respective drying times).

The score plots obtained from the PCA of the NIR spectra acquired on the samples dried at 60 °C, are reported in figure 6 (6a, 6b). Also for 60 °C, the samples are arranged along the PC1 (explained variance 86% and 94%) from right to left, on the basis of the drying time (from 0 to 30 min for one layer (figure 6a) and from 0 to 60 min for two layers in (figure 6b)). A clear separation between samples at different drying times was observed, especially in the first 20 (1L) and 30 (2L) min of drying. In fact, the moisture content of the top and bottom crust continued to decrease also after these times, which is indicative of moisture loss from the product.

In view of the obtained results, it could be more interesting to define the optimal drying moment rather than the exact drying time, by determining the moisture content using NIR spectroscopy. Following this the spectral data to estimate the moisture content, were subjected to PLS regression and the results are reported in table 2. In general, satisfactory results were achieved for both the temperature and bread surfaces with a R^2 in test set ranging from 0.902 to 0.963. Analyzing the calibration, the full cross and the test set validation, the best model concerns the sample dried at 60 °C and covered by two layers of coating (top: R^2=0.963, RMSET=2.87%; bottom: R^2=0.937, RMSET=3.15%). The errors may be attributable to the moisture reference data that were affected by the samples preparation operations.

Table 2. PLS regression calibration parameters of the NIR spectra for predicting moisture content (%) in coated bread.

		Calibration			Full Cross Validation			Test set		
		LVs	R^2	RMSEC (%)	LVs	R^2	RMSECV (%)	LVs	R^2	RMSET(%)
25°C 1L	Top	1	0.927	2.25	1	0.921	2.45	2	0.918	2.51
	Bottom	8	0.986	1.07	8	0.933	2.28	7	0.922	2.66
60°C 1L	Top	5	0.968	1.58	5	0.950	2.04	5	0.932	2.26
	Bottom	2	0.924	2.84	2	0.914	3.08	2	0.902	3.12
60°C 2L	Top	1	0.973	2.29	1	0.969	2.49	1	0.963	2.87
	Bottom	2	0.958	2.91	2	0.954	3.08	2	0.937	3.15

4. Conclusion

The results of the presented study show the application of NIR spectroscopy to monitor and identify the drying behaviour of coating on bread surfaces. In particular, PCA analysis of the spectral data was able to differentiate samples on the basis of decrease in moisture content along the drying time. The technique was useful to track the variances evolving mainly from the event of water evaporation, as the spectral differences reflect the resonance bands of the O–H stretch of water. Also, a clear differentiation of different bread surfaces was observed. Furthermore, PLS regression built on the basis of drying temperature and type of surface was found to provide satisfactory results for estimating the optimal drying moment within the tested parameters. The developed method is fast and able to predict in a satisfactory way the moisture decrease of the coating and can be a potential technique to estimate drying times. However, further studies will be needed to verify the drying of the coatings alone and the effect on interaction with substrate.

Declarations of interest: None

References

Amigo, J.M., Del Olmo Alvarez, A., Engelsen, M.M., Lundkvist, H., Engelsen, S.B., 2016. Staling of white wheat bread crumb and effect of maltogenic α-amylases. Part 1: Spatial distribution and kinetic modeling of hardness and resilience. Food Chem. 208, 318–325. https://doi.org/10.1016/j.foodchem.2016.02.162

Baeva, M., Panchev, I., 2005. Investigation of the retaining effect of a pectin-containing edible film upon the crumb ageing of dietetic sucrose-free sponge cake. Food Chem. 92, 343–348. https://doi.org/10.1016/j.foodchem.2004.03.060

Balaguer, M.P., Lopez-Carballo, G., Catala, R., Gavara, R., Hernandez-Munoz, P., 2013. Antifungal properties of gliadin films incorporating cinnamaldehyde and application in active food packaging of bread and cheese spread foodstuffs. Int. J. Food Microbiol. 166, 369–377. https://doi.org/10.1016/j.ijfoodmicro.2013.08.012

Bartolozzo, J., Borneo, R., Aguirre, A., 2016. Effect of triticale-based edible coating on muffin quality maintenance during storage. J. Food Meas. Charact. 10, 88–95. https://doi.org/10.1007/s11694-015-9280-1

Besbes, E., Jury, V., Monteau, J.-Y., Le Bail, A., 2014. Effect of baking conditions and storage with crust on the moisture profile, local textural properties and staling kinetics of pan bread. LWT - Food Sci. Technol. 58, 658–666. https://doi.org/10.1016/j.lwt.2014.02.037

Bouman, J., de Vries, R., Venema, P., Belton, P., Baukh, V., Huinink, H.P., van der Linden,

E., 2015. Coating Formation During Drying of β-Lactoglobulin: Gradual and Sudden Changes. Biomacromolecules 16, 76–86. https://doi.org/10.1021/bm501549b

Büning-Pfaue, H., 2003. Analysis of water in food by near infrared spectroscopy. Food Chem. 82, 107–115. https://doi.org/10.1016/S0308-8146(02)00583-6

Campos, C.A., Gerschenson, L.N., Flores, S.K., 2011. Development of Edible Films and Coatings with Antimicrobial Activity. Food Bioprocess Technol. 4, 849–875. https://doi.org/10.1007/s11947-010-0434-1

Cevoli, C., Gianotti, A., Troncoso, R., Fabbri, A., 2015. Quality evaluation by physical tests of a traditional Italian flat bread Piadina during storage and shelf-life improvement with sourdough and enzymes. Eur. Food Res. Technol. 240, 1081–1089. https://doi.org/10.1007/s00217-015-2429-7

Chen, Q., Zhang, C., Zhao, J., Ouyang, Q., 2013. Recent advances in emerging imaging techniques for non-destructive detection of food quality and safety. TrAC Trends Anal. Chem. 52, 261–274. https://doi.org/10.1016/j.trac.2013.09.007

Chin, N.L., Abdullah, R., Yusof, Y.A., 2011. Glazing effects on bread crust and crumb staling during storage. J. Texture Stud. 42, 459–467. https://doi.org/10.1111/j.1745-4603.2011.00307.x

Costa, M.J., Maciel, L.C., Teixeira, J.A., Vicente, A.A., Cerqueira, M.A., 2018. Use of edible films and coatings in cheese preservation: Opportunities and challenges. Food Res. Int. 107, 84–92. https://doi.org/10.1016/j.foodres.2018.02.013

Czaja, T., Kuzawińska, E., Sobota, A., Szostak, R., 2018. Determining moisture content in pasta by vibrational spectroscopy. Talanta 178, 294–298. https://doi.org/10.1016.2017.09.050

Debeaufort, F., Quezada-Gallo, J.A., Voilley, A., 1998. Edible films and coatings: tomorrow's packagings: a review. Crit. Rev. Food Sci. Nutr. 38, 299–313. https://doi.org/10.1080/10408699891274219

Dehghani, S., Hosseini, S.V., Regenstein, J.M., 2018. Edible films and coatings in seafood preservation: A review. Food Chem. 240, 505–513. https://doi.org/10.1016/j.foodchem.2017.07.034

Di Scala, K., Crapiste, G., 2008. Drying kinetics and quality changes during drying of red pepper. LWT - Food Sci. Technol. 41, 789–795. https://doi.org/10.1016/j.lwt.2007.06.007

Falguera, V., Quintero, J.P., Jiménez, A., Muñoz, J.A., Ibarz, A., 2011. Edible films and coatings: Structures, active functions and trends in their use. Trends Food Sci. Technol. 22, 292–303. https://doi.org/10.1016/j.tifs.2011.02.004

Ferreira Saraiva, L.E., Naponucena, L. de O.M., da Silva Santos, V., Silva, R.P.D., de Souza,

C.O., Evelyn Gomes Lima Souza, I., de Oliveira Mamede, M.E., Druzian, J.I., 2016. Development and application of edible film of active potato starch to extend mini panettone shelf life. LWT 73, 311–319. https://doi.org/10.1016/j.lwt.2016.05.047

Foca, G., Ferrari, C., Sinelli, N., Mariotti, M., Lucisano, M., Caramanico, R., Ulrici, A., 2011. Minimisation of instrumental noise in the acquisition of FT-NIR spectra of bread wheat using experimental design and signal processing techniques. Anal. Bioanal. Chem. 399, 1965–1973. https://doi.org/10.1007/s00216-010-4431-z

Galus, S., Kadzińska, J., 2015. Food applications of emulsion-based edible films and coatings. Trends Food Sci. Technol. 45, 273–283. https://doi.org/10.1016/j.tifs.2015.07.011

Giangiacomo, R., 2006. Study of water–sugar interactions at increasing sugar concentration by NIR spectroscopy. Food Chem. 96, 371–379. https://doi.org/10.1016/j.foodchem.2005.02.051

Gray, J.A., Bemiller, J.N., 2003. Bread Staling: Molecular Basis and Control. Compr. Rev. Food Sci. Food Saf. 2, 1–21. https://doi.org/10.1111/j.1541-4337.2003.tb00011.x

Guldas, M., Bayizit, A.A., Yilsay, T.O., Yilmaz, L., 2010. Effects of edible film coatings on shelf-life of mustafakemalpasa sweet, a cheese based dessert. J. Food Sci. Technol. 47, 476–481. https://doi.org/10.1007/s13197-010-0081-6

He, H.-J., Wu, D., Sun, D.-W., 2014. Rapid and non-destructive determination of drip loss and pH distribution in farmed Atlantic salmon (Salmo salar) fillets using visible and near-infrared (Vis-NIR) hyperspectral imaging. Food Chem. 156, 394–401. https://doi.org/10.1016/j.foodchem.2014.01.118

He, H., Hoseney, R.C., 1990. Changes in Bread Firmness and Moisture During Long-Term Storage. Cereal Chem. 67, 603–605.

Huang, H., Yu, H., Xu, H., Ying, Y., 2008. Near infrared spectroscopy for on/in-line monitoring of quality in foods and beverages: A review. J. Food Eng. 87, 303–313. https://doi.org/10.1016/j.jfoodeng.2007.12.022

Javanmard, M., Golestan, L., 2008. Effect of olive oil and glycerol on physical properties of whey protein concentrate films. J. Food Process Eng. 31, 628–639. https://doi.org/10.1111/j.1745-4530.2007.00179.x

Jirsa, O., Hrušková, M., Švec, I., 2007. Bread features evaluation by NIR analysis. Czech J. Food Sci.

Kester, J.J., Fennema, O.R., 1986. Edible films and coatings: a review. Food Technol. (Chicago, IL, United States).

Kozempel, M., McAloon, A.J., Tomasula, P.M., 2003. Drying kinetics of calcium caseinate. J. Agric. Food Chem. 51, 773–6. https://doi.org/10.1021/jf020634k

Lahsasni, S., Kouhila, M., Mahrouz, M., Jaouhari, J.T., 2004. Drying kinetics of prickly pear fruit (Opuntia ficus indica). J. Food Eng. 61, 173–179. https://doi.org/10.1016/S0260-8774(03)00084-0

Licciardello, F., Cipri, L., Muratore, G., 2014. Influence of packaging on the quality maintenance of industrial bread by comparative shelf life testing. Food Packag. Shelf Life 1, 19–24. https://doi.org/10.1016/j.fpsl.2013.10.001

Licciardello, F., Giannone, V., Del Nobile, M.A., Muratore, G., Summo, C., Giarnetti, M., Caponio, F., Paradiso, V.M., Pasqualone, A., 2017. Shelf life assessment of industrial durum wheat bread as a function of packaging system. Food Chem. 224, 181–190. https://doi.org/10.1016/j.foodchem.2016.12.080

Mohammadi-Moghaddam, T., Razavi, S.M.A., Taghizadeh, M., Pradhan, B., Sazgarnia, A., Shaker-Ardekani, A., 2018. Hyperspectral imaging as an effective tool for prediction the moisture content and textural characteristics of roasted pistachio kernels. J. Food Meas. Charact. 1–10. https://doi.org/10.1007/s11694-018-9764-x

Ncama, K., Magwaza, L.S., Mditshwa, A., Tesfay, S.Z., 2018. Plant-based edible coatings for managing postharvest quality of fresh horticultural produce: A review. Food Packag. Shelf Life 16, 157–167. https://doi.org/10.1016/j.fpsl.2018.03.011

Osborne, B.G., 1996. Near Infrared Spectroscopic Studies of Starch and Water in Some Processed Cereal Foods. J. Near Infrared Spectrosc. 4, 195–200. https://doi.org/10.1255/jnirs.90

Osborne, B.G., Fearn, T., Miller, A.R., Douglas, S., 1984. Application of near infrared reflectance spectroscopy to the compositional analysis of biscuits and biscuit doughs. J. Sci. Food Agric. 35, 99–105. https://doi.org/10.1002/jsfa.2740350116

Otoni, C.G., Avena-Bustillos, R.J., Azeredo, H.M.C., Lorevice, M. V., Moura, M.R., Mattoso, L.H.C., McHugh, T.H., 2017. Recent Advances on Edible Films Based on Fruits and Vegetables-A Review. Compr. Rev. Food Sci. Food Saf. 16, 1151–1169. https://doi.org/10.1111/1541-4337.12281

Otoni, C.G., Pontes, S.F.O., Medeiros, E.A.A., Soares, N.D.F.F., 2014. Edible Films from Methylcellulose and Nanoemulsions of Clove Bud (Syzygium aromaticum) and Oregano (Origanum vulgare) Essential Oils as Shelf Life Extenders for Sliced Bread. J. Agric. Food Chem. 62, 5214–5219. https://doi.org/10.1021/jf501055f

Özdemir, İ.S., Öztürk, B., Çelik, B., Sarıtepe, Y., Aksoy, H., 2018. Rapid, simultaneous and non-destructive assessment of the moisture, water activity, firmness and SO 2 content of the intact sulphured-dried apricots using FT-NIRS and chemometrics. Talanta 186, 467–472. https://doi.org/10.1016/j.talanta.2018.05.007

Planinić, M., Velić, D., Tomas, S., Bilić, M., Bucić, A., 2005. Modelling of drying and rehydration of carrots using Peleg's model. Eur. Food Res. Technol. 221, 446–451.

https://doi.org/10.1007/s00217-005-1200-x

Sinelli, N., Casiraghi, E., Barzaghi, S., Brambilla, A., Giovanelli, G., 2011. Near infrared (NIR) spectroscopy as a tool for monitoring blueberry osmo-air dehydration process. Food Res. Int. 44, 1427–1433. https://doi.org/10.1016/j.foodres.2011.02.046

Sørensen, L.K., 2009. Application of reflectance near infrared spectroscopy for bread analyses. Food Chem. 113, 1318–1322. https://doi.org/10.1016/j.foodchem.2008.08.065

Soukoulis, C., Yonekura, L., Gan, H.H., Behboudi-Jobbehdar, S., Parmenter, C., Fisk, I., 2014. Probiotic edible films as a new strategy for developing functional bakery products: The case of pan bread. Food Hydrocoll. 39, 231–242. https://doi.org/10.1016/j.foodhyd.2014.01.023

Suzuki, K., McDonald, C.E., D'Appolonia, B.L., 1986. Near-infrared reflectance analysis of bread. Cereal Chem.

Todt, H., Guthausen, G., Burk, W., Schmalbein, D., Kamlowski, A., 2006. Water/moisture and fat analysis by time-domain NMR. Food Chem. 96, 436–440. https://doi.org/10.1016/j.foodchem.2005.04.032

Tongnuanchan, P., Benjakul, S., 2014. Essential oils: extraction, bioactivities, and their uses for food preservation. J. Food Sci. 79, R1231-49. https://doi.org/10.1111/1750-3841.12492

Wilson, R.H., Goodfellow, B.J., Belton, P.S., Osborne, B.G., Oliver, G., Russell, P.L., 1991. Comparison of fourier transform mid infrared spectroscopy and near infrared reflectance spectroscopy with differential scanning calorimetry for the study of the staling of bread. J. Sci. Food Agric. 54, 471–483. https://doi.org/10.1002/jsfa.2740540318

Wu, D., Wang, S., Wang, N., Nie, P., He, Y., Sun, D.-W., Yao, J., 2013. Application of Time Series Hyperspectral Imaging (TS-HSI) for Determining Water Distribution Within Beef and Spectral Kinetic Analysis During Dehydration. Food Bioprocess Technol. 6, 2943–2958. https://doi.org/10.1007/s11947-012-0928-0

Xie, F., Dowell, F.E., Sun, X.S., 2003. Comparison of near-infrared reflectance spectroscopy and texture analyzer for measuring wheat bread changes in storage. Cereal Chem. 80, 25–29. https://doi.org/10.1094/CCHEM.2003.80.1.25

Yousuf, B., Qadri, O.S., Srivastava, A.K., 2018. Recent developments in shelf-life extension of fresh-cut fruits and vegetables by application of different edible coatings: A review. LWT - Food Sci. Technol. 89, 198–209. https://doi.org/10.1016/j.lwt.2017.10.051

IV

Drying of coating on bun bread: heat and mass transfer numerical model

Bio systems Engineering (Submitted)

Cevoli C., Nallan Chakravartula SS., Dalla Rosa M., Fabbri A. (2019)

Drying of coating on bun bread: heat and mass transfer numerical model

Chiara Cevoli[a,b], Swathi Sirisha Nallan Chakravartula[a], Marco Dalla Rosa[a,b], Angelo Fabbri[a,b*]

[a]*Department of Agricultural and Food Sciences, Alma Mater Studiorum, Università di Bologna, P.zza Goidanich 60 - 47521, Cesena (FC), Italy.*

[b]*Interdepartmental Centre for Agri-Food Industrial Research, Alma Mater Studiorum, Università di Bologna, Via Quinto Bucci 336, Cesena (FC), Italy.*

*Corresponding author: angelo.fabbri@unibo.it

Abstract

The application of edible coating in bakery products could be a suitable alternative to maintain safety, textural and organoleptic characteristics during the storage. To achieve a continuous coating layer, the coating solvent should be eliminated by a drying process, avoiding the food internal dehydration. The main factors that influence the drying time of the coating are the temperature, thickness of the coating and the solvent concentration. In order to define the optimal drying time, numerical modeling could provide a suitable alternative to experimental techniques. In this study, finite elements models able to describe the heat and moisture transfer inside and on the surface of coated bun breads, as function of drying temperature, time and coating thickness were developed and validated. A good agreement was obtained between calculated and experimental data reporting RMSE of 0.04 and 0.05 $kg_{water}\,kg_{solid}^{-1}$ for the samples dried at 25 and 60°C, respectively. A relation between the optimal drying time, coating thickness and the drying temperature was determined (R^2=0.981, 95% confidence bounds). The model could be used for other coating formulations and bakery products, simply by changing material properties and geometrical dimensions.

Keywords: finite elements model; edible coating; drying; heat transfer; mass transfer.

1. Introduction

Staling and mold spoilage are the main factors that restrict the quality of bread. The stability during storage can be defined as the maintenance of the microbiological, physical and sensorial attributes related to freshness, such as tenderness, compressibility and humidity (Paeschke, 1997). Shelf-life of bread without any preservatives is generally about 3-4 days (Muizniece Brasava et al., 2012; Noshirvani et al., 2017). Due to water activity of around 0.96, bread is susceptible to mold growth (Cioban et al., 2010). The fungal proliferation determines the shelf-life of bread and bakery products. Along with mold contamination, staling is another important attribute for the bakery product quality (Bartolozzo et al., 2016). Staling is defined as a term which indicates decreasing consumer acceptance of bakery products caused by changes in crumb and crust other than those resulting from the action of spoilage organisms (Bechtel et al., 1953). Particularly, staling includes complex processes that induce changes in mouth-feel, texture, loss of tenderness, humidity redistribution and partial dryness (Bartolozzo et al., 2016).

Coating and edible films have been taken into consideration in food preservation due to their ability to improve global food quality and increase the shelf-life (Chillo et al., 2008). These substances have been used to improve mechanical properties, the gas and moisture barriers, sensory perceptions, convenience, microbial protection (Galus and Kadzinska, 2015). In this way, the application of edible coating or films in bread products could be a suitable alternative to maintain safety, textural and organoleptic characteristics during the storage (Ferreira Saraiva et al., 2016).

An edible film or coating has been defined as thin layered structures of biopolymer that can be consumed and is usually applied onto a product surface in a liquid form by brushing, dipping or spraying (Soukoulis et al., 2014; Bourtoom, 2008). One or more fluid layers can be deposited and subsequently dried to form solid films. To set up a suitable coating procedure, food product parameters such as composition, shape, dimension and density, processing factors (temperature, static/dynamic, time), and coating formulation (solvent, viscosity, composition) have to be taken into account (Embuscado and Huber, 2009). To achieve a continuous layer, the solvent can be eliminated by drying at ambient or controlled conditions (Galus and Kadzinska, 2015). Various factors are relevant in the drying of coating: the temperature at which the process is performed, the thickness of the coating and the solvent concentration (Blandin et al., 1987). The time and the method of drying can significantly affect

the physical properties of the final film (Soazo et al., 2011; Perez-Gago and Krochta 2000). To optimize the drying of coating, it is essential to study the relation between temperatures, time and type fluid dynamics or flow conditions (e.g natural or forced convection). The optimal drying time can be seen as the time necessary to completely remove the solvent from the product surface, avoiding the food internal dehydration. Regarding the research works on the application of the coating on bakery products, the drying time of the edible films appears to have been empirically selected and a justification was not reported. Low temperature drying at 60 °C for 10 min in an air circulating drying chamber, and high temperature-short time drying (180 °C for 2 min) have been used by Soukoulis et al. (2014) to dry a probiotic edible coating on the crust of the bread. Ferreira Saraiva et al. (2016) reported a temperature of 180 °C for 5 minutes to dry coated panettones with an edible film of active potato starch. Lower temperatures for longer time (40 °C for 40 minutes, 60 °C for 2 hours and 1 hour at ambient temperature under forced ventilation) have been used on coated muffin, commercial crackers and bread, respectively by Bartolozzo et al. (2016), Bravin et al. (2006) and Noshirvani et al. (2017).

In order to define the optimal drying time, numerical modeling could provide a suitable alternative to experimental techniques (Defraeye, 2014). In experiments, some biological and experimental variability will be inherently present, which makes extensive parametric studies challenging. A particular advantage is that the properties of the thin film (e.g. thickness, solvent concentration, position on the product) can be exactly controlled, such as the shape and size of the coated product. Furthermore, the modeling provides high spatial and temporal resolution on moisture transport predictions (Defraeye and Verboven, 2017). The aim of this study was to develop and validate a finite elements model able to describe the drying of an edible coating on a bun bread, varying several process conditions (temperature, time and heating properties), coating properties (moisture content, thickness, position) and product characteristics. The model was used to determine the optimal coating drying time, avoiding the food internal dehydration.

2. Materials and Methods

2.1 Model development

The main physical phenomena that should be considered in the process of drying are the diffusion of the solvent (water) through the solid ingredients of coating and then the

evaporation. To study the drying time of coating on the bread surface, a 1D finite element model was developed by using Comsol Multiphysics (Comsol, Inc., Burlington, MA). A 2D axisymmetric model based on the geometry reported in figure 1, was exclusively developed to evaluate the influence of the surface temperature distribution on the mass flux. Indeed the surface temperature depends on the shape of the sample and so it is important to evaluate the effect of the temperature distribution on the mass flux. If this effect is negligible, the simpler 1D model could be used.

The dimension values are the average of the measurement carried out on ten breads. Both the models describe the heat and moisture transfer inside and on the surface of coated breads. The main model assumptions are that the shrinkage of the coating was not considered, that the evaporation occurs only at the air-coating interface, and that the initial moisture concentrations are uniform. The model geometry was composed by 5 different zones, as reported in figure 1, parametrically defined by the distance from the edge. Each zone is characterized by its own physical properties.

The mesh of the 1D model was characterized by edge elements symmetrically distributed in relation to the geometrical center, with a ratio between bigger and smaller elements being 500. For the 2D model, an unstructured mesh with triangular elements was generated. Furthermore, 6 layers of quadrilateral boundary elements characterized by a stretching factor of 1.2 (increase in thickness between two consecutive boundary layers) has been applied on all boundaries. For both models the mesh was refined up to a level for which the calculus improvements were not significant.

2.1.1 Governing equations

Mass transfer

The moisture transfer inside the product was governed by the following mass transfer equation conformal to the second Fick's law:

$$\frac{\partial C}{\partial t} = \nabla \cdot (D \nabla C) \qquad (1)$$

where C (mol m^{-3}) is the calculated moisture concentration at time t (s), D (m^2 s^{-1}) is the water diffusion coefficient through the involved material. The diffusion coefficient of crust and crumb were set on the basis of the values found in literature (Monteau, 2008; Purlis, 2011). The coating diffusion coefficient ($D_{coating}$) was experimentally determined combining drying experimental data and inverse numerical method (Zogzas et al., 1994, Fabbri et al., 2011). A relation between diffusion coefficient, moisture concentration and temperature was determined (Blandin et al., 1987):

$$D_{coating} = aexp\left(-\frac{b}{T}\right) exp\ \left(-\frac{d}{C}\right), \quad (2)$$

where T (K) is the calculated temperature at time t(s) and a, b and d are the equation parameters. The drying experimental curves were obtained by using a thermobalance (i-Thermo 163M, Exacta-Optech, Italy) following the procedure proposed by Arranz et al. (2017). Three mm of coating (the same formulation used for the model validation) was applied on to an aluminium plate (diameter of 10 cm) and then exposed to drying at different temperatures (25, 40, 60 and 80°C). The sample weight was automatically recorded. A simple numerical model replacing the experimental geometry dimensions and drying conditions was developed. By the inversion of the numerical model, the computed mean moisture content values were compared to the experimental ones and the parameters of the diffusion coefficient equation were estimated as shown in table 1. The optimization procedure was the same as proposed by Fabbri et al. (2014). All the values of the material properties are given in table 1.

Heat transfer

Inside the product heat is transferred by conduction and is described by the following partial differential equation:

$$\rho C_P \frac{\partial T}{\partial t} = \nabla \cdot (k \nabla T) \quad (3)$$

where:

C_P (J $K^{-1}kg^{-1}$), k (W $m^{-1}K^{-1}$) and ρ (kg m^{-3}) are the specific heat, thermal conductivity and density of the different parts of the product (coating, crust and crumb), respectively. Thermal conductivity and the thermal diffusivity (θ, m^2 s^{-1}) have been experimentally determined by using the needle probe KD2 (Decagon Device Inc., Pullman, USA) on the same type of bun bread used for the model validation. The density ρ (kg m^{-3}) was also experimentally

determined (Zanoni et al., 1995). The specific heat (J $K^{-1}kg^{-1}$) was consequently calculated by the following equation:

$$C_P = \frac{k}{\rho\theta} \quad (4)$$

The values of material properties are given in table 1.

Table 1. Material properties and initial conditions implemented in the model.

	Crumb	Crust top/bottom	Coating	Air
Material properties				
Thermal conductivity, k ($Wm^{-1}K^{-1}$)	0.31	0.21	0.52	-2.28E-3+1.155E-4T-7.9E-8T^2+4.12E-11T^3-7.44E-15T^4
Density, ρ (kgm^{-3})	310	200/230	950	346.52/T
Specific heat, C_P ($Jkg^{-1}K^{-1}$)	2600	2200	3900	1.05E+3-3.73E-1T+9.45E-4T^2 -6.02E-7T^3 + 1.28E-10T^4
Diffusion coefficient, D (m^2s^{-1})	5.98E-11	1.00E-10	2.2E-14exp(0.0255T) exp(-444/C)	-2.775E-6+4.479E-8T+1.656E-10T^2
Dynamic viscosity, μ_a (Pas)	-	-	-	-75.20E-10+ 4.427E-8T - 7.887E-12T^2
Initial conditions				
Moisture concentration, C (molm-3, kgwater kgsolid^{-1})	4900, 0.44	2600, 0.23 3100, 0.27	51600, 13.26	-
Temperature, T (°C)	20	20	20	25°C-90°C

2.1.2 Boundary conditions

Concerning the boundary conditions, flux conditions were imposed on the interface between the coated product surface and the air.

Mass flux

$$\mathrm{n}\cdot(-D\nabla \mathrm{C}) = N = h_m\left(\frac{\mathrm{P}_\infty}{\mathrm{RT}_\infty} - \frac{\mathrm{P_S}}{\mathrm{RT_S}}\right) \quad (5)$$

where N (mol $m^{-2}s^{-1}$) is the water molar flux, R (J $mol^{-1}K^{-1}$) is the universal gas constant and h_m (m s^{-1}) is the mass transfer coefficient calculated on the basis of the well-known Chilton-Colburn analogy between the Nusselt number and the Sherwood number (Sh):

$$h_m = \frac{ShD_a}{L} \quad (6)$$

For the 1D model:

top surface : $Sh_t = 0.54(Gr_m Sc)^{1/4}$, (7)

bottom surface : $Sh_b = 0.27(Gr_m Sc)^{1/4}$, (8)

where:

$Sc = \frac{\mu_a}{\rho_a D_a}$: Schmidt numbers, (9)

$Gr_m = \frac{gL^3 \rho_a (\rho_s - \rho_\infty)}{{\mu_a}^2}$: Grashof number for the mass flux, (10)

$\rho_s = X_s \rho_a$: density of humid air at the coated bread surface (kg m^{-3}), (11)

$\rho_\infty = X_\infty \rho_a$: density of humid air far from the coated bread surface (kg m^{-3}), (12)

where ρ_a (kg m^{-3}) and μ_a (Pa s) are the density and dynamic viscosity of the air, respectively (data reported in table 1).

For the 2D axisymmetric model:

$$Sh = 0.59(Gr_m Sc)^{1/4} \quad (13)$$

The vapour pressure in the drying cabinet far from the product surface (P_∞), and the vapour pressure close to coating surface (P_s), are determined on the basis of the vapour relative humidity in the cabinet far from the product surface (RH_c) and the water activity at the interface (aw_s), together with the corresponding temperature, via saturated vapour pressure P_{sat} (T) given by Antoine's law:

$$P_{sat}(T) = \left[10^{\left(8.07131 - \frac{1730.63}{233.426+T}\right)} \frac{10^5}{760}\right] \quad (14)$$

$$P_\infty = RH_c P_{sat}(T_\infty), \quad (15)$$

$$RH_c = \left(\frac{X_\infty P_{atm}}{0.622 P_{sat}(T_\infty) + P_{sat}(T_\infty) X_\infty}\right), \quad (16)$$

$X_\infty = 0.622 \left(\frac{RH_{amb} P_{sat}(T_{amb})}{P_{atm} - RH_{amb} P_{sat}(T_{amb})}\right)$: water content far from the surface ($kg_{water}\, kg_{solid}^{-1}$). (17)

If the RH_c value is known, the value could be directly inserted in the model.

$$P_s = aw_s P_{sat}(T_s), \quad (18)$$

$aw_S = \frac{-B_1 - \sqrt{{B_1}^2 - 4B_0 B_2}}{2B_2}$: water activity of the coating, (19)

determined fitting the experimental drying data by the GAB model, where:

$$B_0 = \frac{1}{C_g K X_m} \quad (20)$$

$$B_1 = \frac{C_g - 2}{X_m C_g} - \frac{1}{X_S} \quad (21)$$

$$B_2 = \frac{K}{X_m}\frac{1}{C_g - 1} \quad (22)$$

$X_s = \frac{CPM_{H2O}}{\rho_s}$: water content at the surface ($kg_{water}\, kg_{solid}^{-1}$) (23)

PM_{H2O} is the water molecular weight (0.018 kg mol^{-1}) and ρ_S is the density of the dried coating (kg m^{-3}) as reported in table 1, whereas the GAB model parameters are: X_m=0.07, K=0.99 and C_g=1.7.

Heat flux

$$n \cdot (-k\nabla T) = q = h(T_\infty - T) - N\left[C_{Pv}\left(T - T_{ref}\right) + L_v\right]PM_{H2O} \quad (24)$$

where q (W m^{-2}) is the heat flux, T_∞ (K) is the drying cabinet temperature, h (W $m^{-2}K^{-1}$) is the convective heat transfer coefficient depending on the product geometry and the ambient flow conditions (natural or forced convection), C_{Pv} (1000 J $Kg^{-1}K^{-1}$) is the specific heat of water vapour, L_v is the water latent heat (2256 kJ kg^{-1}) and T_{ref} is the reference temperature equal to 273.15 K.

For the natural convection in air, the convective heat transfer coefficient (h) can be obtained using the Nusselt number (Nu) by the following equation (Incropera et al., 2006):

$$h = \frac{Nuk_a}{L} \quad (25)$$

Concerning the 1D model:

For the top surface: $Nu_t = 0.27Ra^{1/4}$, (26)

while for the bottom surface: $Nu_b = 0.54Ra^{1/4}$, (27)

$Ra = GrPr$: Rayleigh number, (28)

$Gr = \frac{g\beta L^3 \rho_a^2 (T_s - T_\infty)}{\mu_a^2}$: Grashof number, (29)

$Pr = \frac{C_{Pa}\mu_a}{k_a}$: Prandtl number, (30)

where g (m s^{-2}) is the gravitational constant, β=1/T is the coefficient of thermal expansion, T_s (K) is the temperature at the coated bread surface, k_a (W $m^{-1}K^{-1}$), and C_{Pa} (J $kg^{-1}K^{-1}$) are the thermal conductivity and specific heat of the air, respectively (data reported in table 1).

For the 2D axisymmetric model the local Nusselt number with downstream angular position of the bread surface is represented by the following equation:

$$Nu = Nu_\theta (Gr\mathrm{Pr})^{1/4} \quad (31)$$

Nu_θ values, as function of angular position was obtained by fitting the data graphically reported for sphere by Merk and Prins (1954).

The average moisture content was calculated only for 1D model by the following equation:

$$\bar{C} = \frac{1}{d}\int_0^d C(x)dx$$

where d (m) and C_i (mol m^{-3}) are the thickness and the moisture concentration of the considered zone (crumb, crust and coating) as shown in figure 1.

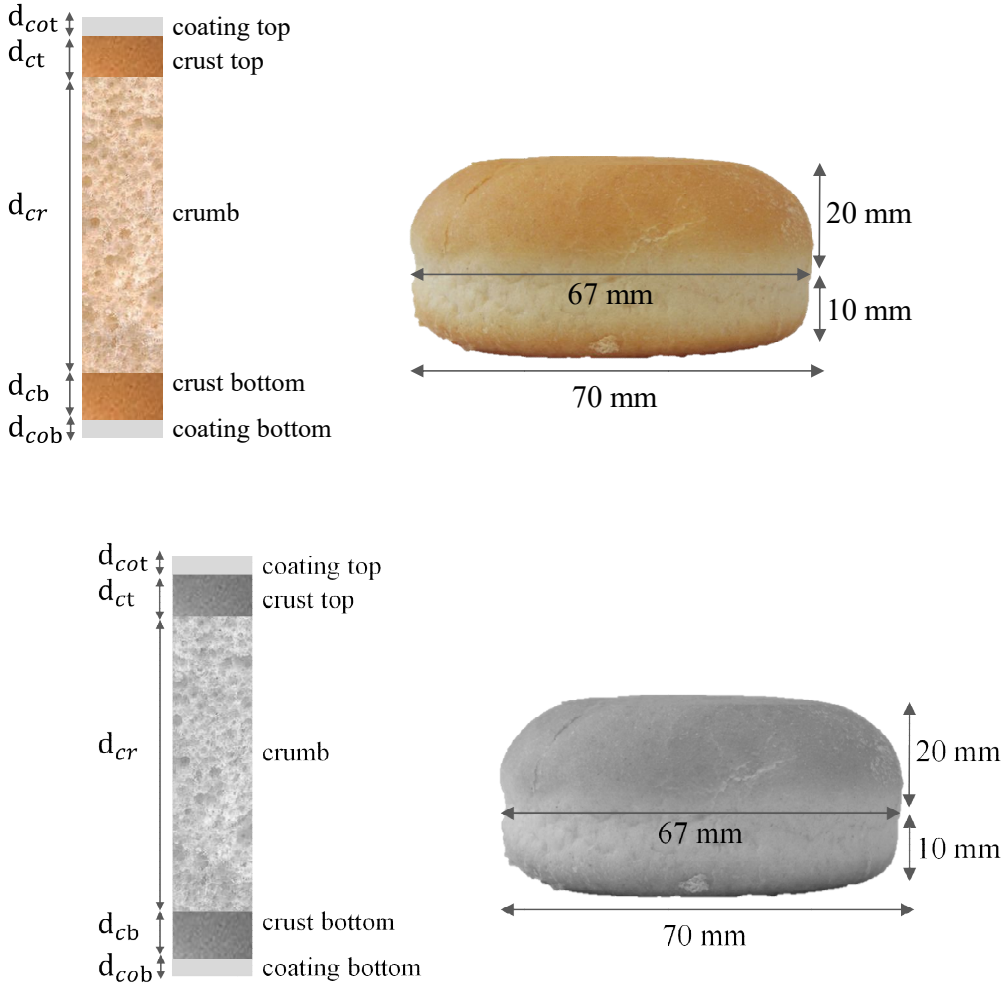

Figure 1. Geometrical dimensions used for model development.

2.2 Model validation

The model was validated comparing the average moisture content calculated and experimentally determined on the top and bottom surfaces of the samples (crust with coating). For the experimental test, the bun bread samples characterized by the geometrical parameters reported in figure 2 were used. 2.5 and 4 g of edible coatings were coated on each bread by a brush for the samples with one layer and two layers respectively, obtaining a coating thickness of about 0.06 mm and 0.1 mm (calculated on the basis of ratio between volume and surface covered by the coating).

The coating solution was prepared with a mixture of pectin, alginate and whey protein concentrate 1.5% w/w each with the addition of 1.5% of glycerol and 0.16% Tween®20, used respectively as plasticizer and emulsifier. It was characterized by an initial moisture content of 93% (13 $kg_{water}\,kg_{solid}^{-1}$) and a water activity of 0.95. The coated breads were subsequently dried in a conditioned cabinet at 25 °C (RH=65%) or at 60 °C (RH=10%). The moisture content of the crust with coating was measured by heating 1 g of sample at 130°C until constant weight, using a thermobalance (i-Thermo 163M, Exacta-Optech, Italy). Five bread samples for each time were taken into account.

Maximum Error (ME), Root Mean Square Error (RMSE), Standard Deviation (SD) and BIAS were used to compare experimental and numerical data. RMSE, SD and BIAS were calculated as average of the values obtained for each time:

$$RMSE = \sqrt{\frac{\sum_i^n (X_{num} - X_{\exp\_i})^2}{n}} \quad (32)$$

$$SD = \sqrt{\frac{\sum_i^n (X_{\exp\_i} - \bar{X}_{exp})^2}{n}} \quad (33)$$

$$BIAS = \frac{\sum_i^n (X_{num} - X_{\exp\_i})}{n} \quad (34)$$

where X_{num}, X_{exp_i}, and $\bar{X}_{exp}$ are the calculated, experimental and average experimentally measured moisture content ($kg_{water}kg_{solid}^{-1}$), respectively. *n* is the number of the experimental replicates (5).

3. Results

3.1 Model validation

The results of models were experimentally validated comparing the experimental and calculated values (1D model) of the mean moisture content of the crust with coating (Figure 2). Drying temperature of 25°C (RH=65%) and 60°C (RH=10%) were evaluated. For the experimental measurements, the average values and standard deviations calculated on five replicates (five breads) are shown. Concerning the drying at 25°C, it can be seen that the moisture content tends to obtain equilibrium after about 150 min, when it reaches a value of 0.19±0.01 $kg_{water}\,kg_{solid}^{-1}$. At this time, the coating water activity (0.66) is rather equal to the relative humidity of air in the cabinet (65%).

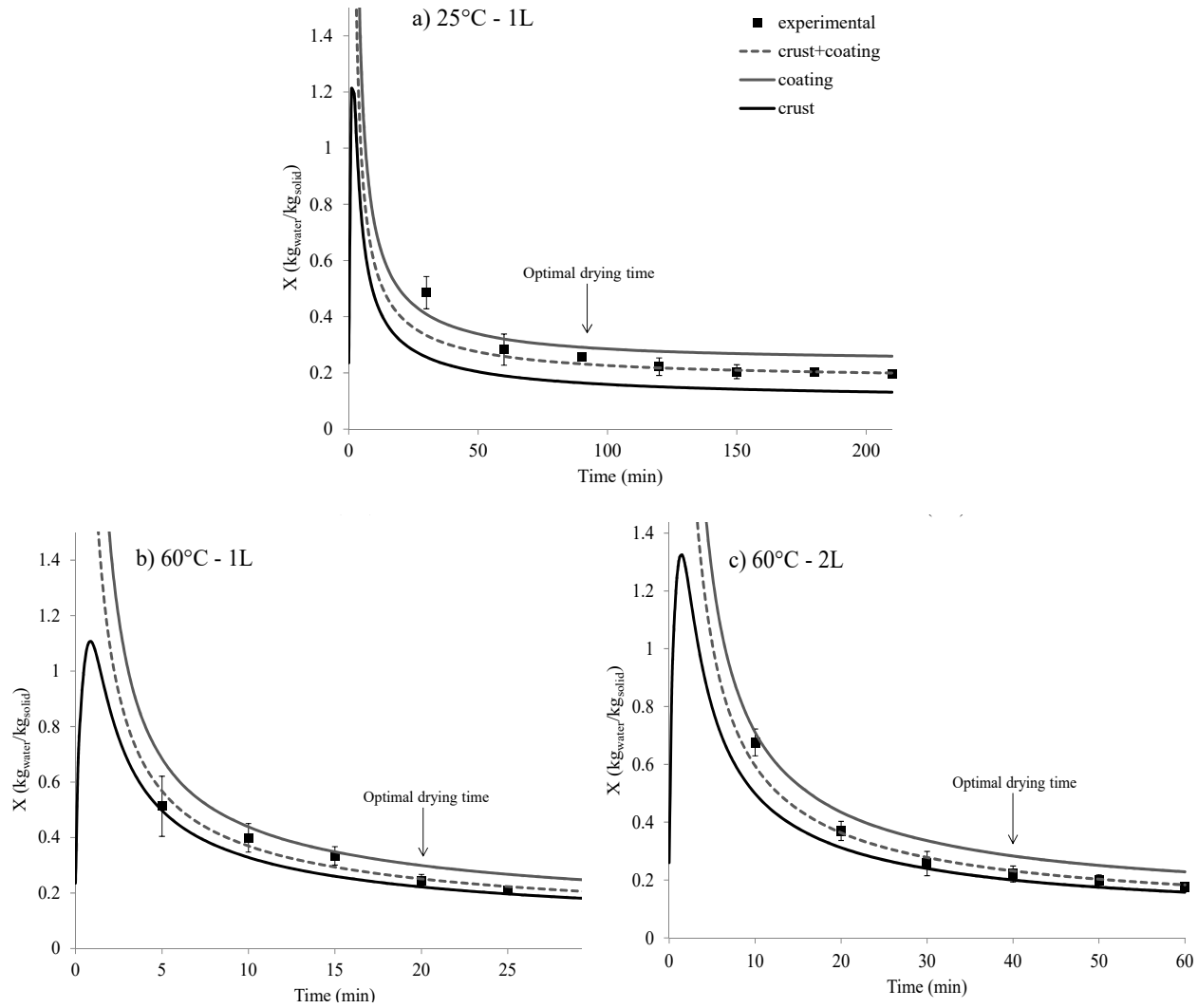

Figure 2. Experimental (●) and calculated (--) moisture content of the coating over the drying time at 25 °C and 60 °C (1L=0.06 mm; 2L=0.1 mm).

On the contrary, the coating moisture content of the samples drying at 60°C appeared to decrease without reaching the equilibrium. This is due to the low relative humidity of the drying cabinet. The calculated data followed the same trend. ME, RMSE, SD and BIAS are reported in table 2. A good agreement was obtained between calculated and experimental data reporting ME of 0.15, 0.15 and 0.19 $kg_{water}\ kg_{solid}^{-1}$ and RMSE of 0.05, 0.04 and 0.04 $kg_{water}\ kg_{solid}^{-1}$ for the samples dried at 25 and 60°C (one and two layer), respectively.

The BIAS and SD values allowed to evaluate the systematic error between calculated and experimental data and the random error between experimental measurements, respectively. In general, the lower BIAS values, suggest that the main component of the error is due to random

errors related to experimental measurements. This could be due to the unsuitable technique of separation of the crust from the bread during the sample preparation.

Subsequently, the calculated optimal drying times were compared with those experimentally obtained. The optimal drying time was arbitrarily defined as the time necessary to remove the water from the coating until it reaches a moisture content of 0.28 $kg_{water}\,kg_{solid}^{-1}$ (about 1100 mol m^{-3}) corresponding to a water activity of about 0.75 (relative humidity of a hypothetic storage ambiente), avoiding the bread internal dehydration. Accordingly, at the same time, the moisture content of the crust should be near to the initial value (0.23 $kg_{water}\,kg_{solid}^{-1}$, 2600 mol m^{-3}). Calculated optimal drying times were about 90, 20 and 40 min, for the samples dried at 25 and 60°C (one and two layers), respectively. Analysing the experimental data, it was not possible to define an accurate time, but only a time range. However, the calculated times were observed to be within these ranges, confirming that by using the model it is possible to identify the correct optimal drying time.

3.2 Model results

For the 2D model, the meshed domain was composed by 111'275 triangular elements characterized by an average element quality (dimensionless quantity between 0 and 1, where 1 represents a perfectly regular element, and 0 represents a degenerated element) of 0.3788 and 14'645 quadrilateral elements placed on all boundaries (figure 3). 500 edge elements with a growth rate of 1.025 and an element length ratio of 0.002 have been selected for the 1D model. The computation was carried out on a PC with 24 CPU (Xeon5675 64 bit 3.07 GHz) and 24 GB RAM. The calculation time was about 3 s and about 250 s for the 1D and 2D models, respectively.

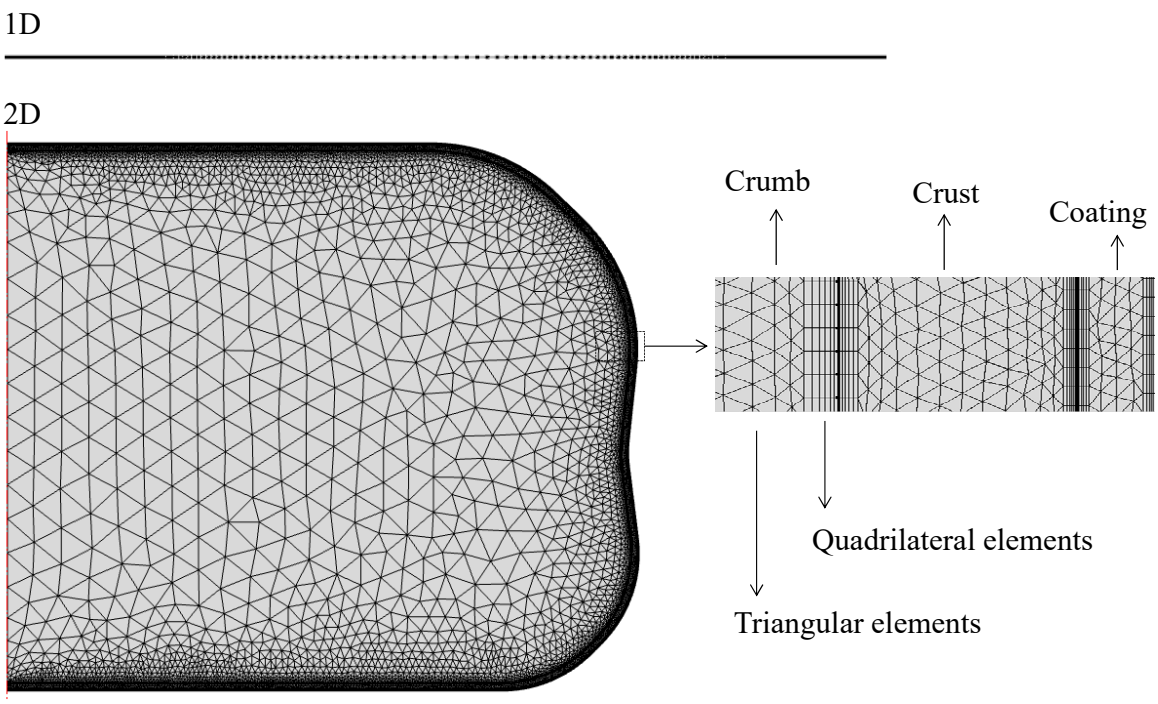

Figure 3. Mesh of the 1D and 2D axisymmetric models.

The mass flux (*N*) distribution on the coated bread surface was evaluated by using the 2D model (figure 4). It can be seen that the positions along the boundary have an important contribution on the *N* value approximately for the first two minutes (considering a drying temperature of 80 °C). After this time, the difference between the maximum and minimum *N* value appears to be negligible. The impact of the mass flux on the moisture concentration in the coating, crust and crumb, considering the bread zones where the minimum (A) and maximum (B) values of mass flux have been calculated, is shown in figure 5. Drying times of 2, 5, 10, 15 and 20 minutes have been considered (drying temperature of 80 °C, coating and crust thickness equal to 0.1 and 0.3 mm). At the same drying time, the moisture concentration profiles calculated in the A and B zones were almost equal, confirming that, for this geometry, the calculated mass flux difference does not significantly affect the moisture migration. Accordingly, the results of the 1D model were used for the following results discussion.

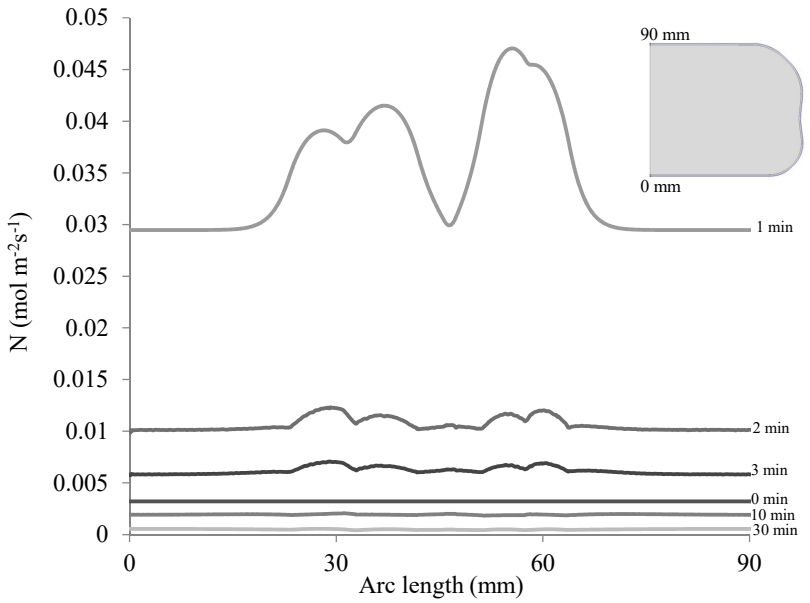

Figure 4. Mass flux calculated on the external boundary by using the 2D axisymmetric model, for different drying times (from 0 min to 30 min).

Crust and coating mean moisture concentrations ($molm^{-3}$), as function of the drying time (drying temperatures of 25, 60 and 80 °C), are reported in figure 6. The high difference between the moisture concentration of the coating and the crust drives the moisture movement from the coating to crust. At the same time, on the opposite front of the coating, the moisture evaporates.

Increasing the drying temperature, decreases the difference between the moisture concentration of the coating and the crust faster, thereby lowering the movement of the moisture in the crust. It can be seen that the moisture content of the crust passes from 2600 mol m^{-3} (0.23 $kg_{water}\,kg_{solid}^{-1}$) to 13'890 mol m^{-3} (1.25 $kg_{water}\,kg_{solid}^{-1}$) and from 2600 mol m^{-3} to 11'890 mol m^{-3} (1.07 $kg_{water}\ kg_{solid}^{-1}$) for the drying temperatures of 25 °C and 80 °C, respectively. Upon reaching the equilibrium between the coating and crust moisture content, the crust moisture starts to move towards the coating where the water evaporates. The rate of this motion depends on the diffusion coefficient of the moisture in the coating which is a function of the temperature and moisture content. Increasing temperature increases molecular mobility and diffusivity. Hence, it induces accelerated movement of water through the coating (Bourlieu et al., 2009).

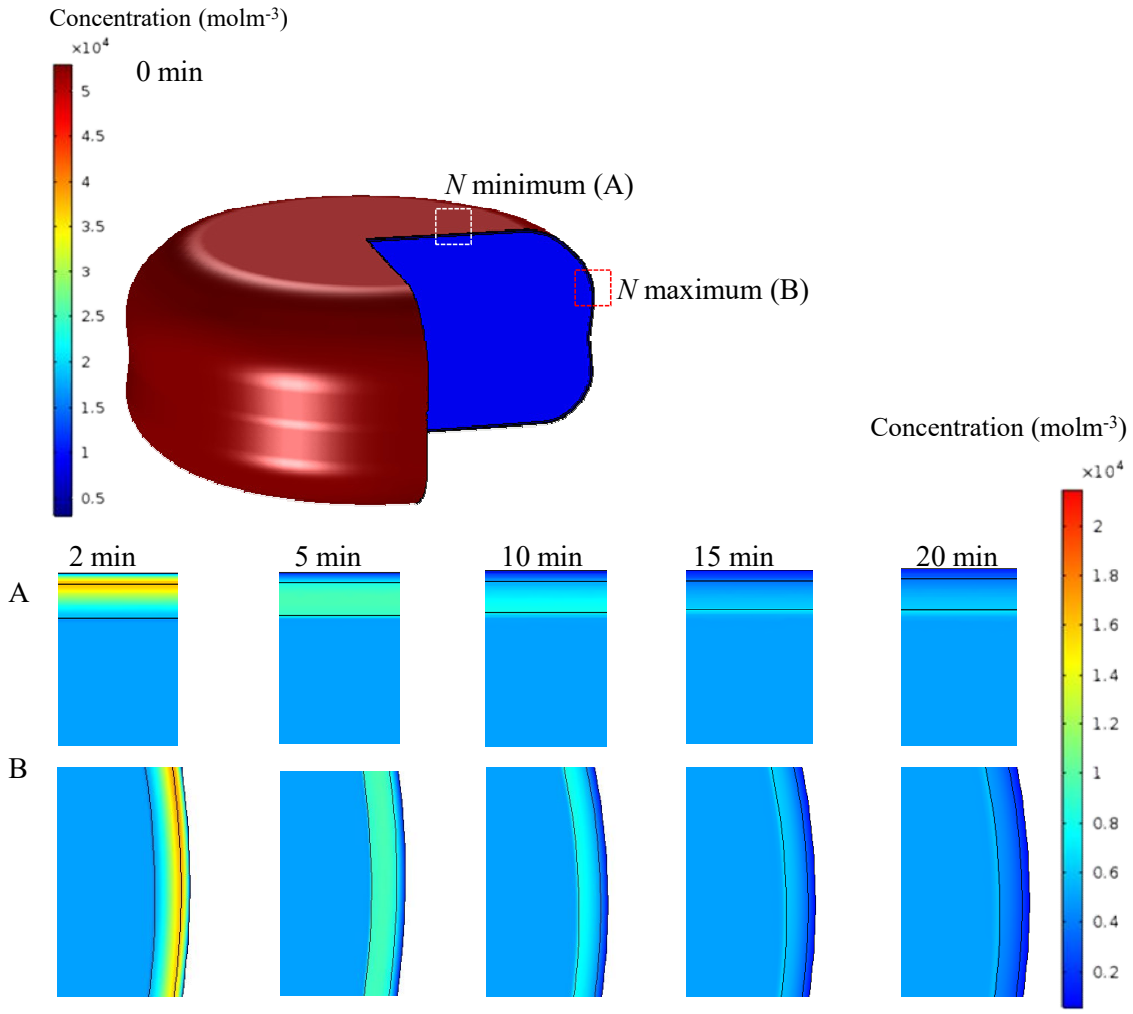

Figure 5. Moisture concentration field calculated at different points in time (0, 2, 5, 15, 10, 15 and 20 min) by using the 2D axisymmetric model (drying temperature of 80 °C) at the zone with the minimum (A) and maximum (B) value of mass flux.

The rate of this phenomenon also depends on the intensity of the starting mass flux (N) that is linearly correlated with the drying temperature (N=0.0001T-0.0359; R^2=0.999) and of the gradient between the vapour relative humidity in the cabinet and the water activity at the interface (figure 7). Furthermore, because of the very small thickness of the coating, the major amount of the moisture content rapidly evaporates (coating moisture content decreases) causing a fast decrease in mass flux. The vapour evaporation energy causes a slowing down of the product temperature rise that starts to rapidly increase when the mass flux tends to decrease.

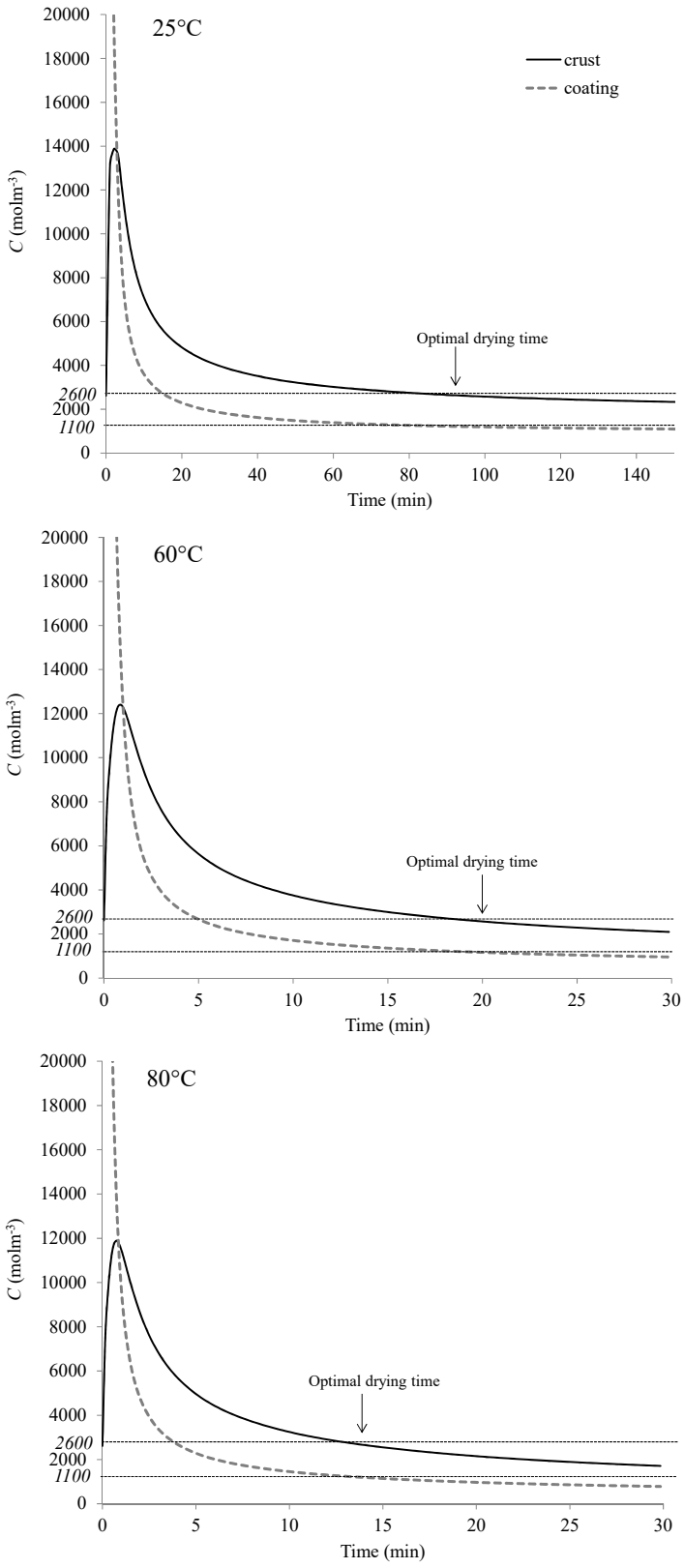

Figure 6. Average moisture concentration calculated at the coating and crust, over the time for 25, 60 and 80°C of drying temperature.

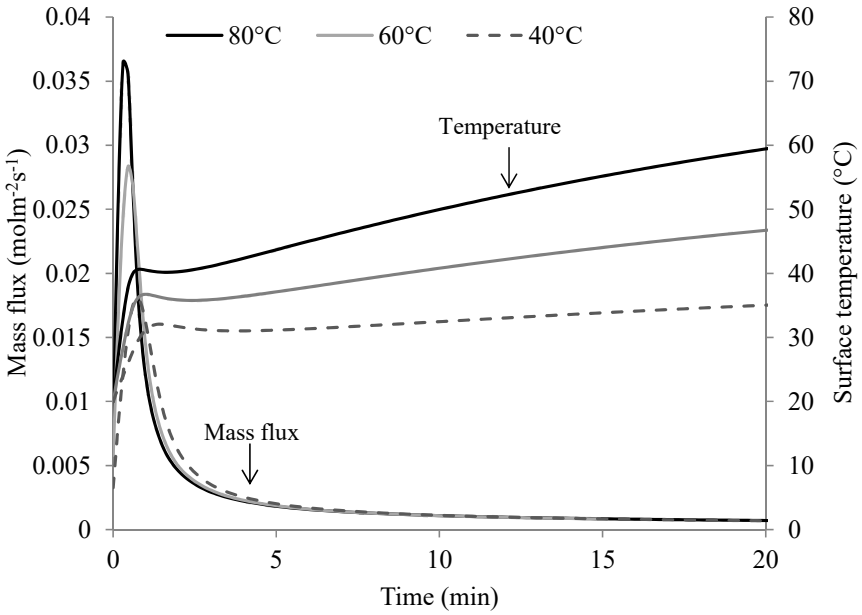

Figure 7. Mass flux and temperature calculated on the coated bread top surface over the time at different drying temperatures (40°C, 60°C and 80°C).

As described in the model validation section, the coating is arbitrarily considered dried when the coating water activity is comparable to relative humidity of the storage ambience (0.75 corresponding to 1100 mol m^{-3}) and the crust moisture concentration returns to the initial value (2600 mol m^{-3} , 0.23 $kg_{water}\, kg_{solid}^{-1}$). In this way, the coating water activity as function of the drying time and moisture concentration is reported in figure 8. It can see that the optimal drying time was reached after about 90, 20, and 14 minutes, for 25, 60 and 80°C of drying temperatures, respectively. The same drying time was also identified evaluating the crust and coating moisture concentration over the drying time (see figure 6).

By using the model results, a relation between the optimal drying time (z), coating thickness (x) (0.06- 0.14 mm) and the drying temperature (y) (from 25 to 90°C) was determined (figure 9). Good results (R^2=0.981, 95% confidence bounds) were obtained by using an equation combining a linear relation between optimal drying time and coating thickness, and a power law relation between the optimal drying time and drying temperature $[z = (-7.197E3 + 3.6E5x)/(y^{1.119})]$.

In general, the estimated optimal drying time appears to be nearer to those reported in literature for coated bakery products (Soukoulis et al. 2014; Bartolozzo et al., 2016; Bravin et al., 2006; Noshirvani et al., 2017; Ferreira Saraiva et al., 2016). However, it is hard to have a

direct comparison because of different product and coating characteristics as well as different drying conditions.

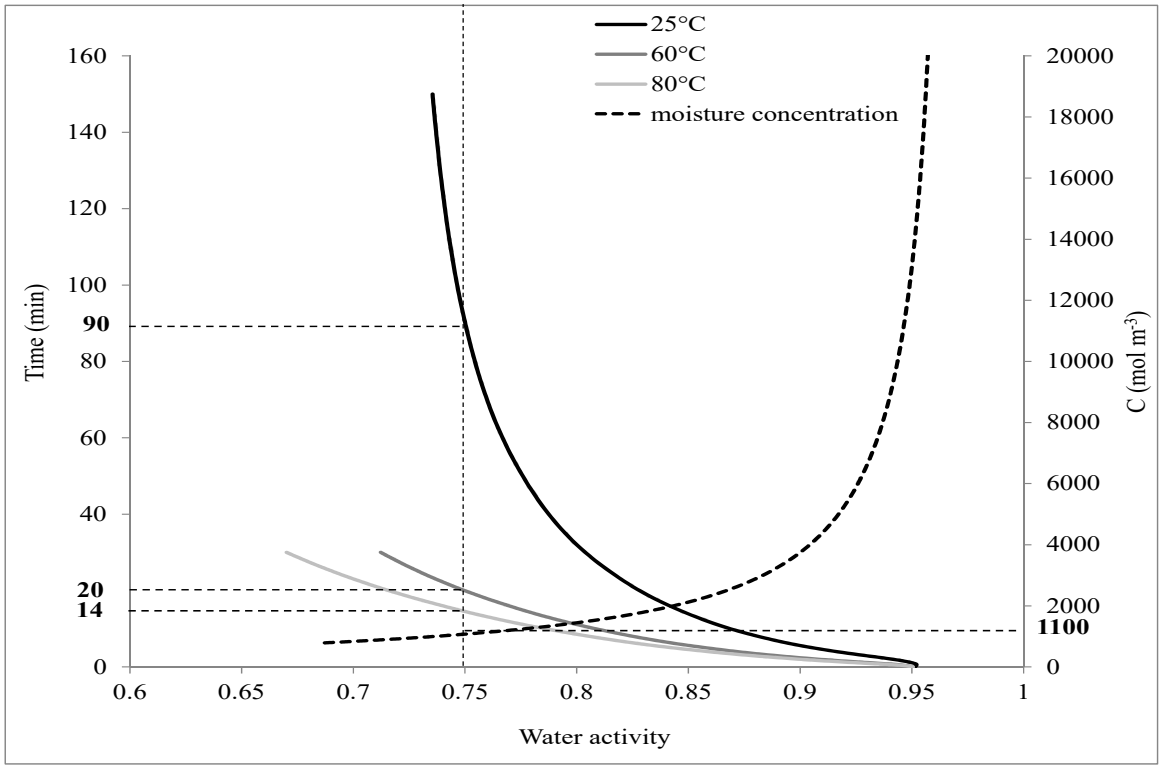

Figure 8. Calculated coating water activity over the time (25, 60 and 80°C of drying temperature) and moisture concentration.

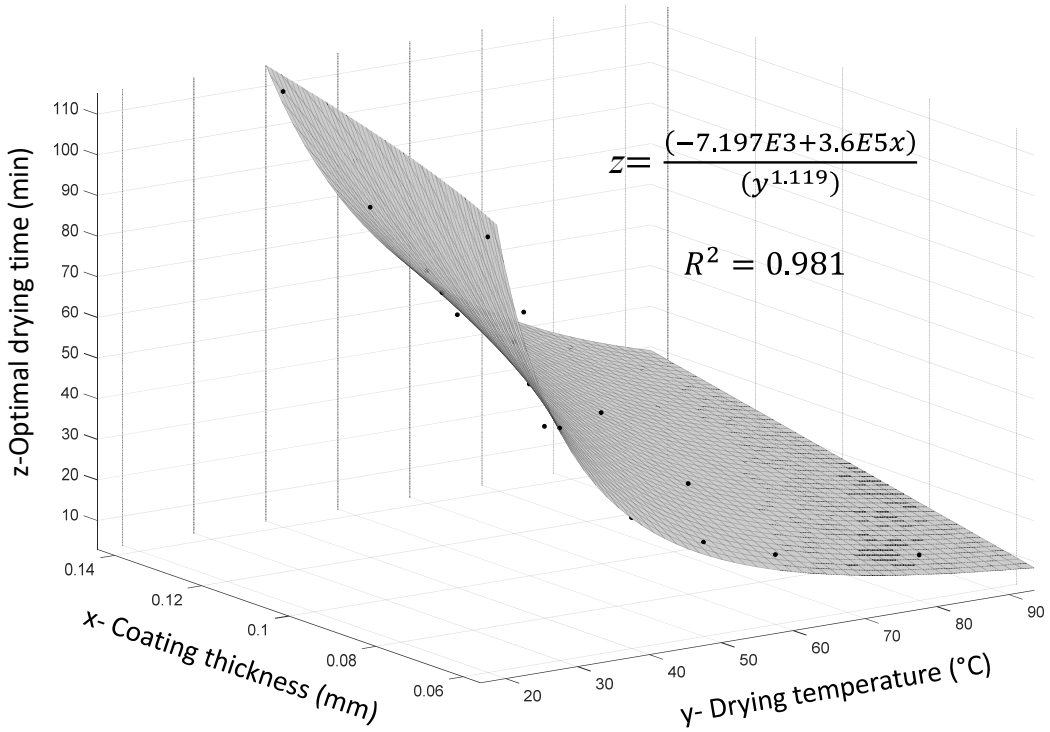

Figure 9. Regression between optimal drying time (min), drying temperature (°C) and coating thickness (mm).

Conclusions

One dimensional and 2D axisymmetric finite elements models able to describe the heat and moisture transfer inside and on the surface of coated breads were developed to determine the proper coating drying time, in order to minimise the food internal dehydration. The 2D axisymmetric model, based on a real geometry, allowed to state that the influence of the surface temperature distribution on the mass flux is weak (drying temperature until 80 °C). The difference between the maximum and minimum mass flux value appeared to be negligible. The model was validated comparing the average moisture content calculated and measured on the coating of the breads dried at 25 °C and 60°C. Good agreement was observed between experimental and numerical data (RMSE of 0.05 and 0.04 $kg_{water}\ kg_{solid}^{-1}$). The mean moisture contents calculated on the top and the bottom zones of the coated breads, as a function of the drying temperature, time and coating thickness, were taken into account. A specific relation between the optimal drying time, drying temperature and coating thickness was determined (R^2=0.98). The study demonstrated the feasibility of the model with particular reference to the approximations adopted, which can represent a good compromise between computational effort, reliability and generalization of results. The same model could be used for many other bakery products and coating formulations, simply by changing geometrical dimensions and the material properties.

References

Arranz, F.J., jimenez-Ariza, T., Diezma, B., Correa, E.C. (2017). Determination of diffusion and convective transfer coefficients in food drying revisited: A new methodological approach. Biosystem Engineering, 162, 30-39.

Bartolozzo, J., Borneo, R., Aguirre, A. (2016). Effect of triticale-based edible coating on muffin quality maintenance during storage. Food Measure, 10, 88-95.

Bechtel, W.G., Meisner, D.F., Bradley, W.B. (1953). The effect of the crust on the stailing of bread. Cereal Chemistry, 30, 160.

Bitog, J.P.P., Lee, I.B., Oh, H.M., Hong, S.W., Seo, I.H., & Kwon, K.S. (2014). Optimised hydrodynamic parameters for the design of photobioreactors using computational fluid dynamics and experimental validation. *Biosystems Engineering*, 122, 42-61.

Blandin, H.P., David, J.C. Vergnaud, J.M. (1987). Modelling of drying of coating: effect of the thickness, temperature and concentration of solvent. Progress in Organic Coating, 15, 163-172.

Bourlieu, C., Guillard, V., Vallès-Pamiès, V., Guilbert, S., & Gontard, N. (2009). Edible moisture barriers: How to assess of their potential and limits in food products shelf life extension? Critical Reviews in Food Science and Nutrition, 49, 474-499.

Bourtoom, T. (2008). Edible films and coatings: characteristics and properties. International Food Research Journal, 15, 237-248.

Bravin, B., Peressini, D., Sensidoni, A. (2006).Development and application of polysaccharide-lipid edible coating to extend shelf-life of dry bakery products. Journal of Food Engeneering,76, 280-290.

Chillo, S., Flores, S., Mastromatteo, M., Conte, A., Gerschenson, L., & del Nobile, M. A. (2008). Influence of glycerol and chitosan on tapioca starch-based edible film properties. Journal of Food Engineering, 88, 159e168.

Cioban, C., Alexa, E., Sumalan, R., & Merce, I. (2010). Impact of packaging on Bread physical and chemical properties. Bulletin UASVM Agriculture, 67(2), 212–217.

Defraeye, T. (2014).Advanced computational modelling for drying processes - A review. Applied Energy, 131, 323-344.

Defraeye, T., Verboven, P. (2017). Moisture barriers to control drying of fresh-cut fruit: Quantifying their impact by modelling. Food and Bioproducts Processing, 101, 205-213.

Embuscado, M., Huber, K.C. (2009). Edible films and coating for food applications. Springer.

Fabbri, A., Cevoli C., Troncoso, R. (2014). Moisture diffusivity coefficient estimation in solid food by inversion of a numerical model. Food Research International, 56, 63-67.

Ferreira Saraiva, L.E., Naponucena, L.D.O.M., da Silva Santos, V., Silva, R.P.D., de Souza, C.O., Evelyn Gomes Lima Souza, I., de Oliveira Mamede, M.E., Druzian, J.I. (2016). Development and application of edible film of active potato starch to extend mini panettone shelf life. LWT - Food Science and Technology, 73, 311-319.

Galus, S., Kadzinska, J. (2015). Food application of emulsion-based edible films and oatings. Trends in Food Science & Technology, 45, 273-283.

Incropera, F.P. DeWitt, D.P., Bergman, T.L., Lavine, A.S. (2006). Fundamentals of heat and mass transfer, 6th Edition. Wiley.

Merk, H.J., Prins, J.A. (1954). Thermal Convection Laminar Boundary Layer II. Applied Scientific Research, A4, 195-221.

Monteau, J. (2008). Estimation of thermal conductivity of sandwich bread using an inverse method. Journal of Food Engineering, 85, 132-140.

Muizniece Brasava, S., Dukalska, L., Murniece, I., Dabina Bicka, I., Kozlinskis, E., Sarvi, S., et al. (2012). Active packaging influence on shelf life extension of sliced wheat bread. World Academy of Science, Engineering and Technology, 67, 1128–1134.

Noshirvani, N., Ghanbarzadeh, B., Mokarram, R.R., Hashemi, M. (2017). Novel active packaging based on carboxymethyl cellulose-chitosan-ZnO NPs nanocomposite for increasing the shelf life of bread. Food Packaging and Shelf Life,11, 106-114.

Paeschke, T. (1997). Shelf life extension of reduced-fat baked goods using fruit powders. Cereal Foods World, 42, 391-395.

Pérez-Gago, M.B., Krochta, J.M. (2002). Drying temperature effect on water vapor permeability and mechanical properties of whey protein-lipid emulsion films. Journal of Agricultural and Food Chemistry, 48, 2689-2692.

Purlis, E. (2011). Bread baking: Technological considerations based on process modelling and simulation. Journal of Food Engineering, 103, 92-102.

Purlis, E., Salvadori, V.O. (2009). Modelling the browning of bread during baking. Food Research International, 42, 865-870.

Soazo, M., Rubiolo., A.C., Verdini, R.A. (2011). Effect of drying temperature and beeswax content on physical properties of whey protein emulsion films. Food Hydrocolloids, 25, 1251-1255.

Soukoulis, C., Yonekura, L., Gan, H.H., Behboudi-Jobbehdar, S., Parmenter, C., Fisk, I. (2014). Probiotic edible films as a new strategy for developing functional bakery products: The case of pan bread. Food Hydrocolloids, 39, 231-242.

Zanoni B., Pierrucci, S. Peri, C. (1994). Determination of the thermal diffusivity of bread as a function of porosity. Journal of Food Engineering, 26, 497-510.

Zhang, A.K. Datta. (2006). Mathematical modeling of bread baking process. Journal of Food Engineering, 75, 78-89.

Zogzas, N.P., Maroulis, Z.B., Marinos-Kouris, D. (1994). Moisture diffusivity methods of experimental determination: a review. drying Technology, 12, 483-515.

Effect of edible coating on mini-buns during storage: Textural and near infrared spectroscopic analysis

Journal of Food Engineering (Submitted)

Nallan Chakravartula SS., Cevoli C., Balestra F., Fabbri A., Dalla Rosa M. (2019)

Effect of edible coating on mini-buns during storage: Textural and near infrared spectroscopic analysis

Swathi Sirisha Nallan Chakravartula[a], Chiara Cevoli[b], Federica Balestra[a], Angelo Fabbri [a,b], Marco Dalla Rosa[a,b]

[a] *Department of Agricultural and Food Sciences, Alma Mater Studiorum, University of Bologna, Campus of Food Science, Cesena, Italy.*

[b] *Interdepartmental Centre for Agri-Food Industrial Research, Alma Mater Studiorum, University of Bologna, Campus of Food Science, Cesena, Italy*

*Corresponding author: chiara.cevoli3@unibo.it

Abstract

Moisture migration plays an important role in the stability and quality of bakery products. In this study, a pectin/alginate/whey protein edible coating was used as an edible barrier to evaluate its effectiveness for retaining the quality of bread by reducing moisture loss and textural changes during storage. Burger mini-buns as model systems were applied with 1 layer and 2 layers of coating and evaluated for moisture and texture attributes by both mechanical and spectroscopic techniques. The coatings displayed a retaining effect with the percentual increase in crumb hardness lower for coated samples (1L: 126.5% and 2L: 231.2%) than control samples (Control: 271.8%). Further, the spectral data for the crust and crumb surfaces were pre-treated and subjected to Principal Component analysis (PCA) for the evolution along storage time. In particular for moisture content, discrimination at 8h for crust and after 24h for crumb was noted for both 1L and 2L coating layers with a $R^2 > 0.85$. Subsequently, PLS models with spectral data described satisfactorily the evolution of hardness with low (<10.8) RMSE values.

Keywords: mini-burger buns; staling; edible coating; near infrared.

1

[1] List of Symbols and Abbreviations

1L- Single layer of coating; 2L- Two layers of coating; C- Control bread samples; T- Coated bread samples; MC- Moisture Content; PC- Principal Components; RH- Relative humidity; MSC- Multiple scatter correction; NIR - Near Infra-red; PCA- Principal Component Analysis; PLS- Partial Least Square; SVN- Standard normal variate; RMSE- Root mean square error; RMSEC- Root mean square error Calibration set; RMSECV- Root mean square error Cross Validation set; RMSET- Root mean square error Test set

1. Introduction

Bread is a widely consumed product, with hamburger buns and mini-buns being one of the fast moving products in both supermarkets and fast food market (Esteller et al., 2005) . These are characterized by uniform crust, crumb characteristics and rapid staling depending on the baking and storage conditions, besides mould growth. The shelf-life of bread is extended usually by addition of anti-microbial agents alone or in combination with high barrier and modified atmospheric packaging (MAP).

Staling is a detrimental change resulting in food waste by altering the eating character and aesthetic value of bread. It is a complex phenomenon involving in starch, protein and water interactions that are further complexed by the re-crystallization of starch. The crust staling phenomenon is constantly linked to the re-distribution of moisture whereas the crumb staling is related to the complex interactions and is less understood (Fadda et al., 2014; Gray and Bemiller, 2003; He and Hoseney, 1990). Many studies investigated reduction of staling by use of additives and changes in formulation (Callejo et al., 1999; Gomes-Ruffi et al., 2012; Gray and Bemiller, 2003). However, the control of moisture loss was observed to have a positive effect on the bread staling with higher softness perceived. Moisture desorption and absorption is regulated usually by packaging, with high barrier packaging being used leading to "*over-packaging*"(Piergiovanni and Fava, 1997). Reduced level and alternative packaging solutions are being explored to reduce the packaging impact apart from use of active packaging (Altan et al., 2018; Jideani and Vogt, 2016; Licciardello et al., 2014; Noshirvani et al., 2017; Sarinthip et al., 2018).

In the spectrum of active packaging, recent studies evidenced that the use of edible coatings and films in combination with or without active components have improved the shelf-life of sliced bread (Balaguer et al., 2013; Otoni et al., 2014), mini panettone (Ferreira Saraiva et al., 2016) and cakes (Baeva and Panchev, 2005; Bartolozzo et al., 2016). Moreover, some researchers found positive effect of coatings on the texture and gluten network of cake type products and bread respectively (Baeva and Panchev, 2005; Galvão et al., 2018). In this aspect, edible films and coatings made up of one or more hydrocolloids with or without the addition of lipids with ability to act as gas and water vapor barrier properties (Falguera et al., 2011; Galus and Kadzińska, 2015; Passarinho et al., 2014) can reduce crumb hardening by minimizing the migration of moisture.

The effectiveness of the coatings can be measured in terms of the moisture and textural changes which are strongly correlated to sensorial acceptance. The textural attributes are frequently evaluated with texture profile analysis and compression tests industrially and as observed in literature (Conte et al., 2018; Licciardello et al., 2017). However, other techniques like near infrared spectroscopy (Cevoli et al., 2015; Piccinini et al., 2012), vibrational spectroscopy (Czaja et al., 2018; Nouri et al., 2017; Ringsted et al., 2017) are being explored for higher reliability and non-destructive nature. In particular, NIR spectroscopy in range of 1100nm and 2400nm was found to be related to the bread staling and was comparable to the texture results as observed by Cevoli et al., (2015) and Xie et al., (2003). Also, it is cost effective in comparison to traditional methods with information on both physical and chemical aspects of staling related to the hydrogen bonding. In relation to staling, the spectral wavelengths relating to the amylo-pectin retrogradation was observed to be the main factor for differentiating the staling. Moreover, the absorption bands of water molecules reflect the evolution of changes in starch and protein along the storage time, with successful application of NIR in products like bread and flat breads (Büning-Pfaue, 2003; Osborne, 1996; Wilson et al., 1991; Xie et al., 2003).

In light of the findings, the objective of the work presented is to evaluate the effect of edible coating on commercial hamburger buns as model systems when applied as single and double layers during short storage using physico-mechanical and NIR spectral analyses.

2. Materials and methods

2.1. Materials

Sodium alginate (Sigma-Aldrich, St. Louis Missouri USA), pectin (derived from Citrus peel, Sigma-Aldrich, St. Louis Missouri USA), and whey protein concentrate (80% protein, Products-Gianni SRL, Milan Italy) were used for preparation of edible coating solution. Glycerol (≥99.5%) (Sigma-Aldrich, St. Louis Missouri USA) and Tween® 20 (Sigma-Aldrich, St. Louis Missouri USA) were used as plasticizing and emulsifying agents respectively. The 'mini-burger buns' (Roberto Industria alimentare s.r.l, Italy) were procured from a local market (IperCoop, Cesena, IT). The ingredients of the mini-burger buns as per the packaging are wheat flour, water, rapeseed oil, yeast, Glucose-Fructose syrup, sugar, salt, and emulsifiers.

2.2. Preparation of coated bread

The coating solutions and the coated bread were prepared as described by Nallan Chakravartula et al., (2019). The coating solution was then spread onto the surface of bread with the aid of a confectionary brush as a single layer (1L) or two layers (2L) with 3-minute interval between applications. The samples coated with single or two layers were initially dried at 60°C for 25 min and 35min respectively. The control samples consisted of uncoated samples randomly selected from the packages.

2.3. Storage Evaluation

To study the effect of edible coating on bread dehydration kinetics and texture evolution, the samples were stored at 25°C, 50% RH in climatic chambers (Constant Climate Chamber with Peltier technology, model HPP 108 / 749- Memmert, Germany) for 48h, without any secondary packaging. The samples were evaluated periodically at 0, 2, 4, 6, 8, 12, and 24 hours for the selected parameters. Furthermore, 36h and 48h samples of storage were also considered for NIR spectroscopy.

2.4. Weight loss and Moisture content

The weight loss (%) during storage was recorded using an analytical balance (KERN and Sohn GmbH) up to the nearest 0.001g. Moisture content of the crust and crumb were separately determined by oven drying method (AOAC, 2000) at 105°C until constant weight was achieved.

2.5. Mechanical characteristics

Mechanical characteristics were evaluated by Texture profile analysis (TPA) using a Texture Analyser (Mod.TA.HDi 500, Stable Micro Systems, Surrey, UK) according to Balestra et al., (2011) with modifications of using a P/75mm cylindrical aluminum probe attached to a 25kg load cell and whole bread similar to Guadarrama-Lezama et al., (2016). The data were acquired by associated software (Textexceed) and the texture parameters namely; hardness, chewiness and cohesivity were calculated. The sample hardness was determined by evaluating the maximum force of the first compression peak and is expressed in Newton's (N). Cohesivity was calculated as the ratio of work during the second compression cycle to that of first compression cycle. Finally chewiness (N) was calculated from product of hardness, cohesivity and springiness.

2.6. NIR spectroscopy

The control and coated samples were submitted to near-infrared spectroscopy (NIR) for acquisition of the spectra using a FT-NIR spectrophotometer (MATRIX ™ -F, Bruker Optics) in diffuse reflectance in the range of 800 and 2500 nm ($8cm^{-1}$ resolution). An average of 32 scans was obtained for each sample at interval of storage by placing the optical fiber probe (IN 261, Bruker Optics, Mass., USA) in direct contact with the bread surface. The probe is characterized by a diameter of 10mm with a bifurcated fiber bundle to illuminate the sample and collect the refracted light. For each spectral wave, the background was acquired by placing the probe in the specific support covered with quartz under the same environmental conditions as the sample (25° C) and subtracted from sample spectra. The bread was scanned at 3 central points of the upper crust, lower crust and crumb; subsequently for each surface, the average spectrum of the three acquisitions was calculated.

2.7. Data analysis

Significant differences between means of mechanical parameters, weight loss and moisture content at different storage times were explored by using ANOVA (post-hoc Tukey HSD, p-level <0.05). Kruskal-Wallis test was used if significant differences emerged between variance means of the Levene test (Statistica-StatSoft, version 7). Pearson's analysis, (p-level <0.05) was performed to evaluate the correlation between moisture content and mechanical parameters.

The NIR spectra acquired on different bread samples were analyzed by multivariate analyses (The Unscrambler ver. 9.7, CAMO, Oslo, Norway). The first part of the spectra until 1,200nm was deleted as it contains no useful chemical information, but only instrumental noise. The absorbance data were normalized by using the Standard Normal Variate (SNV) technique. To remove the effects of light scattering, spectra were pre-treated with multiplicative scattering correction (MSC). To reduce the noise and obtain more band information, the absorbance data were treated by applying the first derivative (Savitsky–Golay). Furthermore, spectral data were subjected to Principal Component Analysis (PCA) and Partial Least Square (PLS) regression to discriminate the samples as function of different storage times, and to predict moisture content and mechanical parameters, respectively. The predictive power of the obtained models were tested by analyzing the calibration results and by performing the full cross and test set validation (30% of the samples). Randomly selecting the samples, the models were solved 5 times and the mean results were analyzed in terms of determination coefficient (R^2) and Root

Mean Square Error (RMSE). To avoid the model over-fitting, optimal number of latent factors was identified by plotting the root mean square error as a function of the number of factors (minimum of the curve).

3. Results & Discussions

3.1. Weight loss and Moisture content

Water is an important aspect of bread which directly determines the consumer perception of freshness. Water within the product is redistributed from crumb to crust and subsequently lost to the environment during storage, causing change in crust/crumb moisture and weight. Table 1 presents the weight loss data for the Control (C), 1L and 2L coated mini-buns increasing significantly for all samples along the storage time. However, the control samples registered a marginal of 1-2% higher weight loss than the coated samples irrespective of the number of layers. Subsequently, the moisture content decreased following an exponential trend with the final moisture loss being 66.1% for control and 62.8% to 64.2% for 1L and 2L coated samples, respectively with 2L coating exhibiting significantly lower moisture loss. It is expected that the moisture content decreases along the storage time and specific behavior with respect to the surface was not observed concerning the top and bottom surfaces. However, a slight decrease in the moisture loss by 2L coating was observed that might be indicative of retaining effect, as observed in dietetic cakes covered with pectin films by Baeva and Panchev, (2005).

Table 1. Weight loss and moisture content of control and coated (1L, 2L) mini buns during storage

Sample		Storage time (hours)						
		0	2	4	6	8	12	24
Weight loss (%)								
Whole bread	1L	0.0 ± 0.0^{a}	-1.5 ± 0.3^{b}	-3.0 ± 0.5^{c}	-3.9 ± 0.3^{cd}	-4.7 ± 0.4^{d}	-11.5 ± 0.9^{e}	-12.4 ± 0.6^{e}
	2L	0.0 ± 0.0^{a}	-1.8 ± 0.3^{b}	-3.6 ± 0.4^{c}	-5.0 ± 0.5^{d}	-6.5 ± 0.5^{e}	-10.4 ± 0.4^{f}	-13.3 ± 0.7^{g}
	Control	0.0 ± 0.0^{a}	-2.5 ± 0.1^{b}	-4.1 ± 0.1^{bc}	-5.6 ± 0.1^{bcd}	-7.4 ± 0.4^{bcd}	-10.8 ± 0.2^{bcd}	-15.7 ± 0.2^{bcd}
Moisture content(%)								
Top crust	1L	22.1 ± 0.9^{a}	19.7 ± 0.3^{b}	19.6 ± 0.5^{b}	19.0 ± 0.8^{b}	18.6 ± 0.5^{b}	16.5 ± 0.8^{c}	14.8 ± 0.5^{d}
	2L	18.2 ± 0.4^{a}	16.1 ± 0.8^{b}	16.0 ± 0.6^{b}	17.6 ± 1.4^{ab}	17.1 ± 1.2^{ab}	13.3 ± 0.9^{c}	12.6 ± 0.8^{c}
	Control	18.7 ± 0.7^{abc}	18.2 ± 0.7^{abc}	17.4 ± 1.3^{abc}	17.2 ± 1.1^{b}	16.4 ± 0.5^{b}	20.5 ± 3.9^{c}	11.6 ± 0.5^{d}
Bottom crust	1L	21.0 ± 0.5^{a}	20.7 ± 0.8^{a}	20.6 ± 0.8^{a}	20.2 ± 1.5^{a}	18.6 ± 0.8^{b}	17.8 ± 0.8^{b}	14.6 ± 0.4^{c}
	2L	22.3 ± 1.4^{a}	19.4 ± 1.2^{b}	17.6 ± 1.1^{b}	19.1 ± 1.7^{b}	18.5 ± 0.6^{b}	14.5 ± 0.7^{c}	13.4 ± 0.9^{c}
	Control	18.8 ± 1.7^{a}	17.8 ± 0.8^{a}	17.4 ± 0.4^{a}	18.0 ± 1.2^{a}	17.1 ± 1.1^{a}	16.8 ± 2.5^{a}	11.4 ± 1.0^{bc}
Crumb	1L	31.4 ± 0.9^{a}	30.6 ± 0.5^{a}	31.0 ± 0.6^{a}	28.1 ± 0.8^{b}	26.2 ± 0.8^{c}	26.5 ± 0.6^{c}	19.7 ± 0.4^{d}
	2L	30.4 ± 0.9^{a}	30.7 ± 0.3^{a}	29.9 ± 0.6^{a}	25.5 ± 0.9^{b}	24.9 ± 0.6^{b}	24.9 ± 0.6^{b}	19.6 ± 0.7^{c}
	Control	31.1 ± 0.7^{a}	29.9 ± 0.4^{b}	30.7 ± 0.5^{ab}	27.5 ± 0.6^{c}	26.5 ± 0.4^{d}	22.4 ± 0.3^{e}	17.3 ± 0.3^{f}

Values are mean ± SD; Different letters row-wise indicate significant differences ($p<0.05$).

3.2. Mechanical parameters

The effect of the coatings in controlling the staling has been evaluated by textural parameters namely hardness, cohesivity and chewiness as presented in table 2 until 24h of storage. Texture is an important characteristic for the acceptance of bread and the parameter hardness is strongly correlated to the consumer purchase decision. The redistribution of moisture from crumb to crust and the retrogradation of starch are the main factors for hardening of the crumb (Fadda et al., 2014; Gray and Bemiller, 2003). A significant increase in the bread hardness and chewiness has been observed with the increase in storage time as expected (He and Hoseney, 1990; Licciardello et al., 2014). The hardness of the coated sample was significantly higher than their respective control at time '0h'. This can be probably due to the fact that whole bread was considered including the crust, to have similar effect as to when a bun is consumed. The addition of coating as expected formed an individual layer on the top of the crust which might have contributed to the additional hardness. Although the coated sample had higher initial hardness, considering the degree of increase in hardness until 24h the control sample registered higher value (Control: 271.8%) than those of the coated samples (1L: 126.5% and 2L: 231.2%), confirming the retaining effect of the coating. Similar inferences on hardness have been observed by Eom et al., (2018) with starch/gum based edible coating for rice cakes. However, cohesivity decreased during storage, irrespective of the presence or absence of coating. Subsequently, chewiness related to the reinforcement and dehydration of bread increased along storage time. This trend is similar to that of the hardness values with a higher increase in the control in comparison to the coated samples.

Table 2. Mechanical parameters of control and coated (1L, 2L) mini buns during storage

Parameter	Storage time (h)						
Hardness (N)	0	2	4	6	8	12	24
1L	21.5 ± 1.5^{a}	23.8 ± 1.4^{ab}	27.5 ± 2.2^{ab}	28.8 ± 1.7^{b}	35.6 ± 3.4^{c}	48.6 ± 4.6^{d}	100.2 ± 4.7^{e}
2L	25.0 ± 3.1^{a}	29.6 ± 1.3^{ab}	28.2 ± 3.3^{ab}	39.8 ± 2.4^{abc}	43.0 ± 3.2^{abc}	82.8 ± 4.9^{bc}	136.3 ± 14.9^{c}
Control	19.4 ± 2.6^{a}	24.7 ± 3.6^{a}	25.6 ± 2.1^{a}	29.6 ± 3.1^{ab}	36.4 ± 3.1^{b}	72.3 ± 7.5^{c}	128.8 ± 9.9^{d}
Cohesivity							
1L	0.43 ± 0.0^{a}	0.42 ± 0.0^{a}	0.40 ± 0.0^{a}	0.41 ± 0.0^{a}	0.40 ± 0.0^{a}	0.41 ± 0.0^{a}	0.42 ± 0.0^{a}
2L	0.41 ± 0.0^{a}	0.40 ± 0.0^{a}	0.39 ± 0.0^{a}	0.39 ± 0.0^{a}	0.37 ± 0.0^{a}	0.36 ± 0.0^{a}	0.38 ± 0.0^{a}
Control	0.42 ± 0.0^{a}	0.38 ± 0.0^{b}	0.39 ± 0.0^{ab}	0.38 ± 0.0^{b}	0.37 ± 0.0^{b}	0.37 ± 0.0^{b}	0.38 ± 0.0^{b}
Chewiness (N)							
1L	6.34 ± 0.3^{a}	7.1 ± 0.6^{a}	7.5 ± 0.6^{a}	8.5 ± 0.9^{ab}	10.6 ± 1.2^{b}	15.1 ± 1.8^{c}	33.3 ± 1.8^{d}
2L	7.0 ± 0.8^{a}	8.3 ± 0.3^{ab}	7.8 ± 0.9^{ab}	11.1 ± 1.0^{abc}	11.4 ± 0.7^{abc}	22.2 ± 2.1^{bc}	39.3 ± 4.2^{c}
Control	5.4 ± 0.9^{a}	6.1 ± 0.8^{ab}	6.7 ± 0.7^{ab}	7.7 ± 0.9^{ab}	9.1 ± 1.1^{b}	19.9 ± 0.8^{c}	37.3 ± 3.8^{d}

Values are mean ± SD; Different letters row-wise indicate significant differences ($p<0.05$)

Furthermore, the moisture and textural parameters correlation was investigated by using *Pearson* test (table 3). As can be observed the moisture content of crust and crumb are positively correlated for both 1L (r=0.86-0.90) and for 2L (r=0.51-0.76). Hardness and chewiness were negatively correlated to the moisture, with a stronger correlation to crumb moisture (r= 0.91-0.96) for both the layers studied. However, cohesivity (Co) was observed to be negatively correlated to the hardness and chewiness irrespective of sample. This observation is similar to that observed by Chin et al., (2011) in sweet buns with different types of glazing.

Table 3. Correlation between moisture content and the mechanical parameters

1L	M_T	M_B	M_C	H	Co	Che
M_T	1.00					
M_B	0.86	1.00				
M_C	0.86	0.89	1.00			
H	-0.85	-0.85	-0.94	1.00		
Co	-0.16	-0.16	-0.23	0.32	1.00	
Che	-0.82	-0.82	-0.91	0.98	0.48	1.00
2L						
M_T	1.00					
M_B	0.67	1.00				
M_C	0.52	0.71	1.00			
H	-0.65	-0.77	-0.91	1.00		
Co	0.25	0.40	0.46	-0.38	1.00	
Che	-0.65	-0.77	-0.91	1.00	-0.32	1.00
Control						
M_T	1.00					
M_B	0.74	1.00				
M_C	0.51	0.76	1.00			
H	-0.56	-0.80	-0.96	1.00		
Co	0.15	0.31	0.39	-0.31	1.00	
Che	-0.57	-0.81	-0.95	1.00	-0.25	1.00

**1L- 1 layer; 2L- 2 layers; M_T – moisture top crust (%); M_B – moisture bottom crust (%); M_C – moisture crumb (%); H- hardness (N); Co- Cohesivity; Che- Chewiness (N).*

3.3. NIR spectroscopy

The characteristic near infrared spectra of coated bread at different storage times are shown in figure 1. In particular, resonance bands of O–H bonds related to water and starch were observed at about 1450 and 1940 nm, and N-H bonds vibrations at 1500–1570 nm and 2050–2070 nm. The absorption peaks at 1730, 1770 and 2310 nm were ascribed to the first overtone of the C–H stretch and to C–H_2 group of the lipids (Cevoli et al., 2015; Giangiacomo, 2006; Nallan Chakravartula et al., 2019).

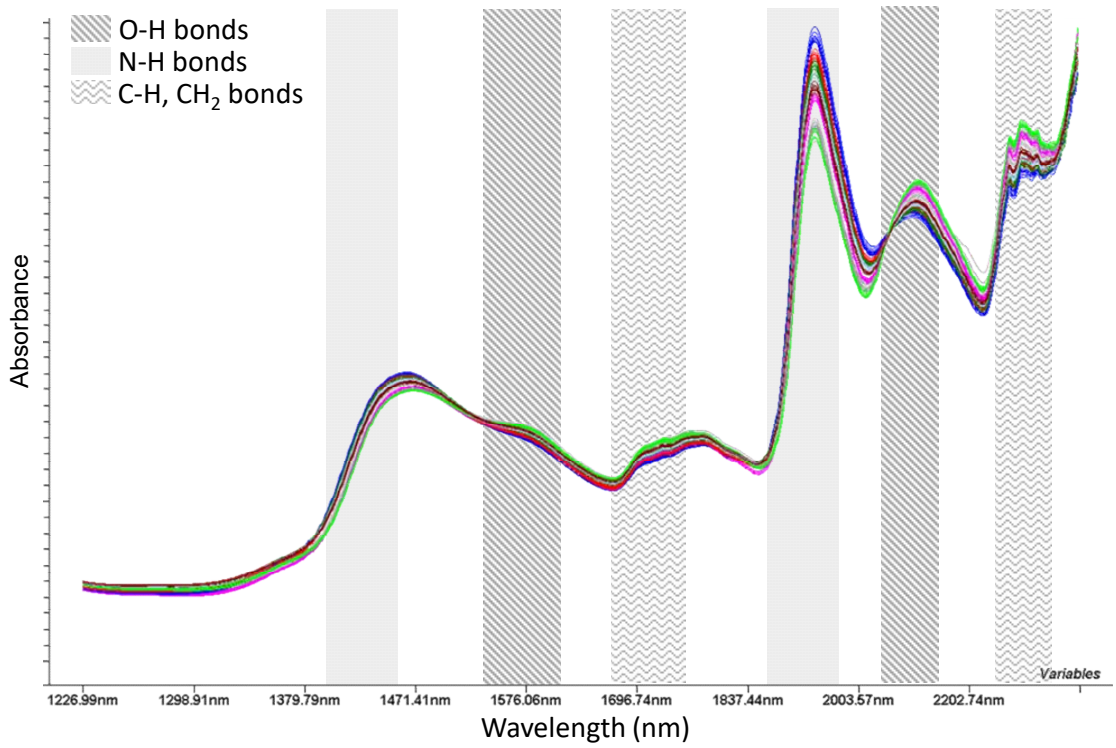

Figure 1. Representative spectra of coated samples during storage.

The PCA score plots for the NIR spectra were performed to discriminate between control samples (C) and coated bread samples (T). Both top and bottom crust surfaces along with crumb were considered. The best results were obtained by using the SNV spectral pre-treatment followed by the Savitzky–Golay. As reported in figure 2, a clear separation between samples was observed along the PC3 (1%). Through the analysis of the X-loading it was possible to observe that the highest variance (PC3) corresponds to 2050-2070nm spectral range (N-H bonds). This is probably due to the protein contributed by the coating on the treated samples. Similar results were obtained for both one and two layers of coating (data not shown).

Considering the storage time, it can be observed that the spectral absorbance decreases in the region related to O-H bonds and reciprocatively increases in the typical spectral range of the fats and proteins, (N-H, C-H and C-H_2 bonds). The PCA score plots (PC1 *vs.* PC2) developed to discriminate the samples on the basis of the storage time are reported in figure 3, for the top, bottom crust and centre crumb, respectively. The samples are arranged along the PC1 (explained variance 98%, 97% and 97%) on the basis of the storage time. A clear separation between samples was observed, for the top and bottom surface, especially after 8 hours of

storage. With regard to the centre, discrimination was detected only after 24 hours of storage as constant moisture content was observed for two days of storage. Following, the spectral data were subjected to PLS to estimate the moisture content and mechanical parameters. Results are reported in Table 4 and 5, for the moisture and mechanical parameters, respectively.

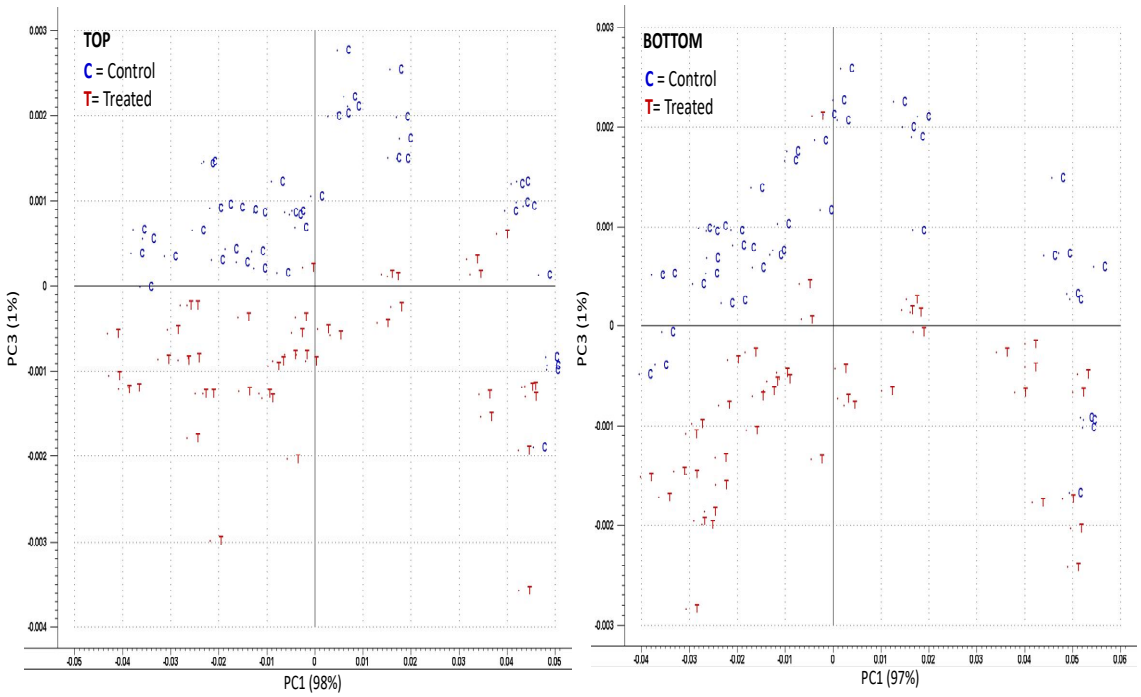

Figure 2. PCA score plots for the top and bottom surface of the control (C) and treated (T) samples with 1L coating.

Table 4. PLS regression parameters for moisture content

Sample		Calibration		Cross-Validation		Test Set Validation	
		R^2	RMSEC	R^2	RMSECV	R^2	RMSET
1L	Top	0.949	0.87	0.948	0.9	0.938	0.9
	Bottom	0.957	0.72	0.955	0.77	0.947	0.85
	Centre	0.969	1.31	0.959	1.4	0.946	1.52
2L	Top	0.915	1.01	0.852	1.31	0.8451	1.36
	Bottom	0.901	1.32	0.899	1.35	0.862	1.45
	Centre	0.957	1.51	0.945	1.72	0.921	1.88

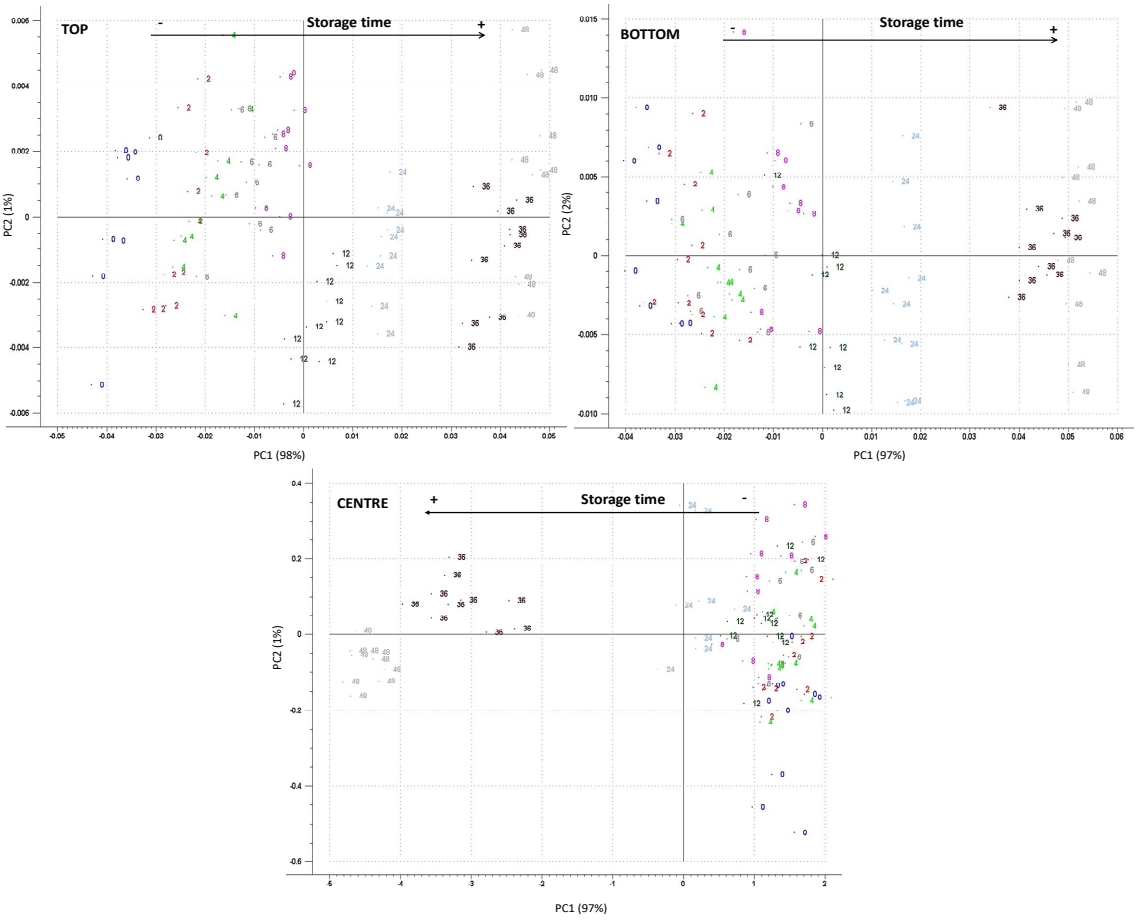

Figure 3. PCA score plots for the samples (1L) along storage time for different bread surfaces.

In general, for the moisture content, satisfactory results were achieved for one and two coating layers and bread position (top, bottom and centre) with a R^2 in test set ranging from 0.938 to 0.947, and from 0.845 to 0.921 respectively. Analyzing the calibration, the full cross and the test set validation, the best models concern the sample characterized by one layer of coating (top: R^2=0.938, RMSET=0.9%; bottom: R^2=0.947, RMSET=0.85%; centre: R^2=0.946, RMSET=1.52%).

Concerning the mechanical parameters, hardness and chewiness were taken into account and PLS models were developed analyzing the NIR spectra acquired on the bread top. Also in this case, good results were obtained in terms of R^2 and RMSE for calibration, cross-validation and test set validation, respectively. The best results were reached for the hardness of the samples with 2 layers of coating (R^2=0.915, RMSET=10.7 N). Recently, Ringsted et al., (2017) reported correlation values (R^2) between bread hardness measured during 7 days of storage, and near-infrared bands ranging from 0.88 to 0.97. More weak results were obtained by Xie et al., (2003) developing a PLS model (NIR spectra) to predict the firmness of bread stored at

27°C for 5 days (R^2=0.80 in calibration). With regard to flat bread tensile tests and near-infrared reflectance spectroscopy were used to monitor flat bread ageing treated by preservatives. Al-Mahsaneh et al., (2018) reported high R^2 values and confirmed that the NIRS along with texture analysis are valuable tools to detect the effect of the preservatives on shelf-life and quality of flat bread.

Table 5. PLS regression parameters for mechanical parameters

Sample	Mechanical parameters	Calibration		Cross-Validation		Test Set Validation	
		R^2	RMSEC	R^2	RMSECV	R^2	RMSET
1L	Hardness (N)	0.947	5.4	0.886	8.1	0.878	8.8
	Chewiness (N)	0.974	1.4	0.901	2.9	0.879	3.4
2L	Hardness (N)	0.973	6.3	0.924	10.6	0.915	10.7
	Chewiness (N)	0.969	2.2	0.915	3.7	0.892	3.7

4. Conclusions

The results of the presented study show that the application of coating has a retaining effect on the product to some extent. The NIR spectroscopy was useful in modeling the textural responses during storage on basis of both changes in moisture and protein bands. The principal component analysis was useful for differentiating the samples based on coating application. Further, PLS modeling established a correlation to the surface moisture and texture which might be useful to track staling. The practical knowledge on coatings effect on staling is useful to develop potential solutions to preserve bread with higher efficiency and lower packaging impact.

References

AOAC, (2000). AOAC Method 945.15, Moisture in cereal adjuncts: air oven method». In *Official Methods of Analysis of AOAC International* (17th ed.). Varlington, Va, USA: Association of Official Analytical Chemists.

Al-Mahsaneh, M., Aljarrah, M., Rababah, T., Alu'datt, M., 2018. Using MR-FTIR and Texture Profile to Track the Effect of Storage Time and Temperature on Pita Bread Staling. J. Food Qual. 2018, 1–9. https://doi.org/10.1155/2018/8252570

Altan, A., Aytac, Z., Uyar, T., 2018. Carvacrol loaded electrospun fibrous films from zein and poly(lactic acid) for active food packaging. Food Hydrocoll. 81, 48–59. https://doi.org/https://doi.org/10.1016/j.foodhyd.2018.02.028

Baeva, M., Panchev, I., 2005. Investigation of the retaining effect of a pectin-containing edible film upon the crumb ageing of dietetic sucrose-free sponge cake. Food Chem. 92, 343–348. https://doi.org/10.1016/j.foodchem.2004.03.060

Balaguer, M.P., Lopez-Carballo, G., Catala, R., Gavara, R., Hernandez-Munoz, P., 2013. Antifungal properties of gliadin films incorporating cinnamaldehyde and application in active food packaging of bread and cheese spread foodstuffs. Int. J. Food Microbiol. 166, 369–377. https://doi.org/10.1016/j.ijfoodmicro.2013.08.012

Balestra, F., Cocci, E., Pinnavaia, G., Romani, S., 2011. Evaluation of antioxidant, rheological and sensorial properties of wheat flour dough and bread containing ginger powder. LWT - Food Sci. Technol. 44, 700–705. https://doi.org/10.1016/j.lwt.2010.10.017

Bartolozzo, J., Borneo, R., Aguirre, A., 2016. Effect of triticale-based edible coating on muffin quality maintenance during storage. J. Food Meas. Charact. 10, 88–95. https://doi.org/10.1007/s11694-015-9280-1

Büning-Pfaue, H., 2003. Analysis of water in food by near infrared spectroscopy. Food Chem. 82, 107–115. https://doi.org/10.1016/S0308-8146(02)00583-6

Callejo, M.J., Gil, M.J., Rodríguez, G., Ruiz, M. V, 1999. Effect of gluten addition and storage time on white pan bread quality: instrumental evaluation. Zeitschrift für Leb. und -forsch. A 208, 27–32. https://doi.org/10.1007/s002170050370

Cevoli, C., Gianotti, A., Troncoso, R., Fabbri, A., 2015. Quality evaluation by physical tests of a traditional Italian flat bread Piadina during storage and shelf-life improvement with sourdough and enzymes. Eur. Food Res. Technol. 240, 1081–1089. https://doi.org/10.1007/s00217-015-2429-7

Chin, N.L., Abdullah, R., Yusof, Y.A., 2011. Glazing effects on bread crust and crumb staling during storage. J. Texture Stud. 42, 459–467. https://doi.org/10.1111/j.1745-4603.2011.00307.x

Conte, P., Del Caro, A., Balestra, F., Piga, A., Fadda, C., 2018. Bee pollen as a functional ingredient in gluten-free bread: A physical-chemical, technological and sensory approach. LWT 90, 1–7. https://doi.org/https://doi.org/10.1016/j.lwt.2017.12.002

Czaja, T., Kuzawińska, E., Sobota, A., Szostak, R., 2018. Determining moisture content in pasta by vibrational spectroscopy. Talanta 178, 294–298. https://doi.org/10.1016.2017.09.050

Eom, H., Chang, Y., Lee, E. sil, Choi, H.D., Han, J., 2018. Development of a starch/gum-based edible coating for rice cakes to retard retrogradation during storage. Lwt 97, 516–

522. https://doi.org/10.1016/j.lwt.2018.07.044

Esteller, M.S., Pitombo, R.N.M., Lannes, S.C.S., 2005. Effect of freeze-dried gluten addition on texture of hamburger buns. J. Cereal Sci. 41, 19–21. https://doi.org/10.1016/j.jcs.2004.08.013

Fadda, C., Sanguinetti, A.M., Del Caro, A., Collar, C., Piga, A., 2014. Bread staling: Updating the view. Compr. Rev. Food Sci. Food Saf. 13, 473–492. https://doi.org/10.1111/1541-4337.12064

Falguera, V., Quintero, J.P., Jiménez, A., Muñoz, J.A., Ibarz, A., 2011. Edible films and coatings: Structures, active functions and trends in their use. Trends Food Sci. Technol. 22, 292–303. https://doi.org/10.1016/j.tifs.2011.02.004

Ferreira Saraiva, L.E., Naponucena, L. de O.M., da Silva Santos, V., Silva, R.P.D., de Souza, C.O., Evelyn Gomes Lima Souza, I., de Oliveira Mamede, M.E., Druzian, J.I., 2016. Development and application of edible film of active potato starch to extend mini panettone shelf life. LWT 73, 311–319. https://doi.org/10.1016/j.lwt.2016.05.047

Galus, S., Kadzińska, J., 2015. Food applications of emulsion-based edible films and coatings. Trends Food Sci. Technol. 45, 273–283. https://doi.org/10.1016/j.tifs.2015.07.011

Galvão, A.M.M.T., Zambelli, R.A., Araújo, A.W.O., Bastos, M.S.R., 2018. Edible coating based on modified corn starch/tomato powder: Effect on the quality of dough bread. LWT 89, 518–524. https://doi.org/https://doi.org/10.1016/j.lwt.2017.11.027

Giangiacomo, R., 2006. Study of water–sugar interactions at increasing sugar concentration by NIR spectroscopy. Food Chem. 96, 371–379. https://doi.org/10.1016/j.foodchem.2005.02.051

Gomes-Ruffi, C.R., Cunha, R.H. da, Almeida, E.L., Chang, Y.K., Steel, C.J., 2012. Effect of the emulsifier sodium stearoyl lactylate and of the enzyme maltogenic amylase on the quality of pan bread during storage. LWT - Food Sci. Technol. 49, 96–101. https://doi.org/https://doi.org/10.1016/j.lwt.2012.04.014

Gray, J.A., Bemiller, J.N., 2003. Bread Staling: Molecular Basis and Control. Compr. Rev. Food Sci. Food Saf. 2, 1–21. https://doi.org/10.1111/j.1541-4337.2003.tb00011.x

Guadarrama-Lezama, A.Y., Carrillo-Navas, H., Vernon-Carter, E.J., Alvarez-Ramirez, J., 2016. Rheological and thermal properties of dough and textural and microstructural features of bread obtained from nixtamalized corn/wheat flour blends. J. Cereal Sci. 69, 158–165. https://doi.org/https://doi.org/10.1016/j.jcs.2016.03.011

He, H., Hoseney, R.C., 1990. Changes in Bread Firmness and Moisture During Long-Term Storage. Cereal Chem. 67, 603–605.

Jideani, V.A., Vogt, K., 2016. Antimicrobial Packaging for Extending the Shelf Life of Bread-A Review. Crit. Rev. Food Sci. Nutr. 56, 1313–24.

https://doi.org/10.1080/10408398.2013.768198

Licciardello, F., Cipri, L., Muratore, G., 2014. Influence of packaging on the quality maintenance of industrial bread by comparative shelf life testing. Food Packag. Shelf Life 1, 19–24. https://doi.org/10.1016/j.fpsl.2013.10.001

Licciardello, F., Giannone, V., Del Nobile, M.A., Muratore, G., Summo, C., Giarnetti, M., Caponio, F., Paradiso, V.M., Pasqualone, A., 2017. Shelf life assessment of industrial durum wheat bread as a function of packaging system. Food Chem. 224, 181–190. https://doi.org/10.1016/j.foodchem.2016.12.080

Nallan Chakravartula, S.S., Cevoli, C., Balestra, F., Fabbri, A., Dalla Rosa, M., 2019. Evaluation of drying of edible coating on bread using NIR spectroscopy. J. Food Eng. 240, 29–37. https://doi.org/10.1016/j.jfoodeng.2018.07.009

Noshirvani, N., Ghanbarzadeh, B., Rezaei Mokarram, R., Hashemi, M., 2017. Novel active packaging based on carboxymethyl cellulose-chitosan-ZnO NPs nanocomposite for increasing the shelf life of bread. Food Packag. Shelf Life 11, 106–114. https://doi.org/10.1016/j.fpsl.2017.01.010

Nouri, M., Nasehi, B., Abdanan Mehdizadeh, S., Goudarzi, M., 2017. A novel application of vibration technique for non-destructive evaluation of bread staling. J. Food Eng. 197, 44–47. https://doi.org/10.1016/j.jfoodeng.2016.11.003

Osborne, B.G., 1996. Near Infrared Spectroscopic Studies of Starch and Water in Some Processed Cereal Foods. J. Near Infrared Spectrosc. 4, 195–200. https://doi.org/10.1255/jnirs.90

Otoni, C.G., Pontes, S.F.O., Medeiros, E.A.A., Soares, N.D.F.F., 2014. Edible Films from Methylcellulose and Nanoemulsions of Clove Bud (Syzygium aromaticum) and Oregano (Origanum vulgare) Essential Oils as Shelf Life Extenders for Sliced Bread. J. Agric. Food Chem. 62, 5214–5219. https://doi.org/10.1021/jf501055f

Passarinho, A.T.P., Dias, N.F., Camilloto, G.P., Cruz, R.S., Otoni, C.G., Moraes, A.R.F., Soares, N.D.F.F., 2014. Sliced Bread Preservation through Oregano Essential Oil-Containing Sachet. J. Food Process Eng. 37, 53–62. https://doi.org/10.1111/jfpe.12059

Piccinini, M., Fois, S., Secchi, N., Sanna, M., Roggio, T., Catzeddu, P., 2012. The Application of NIR FT-Raman Spectroscopy to Monitor Starch Retrogradation and Crumb Firmness in Semolina Bread. Food Anal. Methods 5, 1145–1149. https://doi.org/10.1007/s12161-011-9360-8

Piergiovanni, L., Fava, P., 1997. Minimizing the residual oxygen in modified atmosphere packaging of bakery products. Food Addit. Contam. 14, 765–773. https://doi.org/10.1080/02652039709374587

Ringsted, T., Siesler, H.W., Engelsen, S.B., 2017. Monitoring the staling of wheat bread using

2D MIR-NIR correlation spectroscopy. J. Cereal Sci. 75, 92–99. https://doi.org/10.1016/j.jcs.2017.03.006

Sarinthip, T., Dowan, K., Jongchul, S., Thanakkasaranee, S., Kim, D., Seo, J., 2018. Preparation and characterization of polypropylene/sodium propionate (PP/SP) composite films for bread packaging application. Packag. Technol. Sci. 31, 221–231. https://doi.org/10.1002/pts.2369

Wilson, R.H., Goodfellow, B.J., Belton, P.S., Osborne, B.G., Oliver, G., Russell, P.L., 1991. Comparison of fourier transform mid infrared spectroscopy and near infrared reflectance spectroscopy with differential scanning calorimetry for the study of the staling of bread. J. Sci. Food Agric. 54, 471–483. https://doi.org/10.1002/jsfa.2740540318

Xie, F., Dowell, F.E., Sun, X.S., 2003. Comparison of near-infrared reflectance spectroscopy and texture analyzer for measuring wheat bread changes in storage. Cereal Chem. 80, 25–29. https://doi.org/10.1094/CCHEM.2003.80.1.25

Edible coatings application on bread: Effect of application stage and type of coating in storage

Manuscript

Nallan Chakravartula SS., Balestra F., Romani S., Dalla Rosa M. (2019)

Edible coatings application on bread: Effect of application stage and type of coating in storage

Swathi Sirisha Nallan Chakravartula[a, b], Federica Balestra[b], Santina Romani [a, b],Marco Dalla Rosa[a, b]

[a] *Department of Agricultural and Food Sciences, Alma Mater Studiorum, University of Bologna, Campus of Food Science, Cesena, Italy.*

[b] *Interdepartmental Centre for Agri-Food Industrial Research, Alma Mater Studiorum, University of Bologna, Campus of Food Science, Cesena, Italy*

Abstract

Pan-bread is characterized by thin crust and evenly distributed crumb, with short shelf-life and rapid staling depending on baking and storage conditions contributing to economic losses. Recent research trends towards the use of edible coatings and films in bakery products to preserve freshness and incorporate secondary functionalities. In this context, it was considered interesting to study effect of coating application: before baking (BB), at interrupted baking (PB) and post baking (FB) on bread characteristics. Composite edible coatings based on pectin, sodium alginate and whey protein concentrate without (C) and with butter (B) or corn oil (O) were applied by spreading on bread. The samples were packed in OPA-PP (bi-oriented polyamide-polypropylene) bags, stored in climatic chamber (at 25°C, 50% RH) and evaluated for crust firmness, crumb texture (TPA) and moisture content (AOAC, 2000). The coatings applied on the crust were observed to form an individual layer and have a significant effect ($p<0.05$) on bread characteristics. Considering the stage of application, FB group had marked effect followed by PB and BB groups for moisture retention. The PB group had retained softer crumb majorly due to the type of baking. Whereas, the application of coating BB had a slight degrading effect on the bread shape due to the expulsion of gas. Within each baking group, comparing the coated samples (C, O, B) to that of uncoated (U), samples O had the lowest firming rate (BB-10.09; PB-7.3 N/d). However in FB group, coating without oil or butter registered lowest firming rate, in accordance with lower initial moisture content. In view of the obtained results, as expected the presence of hydrophobic coatings reduced the loss of moisture and rate of crumb firming of the bread during storage. Also, coatings could be a suitable vehicle to incorporate bread with secondary functions without effecting bread characteristics.

Keywords: Hydrophobic coatings; bread; firming behavior.

1. Introduction

Edible coatings can be defined as a preliminary layer of packaging applied on the surface as thin layer(s) by dipping, spreading or spraying to increase the functionality and quality of foods. The major components for the preparation of edible coatings are usually one or more polysaccharide(s), protein(s) with or without addition of lipid(s) (Baeva & Panchev, 2005; Debeaufort & Voilley, 2009; Galus & Kadzińska, 2015). Edible coatings and films were found to be effective in reducing the physico-chemical and physiological changes in many perishable, semi-perishable foods as well as act as physical barriers for moisture loss and fat uptake. Recently, a renewed interest was found in utilizing edible coatings as carriers for active, functional compounds like antioxidants, antimicrobials, vitamins and probiotics for food systems (Altamirano-Fortoul *et al*., 2012; Falguera *et al*., 2011; Galvão *et al*., 2018; Guillard *et al*., 2003; Soukoulis *et al*., 2014).

Bakery products, particularly breads are a staple product which face quality deterioration during storage due to staling and mould spoilage. Staling is a complex phenomenon influencing the textural quality and consumer acceptance of bread contributing to economic losses (Cauvain, 2006). Extensive reviews by (Fadda et al., 2014; Galić et al., 2009) C. *et al*., 2014; Galić *et al*., 2009 provides an overview of anti-staling mechanisms explored in the past decade by use of anti-staling agents, emulsifiers, enzymes; fermentation methods, par-baking and packaging methods like MAP. However, industries continuously search for new alternatives to maintain the fresh quality of food for longer storage periods. Recent research trends towards exploiting the use of edible coatings and films also in bakery products particularly to preserve freshness and improve functionality. Studies on crumb firming kinetics and textural changes of cake and cake-type products were observed to be delayed by use of edible coatings (Baeva and Panchev, 2005; Bartolozzo et al., 2016; Ferreira Saraiva et al., 2016).

Otoni, et. al., (2014), observed that use of active films based on methylcellulose and emulsions of Oregon and clove oils effectively reduced the growth of yeasts and moulds in packaged bread slices. Similarly, Ferreira Saraiva *et al*., (2016) demonstrated the effect of potassium sorbate and citric acid incorporation in potato starch edible coatings on yeast and mould growth in mini-pannetones. Though there was a specific increase in hardness, the authors considered this change as a desirable maturation step for enhanced organoleptic profile.

However, the active coatings were successful in extending the shelf life of mini-panettones by 2-4 times for different coatings.

In another study on probiotic coatings application by Soukoulis *et al*., (2014) in pan breads, it was observed that the temperature of coat drying rather had an effect on moisture changes than the specific presence of coating. Moreover, it was suggested that coatings might have limited effect on the staling of crumb as evaluated by thermal analysis. Similarly, Altamirano-Fortoul *et al*., (2012), during a short storage of partially baked bread with probiotic coatings evidenced that the coatings induced a slight change in water activity of the crust initially but did not affect the trend of water or textural changes during storage. In most of the studies the coating was applied in a subsequent process step after baking necessitating a drying step, except for par baked bread, where the coating was applied before complete baking. Chin *et al*., 2011, studied the effect of glazes on texture and demonstrated reduced moisture loss and crumb firming kinetics in storage when corn starch, egg yolk and skim milk glazing were applied on sweet buns before baking. In general, in the literature the effects of coating or glazing on texture varied based on the type of coating, application stage and also type of cake or bread, and level of baking prior to application: fully baked or par-baked.

Therefore, it was hypothesized that the stages of application and type of coating might have an effect on the moisture and textural characteristics of the bread during storage. In this study, the recipe for pan bread was used which is typically characterized by a thin crust and evenly distributed crumb, with a short shelf-life and rapid staling depending on the baking and storage conditions. Three different experimental trials were run to select the stages of coating application, type of coating and amount of hydrophobic component and finally to integrate the stages and type of coating to evaluate the moisture and textural changes of the crust and crumb during a short storage with commercial packaging.

2. Materials and Methods

2.1. Coating Preparation

The edible coating was prepared according to the procedure described in our previous work Nallan Chakravartula *et al*., 2019. The coating solution was then spread onto the surface of bread at various stages as explained in sections 2.3-2.6 with the aid of a confectionery brush as a single layer (1L).

2.2. Bread Preparation

The bread was prepared according to AACC method 10-09 (1995) with modifications using the following composition (%w/w of flour basis) of pan bread: Manitoba type '0' soft wheat flour (100g); water (66g), extra virgin olive oil (28g); active dry yeast (1.25g); sugar (5g) and salt (0.75g). The yeast was dissolved in lukewarm water for 10min with sugar. The dry ingredients are mixed with a planetary mixer (Major 1200W model, Kenwood, Italy) for 30s at low speed, added with yeast water and oil was added subsequently while mixing for 6min until gluten formation. Further, the dough was kneaded for 3min and leavened in climatic cell at 30°C for 30min. The dough was then divided; hand worked into 25g pieces, placed in dusted moulds (diameter 5.5cm, diameter 8.5cm, height 3.5cm) and fermented at 28 (± 2)°C for 60min. The baking step was carried out in an oven at 200°C for 12min and cooled for 1h. All the samples were cooled for 1h and analyzed for selected quality parameters – moisture content, crust and crumb colour, texture analysis as explained in sections 2.6 – 2.8.

2.3. Stage 1: Selection of the stage of coating application

Each coating was prepared for the given batch of bread baked and were applied uniformly by a clean silicone pastry brush. The buns were divided into 4 sets (application stages) as: BF-Before second fermentation; BB-Before Baking; PB-Interrupted baking: coat application after 8min of cooking + 4min to complete baking; FB-Post bake: coat application after 12min baking + 25min at 60°C to dry coating; along with 2 sets of control samples CF - Control for BF, BB & FB; and CP- Control for Par-baked.

2.4. Stage 2: Type of coating and amount of hydrophobic component

Coating was prepared as explained previously was prepared and cooled to a temperature of 50(± 2)°C and added with butter and corn oil (Oleificio Zucchi SpA cremona for Coop Italia SC), in different percentages: 0%, 0.5%, 3% and 6% and then homogenized at 10,000rpm for 8min with a homogenizer (ULTRA-TURRAX® T25 digital model, IKA®, GmbH & Co. KG, Germany) and subjected to vacuum at 60mbar for 10min to eliminate any air bubbles. The coatings were applied onto bread with drying step at 60°C for 25min, to choose effective percentage of hydrophobic components. The weight loss of samples was monitored for 30h and fitted with Pelegs' model as described by Nussinovitch & Peleg, 1988.

2.5. Stage 3: Integrated application of different types of coating at baking stages

Coatings selected from stage 2 were prepared for each batch of bread baked and were applied uniformly by a clean silicone pastry brush. The buns were divided into 3 x 3 (application

stages x coatings) as: BB-Before Baking: coat application after 40min fermentation + 20min to complete fermentation; PB-Interrupted baking: coat application after 8min of cooking + 4 min to complete baking; FB-Post bake: coat application after 12min baking + 25min at 60°C to dry coating. The baking step was carried out in an oven at 200°C for 12min and cooled for 1h. All the samples were packed in OPA (bi-oriented polyamide) + PP (polypropylene) bags, heat sealed and stored in a climatic chamber at 25°C, 50% RH and evaluated for moisture content and texture on 0, 1, 4 and 7 days for crust and crumb.

2.6. Bread crust and crumb colour

The colour of the bread crust and crumb were measured with a Spectrophotocolorimeter (HUNTERLAB ColorFlexTM, mod. A60-1010-615, U.S.A) using CIELAB parameters. The instrument was calibrated with a black tile and a white standard tiles under illumination D65 (6500K). The L*, a*, b* parameters and total colour difference (ΔE) were calculated as described by Soukoulis *et al*., (2014).

2.7. Moisture Content

The moisture content (%) of the crust and the crumb was determined by the hot air oven drying (Universal Oven UF110, MEMMERT GmbH + Co. KG, Germany) in accordance with the AOAC (2000) method at 105 ° C up to constant weight. The crust was taken from the lower and upper surface, while the crumb was taken from the centre of the bread.

2.8. Texture analysis

The crust and crumb firmness were measured by Texture Analyzer model TA.HDi 500 (Stable Micro Systems, Surrey, UK). The crust firmness was measured by penetration test with modifications in AIB standard procedure with a cylindrical probe of 2mm (P / 2) and a load cell of 50N (5kg) with test parameters: 0.25mm/s; pre and post-test speed of 2mm/s and a penetration distance of 3mm. The peak force required to penetrate the crust is considered as crust hardness (Altamirano-Fortoul *et al*., 2013; Soukoulis *et al*., 2014). The crumb firmness was determined using Texture Profile Analysis (TPA) on the whole surface of buns after careful separation of the crust with a cylindrical aluminium probe P/75 mm and a load cell of 25kg with the test parameters: pre-test speed of 2.0 mm/s; test and post-test speed of 3.0 mm/s and deformation of 40.0%.

The obtained curves were analyzed with Texture Expert Exceed software (Version 2.64, Stable Micro Systems, 2003) to obtain the texture parameters Failure force (N- the peak force at crust

puncture) for crust; crumb Firmness (N), (peak force at the first compression to the pre-determined deformation); Cohesivity (work during the second compression cycle divided by work during the first compression cycle); Resilience (ratio of energies), Springiness (m, distance 1), Chewiness (derived from hardness*cohesivity*springiness) respectively. The firming rate of crust and crumb was calculated from the slopes of crust or crumb firmness along the storage time (Chin et al., 2011).

2.9. Statistical Analysis

Significant differences ($p<0.05$) between different samples and storage times were explored by means of the analysis of variance (ANOVA with post-hoc Tukey HSD); and Kruskal-Wallis test was used if Levene's test was significant (Statistica-StatSoft, version 7).

3. Results and Discussion

3.1. Stage 1: Stages of coating application

3.1.1. Crust and crumb colour

Colour is an important characteristic for bread and in general bakery products as it is a detrimental trait for aesthetics and is a result of ingredients, their interaction and maillard/ caramelization reactions during baking. Table 1 presents the colour parameters for the crust and crumb of uncoated and coated breads. Significant differences ($p<0.05$) for all parameters (L*, a*, b* and ΔE) were observed between the stages of coating application. Luminosity values in general decreased upon the presence of coating as also observed by other authors (Altamirano-Fortoul *et al*., 2012; Soukoulis *et al*., 2014), except for BF, wherein the luminosity increased and decreased the reddish hue indicative of lowering of browning (Liu *et al*., 2018). The slight increase in reddish hue in BF and PB samples might be due to the possible maillard reaction between the WPC and sugars (Soukoulis *et al*., 2014). However, there was no significant ($p>0.05$) change in luminosity of crumb and only slight changes in a* and b* values. However, in BB and PB the yellowness of crumb was slightly promoted. The total colour difference for both crust and crumb were calculated as described by Soukoulis *et al*., (2014) with control sample as standard. All the samples for crust exceeded the threshold of value 3.0 proposed to distinguish differences, except FB crust samples. This might be due to the lightening of color due to coating presence and less aggressive temperature at which the coating and product interact (60° vs 180°C) as evidenced also by Soukoulis *et al*., (2014). Whereas, in case of crumb all samples had ΔE values lower than the threshold except in samples BF indicating interaction between the coating and the dough (Galvão et al., 2018).

Table 1. Colour parameters of coated and uncoated bread crust and crumb for different stages of coat application

	Crust				Crumb			
Sample	L*	a*	b*	ΔE	L*	a*	b*	ΔE
CF	55.8±2.16^{ab}	12.3±0.93^{ab}	30.6±1.78^{ab}	-	57.8±1.91^{a}	-0.4±0.21^{ab}	12.7±1.13^{ab}	-
BF	61.4±0.48^{c}	10.8±0.06^{a}	30.5±0.40^{ab}	5.9±0.47^{b}	61.7±1.19^{a}	-0.4±0.05^{ab}	11.9±0.70^{a}	4.0±1.29^{a}
BB	51.8±1.00^{a}	14.1±2.00^{c}	33.5±0.64^{b}	5.5±0.79^{b}	58.9±1.67^{a}	0.1±0.15^{c}	14.2±0.82^{b}	2.3±0.91^{a}
FB	55.6±1.47^{ab}	11.8±1.07^{ab}	30.0±1.68^{a}	2.3±0.77^{a}	59.7±1.11^{a}	-0.5±0.14^{a}	11.90.65^{a}	2.2±1.00^{a}
CP	59.4±3.99^{bc}	11.1±1.63^{ab}	28.4±2.82^{a}	-	58.8±0.99^{a}	-0.5±0.07^{a}	12.1±0.31^{a}	-
PB	52.3±3.09^{a}	13.4±0.68^{bc}	29.7±1.78^{a}	5.1±2.78^{b}	60.1±1.65^{a}	-0.1±0.24^{bc}	13.0±0.67^{ab}	2.1±1.05^{a}

**Values are means ± SD; Means in a column without a common superscript letter in lowercase differ significantly ($p<0.05$) between treatments*

3.1.2. Moisture and texture parameters

Moisture is known to have a pronounced effect on the texture of bread. It can be observed from table 2 that the edible coating significantly ($p<0.05$) increased the crust moisture content irrespective of stage of application approximately by 3-6%. However, the crumb moisture content ranged between 40-43% in comparison to the 40-41% for the control samples. Also, in this case significant differences were observed between the stages of application with BB samples having noticeably higher values due to the restriction of moisture migration during baking from the bread surface. Similar inferences of surface water retention by coating were noticed by Liu *et al*., (2018) and Hossein *et al.,* (2011) in their study of starch coating application on pan-bread and polyol-coating on flat Barbari breads prior to baking, respectively. As expected the coated samples with post bake drying step recorded lower crust moisture than other stages but higher than that of the control, indicating moisture loss during post bake drying step.

Moisture redistribution directly affects the texture of the product with loss of texture resulting in the loss of freshness and consumer acceptability (Bartolozzo *et al*., 2016). Hence, the crust and crumb textural properties were evaluated to estimate the extent of textural changes upon coating addition as presented in table 1. The crust puncture force decreased upon the addition of coating at BF, BB and PB stages indicating a softer crust than control and FB samples (Altamirano-Fortoul *et al*., 2012). However, the post drying step did not significantly change the crust hardness and were comparable to control bread, indicating that drying step does not negatively affect the texture characteristics.

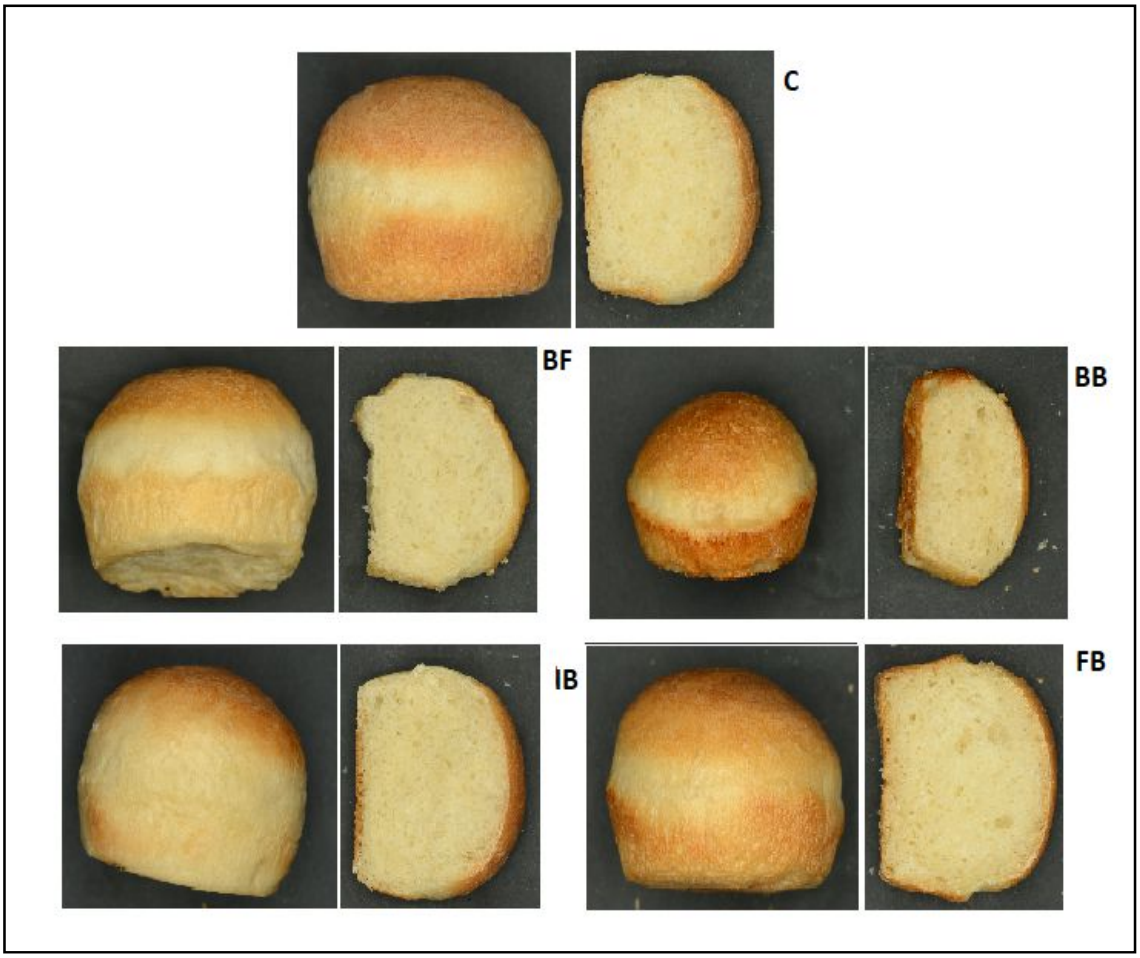

Figure 1. Representative image of bread samples coated at different stages of baking and control bread without coating

In consideration of the crumb characteristics, it can be noticed that the presence of coating did not significantly change bread characteristics. In particular, the stage of coating 'BB' was observed to have a deteriorative effect probably due to the gas expulsion during handling and lack of sufficient rebound time between coat application and baking (figure 1). However, Galvão *et al*., (2018); Theóphilo Galvão *et al*., (2018) observed that coating application prior to baking had positive effects on the dough expansion and final crumb hardness. The resilience values ranged between 0.54-0.56 and springiness values between 0.93-0.94 with no significant differences ($p>0.05$) between the stages of baking. Chewiness values followed similar trend as hardness, and cohesivity slightly increased upon the addition of coating.

Table 2. Moisture content and texture parameters of coated and uncoated baked bread for different stages of coat application

Sample	Moisture content		Texture parameters			
	Crust (%)	Crumb (%)	Crust PF (N)	Hardness (N)	Cohesivity	Chewiness (N)
CF	17.89±0.84^{a}	41.45±0.50^{ab}	1.39±0.40^{b}	2.78±0.19^{a}	0.81±0.01^{a}	2.11±0.13^{a}
BF	23.78±1.27^{cd}	42.64±0.33^{b}	0.93±0.15^{a}	2.10±0.18^{a}	0.85±0.01^{cd}	1.65±0.13^{a}
BB	25.60±1.19^{d}	43.18±0.20^{b}	1.04±0.12^{a}	7.81±1.10^{b}	0.87±0.02^{d}	6.27±1.01^{b}
FB	20.01±0.64^{ab}	41.75±0.08^{ab}	1.28±0.30^{b}	2.39±0.20^{a}	0.83±0.01^{bc}	1.84±0.18^{a}
CP	18.51±0.42^{a}	40.81±0.35^{a}	1.05±0.42^{ab}	2.80±0.27^{a}	0.82±0.01^{ab}	2.17±0.21^{a}
PB	22.09±1.84^{bc}	41.62±0.53^{ab}	1.16±0.22^{ab}	2.76±0.19^{a}	0.82±0.00^{ab}	2.10±0.15^{a}

**Values are means ± SD; Means in a column without a common superscript letter in lowercase differ significantly ($p<0.05$) between treatments*

3.2. Stage 2: Type of coating and amount of hydrophobic component

To identify a suitable hydrocolloid coating, the weight loss as a function of dehydration was periodically measured for 30h of storage. As hydrocolloids in bread and cake formulations were observed to improve the water retention and better distribution during storage, it was expected that coatings affect the rate of bread dehydration. As the weight loss is primarily due to the migration of moisture, the weight loss was elaborated by Peleg's model to determine the loss rate as presented in table 3. The relative weight loss rates resulted in significant ($p<0.001$) coefficients with $r^2>0.85$. The lowest loss rate ($1/k_1$) was calculated in 6% butter and for oil the loss was similar irrespective of concentration (*table 3)*. Also, the coatings increased the equilibrium moisture content, with lower K_2 values generally for coatings with oil/ butter. For further consideration on textural properties, coating with 6.0% oil and butter were chosen following their positive effects on weight loss.

Table 3. Pelegs' constants for weight loss in coated and uncoated bread during storage

Samples	Uncoated	Coated	0.5%Oil	3.0%Oil	6.0%Oil	0.5%Butter	3.0%Butter	6.0%Butter
k_1 (h)*	47.09	64.27	77.79	70.00	75.38	52.87	62.41	73.95
k_{2*}	3.12	3.10	2.71	2.91	2.88	2.91	3.03	2.96
Calculated loss rate ($1/k_1$, h^{-1})*	0.021	0.016	0.013	0.014	0.013	0.019	0.016	0.014
R^2	0.97	0.97	0.94	0.94	0.87	0.97	0.97	0.86

**All values are significant at $p\leq0.001$*

3.3. Stage 3: Integrated approach with different types of coating at selected baking stages

3.3.1. Moisture content: Bread Crust and Crumb

The bread after baking is cooled during which a moisture gradient forms between the crust and crumb of the bread. This gradient forms the driving force for moisture migration from crumb to crust, which further moves from crust to surrounding environment during cooling (Gray and

Bemiller, 2003). To avoid this interference the initial moisture values were evaluated after one hour of cooling. Moreover, the bread was packaged further for storage which prevents the moisture transfer from crust to environment enabling retention of water in crust. To indicate the moisture transfer, the crust and crumb moisture contents were individually evaluated and presented in table 4. The average initial moisture content was in the ranges of 17-22% for crust 36-42% for crumb depending on type of coating and moment of application. As expected the moisture of the crumb decreased and the crust increased as a function of storage time due to the moisture redistribution from crumb to crust as observed by Baik and Chinachoti (2000). The crumb moisture reduction suggests the initiation and progression of staling and subsequently harder texture (Chin *et al*., 2011).

3.3.2. Texture characteristics: Bread Crust and Crumb

Table 5 presents the crust and crumb texture characteristics of the samples along the storage time. The trends of decrease in crust firmness and increase in crumb firmness is similar to other bread storage studies (He and Hoseney, 1990; Soukoulis *et al*., 2014). The textural parameters beyond 4 days were not taken into account due to the growth of mould on the bread surfaces. The coatings applied on the surface of bread produced significant modifications in the crust mechanical properties.

Table 4. Moisture content of coated and uncoated baked bread during storage

Sample	Crust				Crumb			
	T0	T1	T4	%	T0	T1	T4	%
BBU	17.92 ± 0.59^{A}	24.68 ± 0.81^{B}	25.40 ± 1.71^{B}	42	39.42 ± 1.28^{bC}	36.94 ± 0.45^{abB}	33.32 ± 0.49^{abA}	-15
BBC	21.27 ± 0.52^{A}	26.68 ± 0.23^{bcdB}	30.34 ± 0.59^{C}	43	42.74 ± 0.78^{cdC}	38.75 ± 0.8^{bcB}	36.33 ± 0.7^{cdA}	-15
BBO	20.58 ± 0.67^{bcdA}	26.71 ± 0.44^{bcdAB}	30.43 ± 6.46^{abB}	48	41.05 ± 0.41^{bcC}	37.30 ± 0.43^{abcB}	36.21 ± 0.36^{bcdA}	-12
BBB	22.75 ± 1.13^{deA}	27.74 ± 0.57^{cdB}	30.89 ± 0.79^{abC}	36	41.88 ± 1.57^{bcdC}	$38.61\pm0.76b^{cB}$	35.92 ± 0.39^{bcdA}	-14
PBU	19.89 ± 0.61^{abcA}	24.46 ± 0.72^{abB}	26.83 ± 0.27^{abC}	35	41.88 ± 0.75^{bcdC}	38.52 ± 0.46^{bcB}	33.66 ± 0.85^{abcA}	-20
PBC	23.37 ± 0.61^{eA}	29.23 ± 1.15^{dB}	32.88 ± 1.39^{bC}	41	43.96 ± 0.18^{dC}	40.39 ± 0.42^{cB}	38.53 ± 0.62^{dA}	-12
PBO	20.44 ± 0.05^{bcA}	24.38 ± 0.29^{abB}	29.58 ± 0.64^{abC}	45	42.39 ± 1.19^{cdC}	37.17 ± 0.70^{abB}	34.36 ± 0.98^{abcA}	-19
PBB	20.27 ± 1.02^{bcA}	25.58 ± 0.69^{abcB}	29.07 ± 0.76^{abC}	43	43.18 ± 0.27^{cdC}	$38.32\pm0.25b^{cB}$	33.65 ± 1.31^{abcA}	-22
FBU	17.93 ± 0.59^{aA}	24.68 ± 0.81^{abB}	25.40 ± 1.71^{aB}	42	39.42 ± 1.28^{bC}	36.94 ± 0.45^{abB}	33.32 ± 0.4^{9abA}	-15
FBC	21.72 ± 0.26^{cdeA}	39.37 ± 2.74^{eB}	26.94 ± 1.27^{abC}	24	36.48 ± 1.06^{aA}	35.72 ± 0.45^{abA}	32.84 ± 2.25^{aA}	-10
FBO	19.74 ± 1.45^{abcA}	25.66 ± 0.85^{abcB}	28.07 ± 1.94^{abB}	42	41.71 ± 0.30^{bcdB}	34.92 ± 3.18^{aA}	36.04 ± 0.59^{bcdA}	-14
FBB	18.96 ± 0.54^{abA}	23.54 ± 0.32^{aB}	29.24 ± 0.32^{abC}	54	39.49 ± 0.20^{bB}	35.02 ± 0.50^{aA}	34.97 ± 0.69^{abcA}	-11

**Values are means ± SD; Means in a column without a common superscript letter in lowercase differ significantly ($p<0.05$) between treatments; Means in a row without a common superscript letter in uppercase differ significantly ($p<0.05$) during storage in the same sample*

The crust puncture force decreased significantly ($p < 0.05$) in samples applied with coatings irrespective of application stage justified by the slight increase in crust moisture. Considering

the application stage, the interrupted baking group had the lowest crust firmness and were significantly not different for coated and uncoated samples. During storage the failure force, crust rupture work and the failure firmness (until day 1) were observed to decrease which indicates loss of crispness and the formation of a soft leathery bread crust.

Table 5. Puncture and Texture profile analysis characteristics of coated and uncoated baked bread during storage

Failure Force (N)	T0	T1	T4
BBU	1.23 ± 0.11^{dC}	0.57 ± 0.08^{cdeB}	0.45 ± 0.07^{cdA}
BBC	1.08 ± 0.18^{cC}	0.52 ± 0.08^{bcdB}	0.49 ± 0.08^{dA}
BBO	0.77 ± 0.09^{aC}	0.54 ± 0.15^{bcdeB}	0.38 ± 0.04^{abcA}
BBB	0.81 ± 0.12^{aC}	0.45 ± 0.09^{abB}	0.39 ± 0.13^{abcdA}
PBU	0.74 ± 0.11^{aB}	0.49 ± 0.07^{bcA}	0.49 ± 0.11^{dA}
PBC	0.79 ± 0.15^{aB}	0.36 ± 0.05^{aA}	0.32 ± 0.05^{aA}
PBO	0.74 ± 0.10^{aB}	0.49 ± 0.11^{bcA}	0.34 ± 0.05^{abA}
PBB	0.76 ± 0.10^{aB}	0.48 ± 0.09^{bcA}	0.43 ± 0.05^{bcdA}
FBU	1.23 ± 0.11^{dC}	0.57 ± 0.08^{cdeB}	0.45 ± 0.07^{cdA}
FBC	0.82 ± 0.25^{aC}	0.64 ± 0.09^{eB}	0.47 ± 0.12^{cdA}
FBO	1.00 ± 0.24^{bcC}	0.62 ± 0.08^{deB}	0.39 ± 0.06^{abcdA}
FBB	1.05 ± 0.25^{cC}	0.57 ± 0.11^{cdeB}	0.34 ± 0.06^{abA}
Crumb Firmness (N)			
BBU	6.40 ± 1.65^{bcdA}	27.82 ± 1.63^{cdB}	49.30 ± 7.89^{cdeC}
BBC	10.41 ± 0.57^{eA}	38.72 ± 2.56^{eB}	65.63 ± 3.38^{fC}
BBO	8.44 ± 0.82^{deA}	28.69 ± 2.32^{cdB}	51.72 ± 3.32^{cdeC}
BBB	9.98 ± 0.87^{eA}	29.57 ± 3.16^{cdB}	58.91 ± 5.36^{efC}
PBU	4.77 ± 1.13^{abA}	22.44 ± 3.98^{bB}	42.09 ± 5.36^{abcC}
PBC	5.50 ± 0.22^{bcA}	21.48 ± 2.90^{bB}	39.27 ± 5.45^{abC}
PBO	2.65 ± 0.65^{aA}	16.31 ± 2.45^{aB}	33.66 ± 3.86^{aC}
PBB	3.98 ± 0.70^{abA}	19.46 ± 1.15^{abB}	44.70 ± 3.37^{bcdC}
FBU	6.40 ± 1.65^{bcdA}	27.82 ± 1.63^{cdB}	49.30 ± 7.89^{cdeC}
FBC	24.22 ± 0.20^{fA}	31.00 ± 3.45^{dB}	49.82 ± 5.09^{cdeC}
FBO	7.76 ± 1.73^{cdeA}	24.37 ± 2.62^{bcB}	54.83 ± 4.36^{efC}
FBB	9.12 ± 3.57^{deA}	29.20 ± 2.49^{cdB}	53.68 ± 3.19^{deC}
Cohesiveness			
BBU	0.83 ± 0.03^{bC}	0.71 ± 0.07^{abB}	0.61 ± 0.10^{abA}
BBC	0.85 ± 0.01^{bC}	0.73 ± 0.06^{bB}	0.61 ± 0.02^{abA}
BBO	0.84 ± 0.01^{bC}	0.67 ± 0.02^{abB}	0.56 ± 0.02^{abA}
BBB	0.84 ± 0.03^{bC}	0.66 ± 0.02^{abB}	0.53 ± 0.01^{aA}
PBU	0.82 ± 0.01^{bC}	0.70 ± 0.07^{abB}	0.55 ± 0.01^{abA}
PBC	0.84 ± 0.01^{bB}	0.68 ± 0.01^{abA}	0.65 ± 0.14^{bA}
PBO	0.85 ± 0.01^{bC}	0.68 ± 0.01^{abB}	0.53 ± 0.01^{abA}
PBB	0.85 ± 0.01^{bC}	0.68 ± 0.01^{abB}	0.53 ± 0.01^{abA}
FBU	0.83 ± 0.03^{bC}	0.71 ± 0.07^{abB}	0.61 ± 0.10^{abA}
FBC	0.73 ± 0.06^{aC}	0.67 ± 0.01^{abB}	0.58 ± 0.01^{abA}
FBO	0.84 ± 0.01^{bC}	0.63 ± 0.01^{aB}	0.54 ± 0.04^{abA}
FBB	0.83 ± 0.01^{bB}	0.70 ± 0.07^{abB}	0.57 ± 0.03^{abA}

Resilience			
BBU	0.52±0.02^{bcdC}	0.42±0.03^{bB}	0.35±0.04^{abA}
BBC	0.56±0.01^{eC}	0.45±0.03^{cB}	0.37±0.02^{cA}
BBO	0.54±0.02^{cd}eC	0.41±0.01^{abB}	0.32±0.02^{abA}
BBB	0.55±0.01^{deC}	0.40±0.01^{abB}	0.31±0.01^{aA}
PBU	0.51±0.03^{bcC}	0.42±0.03^{bB}	0.31±0.02^{abA}
PBC	0.56±0.01^{eC}	0.42±0.01^{bB}	0.36±0.07^{abA}
PBO	0.57±0.02^{eC}	0.42±0.01^{abB}	0.31±0.01^{aA}
PBB	0.57±0.01^{eC}	0.43±0.01^{bB}	0.30±0.01^{aA}
FBU	0.52±0.02^{bcdC}	0.42±0.03^{bB}	0.35±0.04^{abA}
FBC	0.42±0.03^{aB}	0.40±0.01^{abB}	0.32±0.02^{abA}
FBO	0.54±0.01^{bcdeC}	0.38±0.01^{aB}	0.30±0.03^{aA}
FBB	0.51±0.02^{bC}	0.40±0.03^{abB}	0.32±0.02^{abA}
Springiness			
BBU	0.94±0.01^{bB}	0.94±0.02^{aB}	0.90±0.03^{aA}
BBC	0.95±0.01^{bB}	0.94±0.01^{aB}	0.91±0.02^{aA}
BBO	0.95±0.01^{bC}	0.93±0.01^{aB}	0.92±0.01^{aA}
BBB	0.95±0.01^{bB}	0.92±0.02^{aA}	0.92±0.01^{aA}
PBU	0.94±0.01^{bB}	0.94±0.02^{aB}	0.91±0.01^{aA}
PBC	0.95±0.01^{bA}	0.94±0.01^{aA}	0.93±0.03^{aA}
PBO	0.94±0.01^{bB}	0.93±0.01^{aAB}	0.92±0.02^{aA}
PBB	0.95±0.01^{bB}	0.94±0.01^{aB}	0.92±0.01^{aA}
FBU	0.94±0.01^{bB}	0.94±0.02^{aB}	0.90±0.03^{aA}
FBC	0.91±0.02^{aAB}	0.93±0.01^{aB}	0.90±0.01^{aA}
FBO	0.94±0.02^{bA}	0.93±0.01^{aA}	0.92±0.02^{aA}
FBB	0.94±0.01^{bA}	0.93±0.01^{aA}	0.93±0.01^{aA}
Chewiness (N)			
BBU	4.98±1.24^{bcdeA}	18.62±2.03^{deB}	27.73±8.53^{bcC}
BBC	8.45±0.43^{eA}	26.75±3.40^{eB}	34.81±3.27^{cC}
BBO	6.74±0.64^{deA}	17.95±1.07^{cdeB}	26.08±1.62^{bC}
BBB	8.01±0.79^{eA}	18.12±2.51^{cdeB}	28.44±2.75^{bcC}
PBU	3.67±0.88^{abA}	14.86±3.18^{bcdB}	20.88±2.45^{abC}
PBC	4.39±0.22^{abcA}	13.80±2.00^{abB}	23.75±6.21^{abC}
PBO	2.12±0.52^{aA}	10.35±1.63^{aB}	16.43±2.09^{aC}
PBB	3.20±0.60^{abA}	12.43±0.78^{abB}	21.91±1.58^{abC}
FBU	4.98±1.24^{bcdeA}	18.62±2.03^{deB}	27.73±8.53^{bcC}
FBC	16.18±1.65^{fA}	19.50±2.15^{fB}	26.00±2.75^{bC}
FBO	6.13±1.39^{cdA}	14.25±1.38^{abcB}	27.17±2.28^{bcC}
FBB	7.08±2.74^{deA}	19.11±1.47^{eB}	28.60±2.67^{bcC}

**Values are means ± SD; Means in a column without a common superscript letter in lowercase differ significantly ($p<0.05$) between treatments; Means in a row without a common superscript letter in uppercase differ significantly ($p<0.05$) during storage in the same sample*

Considering the crumb, it is well established that the texture of bread is influenced by the amylo-pectin retrogradation and water redistribution along the storage time. The moisture migration from crumb to crust results in formation of hard crumb due to the formation of hydrogen bonds between starch globules and gluten (Gray and Bemiller, 2003; He and Hoseney, 1990). For all types of bread studied, crumb firmness and chewiness increased significantly ($p<0.05$), while crumb cohesiveness, resilience and springiness decreased

significantly ($p<0.05$) over the storage period. The PB samples showed the lowest hardness compared to BB and FB samples regardless of the type of coating present. Within the PB group, lower hardness values were found in the PBO samples from day 1 to day 4 in comparison to other samples of the same group. As for the groups BB and FB; in BB samples, the increase in hardness was lower for the coating with oil and butter, while in the FB samples the lowest hardness on day 4 was observed in FBC, a result that is expected with regard to the decrease in the humidity of the crumb. The largest percentage reductions in Cohesivity values were achieved in PB samples with oil and butter coating, while the lowest reduction is in the FBC samples. Increase in crumb firmness leads to decreased resilience of bread due to decreased gluten flexibility, hence staling results in loss of resilience (Goasaert et. al, 2009). The greatest reduction in percentage terms of this parameter was observed for the PB samples and in particular in those with oil and butter coating, which can be associated with their high increase in hardness, while a minor reduction was observed in the FBC samples. Whereas the springiness of the samples, described as a parameter linked to the ability of the bread to return to its original shape, had a general decrease due to aging in all the samples with no significant differences between presence of different coatings or not; or the application stage. Similar to the values observed for the hardness, the highest percentage increase in terms of chewiness was observed for the PBO and PBB samples, while the lowest for FBC.

Table 6. Crust and crumb firming rates of coated and uncoated baked bread during storage

Firming rate (N/day)		BB	PB	FB
Crust	U	-0.16±0.03^{b}	-0.07±0.03^{a}	-0.16±0.03^{b}
	C	-0.10±0.03^{a}	-0.09±0.04^{a}	-0.10±0.03^{a}
	O	-0.09±0.03^{a}	-0.09±0.03^{a}	-0.15±0.05^{b}
	B	-0.09±0.05^{a}	-0.07±0.02^{a}	-0.16±0.05^{b}
Crumb	U	10.78±1.47 ^{ab}	8.6±1.48^{ab}	10.78±1.47^{b}
	C	12.69±1.06 ^{b}	7.86±1.42^{ab}	6.37±1.13^{a}
	O	10.09±0.78 ^{a}	7.30±1.05^{a}	11.39±1.29^{b}
	B	11.67±1.56 ^{ab}	9.77±1.00^{b}	10.45±1.43^{b}

**Values are means ± SD; Means in a column without a common superscript letter in lowercase differ significantly ($p<0.05$) between treatments*

However, if the rate of firming (table 6) is taken into account, the samples with coating exhibited varied behaviour based on the type and stage of application of coating. The crust softening rates were lower in general for coated breads in BB group. Within each baking group, comparing the samples with coating (C, O and B) to that of without coating (U), it can be observed that for BB and PB groups, sample O had the lowest firming rate whereas for FB

group, coating without oil or butter registered lowest firming rate, in accordance to the lower moisture and texture loss.

3.3.3. Relationship between firmness and moisture

It is well known that the distribution of water plays an important role in the hardness of bread, as well as the retrogradation of amylo-pectin, because an increase in water content decreases the hardness of bread (Baik and Chinachoti, 2000; He and Hoseney, 1990). It is also established that the rate of firming has an inverse relationship to the crumb moisture content.

Taking into account each baking group individually, for the BB group of samples, the lowest crumb moisture loss was registered in sample BBO corresponding to a lower crumb firming rate. However, the crust softening rate was not high with respect to high moisture uptake. Similarly, for the PB group of samples, coated samples PBC and PBO had lower moisture loss and crumb firming rates. Though the crust moisture uptake was higher, no significant differences were found in the crust softening rates. This anomaly might be due to the lower rate of moisture transfer from crust to surrounding compared to that of near-crumb to crust regions, leading to higher water uptake but relatively slower rate of firmness loss (Chin *et al*., 2011). Finally, in the FB group of samples, FBC was observed to have the lowest firming rates in accordance to its moisture values. However, it is important to note that this sample presented the highest initial crumb firmness, which shows that the additional drying step although controlled induced hardness in the samples. However this effect was negligent in coatings with oil and butter, probably due to their protective effect resulting in similar hardness to uncoated samples. Accordingly, no significant differences were observed in the crust and crumb firming rates, compared to the control, although a marked retention of crumb moisture was observed. It is interesting to note that though oils and fats are used to retard staling in formulations, its use for superficial coating in general did not produce softer crust or softer crumb.

4. Conclusions

Overall results show that the presence of coatings has some desirable effects on the loss of moisture and rate of crumb firming of the bread during storage. However, it is evident that sole retention of moisture does not directly equate into reduction of staling with a significant but not substantial improvement. With regards to the stage of application, FB group had a marked effect followed by BB and PB groups for moisture retention. Whereas, considering the firmness, the stage of application had a prominent effect than the type of coating. In

conclusion, from the results obtained, the optimal stages to apply the coating are before baking (BB) and after complete baking (FB). It is however necessary to underline that to increase the efficiency of the film, coat application might be carried before second fermentation so as preserve the dough form. Currently, studies are undertaken to extend the possibility of improving the coatings for texture retention and secondary functionalities like antimicrobial effects.

References

Altamirano-Fortoul, R., Hernando, I., Rosell, C.M., 2013. Texture of Bread Crust: Puncturing Settings Effect and Its Relationship to Microstructure. J. Texture Stud. 44, 85–94. https://doi.org/10.1111/j.1745-4603.2012.00368.x

Altamirano-Fortoul, R., Moreno-Terrazas, R., Quezada-Gallo, A., Rosell, C.M., 2012. Viability of some probiotic coatings in bread and its effect on the crust mechanical properties. Food Hydrocoll. 29, 166–174. https://doi.org/https://doi.org/10.1016/j.foodhyd.2012.02.015

Baeva, M., Panchev, I., 2005. Investigation of the retaining effect of a pectin-containing edible film upon the crumb ageing of dietetic sucrose-free sponge cake. Food Chem. 92, 343–348. https://doi.org/10.1016/j.foodchem.2004.03.060

Bartolozzo, J., Borneo, R., Aguirre, A., 2016. Effect of triticale-based edible coating on muffin quality maintenance during storage. J. Food Meas. Charact. 10, 88–95. https://doi.org/10.1007/s11694-015-9280-1

Chin, N.L., Abdullah, R., Yusof, Y.A., 2011. Glazing effects on bread crust and crumb staling during storage. J. Texture Stud. 42, 459–467. https://doi.org/10.1111/j.1745-4603.2011.00307.x

Debeaufort, F., Voilley, A., 2009. Lipid-Based Edible Films and Coatings, in: Huber, K.C., Embuscado, M.E. (Eds.), Edible Films and Coatings for Food Applications. Springer New York, New York, NY, pp. 135–168. https://doi.org/10.1007/978-0-387-92824-1_5

Fadda, C., Sanguinetti, A.M., Del Caro, A., Collar, C., Piga, A., 2014. Bread staling: Updating the view. Compr. Rev. Food Sci. Food Saf. 13, 473–492. https://doi.org/10.1111/1541-4337.12064

Falguera, V., Quintero, J.P., Jiménez, A., Muñoz, J.A., Ibarz, A., 2011. Edible films and coatings: Structures, active functions and trends in their use. Trends Food Sci. Technol. 22, 292–303. https://doi.org/10.1016/j.tifs.2011.02.004

Ferreira Saraiva, L.E., Naponucena, L. de O.M., da Silva Santos, V., Silva, R.P.D., de Souza, C.O., Evelyn Gomes Lima Souza, I., de Oliveira Mamede, M.E., Druzian, J.I., 2016.

Development and application of edible film of active potato starch to extend mini panettone shelf life. LWT 73, 311–319. https://doi.org/10.1016/j.lwt.2016.05.047

Galić, K., Ćurić, D., Gabrić, D., 2009. Shelf Life of Packaged Bakery Goods—A Review. Crit. Rev. Food Sci. Nutr. 49, 405–426. https://doi.org/10.1080/10408390802067878

Galvão, A.M.M.T., Zambelli, R.A., Araújo, A.W.O., Bastos, M.S.R., 2018. Edible coating based on modified corn starch/tomato powder: Effect on the quality of dough bread. LWT 89, 518–524. https://doi.org/https://doi.org/10.1016/j.lwt.2017.11.027

Gray, J.A., Bemiller, J.N., 2003. Bread Staling: Molecular Basis and Control. Compr. Rev. Food Sci. Food Saf. 2, 1–21. https://doi.org/10.1111/j.1541-4337.2003.tb00011.x

Guillard, V., Broyart, B., Bonazzi, C., Guilbert, S., Gontard, N., 2003. Preventing moisture transfer in a composite food using edible films: Experimental and mathematical study. J. Food Sci. 68, 2267–2277. https://doi.org/10.1111/j.1365-2621.2003.tb05758.x

He, H., Hoseney, R.C., 1990. Changes in Bread Firmness and Moisture During Long-Term Storage. Cereal Chem. 67, 603–605.

Liu, J., Liu, X., Man, Y., Liu, Y., 2018. Reduction of acrylamide content in bread crust by starch coating. J. Sci. Food Agric. 98, 336–345. https://doi.org/10.1002/jsfa.8476

Nallan Chakravartula, S.S., Cevoli, C., Balestra, F., Fabbri, A., Dalla Rosa, M., 2019. Evaluation of drying of edible coating on bread using NIR spectroscopy. J. Food Eng. 240, 29–37. https://doi.org/10.1016/j.jfoodeng.2018.07.009

Otoni, C.G., Pontes, S.F.O., Medeiros, E.A.A., Soares, N. de F.F., 2014. Edible films from methylcellulose and nanoemulsions of clove bud (Syzygium aromaticum) and oregano (Origanum vulgare) essential oils as shelf life extenders for sliced bread. J. Agric. Food Chem. 62, 5214–9. https://doi.org/10.1021/jf501055f

Soukoulis, C., Yonekura, L., Gan, H.H., Behboudi-Jobbehdar, S., Parmenter, C., Fisk, I., 2014. Probiotic edible films as a new strategy for developing functional bakery products: The case of pan bread. Food Hydrocoll. 39, 231–242. https://doi.org/10.1016/j.foodhyd.2014.01.023

Theóphilo Galvão, A.M.M., de Oliveira Araújo, A.W., Carneiro, S.V., Zambelli, R.A., do Socorro Rocha Bastos, M., 2018. Coating development with modified starch and tomato powder for application in frozen dough. Food Packag. Shelf Life 16, 194–203. https://doi.org/https://doi.org/10.1016/j.fpsl.2018.04.003

Tongnuanchan, P., Benjakul, S., 2014. Essential oils: extraction, bioactivities, and their uses for food preservation. J. Food Sci. 79, R1231-49. https://doi.org/10.1111/1750-3841.12492

VI

Preparation and characterization of Cassava Starch/Chitosan films activated with Pitanga leaf extract (Eugenia Uniflora L.) and Natamycin

Manuscript

Nallan Chakravartula SS., Lourenço RV., Balestra F., Bittante AMBQ., Sobral PJA., Dalla Rosa M. (2019)

Preparation and characterization of Cassava Starch/Chitosan films activated with Pitanga leaf extract (*Eugenia Uniflora L.)* and Natamycin

Swathi Sirisha Nallan Chakravartula[a,], Rodrigo Vinicius Lourenço[c], Federica Balestra[a], Ana Mônica Barbosa Quinta Bittante[c], Paulo José do Amaral Sobral[c], Marco Dalla Rosa[a,b]

[a] *Department of Agricultural and Food Sciences, Alma Mater Studiorum, University of Bologna, Campus of Food Science, Cesena, Italy*

[b] *Interdepartmental Centre for Agri-Food Industrial Research, Alma Mater Studiorum, University of Bologna, Campus of Food Science, Cesena, Italy*

[c]*Department of Food Engineering, FZEA, University of São Paulo, Av. Duque de Caxias Norte, 225, 13635-900, Pirassununga, SP, Brazil*

*Corresponding author: swathisirisha.nalla2@unibo.it

Abstract

Edible coatings and films with anti-oxidant and anti-microbial activity by addition of plant extracts and commercial compounds are of interest for active packaging. The aim of this work was to develop and characterize coating and film blends of cassava starch/chitosan (CS/CH) incorporated with Pitanga extract (PE), Natamycin (NA) by casting and studying the effect of PE and NA addition on selected physical properties, antioxidant and anti-fungal activities of films. The addition of extract did not affect the film mechanical properties whereas; Natamycin significantly decreased the flexibility of films due to the change in polymer behaviour from ductile to brittle. Structural analyses by FTIR and XRD indicated interaction among the components particularly with presence of new C=O vibration peaks and shift in the characteristic CS/CH blend wave numbers. The antioxidant activity of the films increased significantly with extracts although the combination of additives resulted in activity reduction. The anti-fungal activity was assayed against *Aspergillus flavus* and *Aspergillus parasiticus*, with positive effects for NA containing films. Overall, these novel materials with both the active components have potential to act as eco-friendly and economic matrices for active food packaging applications.

Keywords

Active coatings-films; physico-chemical properties; antioxidant capacity

[1]

[1] List of symbols and abbreviations

AFM- Atomic Force Microscopy; CH- Chitosan; CS- Cassava starch; DSC- Differential scanning calorimetry; E- Elastic modulus (%/MPa); ε^B- Elongation at break (%); FFS- Film Forming Solutions; FTIR-Fourier Transform Infrared spectroscopy; MC- Moisture Content; NA- Natamycin; PE- Pitanga extract; RH- Relative humidity; TGA- Thermo-gravimetric analysis; WCA- Water contact angle (Θ); WVP- Water vapour permeability; XRD- X-ray diffraction; σ^B-Tensile strength (MPa)

1. Introduction

The development of bio-based polymers to improve bio-degradability of synthetic polymers and to partially or fully replace synthetic packaging materials has been a subject of interest for researchers in the past few years. In particular, the development of edible films and coatings has seen extensive growth in research as an eco-friendly technology that potentially resolves environmental problems and promotes global food quality (Falguera, Quintero, Jiménez, Muñoz, & Ibarz, 2011; Galus & Kadzińska, 2015; Siracusa, Rocculi, Romani, & Rosa, 2008; Valencia-Sullca, Vargas, Atarés, & Chiralt, 2018). This increase in interest is also due to the offered edibility of the packaging, particularly in form of coating, and reutilization of food and agricultural wastes like chitins, whey proteins, collagen, gelatin, pectin, fibers and other renewable resources (Vásconez, Flores, Campos, Alvarado, & Gerschenson, 2009).

Among the various polysaccharides studied cassava starch is considered as promising polymer due to its wide availability, pricing and thermoplastic behaviour. It is a natural polymer, abundantly available with ease of casting as films due to its viscous and gelling properties (Bergo et al., 2008; Pelissari, Grossmann, Yamashita, & Pineda, 2009). Despite the advantages, starch-based films are considered to have poor physical properties like high water solubility and poor mechanical properties which are usually compensated by blending with other biopolymers that are either synthetic to produce bio-degradable films (Bonilla et al., 2014; Elizondo et al., 2009) or other biopolymers to produce edible films (Chillo et al., 2008; Liu et al., 2013; Thakur et al., 2016; Vásconez et al., 2009) with successful improvement in the overall properties of the films. In this context, chitosan was found to have synergistic interactions with cassava starch resulting in improved film performance, suitability for extrusion and thermal compression moulding (Pelissari et al., 2009; Valencia-Sullca, Atarés, Vargas, & Chiralt, 2018). Chitosan is a cationic, linear polysaccharide which is a deacetylated derivative of chitin and is the second most abundant polymer after cellulose. It has increasing applications due to its non-toxicity, biocompatibility, antimicrobial and antifungal properties (Bonilla & Sobral, 2016; Elsabee & Abdou, 2013; Hosseini et al., 2009; Sullca et al., 2018).

Moreover, within the aim to improve the shelf life of foods, incorporation of antioxidants and antifungal compounds in films and coatings has been evidenced to have promising results (Balaguer et al., 2014; Mannozzi et al., 2018; Otoni et al., 2014; Silveira et al., 2007). However, with the increasing consumer concerns over use of food additives and the new food safety directives, plant extracts and natural antimicrobials are potential alternatives for active

coatings and films. Also, these activated films assist in the controlled release of the components, thus sustaining effective diffusion and maintenance of high concentrations of the active components in the packaged product during storage (Bonilla et al., 2018; Kechichian et al., 2010; Sanches-Silva et al., 2014). Also, the combination of active agents can result in synergistic action with improved effectiveness. Among different plant extracts, the leaf extract of Pitanga (Eugenia Uniflora L.) or Brazilian cherry, commonly found in Brazil, Argentina, Chile is known to exhibit antioxidant properties and antifungal properties as they contain flavonoids, tannins and phenolic compounds (dos Santos et al., 2018; Vargas, Arantes-Pereira, Costa, Melo, & Sobral, 2016). Also, being widely used in folk medicine for its pharmacological relevance (de Souza et al., 2018) has been receiving increasing interest for use as active component for food applications (Jeannine Bonilla & Sobral, 2016; Vargas et al., 2016). Natamycin or Pimaricin is a widely used anti-mycotic agent in food industry with generally recommended as safe (GRAS) status by FDA and natural preservative status by EU. It is a polyene macrolide known to primarily act against yeasts and moulds by binding specifically with ergosterol of fungal membranes, thereby impairing the membrane permeability. It has been applied to extend the shelf life of cheese, delay the fungal incidence in fruits like strawberries by direct spray application and as edible films or coatings (Balaguer et al., 2014; Cé, Noreña, & Brandelli, 2012; de Oliveira, de Fátima Ferreira Soares, Pereira, & de Freitas Fraga, 2007; Duran et al., 2016).

In this context, the objective of this work was to study the effect of Pitanga leaf ethanolic extract, Natamycin and their combination on selected characteristics of film forming solutions (FFS) and films based on blends of cassava starch/chitosan.

2. Materials and Methods

2.1. Materials

Cassava starch (Yoki Food Industry, São Paulo, Brazil) and Chitosan (medium molecular weight, Sigma Aldrich) were used as the film forming biopolymers. Natamycin (50% Natamycin, 50% Lactose and salt recipients) was kindly provided by LactoLab (Brazil) and Pitanga leaf extract was prepared by an in-house method with a series of drying, ethanolic extraction and freeze drying operations. Glycerol (Purity>95%; Sigma Aldrich, Brazil) was used as a plasticizer and distilled water was used as the solvent.

2.2. Methods

2.2.1. Preparation of Film forming solutions and Films

The cassava starch (CS) and chitosan (CH) film forming solutions (FFS) were prepared as elaborated by Valencia et al. (2018) and Baron et al. (2017), with modifications. In brief, stock solutions of 2% (w/w) CS was prepared by gelatinization at 90°C for 30min with mechanical stirring, and 1% (w/w) CH was prepared by dispersion in 1.0% (v/v) glacial acetic acid solution at 40°C, overnight with continuous stirring and filtered through gauge cotton to remove impurities. The blended solution was obtained by mixing 1:1 ratio of CS and CH stock solutions and for active solutions the selected compounds Pitanga leaf extract (PE) and/or Natamycin (NA) were added subsequently as a last step by magnetic stirring. The samples were denominated as 'T' representing treatments and numeral 0-3 indicative of different compositions as elaborated in table 1. Glycerol (25g/100 g of biopolymers) was added as plasticizer and homogenized at 5,000 rpm for 5 min (T25 Ultra-turrax). Finally, ultrasound (2min) was applied to remove air bubbles following which the FFS was cast in petriplates (area-170cm^2) and dried in a conventional oven at 30°C, 55% R.H for 16-20h to give a final thickness of 0.080 (±0.040) mm. The films were peeled off and conditioned for 7 days at 25°C and 58% relative humidity in desiccators containing saturated solutions of NaBr, prior to characterizations. For atomic force microscopy (AFM), X-ray diffraction (XRD) and Fourier Transform Infrared spectroscopy (FTIR) analyses, samples were conditioned over silica gel. All analyses were made on triplicates of duplicated runs, except in cases mentioned otherwise.

2.2.2. Film forming solutions characterization

The film forming solutions were characterized for pH (Digital pH-meter PG1400, Gehaka Ltda., São Paulo, Brazil), water activity (Acqualab, Model, Decagon, Pullman, USA) and density (Pycnometer) at 25ºC. Colour (CIEL*a*b*) was measured by using a colorimeter MiniScan MSEZ 1049 (HunterLab, Reston, VA, USA) with the solution level standardized to 1cm height in the cup so as to minimize the effect of variable quantity.

Rheological measurements were performed at 25°C, with an AR2000 Advanced Rheometer (TA Instruments, West Sussex, UK), using cone and plate geometry (cone diameter of 60.0mm, angle of 2°, gap of 2.0mm). Steady-state flow measurements were carried out in the range of 0.1-1000 s^{-1}, and rheological parameters (shear stress, shear rate) were obtained with software Rheology Advantage Data Analysis V.5.3.1 (TA Instruments). The power-law model was fitted to the rheological data allowing the calculation of flow index (n, dimensionless) and

consistency index (K, $Pa.s^{-n}$), and also, the apparent viscosity (η_{ap}, mPa.s) at a shear rate of $100s^{-1}$ was considered.

Table 1. Composition of activated films based on cassava starch/chitosan

Formulations		Treatments			
		T0	T1	T2	T3
Cassava Starch:Chitosan	(g/200g FFS)	2:1	2:1	2:1	2:1
Pitanga Leaf extract	(g/200g FFS)	0.0	4.5	0.0	4.5
Natamycin	(g/ 200g FFS)	0.0	0.0	2.0	2.0

2.2.3. Films Characterization

2.2.3.1. Optical properties

The colour and opacity of the films was determined according to Valencia et al. (2018) using a MiniScan MSEZ 1049 (HunterLab, Reston, VA, USA), in the reflectance mode adopting the CIEL*a*b* scale, with an illuminant/angle D65/10° and an opening of 30mm. The total colour difference (ΔE*) was calculated from L*, a* and b* values. Opacity was measured according to the Hunterlab method, in reflectance mode and calculated according to 'Y = (Y_b/Y_w)' relation by superimposition of opacity over the black standard (Y_b) to that of white standard (Y_w).

2.2.3.2. Light transmission

The ultraviolet and visible light barrier property of films was determined by analysing 10x10mm film strips, using a UV-VIS spectrophotometer (Perkin Elmer, USA) in the wavelength range of 200 – 900nm, as described by Bitencourt et al., (2014).

2.2.3.3. Morphological properties

Atomic force microscopy (AFM) was used for analyzing the films surface topography and roughness, calculated as the mean root square, according to Ma et al., (2012). Analyses were performed in areas of 2.5x2.5mm at random positions of films pasted onto the sample stage with a scan size of 20x20μm on the air side of films.

2.2.3.4. Fourier transform infrared spectroscopy (FTIR)

FTIR analysis was performed using a Perkin Elmer Spectrometer (One spectrum, Perkin Elmer, USA) to analyze the molecular interactions in films. The spectra were determined in range of $600cm^{-1}$ and $4000cm^{-1}$ in transmission mode and $1cm^{-1}$ resolution (Bonilla et al.,

2014). The spectra were converted to absorbance and normalized prior to peak identification by integrated one spectrum software (Perkin Elmer).

2.2.3.5. X- Ray Diffraction (XRD)

XRD measurements were carried out by using an X-ray diffractometer (Rigaku, USA), with Cu source, operating at room temperature, 40kV and 30mA current. The samples were cut as 7 x 12mm^2 and placed in the chamber with the angle being varied from 10° to 60° at 2θ=2° (Bergo & Sobral, 2007).

2.2.3.6. Moisture Content and Solubility

For moisture content determination, the equilibrated film samples of each formulation were weighed to the nearest 0.0001g and dried in an oven at 105°C for 24h, and weighed after drying (Bitencourt et al., 2014). The film solubility in water was determined by immersing film samples in 50mL of distilled water at 20°C for 24h under stirring at 68rpm (shaker incubator, MA-41, Marconi, Brazil). After this period, the samples were dried in an oven at 105°C for 24h, weighed and film solubility was calculated as described by Gontard, Duchez, Cuq, & Guilbert, (1994).

2.2.3.7. Water vapour permeability

Water vapour permeability (WVP) of films was determined gravimetrically at 25°C according to ASTM E96-80 and calculated according to Sobral et al., (2001). In brief, round samples of 30mm diameter were cut and randomly measured for thickness, and fixed onto water permeability cups containing silica gel. The weighed cells were placed in desiccators containing distilled water (100% RH) at 25°C, and weighed daily in a semi analytical balance for 7 days.

2.2.3.8. Water contact angle

Water contact angle (WCA, Ɵ) was used to measure the surface hydrophobicity of air side film's surface, with a goniometer (Kruss Gmbh, Germany) equipped with image analysis software for Drop Shape Analysis (Kruss Gmbh, Germany) using Young-Laplace equation at 15th second of contact (Marcuzzo, Peressini, Debeaufort, & Sensidoni, 2010).

2.2.3.9. Thickness and Mechanical Properties

The thickness was measured using a digital micrometer (Mitutyo, Japan) to the nearest 0.001mm on ten random positions (Bitencourt et al., 2014). The mechanical properties of the films were evaluated using texture analyzer TA XT2i (Stable Micro system, UK). For the tensile test, the samples were cut into 15mm x 100mm strips and loaded with a grip separation of 50mm and speed rate of 1mm/s, according to ASTM D882-12 standard to give the tensile strength (σ^B; MPa), elongation at break (ε^B, %) and elastic modulus (E, %/MPa). The puncture tests were carried out on samples of 60mm diameter, with a 3mm probe and velocity of 1mm/s. The force of puncture was determined from the curve and the deformation during perforation was calculated according to an equation given by Sobral et al., (2001).

2.2.3.10. Thermal Analysis

Thermal properties were measured by differential scanning calorimetry, using a DSC TA 2010 (TA Instruments, USA) with cryogenic quench cooling accessory. Samples of 10mg, weighed to the nearest 0.00001g were placed and hermetically sealed in the Aluminium pans, and heated at 5 °C/min, between -150 and 150 °C, in inert atmosphere (45 mL/min of N_2) with empty reference pan (Sobral et al., 2001). The films were analysed for glass transition temperature (T_g), calculated at the baseline inflexion point, with the auxiliary Universal analysis 2000 XP software, V1.7F (TA instrument).

Thermogravimetric analysis was performed according to Bonilla et al., (2014) using a Thermogravimetric analyzer (TGA, Seiko Exstar 6300) to measure the thermal sensitivity and weight loss (TG) of films in the temperature range between 30°C and 900°C, with a heating rate of 10°C/min under nitrogen stream (50mL/min). The onset temperature (T_0), maximum thermal degradation temperature (T_{max}) and final residue (%) were calculated.

2.2.3.11. Antioxidant Assay

The antioxidant activity of films was determined with the methods of capturing the DPPH• radical, ABTS•+ radical and the reduction assay by FRAP. To carry out these analyses, 0.1g of film was dissolved in 6ml of distilled water and 4ml ethanol (99%), dissolved overnight and homogenized for 1 min. at 4000rpm, in triplicates.

DPPH Assay - The antioxidant activity of films was determined using the free radical 2, 2-diphenyl-1-picryl-hydrazyl or *DPPH• scavenging ability* as described by Brand-Williams et al., (1995) with modifications of Bitencourt et al., (2014). *DPPH•* solution was prepared by

dissolving 2.4mg *DPPH•* in ethanol to a volume of 100ml in a volumetric flask. The absorbance was corrected by a UV/VIS spectrophotometer to 0.70 (±0.05) at 517nm with 99% ethanol for dilution. An aliquot of 0.4ml of the previously dissolved film was added to 3.6ml of *DPPH•* solution, allowed to stabilize for 60min and the absorbance was read at 517nm. The antioxidant capacity was then calculated using equation 1.

$$\%\, DPPH \bullet\ Scavenging\ effect = \frac{(ABS_{\,DPPH} - ABS_{\,sample})}{ABS_{\,DPPH}} \times 100 \qquad (1)$$

ABTS•+ radical capture Assay - The 2,2′- azinobis (3-ethylbenzothiazoline-6-sulfonic acid) or ABTS•+ cation decolorization ability based on the protocol of Re et al. (1999), with slight modifications was used. ABTS•+ working standard was prepared by dissolving ABTS in water to give 7mM concentration stock solution. This was reacted with 2.45mM Potassium persulphate at a ratio of 1:0.5 (ABTS: Pot. Persulphate) and stored in dark for 16h. Further, the absorbance of an aliquot was adjusted to 0.70 (±0.03) at 734nm with 99% ethanol for dilution. 60µl of solubilised film solution was added to 2940µl of working standard, incubated at 37°C for 6min in dark and read for absorbance at 734nm. The antioxidant capacity was calculated with the equation 2.

$$\%\ \mathrm{ABTS} \bullet + Scavenging\ effect = \frac{(ABS_{\,\mathrm{ABTS}\bullet+} - ABS_{\,sample})}{ABS_{\,\mathrm{ABTS}\bullet+}} \times 100 \qquad (2)$$

FRAP assay- The *Ferric reducing ability (FRAP) assay* was carried out as described by Benzie & Strain (1996), with modifications according to Gómez-Guillén et al., (2007). 30µl aliquot of the previously prepared film solution was added with 90µl distilled water and 900µl FRAP reagent (containing TPTZ and $FeCl_3$). Absorbance values were read every 4min and 30min. A calibration curve was performed with $FeSO_4.7H_2O$ solution. Results were expressed as equivalent concentration of $FeSO_4.7H_2O$ mM at 4 and 30 minutes, respectively.

2.2.3.12. Antifungal activity of films

Fungal cultures were prepared as described by Balaguer et al. (2013) with modifications. *Aspergillus flavus* and *Aspergillus parasiticus* cultures were grown on potato dextrose agar petri dishes (9cm diameter) for 7 days at 30°C. Conidia were collected by flooding the surface of the plates with sterile peptone water and gently scraping the mycelial surface with a spatula. 10 ml of this suspension was transferred to sterile tubes, and vortexed to obtain a homogenous

suspension of conidia. The conidial suspensions were adjusted to 1-5 x 10^6 $CFUml^{-1}$ with peptone water. The PDA plates were then inoculated with 0.1ml of the culture and spread evenly with a spreader. The sterilized discs of the prepared films (2mm) of the control and active formulations containing the test compounds were placed on the PDA agar surfaces. The prepared plates in triplicates were incubated at 35°C for 24h and the halos of inhibition were measured using callipers. The results were expressed as zone of inhibition (mm).

2.3. Statistical analysis

Significant differences ($p<0.05$) between different samples were interpreted by means of analysis of variance (ANOVA) with post-hoc Tukey HSD; in case of significant Levene's test, Kruskal-Wallis test was used (Statistica-StatSoft, version 7).

3. Results and Discussion

3.1. Film forming solution (FFS) characteristics

In general, the addition of Pitanga leaf extracts (PE) and/or Natamycin (NA) did not affect the studied physical properties of FFS, except for consistency index and viscosity calculated at $100s^{-1}$ (table 2). The pH of the FFS remained constant ($p>0.05$) between 3.5 and 3.8 (table 2). Similar behaviour was observed for water activity, which was around 0.992 ($p>0.05$). Density of FFS was observed to be around 1.008 g/cm^3 at 25°C with no significant differences ($p>0.05$) despite the addition of PE and/or NA, as also observed by Zhong, Cavender, & Zhao, (2014) in Sodium alginate/Chitosan film forming solutions.

The rheological properties of solutions are consistently used among literature to provide data on film's microstructure, coating spreadability, thickness, performance and uniformity on substrates. In general high viscosity of solutions tend to retain air bubbles and hinder casting process, whereas, FFS with low viscosity is easily spreadable and can be casted by free flow (Cuq et al., 1995; Peressini et al., 2003). All FFS, irrespective of the addition of active components, had similar non-Newtonian behaviour (Figure 1). The studied FFS exhibited pseudo-plastic behaviour, with '*n*' changing from 0.67 to 0.69 ($P>0.05$) as a consequence of addition of PE and/or NA (table 2). Nevertheless, '*k*' was higher ($P<0.05$) for film forming solution without additives (0.44 $Pa.s^{-n}$) comparing with other formulations (0.30-0.34 $Pa.s^{-n}$) (table 2). The addition of PE and/or NA tended to slightly decrease the consistency index and the apparent viscosity of the solutions (table 2). These results indicate that the additives decreased slightly the viscous nature of the polymer solution probably due to weakening of

interactions and lesser structural compactness (Dammak & Sobral, 2017). The viscosity of the FFS at $100s^{-1}$ was lower than 700mPa.s (table 2), a value suggested for appropriate film casting (Peressini et al., 2003).

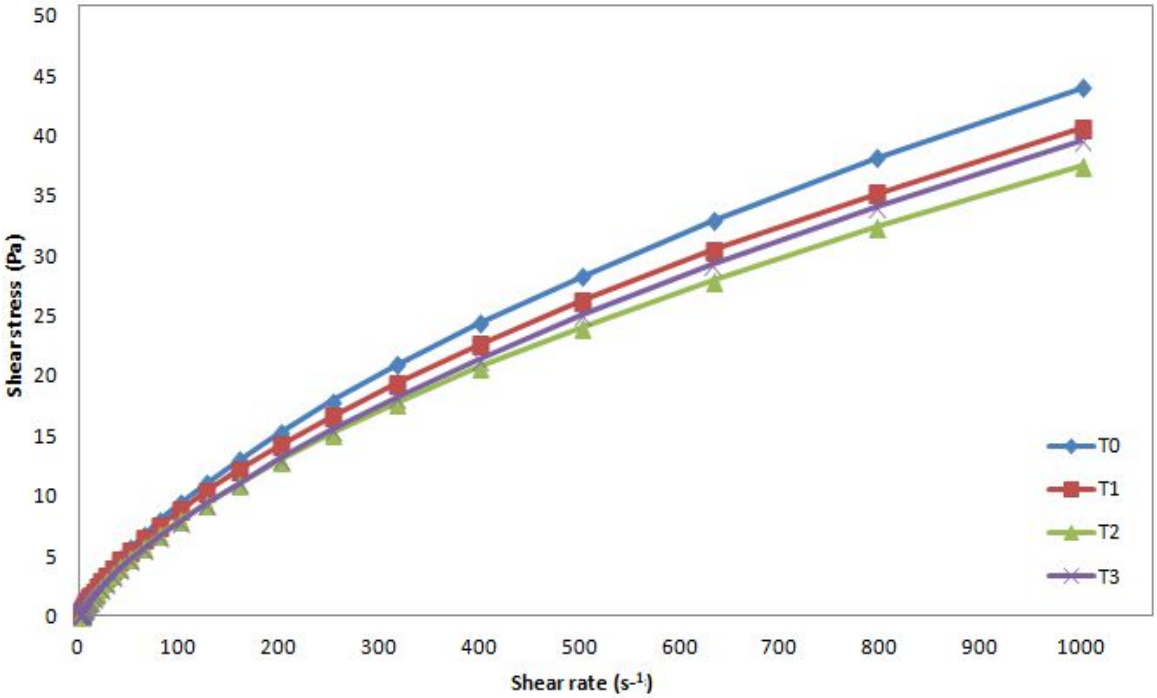

Figure 1. Representative plots of shear stress vs. shear rate for all the formulations T0-T3.

3.2. Optical parameters of film-forming solutions and films

The optical properties of film forming solutions (table 2) and films (table 3) are important parameters as they directly affect the product appearance and consumer acceptance (Galus & Lenart, 2013). The FFS were clear and subsequently, films were clear and transparent indicating homogenous distribution of the components for CS/CH whereas, insoluble particles were observed upon addition of PE and/or NA. In general, all colour parameters of FFS and films were affected by addition of PE and/or NA. Luminosity (L*) decreased upon addition of PE, while it increased with NA addition. As for other parameters a* and b*, they have contrasting behaviour with increase of value upon addition of PE and decrease with NA addition. FFS and films containing PE were the most coloured samples as indicated by higher ΔE* (table 3), due to the greenish-yellow colour of the PE (L*= 30.4, a*= 12.1, b*= 41.3) as observed by Vargas *et al.,* (2016).

Table 2. Physical properties of film forming solutions.

Properties	Treatments			
	T0	T1	T2	T3
pH	3.7±0.1[a]	3.8±0.2[a]	3.5±0.0[a]	3.6±0.0[a]
Water activity, a_w	0.991±0.001[a]	0.993±0.003[a]	0.991±0.001[a]	0.993±0.001[a]
Density g/cm^3)	1.008±0.002[a]	1.006±0.001[a]	1.008±0.001[a]	1.009±0.001[a]
Consistency index, K† (Pa.s^{-n})	0.44±0.03[b]	0.34±0.05[a]	0.32±0.03[a]	0.30±0.01[a]
Flow index, n† (-)	0.67±0.01[a]	0.69±0.01[a]	0.69±0.02[a]	0.69±0.02[a]
Apparent viscosity, η_{ap} at 100 s$^{-1\dagger}$ (mPa.s)	95±0.2[b]	80±0.6[a]	78±0.3[a]	75±0.5[a]
L*	66.93±0.04[b]	54.08±0.04[a]	74.10±1.27[c]	66.29±0.50[b]
a*	-0.08±0.03[b]	1.88±0.02[d]	-2.36±0.05[a]	0.12±0.02[c]
b*	5.87±0.12[a]	27.22±0.03[d]	8.84±0.45[b]	18.08±0.59[c]
ΔE*	26.57±0.03[b]	46.82±0.04[d]	20.43±1.03[a]	31.54±0.15[c]

** Values are means ± SD; Means in a row with different superscripts indicate significant differences ($p<0.05$) between samples. † For rheological parameters all samples had SE< 6% and $r^2 \geq 0.99$. Treatments T0, T1, T2 and T3 are described in Table 1.*

With regard to the film opacity (table 3), addition of NA rendered the films opaque with significantly higher values (36.0 for NA and 47.7 for NA+PE) due to its low solubility which avoided light transmission, thereby producing a shadow. Addition of only PE slightly increased the opacity (from 2.2 to 3.2, $p>0.05$), as also evidenced by Bonilla & Sobral, (2016) upon addition of plant ethanolic extracts in gelatin/chitosan films.

3.3. Light transmission of films

The films without additives were observed to be poor barriers to UV/light (Figure 2) presenting transmittance only until 220nm. This could be expected because neither starch nor chitosan has ability to absorb UV/Light. On other hand, films with PE and/or NA exhibited very low transmittance until 400nm, and hence, can be considered as a good UV barrier, in agreement to that observed by Bonilla *et al.,* (2018) on Chitosan/Gelatin films. But, only films with NA can be considered as high barriers to visible light, as they presented very low transmittance from 400 to 900 nm (figure 2), probably due to low opacity (table 3) of these films. The barrier effect in films with PE can be attributed to the presence of phenolic components (Bonilla *et al.*, 2013). These results indicate that the active films tested can be used to prevent lipid oxidation in foods (Bitencourt *et al*., 2014; Bonilla *et al*., 2013).

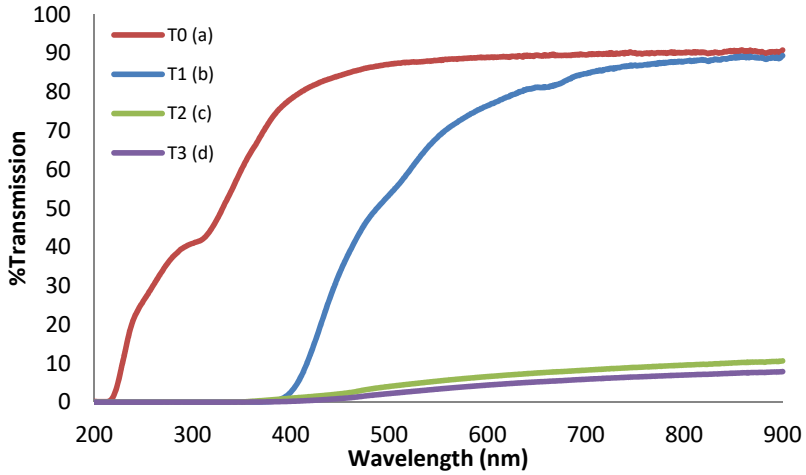

Figure 2. Ultraviolet and visible light barrier properties (200-900nm) of CS/CH films with additives (a) T0 (b) T1 (c) T2 (d) T3.

3.4. Morphological properties of films

The film without additives and with PE (T1) presented a high quantity of finer peaks, whereas, the films containing NA (T2 and T3) showed a small quantity of big structures (figure 3). Apparently, the presence of NA displayed an effect on changing the surface microstructure of films, probably due to its low solubility.

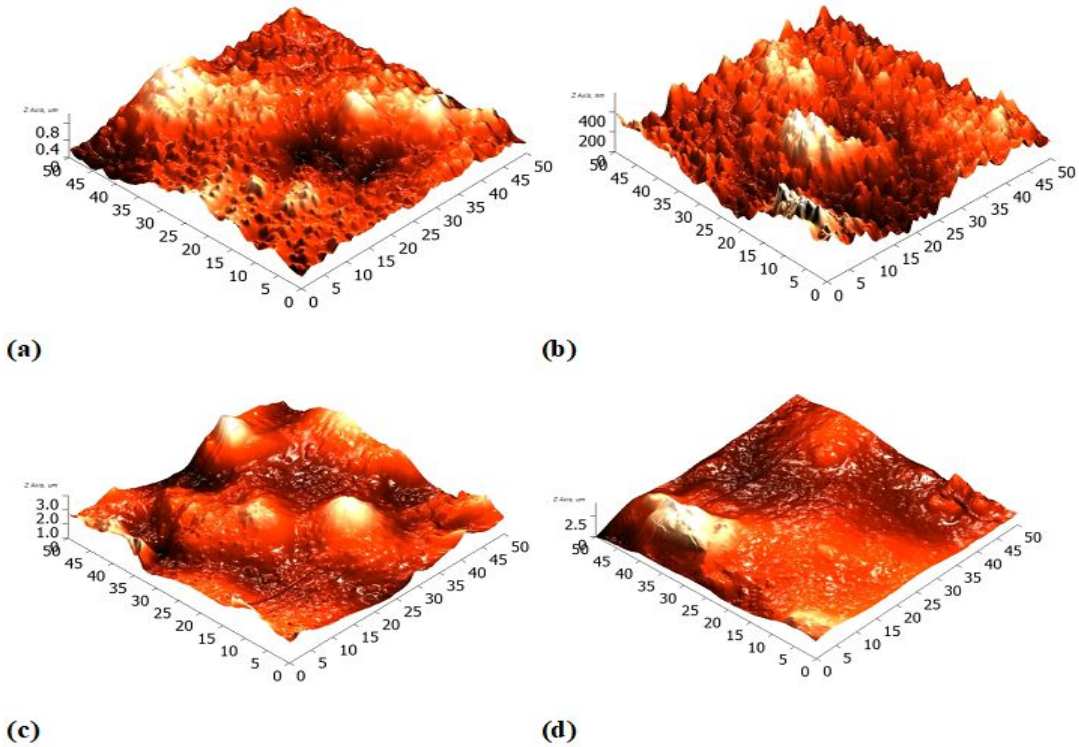

Figure 3(a-d). Representative atomic force micrographs of CS/CH films (a) T0 (b) T1 (c) T2 (d) T3.

The roughness (R_a and R_q) corroborated with the effect of NA on surface microstructure of films (table 3). The addition of PE slightly decreased the R_a and R_q values from 73.4 to 70.2 nm and from 93.6 to 91.0 nm, respectively, with no significant differences ($p>0.05$), whereas, the addition of NA (T2, T3) drastically increased ($p<0.05$) these values to 239-224nm and 300-284nm, respectively (table 3). This behaviour was due to the insoluble characteristic as well as the formation of NA particle agglomerates during the drying process (Ollé Resa *et al.,* 2013; Ollé Resa *et al.,* 2014). The slight decrease of roughness upon addition of PE might be attributed to the interaction of the biopolymer with the extract.

Table 3. Physical properties of films.

Properties	Treatments			
	T0	T1	T2	T3
L*	89.6±0.2^{c}	76.5±0.8^{b}	89.2±1.4^{c}	70.3±1.3^{a}
a*	-1.11±0.04^{b}	-0.57±0.15^{b}	-2.13±0.12^{a}	8.06±0.69^{c}
b*	4.83±0.60^{a}	46.56±2.36^{c}	19.31±5.63^{b}	44.20±0.56^{b}
ΔE*	5.53±0.39^{a}	48.48±2.48^{c}	18.65±5.80^{b}	49.74±1.17^{c}
Opacity	2.2±0.4^{a}	3.2±0.6^{a}	36.0±5.3^{b}	47.7±1.4^{c}
Average roughness, R_a (nm)	73.4±1.8^{a}	70.2 ±5.7^{a}	239.2±39.3^{b}	224.4 ±6.9^{b}
Root mean square roughness, R_q (nm)	93.6 ±2.5^{a}	91.0 ±6.0^{a}	300.3±34.3^{b}	283.5±11.5^{b}
Moisture content, MC (%)	17.9±0.8^{c}	12.7±0.6^{ab}	13.1±0.4^{b}	11.6±0.6^{a}
Solubility in water, S (%)	32.4±0.4^{b}	32.9±0.7^{b}	28.6±0.3^{a}	28.4±1.0^{a}
Water vapor permeability, WVP (x 10^{8} g.mm/h.cm^{2}.Pa)	2.70±0.33^{b}	2.63±0.65^{b}	1.98±0.38^{a}	1.90±0.51^{a}
Water contact angle, WCA (º)	80.3±5.1^{c}	73.8±2.7^{b}	64.8±1.5^{a}	71.6±0.5^{b}
Thickness (mm)	0.084±0.005^{a}	0.084±0.003^{a}	0.080±0.004^{a}	0.082±0.003^{a}
Tensile strength, σ^{B} (MPa)	9.4±1.9^{a}	10.9 ±1.4^{a}	13.3 ±1.4^{b}	10.6 ±1.6^{a}
Elongation at break, ε^{B} (%)	24.3±3.9^{c}	18.4±2.3^{b}	2.8±0.7^{a}	3.7±0.7^{a}
Elastic modulus, E (MPa/%)	2.7±0.5^{a}	2.7 ±0.9^{a}	6.0 ±1.2^{c}	4.3±1.1^{b}
Puncture Force, PF (N)	14.0±1.3^{c}	11.5±1.2^{b}	6.8±1.5^{a}	6.6±0.5^{a}
Puncture Deformation, PD (%)	4.2±1.5^{c}	1.7±0.6^{b}	0.4±0.1^{a}	0.4±0.1^{a}
1st Glass transition temperature, T_{g1} (ºC)	-67.0±2.2^{a}	-56.9±4.8^{b}	-52.9±4.8^{bc}	-47.9±1.7^{c}
2nd Glass transition temperature, T_{g2} (ºC)	14.8±1.9^{a}	18.7±5.4^{ab}	29.7±8.8^{b}	28.2±5.4^{b}
Onset temperature, T_o (ºC)	227.3	249.8	242.0	241.1
Maximum temperature, T_{max} (ºC)	339.6	337.9	358.6	352.2
Residue at 900 °C (%)	25.5	23.9	25.0	25.7

** Values are means ± SD; Means in a row with different superscripts indicate significant differences ($p<0.05$) between samples. Treatments T0, T1, T2 and T3 are described in Table 1.*

3.5. Fourier Transform Infrared spectroscopy

Figure 4 shows the FTIR spectra obtained for CS/CH blend films and those activated with PE and/or NA. As known, molecules of CS/CH as well as PE, NA are capable of hydrogen bonding and specific interactions were observed in the spectra reflected in shifts of characteristic absorption bands. For the film without additives (T0) the characteristic peaks were identified and assigned, as presented in table 4.

Figure 4. Representative FTIR Spectral patterns of CS/CH films (a) T0, (b) T1, (c) T2 and (d) T3.

The common absorption bands at wave-numbers 3276 cm^{-1} - 2925 cm^{-1} - 2881 cm^{-1} represent the OH and the C-H stretching vibrations (Bergo *et al.*, 2008; Dang & Yoksan, 2015; Pelissari *et al.*, 2009). The band at 3200cm^{-1} can be attributed also to the intermolecular hydrogen bonding of the components. The smaller, intensive bands in the region ranging from 1180-953cm^{-1} consists of the typical saccharide structures, known as the finger print region (Bergo *et al.*, 2008; Liu *et al.*, 2013). The bands at 1559 cm^{-1} and 1638 cm^{-1} represent interaction between the hydroxyl and amino groups of starch and chitosan respectively (Bonilla *et al.*, 2014; Liu *et al.*, 2013). Furthermore, the broad peak at 1560 cm^{-1} to 1570cm^{-1} is indicative of the ionization of primary amine of chitosan due to solubilisation in acetic acid (Mathew *et al.,* 2006). As can be observed in figure 4, the characteristic peaks were displaced slightly in films with addition of PE and/or NA. In addition, a new peak was observed at 1261-1267 cm^{-1} for T1, T2 and T3 which can be attributed to the amino group of chitosan that reappeared in films with additives. Also, only in T2 and T3 another new peak at 1713 cm^{-1} and 1714 cm^{-1} was observed which refers to the -C=O vibration characteristic of Natamycin as also observed by

Cevher et al., (2008). Other characteristic peaks of NA that were observed in NA powder (not shown in figure) and subsequently in T2 and T3 films were: 1567 cm^{-1} to 1561 cm^{-1} (CH=CH stretch); 1267 cm^{-1} to 1266 cm^{-1} (C-O-C epoxy); 1144 cm^{-1} shifted to 1150 cm^{-1} and 1150 cm^{-1} relates to (=C-O-C=) vibration; 1106 cm^{-1} shifted to 1103 cm^{-1} and 1107 cm^{-1} indicate (C-OH) symmetric vibration. The shift in the peaks and appearance of new peaks can be considered as polymeric interaction probably by H-bonding in the blend films.

Table 4. Assignment of main bands of FTIR spectra for CS/CH film without additives.

Wavenumber (cm^{-1})	Functional group assignment CS/CH
3600-3100 (3276)*	Broad peak of overlapping hydrogen bonds; O-H and N-H stretch
2926; 2881	C-H stretch vibrations; Pyranose ring
1638	Overlapping δ H_2O bending of cassava and Amide I of chitosan
1580-1548 (1559)*	Amide II: NH_3+ symmetric deformation
1408	OH of primary alcohol
1376; 1331	Amide III- $CH2_3$
1180-953	Typical saccharide bands: CC and CO stretching and the bending mode of CH bonds
1150.75	COC asymmetric bridge stretch
1077	C-O stretch
1019	COH Vibrations; Amorphous crystalline transitions
995	Ether group; Amorphous crystalline transitions

**Wave number ranges presented in literature with the number in parenthesis representing the observed peak.*

3.6. X-ray diffraction of films

X-ray diffractograms of films are shown in figure 5, in which a semi-crystalline pattern with broad amorphous regions and peaks of crystalline regions can be observed. The typical crystalline peaks of chitosan were suppressed and a broad amorphous peak was observed around 2θ ≈20º which indicates the interaction of cassava with chitosan. The presence of smaller peak at 2θ ≈ 15º in T0 can be attributed to the chitosan anhydrous crystal with the low intensity indicating low crystallinity (Bangyekan *et al*., 2006). However, this peak disappeared in T1 and T2 indicating an interaction between additives and chitosan. Whereas, in T3 several new peaks from 2θ ≈ 10º to 30º with smaller intensities were observed due to the aggregation

of NA with PE. However, this did not seem to negatively affect the barrier properties of the film (as in table 3). Further, the small peaks at 2θ ≈ 37° and 44° can be related to the crystalline phases of chitosan and the sharp peak at 2θ ≈ 29º suggests a conformational change in the polymers due to CS/CH intermolecular interactions. Abugoch et al., (2011) observed similarly a peak at 2θ ≈ 29° and also at 31° and 36° suggesting the intermolecular interaction between quinoa protein and chitosan films.

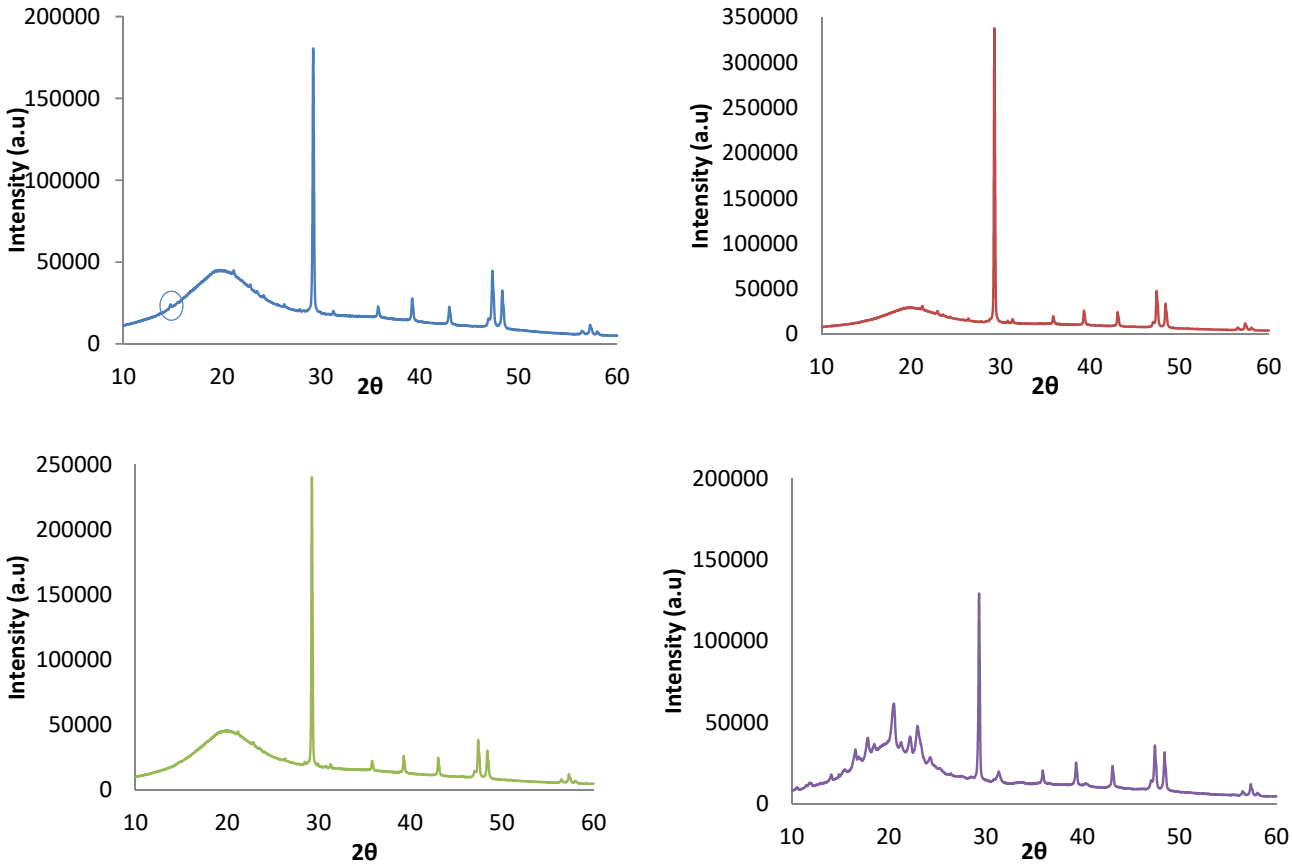

Figure 5 (a-d). X-ray diffraction patterns of CS/CH films (a) T0, (b) T1, (c) T2 and (d) T3

3.7. Moisture Content and solubility in water of films

Moisture content was observed to be highest in film without additives, whereas the additives significantly decreased these values ($p<0.05$) from ~18% to ~12% (table 3). This decrement could be due to the subsequent decrease in availability of glycerol to retain water in the matrix as its content was maintained constant on the basis of CS/CH (Cerqueira, Souza, Teixeira, & Vicente, 2012). The values presented in table 3 are in the usual range for biopolymer-based films (Mathew et al., 2006; Pelissari et al., 2009; Šuput et al., 2016; Valencia-Sullca et al., 2018).

With regard to the film solubility in water (S), the films did not disintegrate after 24h of incubation with stirring, indicative of film integrity. The presented solubility can be attributed to the loss of glycerol, solubilization of amylose and other water soluble components. Similar results were observed in rice starch/chitosan and cassava starch/chitosan films by Bourtoom and Chinnan, (2008) and Vásconez et al., (2009), respectively. In general, the S (%) decreased from ~32% to ~28% ($p<0.05$), due to addition of Natamycin (T2 and T3, table 3), probably due to the low dispersion of NA into biopolymer matrix. On the whole, all films produced in this study presented lower S (%) than the films produced with blends of chitosan/starch (2:1, ~38%) by Bourtoom and Chinnan, (2008), but higher than those produced by Vásconez et al., (2009), working on films based on blends of chitosan/tapioca starch (~25%).

3.8. Water vapor permeability of films

Water vapor permeability (WVP) slightly decreased from 2.70-2.63 to 1.90-198 x 10^8 g.mm/h.cm^2.Pa as a consequence of addition of NA (T2 and T3, table 3), probably due to slight imperfections imbibed into the biopolymer matrix during drying. As such, these CS/CH films are usually characterized as having low barrier to water vapor, but the observed values were lower than those determined for CS/CH (77% starch/5% chitosan) extruded films by Pelissari et al., (2009), and similar to those studied by Vásconez et al., (2009). It was observed that the addition of PE (T1) did not change the WVP, but the addition of NA resulted in decrease of WVP (table 3). Similar trend was observed upon the addition of NA in films based on tapioca starch/Natamycin (Ollé Resa et al., 2013), who also observed an inverse relation between surface roughness and water vapor permeability.

3.9. Water contact angle of films

Contact angle is used to estimate the film surface affinity to water, with contact angles $\theta>65°$ characteristic of hydrophobic surfaces and $\theta<65°$ indicative of hydrophilic surfaces (Karbowiak, Debeaufort, Champion, & Voilley, 2006). In this context, it can be observed that only films produced with NA (T2, WCA = 64.8º) presented slight hydrophilic surface. The most hydrophobic film was that without additives (T0, WCA = 80.3º) (table 3) followed by T1 and T3. However, it was interesting to observe that these results were not relatable to the surface morphology of the films and thus can be estimated to be an effect of the chemical nature of the polymer matrix. In general, as observed by Ollé Resa et al., (2014), increase in surface roughness should result in higher contact angles, but in this case, the values decreased probably due to the hydrophilic nature and high specific surface of starch.

3.10. Thickness and Mechanical Properties of films

The thickness of films was constant around 0.082 mm ($p>0.05$), due to the plating of pre-calculated quantities of filmogenic solutions as mass/plate ratio for different formulations. This was carried out as the thickness is known to directly affect the mechanical properties of films (Bitencourt et al., 2014).

Mechanical properties are related to the structure of films and reflect the films capacity to protect the package integrity and support foods (Rubilar et al., 2013; Talón et al., 2017). Generally, films with high tensile strength have lower values for elongation at break and hence, must be estimated simultaneously (Galus & Lenart, 2013). The tensile strength (σ^B) of the film was observed to slightly increase from 9.4 to 13.3 MPa with the addition of NA alone (T2, table 3), which might be due to inter-molecular hydrogen bonding of the components (Mathew et al., 2006). However, no marked increase in PE incorporated films was noticed (T1 and T3, ~11 MPa) as the presence of starch limits the interaction of phenols with chitosan (Talón et al.,2017). Interestingly, the elongation at break (ε^B) values of the films from 24.3% decreased greatly to 2.8-3.7% upon addition of NA, contrary to that of tensile strength values. However, the addition of PE (T1) only reduced the elongation at break value slightly to 18.4 % ($p<0.05$). Similar inferences were found by Bonilla & Sobral, (2017) in Gelatin films with Boldo and Guarana extracts. Subsequently, the elastic modulus calculated at strains below 5% increased by 40-50% with addition of NA (T2, T3), confirming the loss of film flexibility and stretchability.

Furthermore, the puncture force (PF, N) and puncture deformation (PD, %) were evaluated complementing the mechanical properties of the material. Both puncture force and deformation values decreased ($p<0.05$) upon the addition of PE and NA, but a more pronounceable effect was observed in case of NA addition (table 3). PF decreased from 14 to 11.5N when PE was added, and to 6.6-6.8N, when NA was added (T2 and T3, table 3), with a similar trend for PD values. This behaviour of the films T2, T3 was due to the loss of mobility of macromolecules due to the presence of additives, indicative of brittle behaviour (Ollé Resa et al., 2013). The PF determined in this work were, in overall, higher than that for cassava starch films (~5 N) with 25% of glycerol and conditioned at 58% of relative humidity, with similar deformation values (Lagos et al., 2015).

3.11. Thermal properties of films

The glass transition temperature (T_g) indicative of the film strength is associated with the structural transition from glassy to rubbery state in amorphous components (Cerqueira et al., 2012). Figure 6a shows the typical thermograms for the first scan of the films which exhibited two T_g regions indicating a phase separation (Bergo et al., 2008; Sobral et al., 2001). The T_{g1}, associated to the plasticizer rich fraction, ranged from -67.0°C to -47.9°C, with lowest value in film when PE and NA (T3) was added, and intermediate values for films added with only PE (T1) or NA (T2) (table 3). T_{g1} values were higher than the pure glycerol (-93°C) probably due to the miscibility of CS/CH with glycerol (Yang & Paulson, 2000). Consequently, the T_{g2}, associated to the starch-rich fraction, increased ($p<0.05$) from 14.8°C to 28.2-29.7°C when NA (T2, T3) was added. When PE alone was added (T1), this value was intermediary (18.7ºC), suggesting that the addition of active components stabilized the biopolymer matrix, as also evidenced in Gelatin/Chitosan films by Bonilla et al., (2017).

Figure 6b depicts the representative weight loss curves during thermal degradation of films by thermogravimetric analysis and can be observed that all films presented similar behaviour. A first weight loss step was observed, corresponding to the loss of adsorbed and bound water in films (Mathew et al., 2006). For all films, this first weight loss corresponded to 2 - 3%, and completed around 140°C for films without additives, and about 100-110°C for other films. A second weight loss (II), of about 10%, appeared between 160°C and 200°C which can be attributed to the de-amination of the chitosan chains and degradation of glycerol, as also observed by Homez-Jara et al., (2018) and Valencia-Sullca et al., (2018). Subsequently a third step occurred with 50-70% weight loss, beginning at 227 ºC for films without additives (T0), and reaching 241-250 ºC for films with PE and/or NA (table 3). The maximum degradation temperature ranged between 340 and 359 °C, affected majorly by NA (T2, T3). These values were higher than that noticed in CS/CH films by Mathew et al., (2006) and Pelissari et al., (2009). As an overall consequence, it can be considered that the addition of Natamycin increased the thermal stability of films. However, no differences were specifically observed in the final residue content for different films at 900°C, which remained approximately around 25% (table 3).

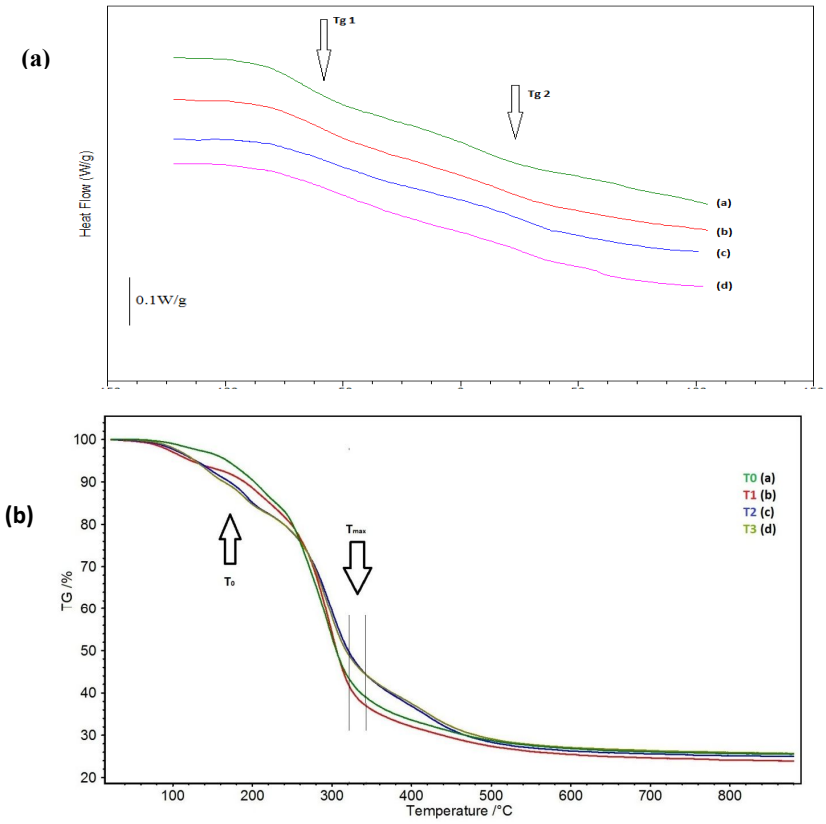

Figure 6 (a-b). Representative DSC thermograms (a) and TGA curves (b) of the CS/CH films.

3.12. Antioxidant properties of films

The incorporation of additives increased ($p<0.05$) the radical scavenging activity as can be observed in table 5. Films without additives (T0) exhibited low antioxidant activity, as expected: 7.68% scavenging effect with ABTS•+ radicals and 3.38% of DPPH• radicals. This activity might be due to the ability of amino groups in CH to react with free radicals as also observed by Ferreira et al., (2014). In case of the films incorporated with PE (T1) an activity of 59.88% and 86.20% for ABTS•+ radicals and DPPH• radicals was observed, respectively. These results affirm that the phenols and pigments in the PE enhanced the antioxidant capacity of the films. The incorporation of NA (T1) alone also increased the antioxidant activity of films, when compared with films without additives, which might be due to its compositional recipients. However, in our knowledge no specific interaction resulting in such activity was found in literature. Nevertheless, when PE and NA (T3) were added into films, a reduction of activity in films, as compared with films with pure PE (T1), was observed which probably can be attributed to the interaction between components as observed in the FTIR spectra (figure 4) and can be hypothesized as antagonist effect.

Table 5. Antioxidant activity of films by DPPH•, ABTS•+ free radical scavenging and FRAP methods

Antioxidant test	T0	T1	T2	T3
ABTS•+ (% Scavenging activity)	7.68±1.57[a]	59.88±2.33[d]	14.33±0.55[b]	37.22±1.62[c]
DPPH• (% Scavenging activity)	3.38±0.11[a]	86.20±1.37[d]	25.79±3.14[b]	71.56±2.99[c]
FRAP- 4 min (µmol $FeSO_4$/g film)	215.25±27.76[a]	4565.34±90.38[c]	325.41±39.04[a]	2918.52±222.37[b]
FRAP- 30 min (µmol $FeSO_4$/g film)	253.85±24.26[a]	5670.98±266.63[c]	508.84±84.23[a]	3594.93±297.30[b]

** Values are means ± SD; Means in a row with different superscripts indicate significant differences ($p<0.05$) between samples. Treatments T0, T1, T2 and T3 are described in Table 1.*

On the other hand, the Ferric reducing ability (FRAP) was notably high in films added with PE (T1, table 4) concurrent with the results of scavenging effects. The antioxidant capacity of different films was proportional to the antioxidant ability of the components, with the phenol-containing extract registering the highest values. Similar inference was observed in case of curcuma extract in gelatin films by Bitencourt et al., (2014).

3.13. Antifungal activity of films

In this study, antifungal activities of activated films with PE and/or NA were tested against *Apergillus flavus* and *Apergillus parasiticus*. NA containing discs demonstrated inhibition zones ranging from 6.5 to 10.5±0.7 mm against *A. flavus* and 11.0±0.1 mm against *A. parasiticus* (figure 7). However, in case of *A. flavus*, the combination of PE and NA (T3) film (Figure 7b, left plate) noted lower inhibition, indicative of slight antagonistic affect upon combination of PE with NA. PE film (T1) was observed to have no effect in the growth of molds, similar to the control film. However, further confirmation is needed through in-vitro studies on more spoilage fungi and real food systems.

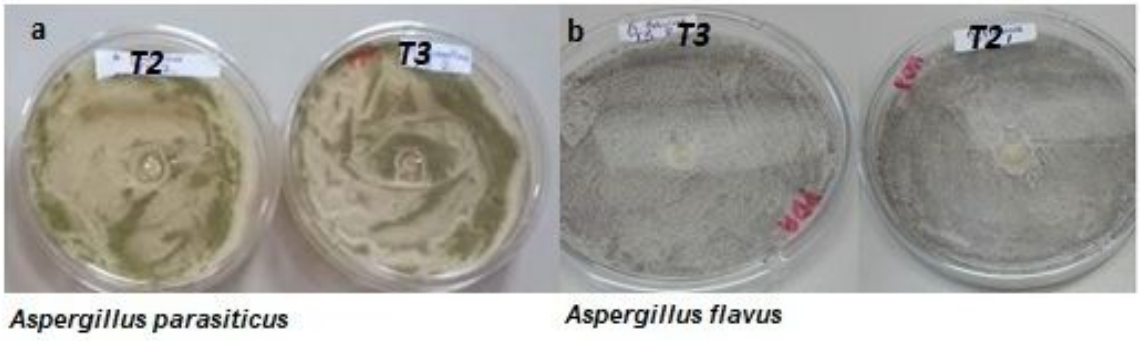

Figure 7 (a-b). Panel displaying representative examples of inhibition zones of Aspergillus parasiticus (a) and Aspergillus flavus (b) exposed to T2 and T3 films.

4. Conclusions

Active films based on blends of cassava starch and chitosan with Pitanga leaf extract and/or Natamycin were prepared successfully by casting technique. The additives were found to alter the morphology and chemical nature of the CS/CH blend films as confirmed by SEM, FTIR and XRD analyses. The addition of PE and NA although adversely affected the opacity improved the UV-Vis barrier property. The film solubility in water and water vapour permeability decreased as a consequence of NA addition, with no specific influence due to plant extract. Within the mechanical properties evaluated, the ε^B, PD and PF were reduced with the presence of PE and/or NA. In addition, PE greatly improved the antioxidant capacity, whereas the incorporation of NA rendered thermal stability and antifungal activity. This study demonstrates that tested compounds and combinations prove to be effective for use as active coatings or films in food applications. However, future directive will be to improve the synergism between the tested components and use of real-food systems for evaluation of effectiveness.

Acknowledgements

The authors acknowledge Marco-Polo financial support for the international mobility of the doctoral student. Paulo J.A. Sobral acknowledges the São Paulo Research Foundation for the grant (FAPESP FoRC, 2013/07914-8), and the Brazilian National Council for Scientific and Technological Development (CNPq) for the Research Fellowship (30.3180/2013-6). Also, we are grateful for the valuable guidance of Prof. Izabel Moraes for rheological measures and Prof. Dr. Andrezza Maria Fernandes, for microbial analysis, from FZEA-USP.

References

Abugoch, L. E., Tapia, C., Villamán, M. C., Yazdani-Pedram, M., & Díaz-Dosque, M. (2011). Characterization of quinoa protein–chitosan blend edible films. *Food Hydrocolloids*, *25*(5), 879–886. https://doi.org/https://doi.org/10.1016/j.foodhyd.2010.08.008

Balaguer, M. P., Fajardo, P., Gartner, H., Gomez-Estaca, J., Gavara, R., Almenar, E., & Hernandez-Munoz, P. (2014). Functional properties and antifungal activity of films based on gliadins containing cinnamaldehyde and natamycin. *International Journal of Food Microbiology*, *173*, 62–71. https://doi.org/https://doi.org/10.1016/j.ijfoodmicro.2013.12.013

Balaguer, M. P., Lopez-Carballo, G., Catala, R., Gavara, R., & Hernandez-Munoz, P. (2013). Antifungal properties of gliadin films incorporating cinnamaldehyde and application in active food packaging of bread and cheese spread foodstuffs. *International Journal of*

Food Microbiology, *166*(3), 369–377. https://doi.org/10.1016/j.ijfoodmicro.2013.08.012

Bangyekan, C., Aht-Ong, D., & Srikulkit, K. (2006). Preparation and properties evaluation of chitosan-coated cassava starch films. *Carbohydrate Polymers*, *63*(1), 61–71. https://doi.org/https://doi.org/10.1016/j.carbpol.2005.07.032

Baron, R. D., Pérez, L. L., Salcedo, J. M., Córdoba, L. P., & Sobral, P. J. A. (2017). Production and characterization of films based on blends of chitosan from blue crab (Callinectes sapidus) waste and pectin from Orange (Citrus sinensis Osbeck) peel. *International Journal of Biological Macromolecules*, *98*, 676–683. https://doi.org/https://doi.org/10.1016/j.ijbiomac.2017.02.004

Benzie, I. F. F., & Strain, J. J. (1996). The Ferric Reducing Ability of Plasma (FRAP) as a Measure of "Antioxidant Power": The FRAP Assay. *Analytical Biochemistry*, *239*(1), 70–76. https://doi.org/https://doi.org/10.1006/abio.1996.0292

Bergo, P., & Sobral, P. J. A. (2007). Effects of plasticizer on physical properties of pigskin gelatin films. *Food Hydrocolloids*, *21*(8), 1285–1289. https://doi.org/10.1016/j.foodhyd.2006.09.014

Bergo, P. V. A., Carvalho, R. A., Sobral, P. J. A., Dos Santos, R. M. C., Da Silva, F. B. R., Prison, J. M., Habitante, A. M. Q. B. (2008). Physical properties of edible films based on cassava starch as affected by the plasticizer concentration. *Packaging Technology and Science*, *21*(2), 85–89. https://doi.org/10.1002/pts.781

Bitencourt, C. M., Fávaro-Trindade, C. S., Sobral, P. J. A., & Carvalho, R. A. (2014). Gelatin-based films additivated with curcuma ethanol extract: Antioxidant activity and physical properties of films. *Food Hydrocolloids*, *40*(Supplement C), 145–152. https://doi.org/10.1016/j.foodhyd.2014.02.014

Bonilla, J., Bittante, A. M. Q. B., & Sobral, P. J. A. (2017). Thermal analysis of gelatin--chitosan edible film mixed with plant ethanolic extracts. *Journal of Thermal Analysis and Calorimetry*, *130*(2), 1221–1227. https://doi.org/10.1007/s10973-017-6472-4

Bonilla, J., Fortunati, E., Atarés, L., Chiralt, A., & Kenny, J. M. (2014). Physical, structural and antimicrobial properties of poly vinyl alcohol–chitosan biodegradable films. *Food Hydrocolloids*, *35*(Supplement C), 463–470. https://doi.org/10.1016/j.foodhyd.2013.07.002

Bonilla, J., Poloni, T., Lourenço, R. V., & Sobral, P. J. A. (2018). Antioxidant potential of eugenol and ginger essential oils with gelatin/chitosan films. *Food Bioscience*, *23*, 107–114. https://doi.org/10.1016/j.fbio.2018.03.007

Bonilla, J., Poloni, T., & Sobral, P. J. A. (2018). Active edible coatings with Boldo extract added and their application on nut products: reducing the oxidative rancidity rate. *International Journal of Food Science & Technology*, *53*(3), 700–708. https://doi.org/10.1111/ijfs.13645

Bonilla, J., & Sobral, P. J. A. (2016). Investigation of the physicochemical, antimicrobial and antioxidant properties of gelatin-chitosan edible film mixed with plant ethanolic extracts. *Food Bioscience*, *16*, 17–25. https://doi.org/10.1016/j.fbio.2016.07.003

Bonilla, J., & Sobral, P. J. A. (2017). Antioxidant and physicochemical properties of blended films based on gelatin-sodium caseinate activated with natural extracts. *Journal of Applied Polymer Science*, *134*(7). https://doi.org/10.1002/app.44467

Bonilla, J., Talón, E., Atarés, L., Vargas, M., & Chiralt, A. (2013). Effect of the incorporation of antioxidants on physicochemical and antioxidant properties of wheat starch-chitosan films. *Journal of Food Engineering*, *118*(3), 271–278. https://doi.org/10.1016/j.jfoodeng.2013.04.008

Bourtoom, T., & Chinnan, M. S. (2008). Preparation and properties of rice starch–chitosan blend biodegradable film. *LWT - Food Science and Technology*, *41*(9), 1633–1641. https://doi.org/10.1016/j.lwt.2007.10.014

Brand-Williams, W., Cuvelier, M. E., & Berset, C. (1995). Use of a free radical method to evaluate antioxidant activity. *LWT - Food Science and Technology*, *28*(1), 25–30. https://doi.org/10.1016/S0023-6438(95)80008-5

Cé, N., Noreña, C. P. Z., & Brandelli, A. (2012). Antimicrobial activity of chitosan films containing nisin, peptide P34, and natamycin. *CyTA - Journal of Food*, *10*(1), 21–26. https://doi.org/10.1080/19476337.2010.537371

Cerqueira, M. A., Souza, B. W. S., Teixeira, J. A., & Vicente, A. A. (2012). Effect of glycerol and corn oil on physicochemical properties of polysaccharide films – A comparative study. *Food Hydrocolloids*, *27*(1), 175–184. https://doi.org/10.1016/j.foodhyd.2011.07.007

Cevher, E., Şensoy, D., Zloh, M., & Mülazımoğlu, L. (2008). Preparation and Characterisation of Natamycin: γ-Cyclodextrin Inclusion Complex and its Evaluation in Vaginal Mucoadhesive Formulations. *Journal of Pharmaceutical Sciences*, *97*(10), 4319–4335. https://doi.org/10.1002/jps.21312

Chillo, S., Flores, S., Mastromatteo, M., Conte, A., Gerschenson, L., & Del Nobile, M. A. (2008). Influence of glycerol and chitosan on tapioca starch-based edible film properties. *Journal of Food Engineering*, *88*(2), 159–168. https://doi.org/https://doi.org/10.1016/j.jfoodeng.2008.02.002

Cuq, B., Aymard, C., Cuq, J.-L., & Guilbert, S. (1995). Edible Packaging Films Based on Fish Myofibrillar Proteins: Formulation and Functional Properties. *Journal of Food Science*, *60*(6), 1369–1374. https://doi.org/10.1111/j.1365-2621.1995.tb04593.x

D882-12, A. (n.d.). ASTM D882-12, Standard Test Method for Tensile Properties of Thin Plastic Sheeting. https://doi.org/10.1520/D0882-12

Dammak, I., & Sobral, P.J.A, (2017). Investigation into the physicochemical stability and rheological properties of rutin emulsions stabilized by chitosan and lecithin. *Journal of Food Engineering*. https://doi.org/https://doi.org/10.1016/j.jfoodeng.2017.09.022

Dang, K. M., & Yoksan, R. (2015). Development of thermoplastic starch blown film by incorporating plasticized chitosan. *Carbohydrate Polymers*, *115*, 575–581. https://doi.org/10.1016/j.carbpol.2014.09.005

de Oliveira, T. M., de Fátima Ferreira Soares, N., Pereira, R. M., & de Freitas Fraga, K. (2007). Development and evaluation of antimicrobial natamycin-incorporated film in gorgonzola cheese conservation. *Packaging Technology and Science*, *20*(2), 147–153. https://doi.org/10.1002/pts.756

de Souza, A. M., de Oliveira, C. F., de Oliveira, V. B., Betim, F. C. M., Miguel, O. G., & Miguel, M. D. (2018). Traditional Uses, Phytochemistry, and Antimicrobial Activities of Eugenia Species – A Review. *Planta Medica*, (EFirst). https://doi.org/10.1055/a-0656-7262

dos Santos, J. F. S., Rocha, J. E., Bezerra, C. F., do Nascimento Silva, M. K., de Matos, Y. M. L. S., de Freitas, T. S., … Morais-Braga, M. F. B. (2018). Chemical composition, antifungal activity and potential anti-virulence evaluation of the Eugenia uniflora essential oil against Candida spp. *Food Chemistry*, *261*, 233–239. https://doi.org/10.1016/j.foodchem.2018.04.015

Duran, M., Aday, M. S., Zorba, N. N. D., Temizkan, R., Büyükcan, M. B., & Caner, C. (2016). Potential of antimicrobial active packaging 'containing natamycin, nisin, pomegranate and grape seed extract in chitosan coating' to extend shelf life of fresh strawberry. *Food and Bioproducts Processing*, *98*, 354–363. https://doi.org/https://doi.org/10.1016/j.fbp.2016.01.007

Elsabee, M. Z., & Abdou, E. S. (2013). Chitosan based edible films and coatings: A review. *Materials Science and Engineering: C*, *33*(4), 1819–1841. https://doi.org/https://doi.org/10.1016/j.msec.2013.01.010

Falguera, V., Quintero, J. P., Jiménez, A., Muñoz, J. A., & Ibarz, A. (2011). Edible films and coatings: Structures, active functions and trends in their use. *Trends in Food Science & Technology*, *22*(6), 292–303. https://doi.org/10.1016/j.tifs.2011.02.004

Ferreira, A. S., Nunes, C., Castro, A., Ferreira, P., & Coimbra, M. A. (2014). Influence of grape pomace extract incorporation on chitosan films properties. *Carbohydrate Polymers*, *113*, 490–499. https://doi.org/https://doi.org/10.1016/j.carbpol.2014.07.032

Galus, S., & Kadzińska, J. (2015). Food applications of emulsion-based edible films and coatings. *Trends in Food Science & Technology*, *45*(2), 273–283. https://doi.org/10.1016/j.tifs.2015.07.011

Galus, S., & Lenart, A. (2013). Development and characterization of composite edible films

based on sodium alginate and pectin. *Journal of Food Engineering*, *115*(4), 459–465. https://doi.org/10.1016/j.jfoodeng.2012.03.006

Gómez-Guillén, M. C., Ihl, M., Bifani, V., Silva, A., & Montero, P. (2007). Edible films made from tuna-fish gelatin with antioxidant extracts of two different murta ecotypes leaves (Ugni molinae Turcz). *Food Hydrocolloids*, *21*(7), 1133–1143. https://doi.org/https://doi.org/10.1016/j.foodhyd.2006.08.006

Gontard, N., Duchez, C., Cuq, J.-L., & Guilbert, S. (2007). Edible composite films of wheat gluten and lipids: water vapour permeability and other physical properties. *International Journal of Food Science & Technology*, *29*(1), 39–50. https://doi.org/10.1111/j.1365-2621.1994.tb02045.x

Homez-Jara, A., Daza, L. D., Aguirre, D. M., Muñoz, J. A., Solanilla, J. F., & Váquiro, H. A. (2018). Characterization of chitosan edible films obtained with various polymer concentrations and drying temperatures. *International Journal of Biological Macromolecules*, *113*, 1233–1240. https://doi.org/https://doi.org/10.1016/j.ijbiomac.2018.03.057

Hosseini, M. H., Razavi, S. H., & Mousavi, M. A. (2009). Antimicrobial, physical and mechanical properties of chitosan-based films incorporated with thyme, clove and cinnamon essential oils. *J. Food Process. Preserv.*, *33*(6), 727.

Karbowiak, T., Debeaufort, F., Champion, D., & Voilley, A. (2006). Wetting properties at the surface of iota-carrageenan-based edible films. *Journal of Colloid and Interface Science*, *294*(2), 400–410. https://doi.org/10.1016/j.jcis.2005.07.030

Kechichian, V., Ditchfield, C., Veiga-Santos, P., & Tadini, C. C. (2010). Natural antimicrobial ingredients incorporated in biodegradable films based on cassava starch. *LWT - Food Science and Technology*, *43*(7), 1088–1094. https://doi.org/https://doi.org/10.1016/j.lwt.2010.02.014

Lagos, J. B., Vicentini, N. M., Santos, R. M. C., Bittante, A.M.Q.B., & Sobral, P.J.A. (2015). Mechanical properties of cassava starch films as affected by different plasticizers and different relative humidity conditions. *International Journal of Food Studies*, *4*(1), 116–125. https://doi.org/10.1017/S0047404500020601

Liu, H., Adhikari, R., Guo, Q., & Adhikari, B. (2013). Preparation and characterization of glycerol plasticized (high-amylose) starch–chitosan films. *Journal of Food Engineering*, *116*(2), 588–597. https://doi.org/10.1016/j.jfoodeng.2012.12.037

Ma, W., Tang, C.-H., Yin, S.-W., Yang, X.-Q., Wang, Q., Liu, F., & Wei, Z.-H. (2012). Characterization of gelatin-based edible films incorporated with olive oil. *Food Research International*, *49*(1), 572–579. https://doi.org/https://doi.org/10.1016/j.foodres.2012.07.037

Mannozzi, C., Tylewicz, U., Chinnici, F., Siroli, L., Rocculi, P., Dalla Rosa, M., & Romani, S.

(2018). Effects of chitosan based coatings enriched with procyanidin by-product on quality of fresh blueberries during storage. *Food Chemistry*, *251*, 18–24. https://doi.org/10.1016/j.foodchem.2018.01.015

Marcuzzo, E., Peressini, D., Debeaufort, F., & Sensidoni, A. (2010). Effect of ultrasound treatment on properties of gluten-based film. *Innovative Food Science & Emerging Technologies*, *11*(3), 451–457. https://doi.org/https://doi.org/10.1016/j.ifset.2010.03.002

Mathew, S., Brahmakumar, M., & Abraham, T. E. (2006). Microstructural imaging and characterization of the mechanical, chemical, thermal, and swelling properties of starch–chitosan blend films. *Biopolymers*, *82*(2), 176–187. https://doi.org/10.1002/bip.20480

Ollé Resa, C. P., Gerschenson, L. N., & Jagus, R. J. (2013). Effect of Natamycin on Physical Properties of Starch Edible Films and Their Effect on Saccharomyces cerevisiae Activity. *Food and Bioprocess Technology*, *6*(11), 3124–3133. https://doi.org/10.1007/s11947-012-0960-0

Ollé Resa, C. P., Jagus, R. J., & Gerschenson, L. N. (2014). Effect of natamycin, nisin and glycerol on the physicochemical properties, roughness and hydrophobicity of tapioca starch edible films. *Materials Science and Engineering: C*, *40*, 281–287. https://doi.org/10.1016/j.msec.2014.04.005

Otoni, C. G., Pontes, S. F. O., Medeiros, E. A. A., & Soares, N. D. F. F. (2014). Edible Films from Methylcellulose and Nanoemulsions of Clove Bud (Syzygium aromaticum) and Oregano (Origanum vulgare) Essential Oils as Shelf Life Extenders for Sliced Bread. *Journal of Agricultural and Food Chemistry*, *62*(22), 5214–5219. https://doi.org/10.1021/jf501055f

Pelissari, F. M., Grossmann, M. V. E., Yamashita, F., & Pineda, E. A. G. (2009). Antimicrobial, mechanical, and barrier properties of cassava starch-chitosan films incorporated with oregano essential oil. *Journal of Agricultural and Food Chemistry*, *57*(16), 7499–504. https://doi.org/10.1021/jf9002363

Peressini, D., Bravin, B., Lapasin, R., Rizzotti, C., & Sensidoni, A. (2003). Starch–methylcellulose based edible films: rheological properties of film-forming dispersions. *Journal of Food Engineering*, *59*(1), 25–32. https://doi.org/10.1016/S0260-8774(02)00426-0

Re, R., Pellegrini, N., Proteggente, A., Pannala, A., Yang, M., & Rice-Evans, C. (1999). Antioxidant activity applying an improved ABTS radical cation decolorization assay. *Free Radical Biology and Medicine*, *26*(9), 1231–1237. https://doi.org/https://doi.org/10.1016/S0891-5849(98)00315-3

Rubilar, J. F., Cruz, R. M. S., Silva, H. D., Vicente, A. A., Khmelinskii, I., & Vieira, M. C. (2013). Physico-mechanical properties of chitosan films with carvacrol and grape seed extract. *Journal of Food Engineering*, *115*(4), 466–474. https://doi.org/10.1016/j.jfoodeng.2012.07.009

Sanches-Silva, A., Costa, D., Albuquerque, T. G., Buonocore, G. G., Ramos, F., Castilho, M. C., Costa, H. S. (2014). Trends in the use of natural antioxidants in active food packaging: a review. *Food Additives & Contaminants. Part A, Chemistry, Analysis, Control, Exposure & Risk Assessment*, *31*(3), 374–95. https://doi.org/10.1080/19440049.2013.879215

Silveira, M. F. A., Soares, N. F. F., Geraldine, R. M., Andrade, N. J., Botrel, D. A., & Gonçalves, M. P. J. (2007). Active film incorporated with sorbic acid on pastry dough conservation. *Food Control*, *18*(9), 1063–1067. https://doi.org/https://doi.org/10.1016/j.foodcont.2006.07.004

Siracusa, V., Rocculi, P., Romani, S., & Rosa, M. D. (2008). Biodegradable polymers for food packaging: a review. *Trends in Food Science & Technology*, *19*(12), 634–643. https://doi.org/https://doi.org/10.1016/j.tifs.2008.07.003

Sobral, P. J. A., Menegalli, F. C., Hubinger, M. D., & Roques, M. A. (2001). Mechanical, water vapor barrier and thermal properties of gelatin based edible films. *Food Hydrocolloids*, *15*(4), 423–432. https://doi.org/10.1016/S0268-005X(01)00061-3

Šuput, D., Lazić, V., Pezo, L., Markov, S., Vaštag, Ž., Popović, L., … Popović, S. (2016). Characterization of starch edible films with different essential oils addition. *Polish Journal of Food and Nutrition Sciences*, *66*(4), 277–285. https://doi.org/10.1515/pjfns-2016-0008

Talón, E., Trifkovic, K. T., Nedovic, V. A., Bugarski, B. M., Vargas, M., Chiralt, A., & González-Martínez, C. (2017). Antioxidant edible films based on chitosan and starch containing polyphenols from thyme extracts. *Carbohydrate Polymers*, *157*, 1153–1161. https://doi.org/10.1016/j.carbpol.2016.10.080

Thakur, R., Saberi, B., Pristijono, P., Golding, J., Stathopoulos, C., Scarlett, C., … Vuong, Q. (2016). Characterization of rice starch-ι-carrageenan biodegradable edible film. Effect of stearic acid on the film properties. *International Journal of Biological Macromolecules*, *93*, 952–960. https://doi.org/10.1016/j.ijbiomac.2016.09.053

Valencia-Sullca, C., Atarés, L., Vargas, M., & Chiralt, A. (2018). Physical and Antimicrobial Properties of Compression-Molded Cassava Starch-Chitosan Films for Meat Preservation. *Food and Bioprocess Technology*, *11*(7), 1339–1349. https://doi.org/10.1007/s11947-018-2094-5

Valencia-Sullca, C., Vargas, M., Atarés, L., & Chiralt, A. (2018). Thermoplastic cassava starch-chitosan bilayer films containing essential oils. *Food Hydrocolloids*, *75*, 107–115. https://doi.org/https://doi.org/10.1016/j.foodhyd.2017.09.008

Valencia, G. A., Luciano, C. G., Lourenço, R. V., & Sobral, P. J. A. (2018). Microstructure and physical properties of nano-biocomposite films based on cassava starch and laponite. *International Journal of Biological Macromolecules*, *107*, 1576–1583. https://doi.org/https://doi.org/10.1016/j.ijbiomac.2017.10.031

Vargas, F. C., Arantes-Pereira, L., Costa, P. A., Melo, M. P., & Sobral, P. J. A. (2016). Rosemary and Pitanga Aqueous Leaf Extracts On Beef Patties Stability under Cold Storage. *Brazilian Archives of Biology and Technology*, *59*. https://doi.org/10.1590/1678-4324-2016160139

Vásconez, M. B., Flores, S. K., Campos, C. A., Alvarado, J., & Gerschenson, L. N. (2009). Antimicrobial activity and physical properties of chitosan–tapioca starch based edible films and coatings. *Food Research International*, *42*(7), 762–769. https://doi.org/10.1016/j.foodres.2009.02.026

Yang, L., & Paulson, A. T. (2000). Mechanical and water vapour barrier properties of edible gellan films. *Food Research International*, *33*(7), 563–570. https://doi.org/10.1016/S0963-9969(00)00092-2

Zhong, Y., Cavender, G., & Zhao, Y. (2014). Investigation of different coating application methods on the performance of edible coatings on Mozzarella cheese. *LWT - Food Science and Technology*, *56*(1), 1–8. https://doi.org/10.1016/j.lwt.2013.11.006